An integrated study of the Gladstone marine system

Babcock RC, Baird ME, Pillans R, Patterson T, Clementson LA, Haywood ME, Rochester W, Morello E, Kelly N, Oubelkheir K, Fry G, Dunbabin M, Perkins S, Forcey K, Cooper S, Adams M, O'Brien K, Donovan A, Kenyon R, Carlin G, Wild-Allen K, Limpus C.
14 April 2015

CSIRO Oceans and Atmosphere

Citation

Copyright and disclaimer

Important disclaimer

Foreword

The work summarised in this report was made possible through the support of the Gas Industry Social and Economic Research Alliance (GISERA). GISERA focuses on public good science related to all facets of the effects of natural gas development in regional areas of Australia. GISERA goes beyond the boundaries of permits held by any one developer and seeks to provide a whole-of-industry focus, using a multi-developer approach to research the impacts of the industry. This is crucial to providing a coherent conduit for knowledge that can inform future regulation and monitoring of natural gas developments around Australia.

GISERA Marine environment research program aims to understand vulnerable components of the marine ecosystem surrounding Gladstone with a view to providing tools and information that can be used to minimise impacts. To do this the GISERA marine environment program has undertaken research into the key areas of water quality and optical properties, seagrass habitat distribution, turtle habitat use and numerical modelling of seagrass growth. The program brings together strands of work essential to building an integrated picture of how major ecosystem processes function in order to begin to provide predictive tools for better understanding and managing the marine habitats and iconic species of Gladstone Harbour.

Current members of GISERA are CSIRO, Australia Pacific LNG and QGC.

Contents

Figures

Tables

Acknowledgments

Executive summary

The overarching goal of the GISERA marine environmental research program has been to make possible more accurate prediction and understanding of impacts and trends in water quality as well as ecological responses in primary producers (seagrass) and grazers (turtles) that have been assessed as being vulnerable due to expansion of development in the Port of Gladstone. In doing this is has also been the aim of the GISERA marine research program to develop tools that can be used to determine management options that may lead to the reduction of impacts on these key ecological assets in the future, well beyond the Port Curtis and the current phase of development.

The GISERA Marine project has made significant progress in integrating environmental and ecological knowledge and towards providing tools, notably a re-locatable seagrass growth model, and a turtle shipping-risk assessment model, that provide for a synoptic picture of conditions within the harbour as well as risks to its key ecological elements. The two major sub-components in the project, 1) Sustaining turtles, dugongs and their habitat – an integrated marine observation system, and 2) Integrated modelling, are presented in five chapters, starting with observations of the biophysical properties of the water column (Chapter I) and seagrasses (Chapter II) that are brought together in a biogeochemical model of seagrass growth (Chapter III), moving up the food web to studies of turtle movements (Chapter IV) and modelling of turtle habitat use and risk from shipping (Chapter V).

The optical data detailed in Chapter I has been vitally important for the development and validation of modelling of coastal waters in Gladstone Harbour, as well as more widely. The data provides confidence in both the use of GISERA optical samples for terrestrially-sourced fine sediment parameterisation in the optical model, as well as in the calculations for converting total suspended solids to remotely-sensed reflectance. The improved confidence in the performance of the model in terms of water column optical properties also means increased confidence in the performance of the model for predicting benthic processes such as seagrass growth.

Seagrass cover and biomass (Chapter II) was low in most areas as expected, confirming the results of other studies which have documented declines in the region since 2010-2011. The exception to this was Pelican Banks where cover of *Zostera* reached as high at 70%. Seagrass biomass estimates were pivotal to the parameterization of the seagrass growth model and surveys of maximum depth range throughout the harbour provide strong validation of the seagrass growth model and indicate that maximum depth of seagrass beds corresponded to approximately 13% of surface irradiation which was similar to the levels shown to be required to sustain seagrass growth. The actual depth of this point varied throughout the harbour according to water quality.

Biogeochemical modelling of seagrass growth has developed efficient new algorithms for the growth of seagrasses that take into account self-shading effects and competition between seagrasses (Chapter III). In Gladstone Harbour, the model was able to produce results that closely reflected the observed values for seagrass depth range and distribution. The model includes two seagrasses, *Zostera* and *Halophila*, and also reflects well the historical distribution of seagrass throughout the harbour. The model has provided an invaluable platform for the development of operational modelling of water quality and seagrass growth in Gladstone Harbour as part of the Gladstone Healthy Harbours Program. Innovations developed in the GISERA seagrass model will also provide a basis for predicting the effects of future impacts on the harbour's natural assets. The model will also have a broader impact through adoption of these innovations into other ecological models in the region.

The iconic fauna of Gladstone Harbour depend on its continued health in terms of water quality and the presence of primary producers such as seagrasses, algae and mangroves. The GISERA tagging program has proven that acoustic tagging and tracking of turtles and dugong is a viable, economical and accurate means of tracking animal behaviour (Chapter IV). It has also shown how turtles use varying components of the harbour's primary producer habitats, depending on the availability of these habitats in any given area. In

areas where seagrasses dominate turtles used them as a primary food source but in areas with little seagrass, such as Wiggins Island, they used other foods such as algae and mangroves. Turtles moved into shallower areas, generally with more food, during high tide, and shifted into slightly deeper waters on the edge of channels at low tide. While many turtles had small home ranges and were resident for all or most of the study, an unusually high proportion left the harbour study areas, for unknown reasons.

Modelling of turtle habitat use (Chapter V) throughout the harbour and the mapping of shipping usage patterns from larger commercial vessels indicated that because most turtle habitat and turtle home range usage is in shallow water, risk from commercial shipping and most passenger ferries may be relatively low. However, improving on this preliminary result and obtaining more accurate assessments of overall risk to turtles will depend on improved information on the overall abundance and distribution of turtles in the harbour as well as an understanding of patterns of smaller vessel usage of the harbour since these may make greater use of shallow water frequented by turtles.

Chapter I   Bio-optical properties of Gladstone Harbour

Lesley Clementson, Mark Baird, Kadija Oubelkheir, Gary Fry

CSIRO

1 Introduction

Coastal environments are impacted by multiple natural and anthropogenic forcing including river runoff, tidal surges, phytoplankton blooms and agriculture, industrial and recreational activities. Resource management of such environments is best achieved by combining *in situ* sampling of bio-optical and biogeochemical parameters, which are spatially and temporally limited, with satellite retrieved estimates of the same parameters, which are spatially broader and temporally more frequent. However, while remotely sensed satellite data provides a large data set, it has been demonstrated that standard global algorithms are inaccurate in near-shore coastal waters (Schroeder et al. 2012).

Light availability is one of the basic requirements for the development and sustainability of phytoplankton within the water column as well as plants on the seabed, and is determined by the optical properties of the dissolved and particulate components within the water column. High levels of particulate and dissolved organic matter in the water column scatter and absorb light which affects both benthic and pelagic photosynthesis and hence primary production. The absorption and scattering properties of the water column will also determine what percentage of incident irradiance is reflected back from the water column to a satellite sensor. Often the absorption and scattering properties of coastal waters can be dominated by high sediment loadings or by high concentrations of Coloured Dissolved Organic Matter (CDOM) that will affect the accuracy of satellite-retrieval of chlorophyll-a, an indicator of phytoplankton biomass. The *in situ* samples can provide data for the development of robust regional algorithms which when employed increases the accuracy of retrieved estimates of parameters. Ultimately they will also be incorporated in other studies beyond GISERA, such as the development of regional satellite (remote sensing) algorithms.

Biogeochemical models can be used to predict the distribution and concentration of biogeochemical parameters under different scenarios. These models also rely on both the *in situ* and satellite-retrieved samples to parameterise the light level throughout the water column, and at the bottom. The models then use these predictions of light to drive photosynthetic processes in phytoplankton and aquatic vegetation such as seagrass.

Gladstone Harbour is a natural deep water harbour that is home to the largest bulk commodity port in Queensland and the sixth largest in Australia. The port exports agriculture products, coal, bauxite and liquefied natural gas (LNG) with coal being the major export (>70%). As a large industrial port, Gladstone is also subject to sediment re-suspension caused by capital dredging operations, maintenance dredging and the passage of shipping. In addition to the working port area, Gladstone Harbour, below the low water mark, is within the Great Barrier Reef World Heritage Area and has in recent years been impacted by significant weather events – the December 2010/January 2011 Queensland floods (Coles et al 2014, Maxwell et al. 2014). Environmental disturbances of various kinds (both natural and anthropogenic) can significantly impact the optical properties of the harbour on varying spatial and temporal scales.

The optical properties reported in this study are critical to the development and improvement of biogeochemical models of the waters of Gladstone Harbour and to the understanding of biogeochemical processes throughout both the pelagic and benthic environments within Gladstone Harbour. Seagrasses are critically dependent on the level of light transmission through the water column (Abal and Dennison 1996, Chartrand Collier et al 2012, Pederson et al. 2012, Collier et al 2012) therefore it is essential for such models to accurately capture processes of sediment resuspension and water column productivity.

2 Methods

2.1 Sample sites and data collection

Two optics field campaigns where undertaken; the first in 2012 had 34 site locations (Figure 1a), and the second in 2013 had 43 site locations which included a repeat of the sites sampled during the first campaign plus some additional offshore sites (Figure 1b). At all stations during both campaigns, an instrument package comprising a WETLabs ac-s, WQM, and WETStar CDOM fluorometer in vertical profiling mode was deployed. A YSI model 6600 water quality probe was deployed simultaneously with the instrument package for comparison. An ac-s with a 10 cm pathlength was used for *in situ* profiling of hyperspectral attenuation and absorption coefficients of total material, (dissolved plus particulate,) between 400 and 730 nm, with a 4 nm resolution. Correction for *in situ* temperature and salinity effects on the optical properties of water was applied (Sullivan et al. 2006). Correction for incomplete recovery of the scattered light in the ac-s absorption tube was performed using the proportional method (Zaneveld et al. 1994). The raw voltage from the WETStar CDOM fluorometer was converted to quinine sulfate units using the calibration coefficients provided by the manufacturer.

Simultaneously with the *in situ* vertical profiling of the water column, discrete samples were collected in the surface layer for the analysis of pigment concentration and composition, particulate and dissolved absorption and total suspended matter (TSM) concentration. The discrete water samples were stored in clear HDPE carboys and stored in the cool and dark until filtration back at the laboratory (approximately 6 hours after collection). Secchi disk readings were also obtained.

2.2 Secchi depth

The secchi depth was measured as the depth in the water column when the Secchi disk (30 cm in diameter disk painted alternately black and white) is no longer visible.

2.3 Total Suspended Matter

Between 0.5 – 2.0 litres of sample water was filtered through a pre-ashed and pre-weighed 47 mm glass fibre filter (Whatman GF/F), under subdued lighting. The filter was washed with approximately 50 mL Milli-Q water to remove any salt in the filter. The filters were stored flat in petri slides (Millipore) at 4°C until analysis. In the laboratory each filter was transferred to a glass petri dish and dried to constant weight at 60°C to determine the total TSM weight. The filters were then placed in a muffle furnace and the furnace was programmed to reach a temperature of 450°C for 3 hours. Once the filters had cooled they were weighed to determine the amount of inorganic material

remaining on the filter. By subtraction from the total TSM an estimate of the organic fraction can be obtained.

2.4   Pigment analysis

One to two litres of sample water was filtered through a 25 mm glass fibre filter (Whatman GF/F) under subdued lighting, and the filter was then stored in liquid nitrogen until analysis. Pigments were extracted and analysed using the method described in Clementson (2013).

2.5   Particulate and detrital absorption

One litre of sample water was filtered through a 25 mm glass fibre filter (Whatman GF/F), under subdued lighting, and then stored flat in liquid nitrogen until analysis. Optical density (OD) spectra for total particulate and detrital matter were obtained using a Cintra 404 UV/VIS dual beam spectrophotometer equipped with integrating sphere. The OD spectrum of the phytoplankton pigment was obtained as the difference between the OD of the total particulate and detrital components. The OD scans were converted to absorption spectra by first normalising the scans to zero at 750 nm and then correcting for the path length amplification using the coefficients of Mitchell (1990).

Figure 1 Site locations for the 2012 optics field campaign (a) and the 2013 optics field campaign (b). See Appendix A for more detail.

2.6 CDOM absorption

Samples for Coloured Dissolved Organic Matter (CDOM) analysis were filtered through a 0.2 μm polycarbonate filter (Millipore) and stored at 4°C, in clean acid washed glass bottles, until analysis within 48 hours. Samples were allowed to equilibrate to room temperature in the dark before the CDOM absorbance was measured in a 10 cm path length quartz cell, from 200–900 nm, using the

normal cell compartment of the Cintra 404 UV/VIS spectrophotometer, with Milli-q water as a reference. Between sample scans, the reference cell was removed from the spectrophotometer and placed in a room temperature water bath to reduce temperature effects in the scans. The CDOM absorption co-efficient (m^{-1}) was calculated using Equation 1.

$$a_{CDOM} = 2.3(a(\lambda)/l) \qquad\qquad \text{Eq. 1}$$

where $a(\lambda)$ is the absorbance (normalised to zero at 680 nm) and l is the cell path length in meters.

2.6.1 CURVE FITTING

An exponential function was fitted to all CDOM and detritus spectra over the wavelength range 350 to 750 nm (Equation 2). A non-linear least-squares technique was used to fit Equation 2 to the untransformed data.

$$a(\lambda) = a_{(350)}.\exp(-S(\lambda - 350)) + b \qquad\qquad \text{Eq. 2}$$

The inclusion of an offset b allows for any baseline correction. In some samples, particularly samples containing cyanobacterial pigments, pigment extraction was incomplete, leaving small residual peaks in detritus spectra at the principal chlorophyll absorption bands. To avoid distorting the fitted detritus spectra, data at these wavelengths were omitted when all spectra were fitted. A linear approximation was used to derive standard errors or the fitted parameters $a(\lambda)$, slope S and offset b.

Total particulate spectra were smoothed using a running box-car filter with width 10 nm, and the fitted detritus spectra subtracted. Subtracting fitted detritus spectra minimised any artefacts due to incomplete extraction of pigments. The resulting phytoplankton spectra were base-corrected by subtracting absorption at 750 nm to obtain $a_{ph}(\lambda)$.

2.6.2 TRUE COLOUR

A Wetlabs ac-s was deployed in Gladstone Harbour at the same time as the HPLC samples were taken. The ac-s measures spectrally-resolved absorption, a_λ, and beam attenuation, c_λ, from which we calculate total scattering, $b_\lambda = c_\lambda - a_\lambda$. The ratio of backscattering to attenuation, u_λ, is then calculated by:

$$u = \frac{\gamma b}{a + \gamma b}$$

where $\gamma = 0.025$ is the backscattering coefficient of particles and takes a value at 555 nm between 0.001-0.05 for north-eastern Australian river plumes (Blondeau-Patissier et al. 2009).

True colour images use intensity in the red, green and blue wavebands. We use u at the MODIS bands 1 (645 nm), 3 (555 nm) and 4 (470 nm), with brightness adjusted by linearly mapping in water surface reflectance at each wavelength from [0 30 60 120 190 255]/255 onto [0 110 160 210 240 255]/255, producing a quasi-true colour (Gumley et al. 2010). These true colour hues are used in plotting to aid in identification of water types.

Later in the analysis we endeavour to relate *in situ* total suspended solids to surface reflectance. The *in situ* surface reflectance, r_r is given by:

$$r_{rs,\lambda} = g_0 u_\lambda + g_1 u_\lambda^2$$

where $g_0 = 0.0949$ and $g_1 = 0.0794$ are empirical constants for the nadir-view in oceanic waters (Gordon et al. 1988; Brando et al. 2012), and these constants result in a change of units from the unitless *u* to a per unit of solid angle, sr^{-1}, quantity $r_{rs,\lambda}$. The above-surface reflectance, through rearranging Lee et al. (2002), is given by:

$$R_{rs,\lambda} = \frac{0.52 \, r_{rs,\lambda}}{1.0 - 1.7 \, r_{rs,\lambda}}$$

3 Results and Discussion

3.1 Hydrodynamic conditions
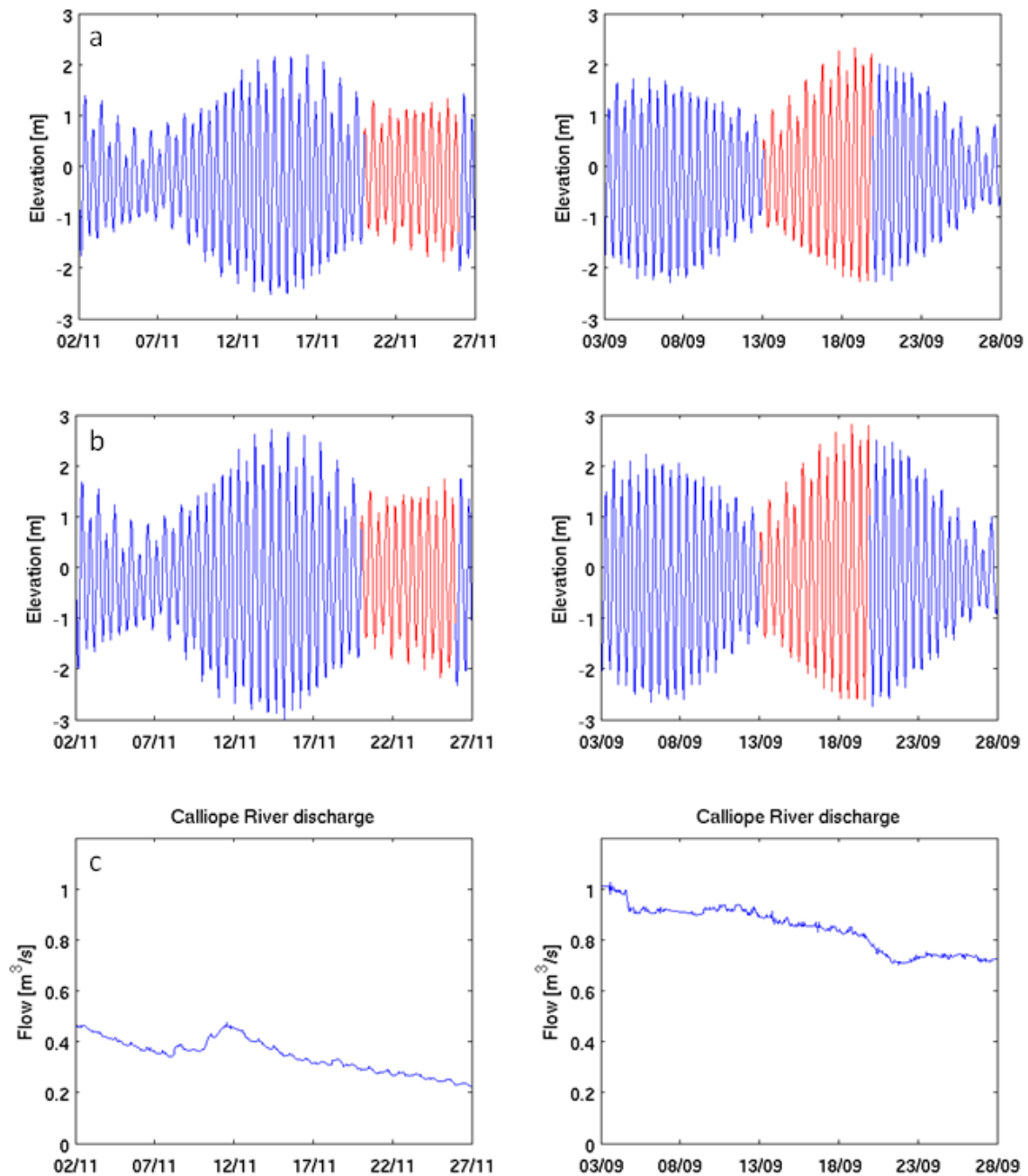
Figure 2 Tidal variation and river discharge during optics sampling periods. (a) Surface elevation near site PBMT1 (northern entrance) in November 2012 (left) and September 2013 (right); (b) Surface elevation near site DCT2 (the Narrows) in November 2012 (left) and September 2013 (right) and (c) Calliope River discharge during November 2012 (left) and September 2013 (right). River discharge was obtained through the eReefs project, surface elevation from the GISERA hydrodynamic model hindcast.

The change in surface elevation and river flow during the period of the observations are shown in Figure 2. Both sets of observations at site PBMT1 (northern entrance; Figure 2a) began under neap tides that occurred on the 21 November 2012 and 13 September 2013. However the 2013 sampling period was one day longer, and occurred during a period of greater tidal amplitudes at the following spring tide. The tidal range at site DCT2 in the Narrows (Figure 2b) is similar, but reaches a maximum range of over 5 m.

The flow from the Calliope River (Figure 2c) was low during both observation periods.

3.2 Secchi depth and total suspended matter

To compare the biogeochemical and optical parameters within Gladstone Harbour, four sites were chosen as representative of the general area where they were located; SFT2, inside the southern entrance to the harbour; PBMT1, inside the northern entrance to the harbour; WIT1, a central location and DCT2, in the Narrows (Figure 1a and b).

Secchi depth in 2013 was deeper at all sites except DCT2 in the Narrows (Figure 3; Table 3.1) than it had been in 2012 and substantially deeper at sites PBMT1 and SFT2 inside the northern and southern entrances respectively (SFT2 – 1.1 m in 2012 compared to 6.2 m in 2013). It then follows that the Total Suspended Matter (TSM) was higher at sites WIT1, PBMT1 and SFT2 in 2012 than it was in 2013 (Figure 3; Table 3.1) with the greatest difference being at the central site, WIT1, where the TSM was approximately 6-7 times greater in 2012 than it was 2013 (37.05 mg L^{-1} in 2012 and 5.52 mg L^{-1} in 2013). At site DCT2 in the Narrows the relationship between Secchi depth and TSM was the same as at the other sites, hence the TSM at this site was higher in 2013 when the Secchi depth was shallower (Figure 3; Table 3.1). It could have been expected that the larger tidal range in 2013 (Figure 2), would have led to more re-suspension and thus higher TSM values would have been observed, compared to those in 2012. However the reverse was observed with higher TSM values in 2012 possibly due to dredging activity at the time of the 2012 trip which had finished by the 2013 trip. Variation due to diurnal variation in winds and time of sampling in relation to ebb or flood tides could also have affected values at individual sites.

During both sampling periods, the composition of the TSM was dominated by the inorganic fraction, being always greater than 77% at all sites (Figure 3; Table 3.1).
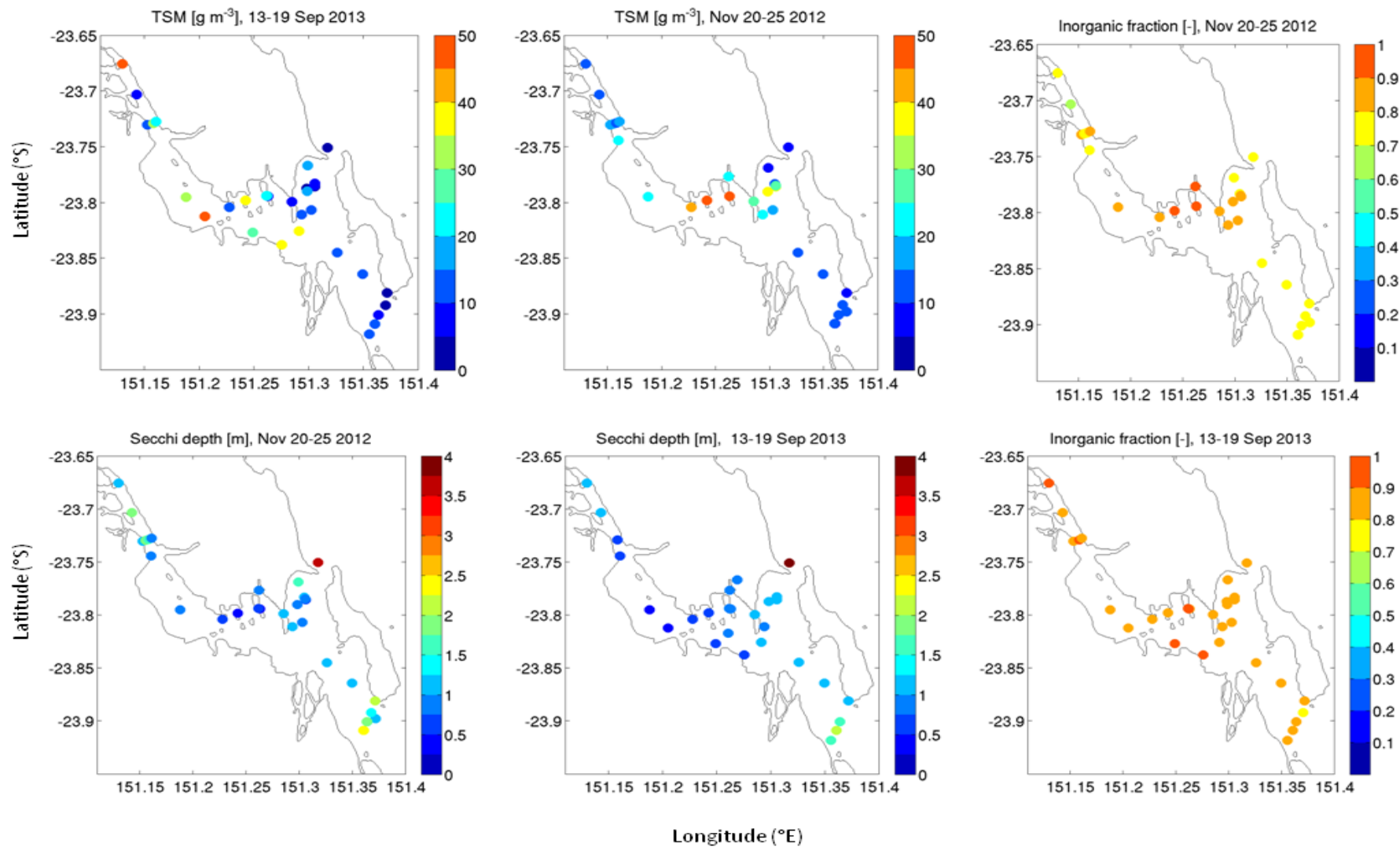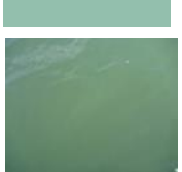
Figure 3 Plots of Secchi depth, TSM and % inorganic fraction for November 2012 (top row) and September 2013 (bottom row).

Table 3.1 Bio-optical parameter measurements at four sites within Gladstone Harbour.

Parameter	Site code			
	DCT2	WIT1	PBMT1	SFT2
	(Narrows)	(Central)	(Inside N. Ent)	(Inside S. Ent)
Secchi depth (m) - 2012	1.8	0.5	0.7	1.1
Secchi depth (m) - 2013	0.5	0.6	5.5	6.2
TSS (mg L^{-1}) – 2012	15.55	81.99	37.05	13.53
TSS (mg L^{-1}) – 2013	32.78	33.04	5.52	6.19
% Inorg. Fraction – 2012	77	91	88	77
% Inorg. Fraction – 2013	91	87	86	85
% Org. Fraction – 2012	23	9	12	23
% Org. Fraction – 2013	9	13	14	15
$a_d(440)$ (m^{-1}) - 2012	0.38	2.69	1.39	0.39
$a_d(440)$ (m^{-1}) - 2013	1.13	0.91	0.46	0.22
$a_{CDOM}(440)$ (m^{-1}) - 2012	0.75	0.34	0.34	0.25
$a_{CDOM}(440)$ (m^{-1}) - 2013	0.32	0.28	NR	0.15
$a_{ph}(440)$ (m^{-1}) - 2012	0.11	0.06	0.15	0.12
$a_{ph}(440)$ (m^{-1}) - 2013	<0.0001	0.01	0.02	0.04
Chlorophyll –a (mg m^{-3}) - 2012	2.56	2.63	4.75	3.21
Chlorophyll –a (mg m^{-3}) - 2013	1.25	1.62	1.46	0.81
Dominant algal species - 2012	Diatoms/ green algae	Diatoms/ green algae	Diatoms/ green algae	Diatoms/ green algae
Dominant algal species - 2013	Diatoms/ green algae	Diatoms/ green algae	Diatoms/ green algae	Diatoms/ green algae
Truecolour - 2012 (top measured by ac-s, below photographs of water where available).				
Truecolour - 2013 (measured by ac-s).				

3.3 Absorption properties

The extent to which the phytoplankton, detrital suspended matter (mineral material and heterotrophic microalgae) and the coloured dissolved organic matter (CDOM) absorb the light will determine what percentage of incident irradiance is available at any one depth.

Absorption (a) is an inherent optical property and therefore the total absorption is the sum of the absorption of the individual components, phytoplankton, detrital matter and CDOM within the water column. Total absorption of any water body can be expressed by

$$a(\lambda) = a_{ph}(\lambda) + a_d(\lambda) + a_{CDOM}(\lambda) + a_w(\lambda) \qquad \text{Eq. 3}$$

where a_{ph}, a_d, a_{CDOM} and a_w represent absorption due to phytoplankton, detrital matter, CDOM and water respectively. Values for a_w were taken from published results (Pope and Fry 1997), whilst values for the other absorption coefficients were determined by laboratory analysis (see methods section).

Values of the absorption coefficients a_{ph}, a_d and a_{CDOM} were determined spectrally between 350 and 800 nm; values were selected at 440 nm to compare the relevance of each component to the total absorption (Table 3.1). Over both sampling periods, a_d(440) values ranged from 0.22 m^{-1} (SFT2, 2013) to 2.69 m^{-1} (WIT1, 2012). As expected a_d(440) values follow the TSM trends and so all sites, except DCT2 in the Narrows had higher a_d(440) values in 2012 than 2013.

CDOM appears to be relatively constant with many of the a_{CDOM}(440) values being around 0.3 m^{-1} during both sampling periods (Figure 4, Table 3.1); the two exceptions were 0.15 m^{-1} (SFT2, 2013) and 0.75 m^{-1} (DCT2, 2012). These values imply that CDOM has less influence than the inorganic or mineral component of the TSM on the clarity of the water in Gladstone Harbour.
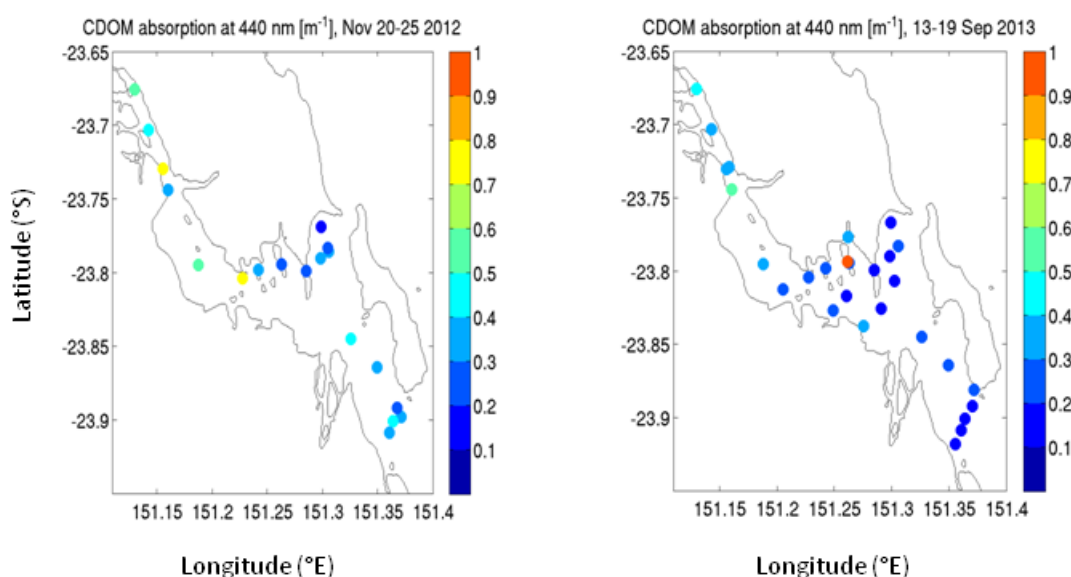
Figure 4 Absorption coefficient for CDOM at 440 nm (m^{-1}) for November 2012 (left) and September 2013 (right).

The $a_{ph}(440)$ values are retrieved by the difference between the total particulate and detrital measurements. In cases such as Gladstone Harbour where the detrital component is so dominant, it is hard to accurately retrieve the phytoplankton component. However the very low $a_{ph}(440)$ values at all sites (Table 3.1) does reflect the situation that due to the high TSM component and hence often shallow Secchi depth, light penetration will be shallow and consequently phytoplankton growth will be low.

3.4 Phytoplankton community composition and biomass as determined by pigment analysis

Pigment analysis is used to estimate algal community composition and concentration. Pigments which relate specifically to an algal class are termed marker or diagnostic pigments (Jeffrey and Vesk 1997; Jeffrey and Wright 2006). Some of these diagnostic pigments are found exclusively in one algal class (e.g. prasinoxanthin in prasinophytes), while others are the principal pigments of one class, but are also found in other classes (e.g. fucoxanthin in diatoms and some haptophytes; 19'-butanoyloxyfucoxanthin in chrysophytes and some haptophytes). The presence or absence of these diagnostic pigments can provide a simple guide to the composition of a phytoplankton community, including identifying classes of small flagellates that cannot be determined by light microscopy techniques. In this report we have based the description of the phytoplankton community composition on the pigments/algal groups listed in Table 2.

Both biomass and composition are represented in Figure 5 (see also Table 3.1); biomass is represented by the radius of the circle and the composition by the different coloured slices of the circle. Biomass was higher at all sites in 2012 compared to 2013, ranging from 1.62 times higher at WIT1 to 4 times higher at SFT2. The higher biomass in 2012 would have resulted from the lower TSM values and deeper Secchi depths recorded during this sampling period. However DCT2 in the

Narrows which had showed reverse trends in both TSM and Secchi depth to the other sites (i.e. lower TSM values and deeper Secchi depths in 2013) also had more biomass in 2012. During both sampling periods, the phytoplankton community composition, as indicated by the pigment composition, was dominated primarily by diatoms (fucoxanthin), but forms of green algae (Chl-b, prasinoxanthin) were also present.

Table 3.2 Biomarker pigments and the algal groups they represent.

Pigment name	Abbreviation	Algal group
Peridinin	Perid	Dinoflagellates
19'-butanoyloxyfucoxanthin	But-fuco	Chrysophytes
Fucoxanthin	Fuco	Diatoms
19'-hexanoyloxyfucoxanthin	Hex-fuco	Haptophytes
Prasinoxanthin	Pras	Prasinophytes
Alloxanthin	Allo	Cryptophytes
Zeaxanthin	Zea	Cyanophytes
Chlorophyll b	Chl b	Green algal groups
Divinyl chlorophyll a	DV chl a	Prochlorophytes

During the 2013 sampling period sites outside of Gladstone Harbour (SCD1, OF1 and OF2) (Figure 1b) were sampled and the phytoplankton composition at these sites was dominated by cyanobacteria (zeaxanthin). Within the harbour the size class of phytoplankton would be nano (2-20 μm) to microplankton (>20 μm), whilst outside the harbour the sites are more influenced by Coral Sea water moving on to the shelf and are dominated by the smallest size class – picoplankton (<2 μm).
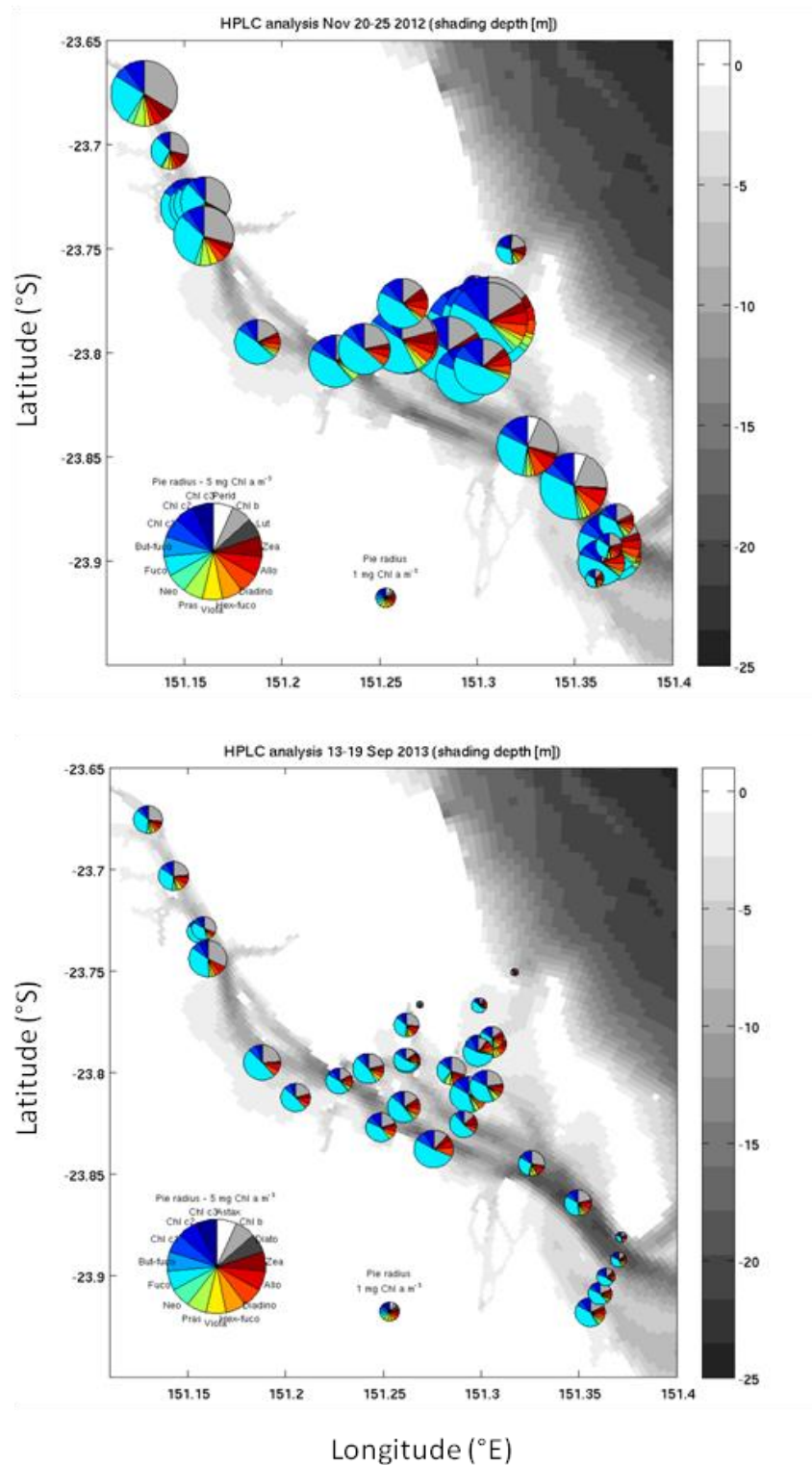
Figure 5 The pigment composition for surface water samples, 20-25 November 2012 (left) and 13-19 September 2013 (right). The radius of the pie quantifies total Chl a concentration, and the slice area gives the relative concentration of the accessory pigments. Pigments are: Chl c3 (chlorophyll-c3); Chl c2 (chlorophyll-c2); Chl c1 (chlorophyll-c1); But-fuco (19'-butanoyloxyfucoxanthin); Fuco (fucoxanthin); Neo (neoxanthin); Pras (prasinoxanthin); Viola (violaxanthin); Hex-fuco (19'-hexanoyloxyfucoxanthin); Diadino (diadinoxanthin); Allo (alloxanthin); Zea (zeaxanthin); Lut (lutein); Diato (diatoxanthin); Chl b (chlorophyll-b); Astax (astaxanthin); Perid (peridinin).

3.5 Spectrally-resolved absorption and scattering

The ac-s measures absorption, a, and attenuation, c, from which total scattering can be determined. In November 2012, total attenuation at 400 nm reached a maximum of almost 60 m^{-1} at site COM1 and WIT1 (central harbour). This extreme attenuation was due mostly to scattering with absorption being 1-2 orders of magnitude lower. The colour of these waters is brown (colouring in Figure 6), illustrating that resuspended inorganic fine sediment was primarily responsible for the optical properties at WIT1. Sites with greater marine influences, such as SFT1-4 (inside southern entrance) had lower total scattering. As a result absorption played a greater role, and the water colour at these sites appeared 'greener'.

The September 2013 observations were similar to those of November 2012, although a few observations were closer to those expected for marine waters, which resulted in less scattering in some sites with greenish coloured waters.

The observations at sites shown in Figure 6 and Figure 7 have been replotted, using the true colouring, on a map of Gladstone Harbour (Figure 8). The more pronounced differences in water colour were evident in September 2013 as a result of a stronger tidal differences in which caused a greater change in scattering.
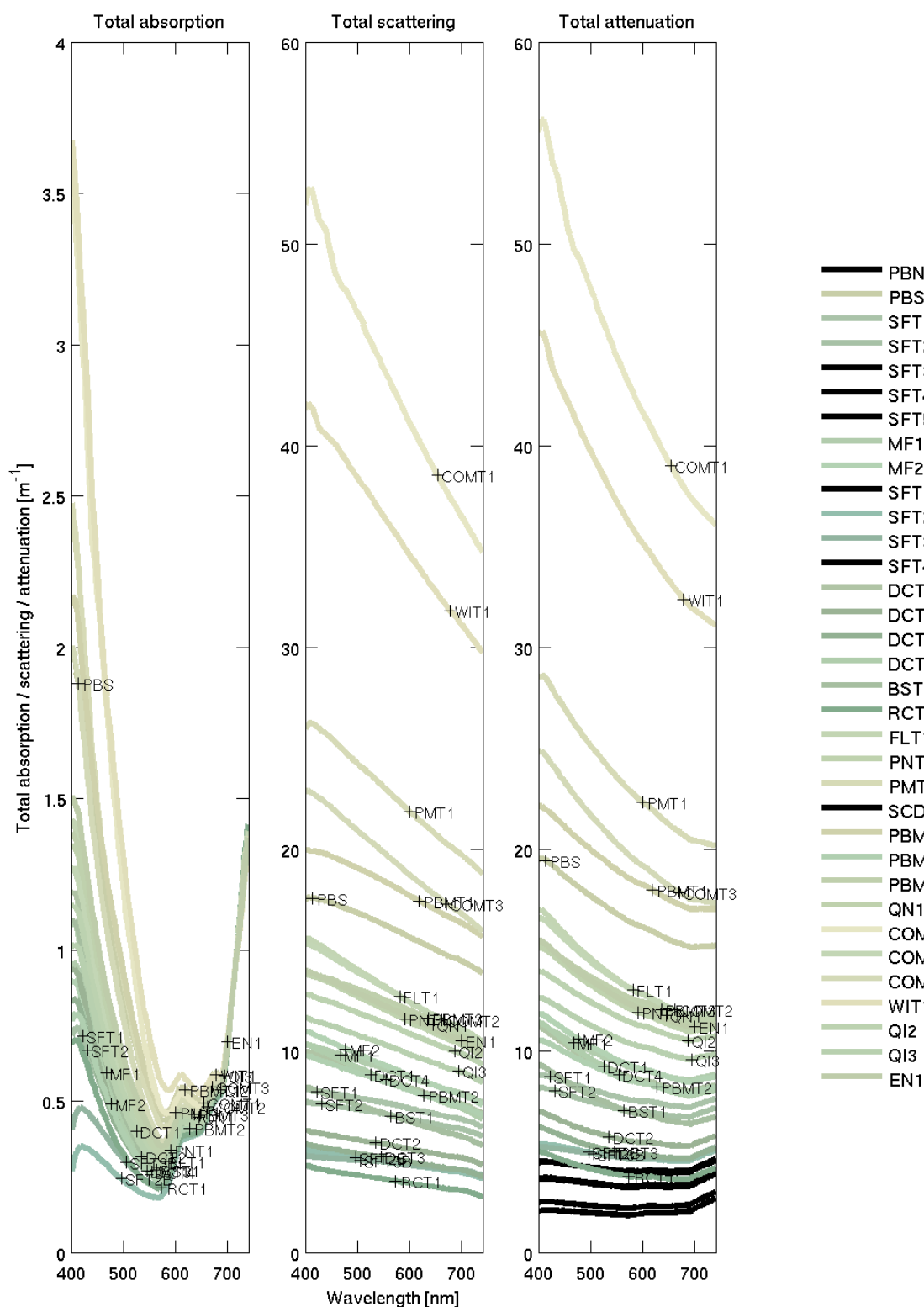
Figure 6 Inherent optical properties at sample sites on 20-25 November 2012. The line colour is rendered using the intensity of *in situ* reflectance at the red (645 nm), green (555 nm), and blue (470 nm) given by 0.03 b_λ / (a_λ + 0.03 b_λ), and scaled using the MODIS true colour brightening. Black lines were excluded due to poor data. The site labelling is ordered in time, from the first sample collected during neap tides at the top, to the last sample collected at spring tides on the bottom.
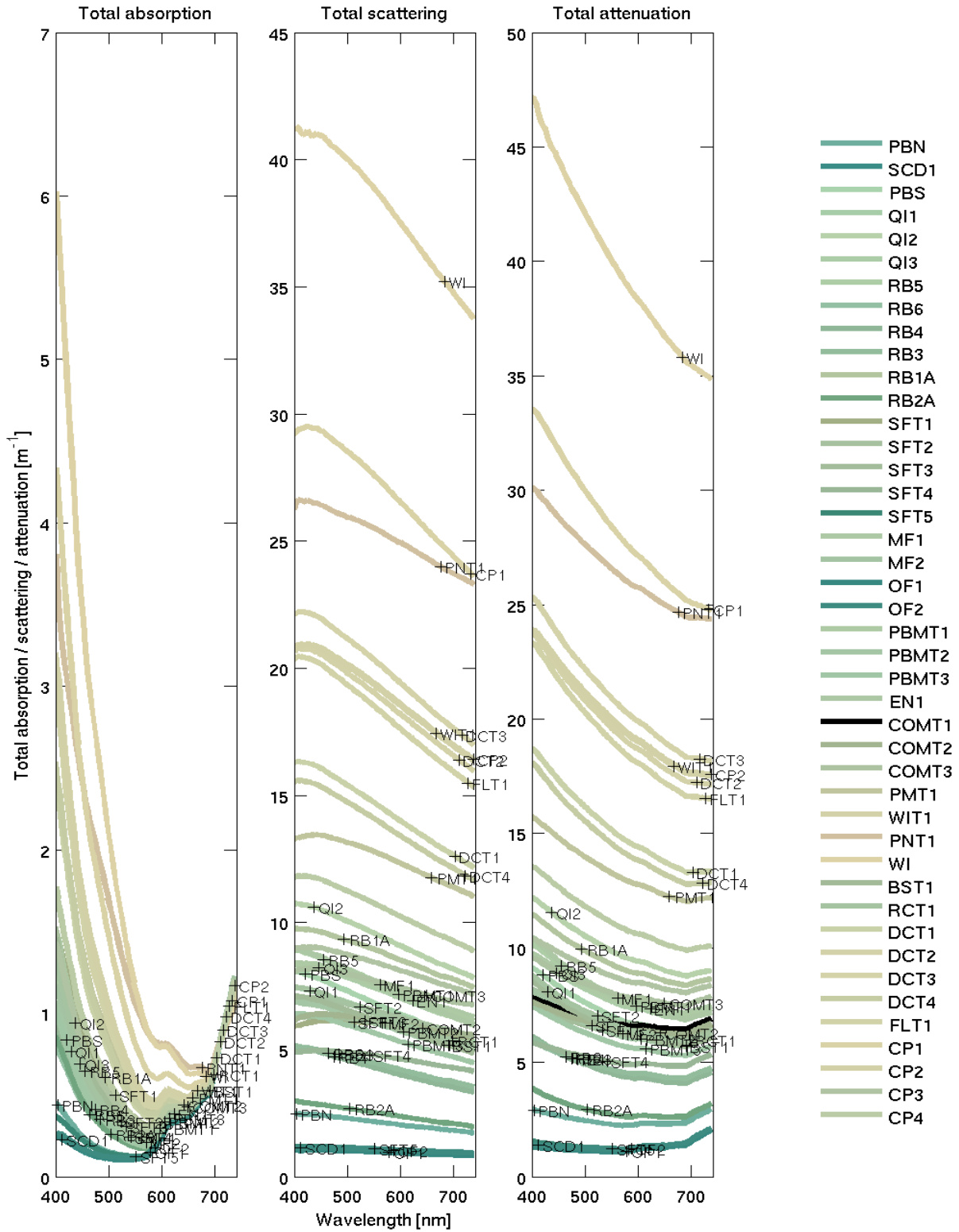
Figure 7 Inherent optical properties at sample sites on 13-19 September 2013. The line colour is rendered using the intensity of *in situ* reflectance at the red (645 nm), green (555 nm), and blue (470 nm) given by 0.03 b / (a + 0.03 b), and scaled using the MODIS true colour brightening. The site labelling is ordered in time, from the first sample collected during neap tides at the top, to the last sample collected at spring tides on the bottom.
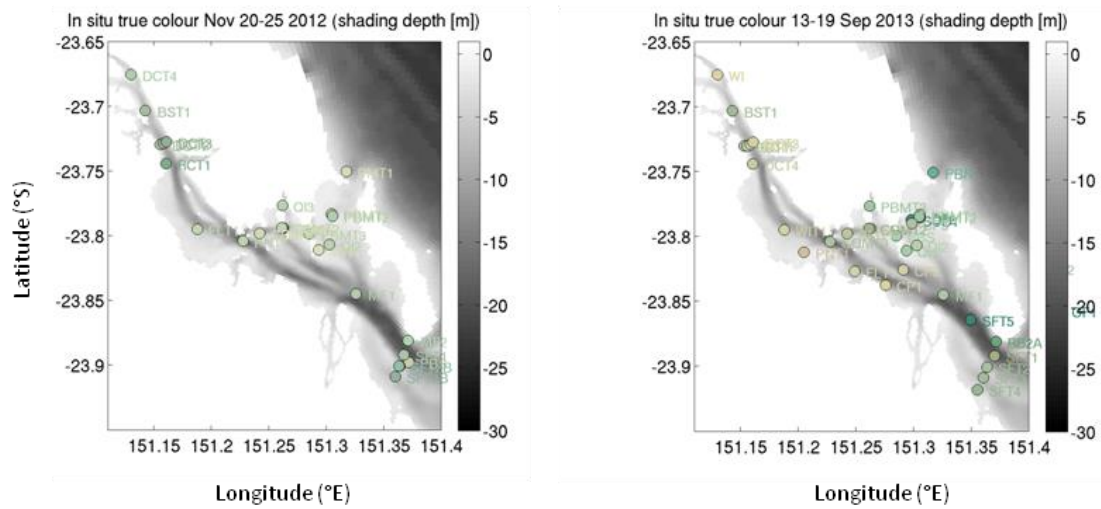
Figure 8 True colour of samples sites 20-25 November 2012 (left) and 13-19 September 2013 (right). The marker colour rendered is the same as the line colour in Figure 6 and Figure 7, based on reflectance calculations and MODIS true colour brightening.

3.6 Applications of optical observations for numerical modelling.

The optical data detailed in this report are important for the modelling of coastal waters in both the modelling component of the GISERA project. Specifically, the observations at WIT1 in November 2012 have been used as an end-member for the optical parameterisation of the mass-specific absorption and total scattering coefficients of fine sediments. Superimposing the observations on a reflectance vs. total suspended matter (TSM) plot (Figure 9) shows that for a given TSM concentration, the observations lie close to a global relationship (Miller and McKee 2004), as well as a local relationship found for Gladstone Harbour (C. Petus pers. comm.), with site WIT1 (black circle) being close to both relationships. This result provides confidence in both the use of WIT1 as an end-member for terrestrial-sourced fine sediments in the optical model parameterisation, as well as the calculations for converting an *in situ* ratio of backscattering over absorption plus backscattering, *u*, to a remotely-sensed reflectance, R_{rs} (Equations in Section 2.4.2).
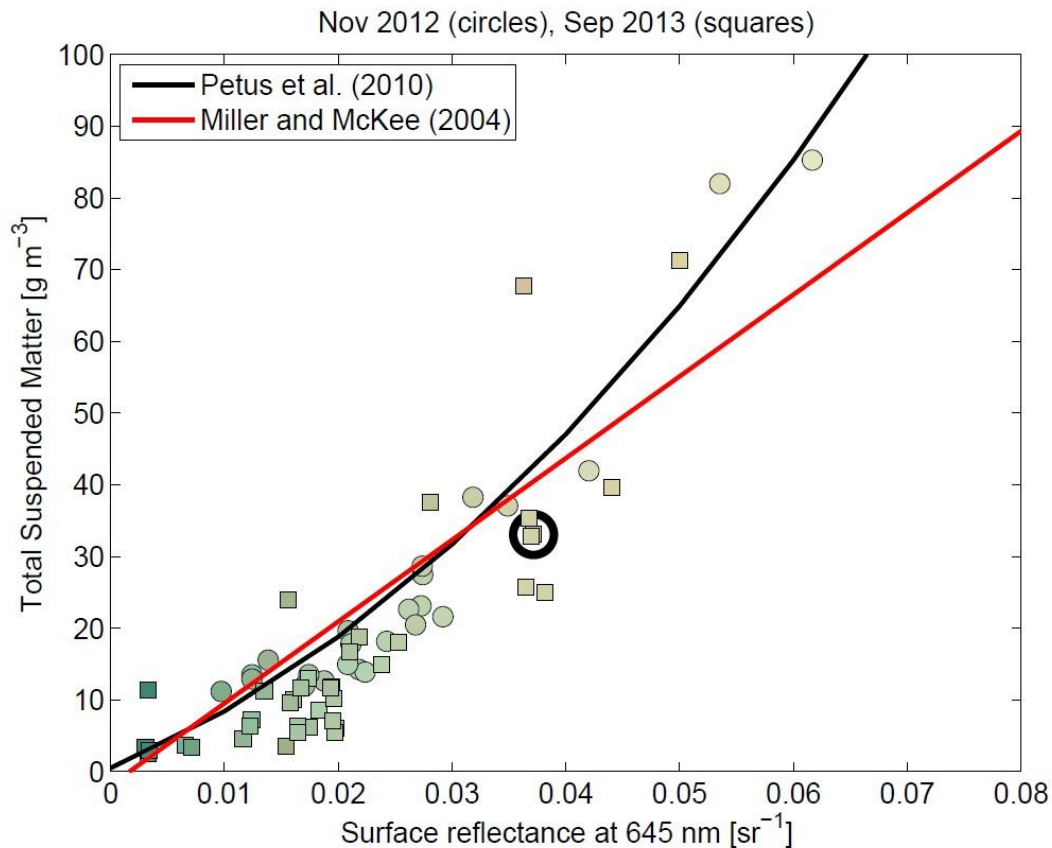
Figure 9 Comparison of reflectance calculated at a range of concentrations of total suspended matter and algorithms used to infer TSM from reflectance at the global scale (Miller and McKee 2004) and for Gladstone Harbour (C Petus pers. comm.). The black circle is centred on the data point used (WIT1, November 2012) that was used as an end-member for the optical model parameterisation of suspended inorganic sediments.

The spectrally-resolved optical model, in collaboration with eReefs, has been critical in developing surface reflectance as a model output. This allows direct comparison of model output with remotely-sensed observations, as well as the use of sophisticated data assimilation of remotely-sensed observations.

The spectrally-resolved optical model allows a synoptic analysis of coastal water quality during periods when remotely-sensed observations are not possible, for example during extreme weather events (Figure 10). The production of simulated true colour images, showing the impacts of sediments, CDOM, bottom reflectance and phytoplankton in one image, is only possible with the calculation of surface reflectance in the red, green, and blue bands, a model innovation developed in part in this project.

The improved confidence in the performance of the model in terms of water column optical properties also means increased confidence in the performance of the model for predicting benthic processes such as seagrass growth (Chapter III).

Gladstone Harbour, eastern Australia

Simulated true color 01-Nov-11 00:00

Elevation 0.643m

SWR 0.63011 W m^{-2}

Gladstone Harbour, eastern Australia

Simulated true color 01-Nov-11 14:00

Elevation 1.1037m

SWR 1.0816 W m^{-2}
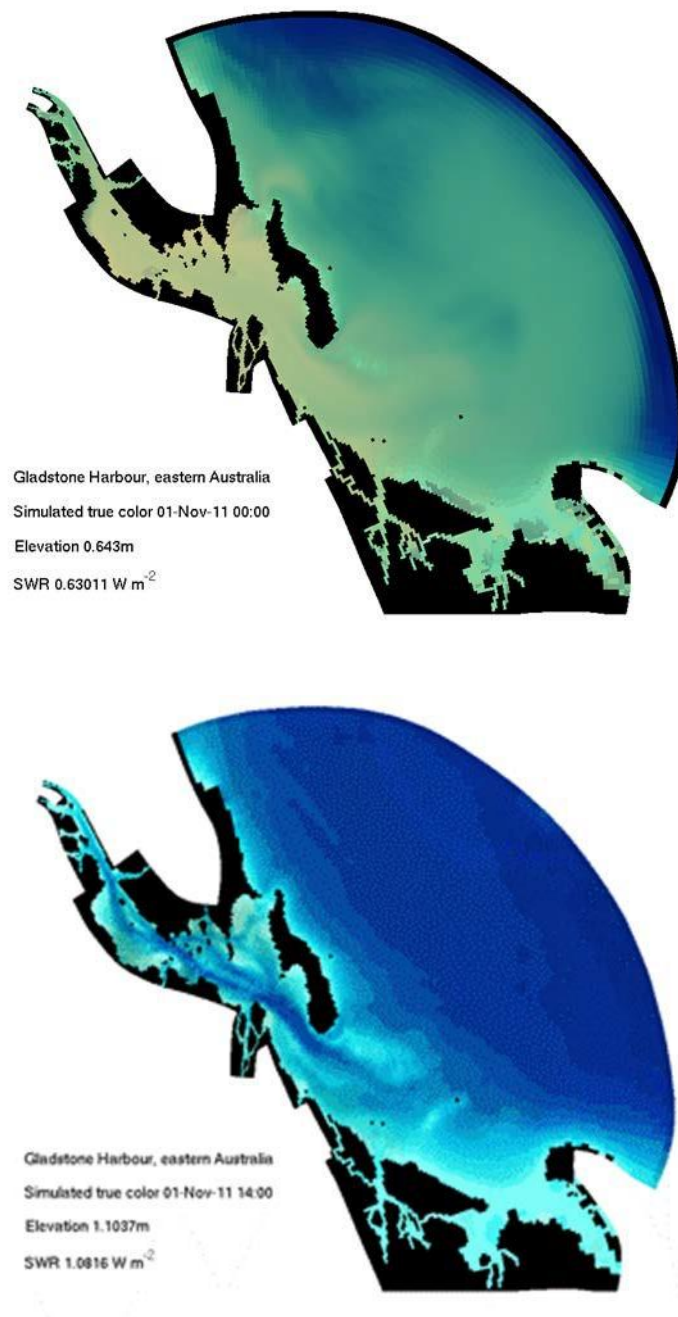
Figure 10 Gladstone Harbour model outputs of water column simulated true colour January (top) and November (bottom) 2011. Simulated true colour is calculated based combining the surface reflectance in the red, green and blue bands. The most significant difference between the two images is the greater CDOM absorption in January compared to November.

3.7 Summary

These results indicate that the variation in optical properties between the sampling periods of November 2012 and September 2013 was less than the variation in space during each sampling period. Some of this spatial variability will be confounded by the time it took to do the sampling (approx. 1 week), nonetheless, the September 2013 sampling was generally undertaken during stronger tidal action, and this is reflected in the mean optical properties.

During both field campaigns, the dominant component of the total absorption was the detrital or non-algal component, being greater than 70% of total absorption in the central region of the harbour. This component was greater than 77% inorganic material at all sites. CDOM was also a significant contributor to the total absorption coefficient and, because of the high particulate and CDOM loadings, light penetration in the water column was low resulting in low phytoplankton biomass. Diatoms were the dominant algal group at all sites within the harbour. Interestingly, although the September 2013 results showed lower particulate and CDOM loadings than the November 2012 results, the phytoplankton biomass, as indicated by chl-a is lower in 2013. This is likely due to the time of year; the September 2013 samples were probably collected prior to the spring bloom while the November 2012 samples were collected during a late spring bloom.

These two sets of data are snapshots in time of the variability in optical parameters within and around Gladstone Harbour. Models developed using these data together with satellite remote sensing estimates of parameters will extend our knowledge of Gladstone Harbour on larger spatial and more frequent temporal scales.

The observations of water quality parameters provided here constitute a key step for GISERA in developing a verifiable biogeochemical model of Gladstone Harbour. They can be used for validation purposes in their own right, but more importantly they form the link between modelling, point observations made in the field, and synoptic broad scale observations of water quality parameters provided by remote sensing platforms. Water quality in turn is a key factor influencing seagrass growth, therefore these observations are integral to the broader goals of GISERA in developing a reliable seagrass growth model for Gladstone Harbour.

Chapter II Port Curtis Seagrass Distribution

Elisabetta Morello, Russ Babcock, Mick Haywood, Gary Fry, Rob Kenyon, Sabina Perkins, Karl Forcey

1 Introduction

Seagrasses dominate many of the inter-reef, soft-bottom and nearshore habitats of the Great Barrier Reef (GBR) region and are often particularly conspicuous in semi-protected embayments of the Queensland coast (Coles et al 2014). These areas are important for a variety of reasons including their value to fisheries (both commercial and recreational), as nursery areas, as for the fact that they support a range of iconic megafauna such as dugong, turtles and dolphins (Stoeckl et al. 2011). Seagrass ecosystems are increasingly recognised both globally and within Australia (Coles et al. 2014) for their economic value (Costanza et al. 2014), their productivity (Rasheed et al. 2008a) and their role as carbon sinks (Macreadie et al. 2014). Seagrasses are an important food source for threatened species such as turtle and dugong (Valentine and Duffy 2006).

Seagrass communities face an array of threats due to human activities ranging from coastal development to climate change that are occurring at an unrelenting pace in coastal ecosystems globally (Orth et al. 2006). The seagrass beds of the GBR region are not immune to these pressures, and despite implementation of a range of management measures to protect seagrasses in GBR coastal areas there have been declines in seagrass cover across a range of habitats (Coles et al. 2014). A wide range of threatening processes are implicated in these declines however the most precipitous decline in seagrasses since 2006 has been linked to extreme weather events (flooding and cyclones) which are likely to have acted synergistically with other long term changes in coastal sediment loads and water quality (Coles et al. 2014). Analysis of expert assessments of threatening processes for seagrasses globally found that, in the Indo-Pacific (including the GBR), port and infrastructure development was considered to have the highest impact, followed by agricultural runoff, trawling and dredging (Grech et al 2012). On the GBR, runoff from various sources is thought to be generally more important than direct coastal development and dredging (Grech et al. 2011), however it was acknowledged that in port areas this ranking was likely to be reversed.

Given the growing threats to seagrasses, and their continued decline, it is essential that managers are provided with up to date information on the status of seagrass beds as well as improved understanding of the environmental requirements of seagrass. In this regard Queensland and the Great Barrier Reef World Heritage Area (GBRWHA) are fortunate in that several long term monitoring programs for seagrass do exist (McKenzie et al. 2000, 2001, 2014; Rasheed and Unsworth 2011) and the areas monitored include the Gladstone region (Bryant and Rasheed 2013; Bryant et al. 2013), site of the most recent and largest port infrastructure upgrade on the east coast of Queensland, and focus of the current GISERA Marine project.

Managing the coastal environmental assets of the greater Gladstone Port and Port Curtis presents considerable challenges given that it is adjacent to the GRBWHA, including the Rodds Bay Dugong Sanctuary on its southern border, and is one of Australia's busiest industrial ports. Despite this fact, the region has until recently held very extensive seagrass beds (Bryant et al. 2013), as well as populations of dugong and turtles. Although flatback turtles have major nesting areas on the eastern beaches of islands such as Curtis and Facing Islands in Port Curtis, green turtles are the most common species in the harbour (Limpus et al. 2013), feeding on seagrass, macroalgae and mangroves. Green turtles also comprised the majority of turtles stranded in Port Curtis including

during 2011, which was a year of severe flooding on the Queensland coast, when there was a spike in the number of strandings recorded (Limpus et al. 2012; Meager and Limpus 2012). Many of the turtles stranded at this time had poor body condition (Limpus et al. 2012), indicating a likely reduction in available food. Large declines in seagrass biomass were also recorded in Port Curtis at this time (Bryant and Rasheed 2013) as well as at Rodds Bay (suggesting that declines in seagrass were related to weather events rather than port related activities).

Monitoring, predicting and managing the impacts of water quality and its interactions with key ecosystem components such as seagrasses and corals, as well as with higher trophic level members of coastal ecosystems, will increasingly rely on modelling such as the Gladstone seagrass model (Chapter III) and eReefs, that can integrate large amounts of data over significant areas, such as the GBRWHA (Schiller et al. 2014). One benefit of such models is that they make large amounts of data much more easily interpretable and accessible but underpinning this they rely on monitoring and other data for validation and calibration, which ensures the validity of model predictions and scenarios. Currently models such as eReefs are predominantly physical models but increasingly they will be able to incorporate biological as well as physical and chemical processes, similar to the GISERA Gladstone seagrass model. GISERA Marine seagrass modelling has made significant contributions to the development of such modelling in eReefs allowing simulations and predictions of seagrass responses to altered water quality. Models of seagrass growth also have terms for grazing/mortality (Chapter III), consequently information on the distribution of higher level organisms can also be linked to seagrass growth. Conversely the distribution of seagrass will also influence factors such as the habitat use and home range size of grazing animals such as turtles and dugong.

The seagrass component of GISERA Marine was designed to complement existing seagrass monitoring of the cover, biomass and extent of seagrass beds conducted through the Western Basin Project and as part of the Gladstone Port's long term seagrass monitoring objectives. Seagrass depth range has been found to be a sensitive indicator of water quality parameters such as light attenuation coefficient, total suspended solids, chlorophyll *a,* total Kjeldahl nitrogen (Abal and Dennison 1996) and our observations specifically focused on measurements to determine the maximum depth of the seagrass bed margin at known seagrass beds in Port Curtis and Rodds Bay. These observations, conducted in 2012 and 2013, were designed to help parameterise the seagrass growth model (Chapter III) ensuring a realistic depiction of potential seagrass growth in Port Curtis. A more detailed survey of Pelican Banks was conducted in 2014 in order to map seagrass cover and biomass in relation to the distribution and habitat use of the tagged green turtle population on the banks, so that we might better correlate turtle habitat use and seagrass distribution.

2 Methods

2.1 Seagrass depth-range sampling 2012 & 2013

2.1.1 YEAR 1: 20–27 NOVEMBER 2012

<u>Sites</u>

Based on the locations of seagrass beds described in previous studies we established 25 sampling sites in Gladstone Harbour (Table 2.1, Figure 11). These sites were classified according to their location within the harbour: "inner", "mid" and "lower" harbour. Sites generally consisted of a transect that crossed the boundary of the seagrass bed's historical extent (Thomas et al. 2010) with samples being taken at 0.1m depth intervals along each transect.

<u>Physical variables recorded</u>

The following information and parameters were recorded at every site:
- Latitude and longitude
- Time
- Depth
- Conductivity and Temperature at the surface and on the bottom, using a Hydrolab Quanta meter
- pH
- Secchi disc depth

Additional physical and optical variables were also collected during the same research trip from another vessel (Chapter I). In this section we report the results of the depth profiles collected at Pelican Banks North using a YSI 6-Series Multiparameter Sonde (Model 6600 V2), recording the following additional parameters:
- Photosynthetically Active Radiation (PAR1 and PAR2)
- Turbidity
- Chlorophyll a
- Blue green algae
- Dissolved oxygen (%)

Depths were adjusted for tide height according to the date and time of the day (rounded to the nearest hour) and are reported as height above datum (Ht, m).

<u>Seagrass biomass</u>

Seagrass biomass was sampled from the RV Julius at 22 of the 25 sites (Figure 11)
The samples were collected using 2 different quantitative methods:
- (i) A van Veen grab: the grab sampled an area of 0.034 m^2 and 7 replicates were taken per site, and
- (ii) A corer: the corer was 15 cm in diameter covering an area of 0.01767 m^2. Seven replicates were taken per site.

Each replicate was bagged and labelled separately, and taken back to the lab for sorting.

Table 2.1 Details of the 26 sites sampled for seagrass in November 2012 with an indication of their location within the harbour and the type of sampling carried out. Notes: B = biomass sampling, DR = depth range sampling, T/C = temperature and conductivity, + = sampled, - = not sampled.

Site name	Latitude	Longitude	Location in harbour	B	DR	Secchi	T/C
Black Swan (BS)	-23.6755	151.1273	Inner	+	-	+	+
Redcliffe (RC1)	-23.70218	151.13666	Inner	+	+	+	+
Redcliffe new (RCnew)	-23.70093	151.13331	Inner	-	+	+	+
Duff Creek (DC1)	-23.7171	151.1591	Inner	+	+	+	+
Graham's Creek (GC1)	-23.7233	151.2229	Inner	+	+	+	+
Graham's Creek (GC2)	-23.7228	151.2240	Inner	-	+	-	-
Fisherman's landing (FL)	-23.7442	151.1602	Inner	-	+	+	+
Wiggins Island 1 (WI1)	-23.81	151.2144	Inner	+	-	+	+
Wiggins new (WInew)	-23.81653	151.20254	Inner	-	+	+	+
Compigne Island (CI)	-23.78322	151.26041	Mid	-	+	+	+
Pelican Banks North (PBN)	-23.7658	151.303	Mid	+	+	+	+
Pelican Banks South (PBS)	-23.7904	151.2985	Mid	+	+	+	+
Facing Island new (FInew)	-23.7905	151.3071	Mid	+	+	+	+
North Banks 1 (NB1)	-23.80447	151.29253	Mid	+	-	+	+
North Banks 2 (NB2)	-23.80934	151.29778	Mid	+	-	+	+
North Banks 3 (NB3)	-23.8121	151.2937	Mid	+	-	+	+
Shoal Bay 1 (SB1)	-23.82956	151.34348	Lower	+	-	+	+
Shoal Bay 2 (SB20	-23.82763	151.34468	Lower	+	-	+	+
South Trees 1 (ST1)	-23.8653	151.324	Lower	+	-	+	+
South Trees 2 (ST2)	-23.8695	151.3243	Lower	+	-	+	+
Boyne Island 1 (BI1)	-23.8755	151.3266	Lower	+	-	+	+
Boyne Island 2 (BI2)	-23.88639	151.32989	Lower	+	+	+	+
Boyne Island 3 (BI3)	-23.89398	151.33261	Lower	+	+	+	+
Boyne Island 4 (BI4)	-23.9012	151.3348	Lower	+	-	+	+
Boyne Island 6 (BI6)	-23.9084	151.3404	Lower	+	+	+	+
Seal Rocks (SL)	-23.9633	151.4814	Lower	+	-	+	+

Figure 11 Sites sampled for seagrass depth range and biomass in November 2012.

In the lab, the seagrass samples were sorted according to species and for each species the following measures were recorded:

    (i)   Total above ground (shoot) and below ground (root) wet weight (g)

    (ii)   Total above ground (shoot) and below ground (root) dry weight (g): this was obtained by drying the samples at 70°C overnight

    (iii)   Number of shoots (No shoots·m^{-2})

    (iv)   For each species the following leaf measurements were measured using a maximum of ten shoots selected randomly:

        -   Leaf length (mm)

        -   Leaf width (mm)

        -   Petiole length (where applicable)

Mean biomasses (g. m^{-1}) were derived from these measurements for above-ground and below-ground components as well as for wet and dry weights. Mean shoot densities (shoots m^{-2}) and mean leaf surface areas were calculated for each sample. For *Zostera muelleri* and *Halodule uninervis* area was calculated using leaf length and width, assuming the leaf was a rectangular shape, while for *Halophila* spp. calculations were based on an elliptical shape.

Seagrass depth ranges

At 12 sites with lower levels of suspended sediment (Table 2.1), the depth range of seagrass was recorded using a drop camera which was cabled to a power supply and video monitor at the surface. Thus, at each site the drop camera was lowered at constant distance intervals from inshore to offshore and the presence or absence of seagrass was recorded. Figure 12 shows the depth range stations sampled at the Boyne Island 6 site.
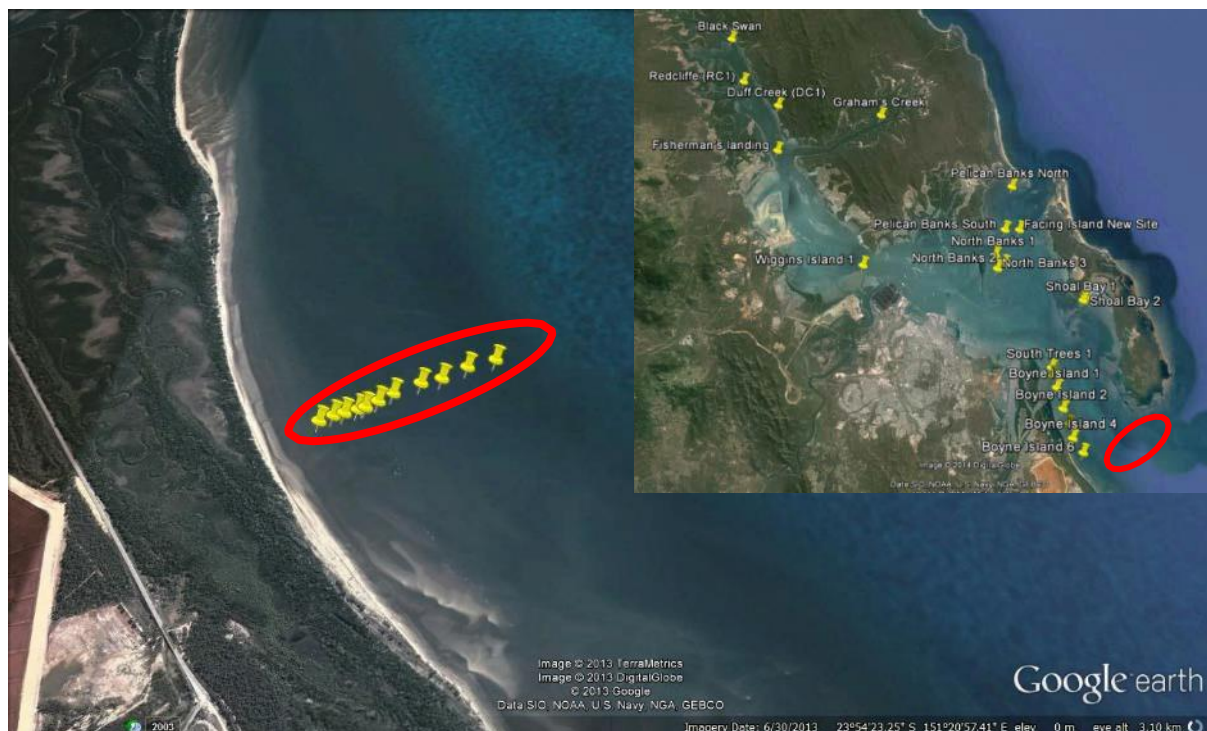
Figure 12 An example of the depth range stations viewed with the drop camera at Boyne Island 6, showing its location in Gladstone Harbour.

2.1.2 YEAR 2: 12–19 SEPTEMBER 2013; 9 NOVEMBER 2013

<u>Sites</u>

Forty-one sites from 17 areas (Figure 13) were sampled between 12 and 19 September 2013, for a total of 621 stations (Figure 13, Table 2.2). An additional 63 stations were sampled in Rodds bay on 9 November 2013 (Figure 13, Table 2.2).
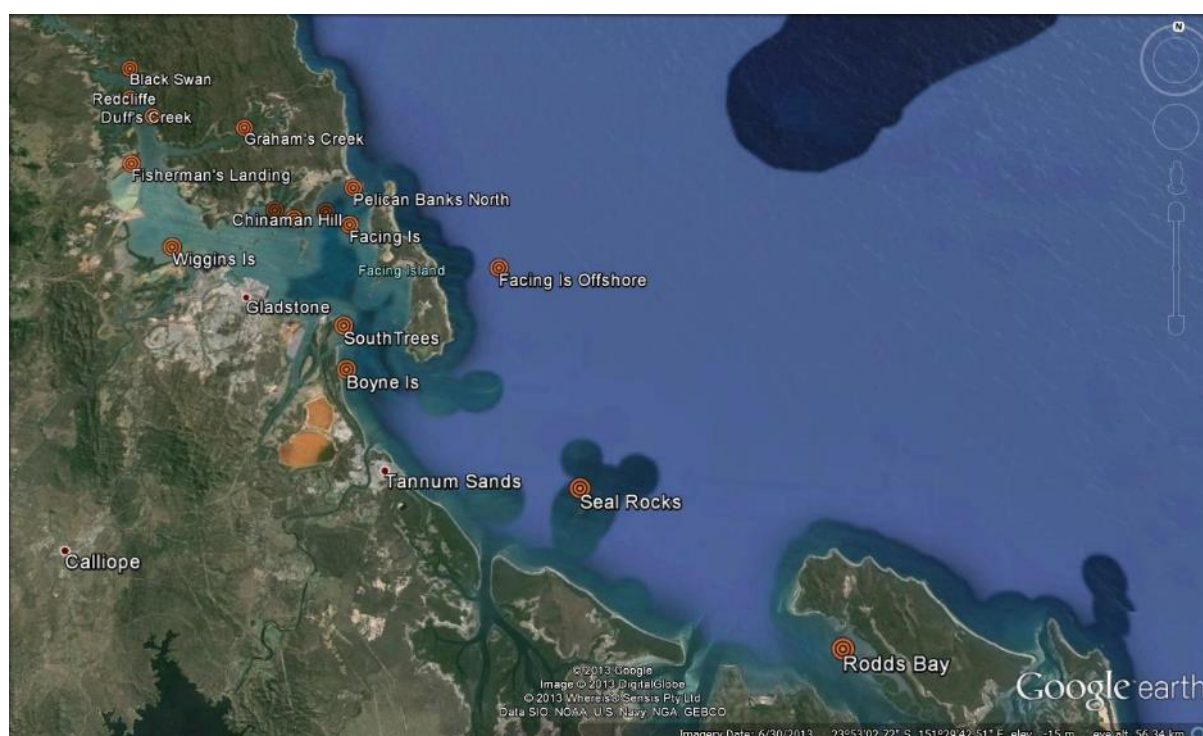
Figure 13 Areas sampled for seagrass depth ranges in September and November 2013

<u>Physical variables recorded</u>

The following information and parameters were recorded at every site:
- Latitude and longitude
- Time
- Depth
- Secchi disc depth

Depths were adjusted for tide height according to the date and time of the day.

<u>Seagrass depth ranges</u>

At all 41 sites (Table 2.2), the depth range of seagrass was recorded using the drop camera. Thus, at each site the drop camera was lowered at constant distance intervals from inshore to offshore and the presence or absence of seagrass was recorded. At each depth range transect where seagrass was recorded, a Naturaliste dredge (dimensions of the frame of the dredges used: small – 0.19 m x 0.44 m, large – 0.2 m x 0.6 m) was towed to obtain a seagrass sample for species identification purposes. Where the water was too shallow to use either of the dredges, a shovel was used (dimensions: 0.2 m x 0.3 m). Each sample was bagged and labelled separately and returned to the lab.

Table 2.2 Depth range sampling sites, September and November 2013.

Site	Latitude	Longitude	Date - Time	No. stations
Black Swan (BS)	-23.67676	151.126004	19/09/2013 10:38	16
Redcliffe 1 (RC1)	-23.703041	151.134005	19/09/2013 9:46	11
Redcliffe new (RCnew)	-23.700897	151.131819	19/09/2013 10:06	9
Duff Creek (DC)	-23.716254	151.158668	19/09/2013 9:04	13
Graham's creek 1 (GC1)	-23.722755	151.222815	17/09/2013 8:57	7
Graham's creek 2 (GC2)	-23.723319	151.222062	17/09/2013 9:16	10
Graham's creek 3 (GC3)	-23.722434	151.224182	17/09/2013 9:51	6
Graham's creek 4 (GC4)	-23.721439	151.226474	17/09/2013 10:11	9
Graham's creek 5 (GC5)	-23.723617	151.221383	17/09/2013 10:33	10
Fisherman's landing (FL)	-23.756566	151.152169	19/09/2013 8:09	16
Wiggins Is 1 (WI1)	-23.823983	151.201091	17/09/2013 6:48	19
Wiggins Is 2 (WI2)	-23.821035	151.185487	19/09/2013 6:47	20
Compigne Is W. 1 (CI1)	-23.781864	151.254804	13/09/2013 15:04	5
Compigne Is W. 2 (CI2)	-23.782482	151.25532	13/09/2013 15:39	5
Compigne Is W. 3 (CI3)	-23.783927	151.255126	13/09/2013 15:53	6
Compigne Is W. 4 (CI4)	-23.78529	151.255574	13/09/2013 16:16	6
Compigne Is. E. 5 (CI5)	-23.78663	151.26075	17/09/2013 8:45	8
Compigne Is. E. 6 (CI6)	-23.782037	151.261236	16/09/2013 11:52	6
Chinaman Hill (CH)	-23.79103	151.27838	17/09/2013 9:43	9
Pelican Banks North 1 (PBN1)	-23.766475	151.306889	13/09/2013 11:39	20
Pelican Banks North 4 (PBN4)	-23.773865	151.313601	18/09/2013 9:40	24
Pelican Banks North 5 (PBN5)	-23.765853	151.315003	18/09/2013 11:01	19
Pelican Banks South 1 (PBS1)	-23.788039	151.299442	16/09/2013 6:30	12
Pelican Banks South 2 (PBS2)	-23.785796	151.288067	16/09/2013 7:13	22
Facing Is. New (FInew)	-23.787963	151.30412	16/09/2013 8:39	14
Facing Is. 2 (FI2)	-23.795735	151.300571	18/09/2013 8:20	17
Facing Offshore (FO)	-23.82433	151.40392	16/09/2013 8:50	46
North Banks 1 (NB1)	-23.804508	151.29085	16/09/2013 10:53	9
North Banks 3 (NB3)	-23.810939	151.290419	16/09/2013 9:57	10
North Banks 4 (NB4)	-23.813639	151.293776	18/09/2013 7:21	32
South Trees 1 (ST1)	-23.865505	151.324014	15/09/2013 7:29	13
South Trees 2 (ST2)	-23.869166	151.326468	15/09/2013 8:32	8
Boyne Is. 1 (BI1)	-23.87466	151.327714	15/09/2013 9:02	10
Boyne Is. 2 (BI2)	-23.884366	151.329043	15/09/2013 9:52	15
Boyne Is. 2parallell (BI2par)	-23.88562	151.329857	15/09/2013 11:05	6
Boyne Is. 3 (BI3)	-23.894116	151.332115	15/09/2013 11:22	13
Boyne Is. 4 (BI4)	-23.901439	151.334045	15/09/2013 11:54	13
Boyne Is. 5 (BI5)	-23.908566	151.338697	15/09/2013 12:25	14

Site	Latitude	Longitude	Date - Time	No. stations
Seal Rocks (SR)	-23.9003	151.3846	15/09/2013 7:39	27
Rodds Bay 1A (RB1 A)	-24.061605	151.648347	14/09/2013 12:53	12
Rodds Bay 2A (RB2 A)	-24.075824	151.644383	14/09/2013 12:18	9
Rodds Bay 3 (RB3)	-24.025832	151.629888	14/09/2013 11:27	13
Rodds Bay 4 (RB4)	-24.020661	151.622218	14/09/2013 10:23	17
Rodds Bay 5(RB5)	-24.039751	151.604772	14/09/2013 7:54	18
Rodds Bay 6 (RB6)	-24.034615	151.573325	14/09/2013 9:05	17
Rodds Bay 7 (RB7)	-24.076449	151.658004	9/11/2013 8:57	63

2.2 Seagrass fine-scale distribution 2014

2.2.1 BACKGROUND

The seagrass at the Pelican Banks meadow is approximately 8.6 km^2 and the Facing Island meadow is ~ 4.4 km^2 (shapefile of seagrass extent provided by Len McKenzie JCU   TropWater; Gladstone_Composite_Seagrass_Dist_2002_2011.shp). There are two sets of overlaying polygons in almost every seagrass bed. One of these represents the survey done in 2011 (based on the shapefile name) while the other overlying polygons (the larger of the two in Figure 14) represent the seagrass extent in 2002.
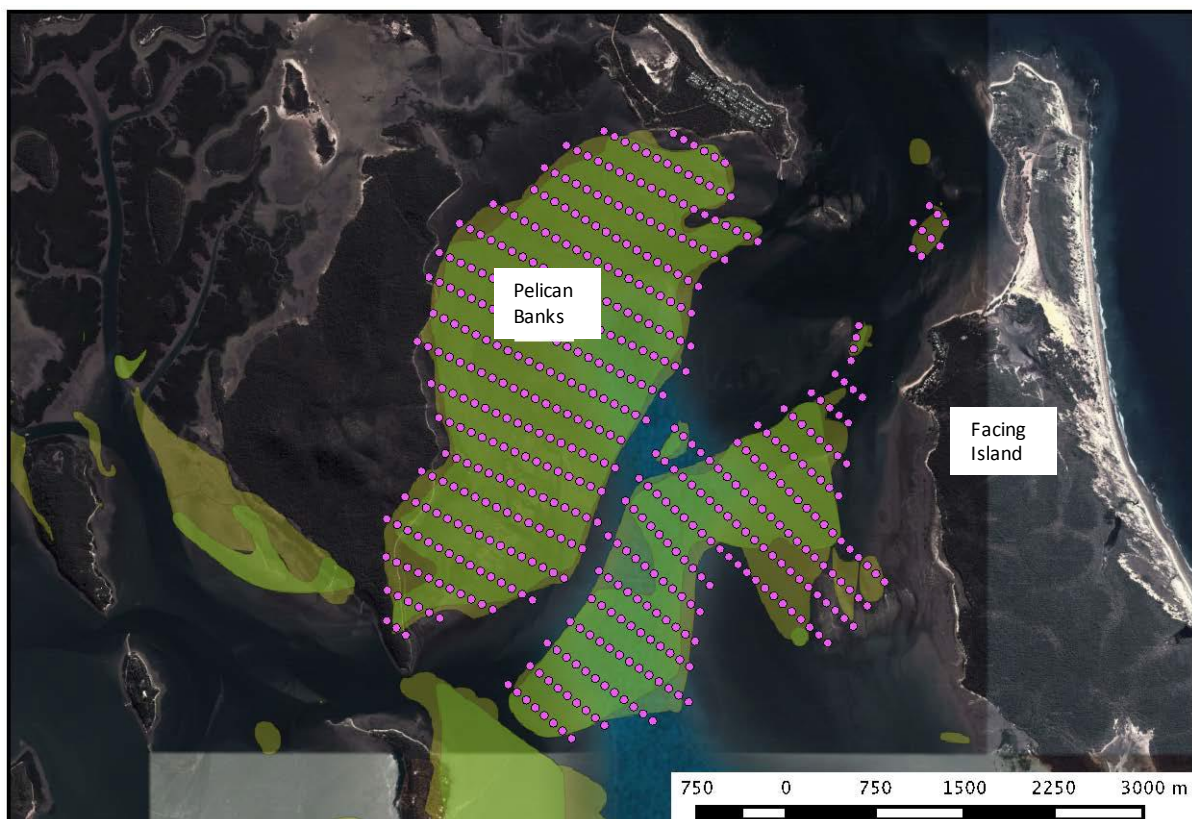
Figure 14 Proposed sites for seagrass sampling at Pelican Banks and west of Facing Island 2014.

We surveyed the seagrass beds at Pelican Banks and to the west of Facing Island by photographing a 0.25 m² quadrat on the seabed at 346 sites throughout the area. Percentage cover of seagrass, algae and substrate components were then visually estimated from the photographs.

2.2.2 SITE SELECTION

The seagrass shapefile Gladstone_Composite_Seagrass_Dist_2002_2011.shp obtained from Len McKenzie (JCU TropWater) was used to plan the areal extent of our sampling. The seagrass shapefile was projected to UTM zone 56 S WGS84 and a series of parallel transect lines 250 m apart were drawn across the seagrass beds to the west of Facing Island and on Pelican Banks. Nodes were then added every 100 m along each transect line in QGIS using the QChainage plugin. The nodes were extracted as points and reprojected to geographics (WGS84) before having lat/long in decimal degrees added to the attribute file. This gave a total of 532 potential sampling sites. The sites were loaded onto a handheld Garmin GPSMAP72 for use in the field.

2.2.3 PHOTOGRAPHY OF SEAGRASS

The large number of planned sites meant that using a diver to photograph the seabed at each site would be time consuming. For this reason, a remotely operated drop camera was used which could be easily operated from a small (5 m) inflatable vessel.

A GoPro 3 Black camera in waterproof housing was chosen for this application. This camera is equipped with WiFi and can be remotely operated using a smartphone. The WiFi signal does not transmit through water but can be transmitted through coaxial cable. A connection between a smartphone and the GoPro was achieved by gluing WiFi antennae to the back of a smartphone housing and the exterior of the GoPro housing, and connecting the two antennae with a 10 m length of coaxial cable. This enabled full remote control of the camera. The camera was mounted facing down in a stainless steel frame fitted with a 0.5 x 0.5 m quadrat (Figure 15).

In the field, at each site the camera frame was lowered to the seabed and a single photograph taken. The vessel was then moved to the next site.

Figure 15 Camera frame used to mount GoPro camera for photography of seagrass

2.2.4 PERCENTAGE COVER OF SEAGRASS

The percentage cover of seagrass (*Zostera muelleri* and *Halophila ovalis*), algae, soft coral, hard coral, mud, sand, gravel and rock were estimated visually by a trained observer. Visual cover estimates were carried out using digitally generated simulation images of a range of different cover values (Figure 16). In order to allow cover estimates to be converted to biomasses, marked areas were photographed, the percent cover of seagrass estimated using CPCE (Kohler and Gill 2006) and the marked area sampled using a 150 mm diameter corer. Seagrass biomasses were measured as described above (Section 2.1.1).

The presence/absence and percentage cover of seagrasses were mapped and a predicted surface of seagrass percentage cover was generated using the kriging routine of the geostatistical analyst extension in ArcMap 10.0.
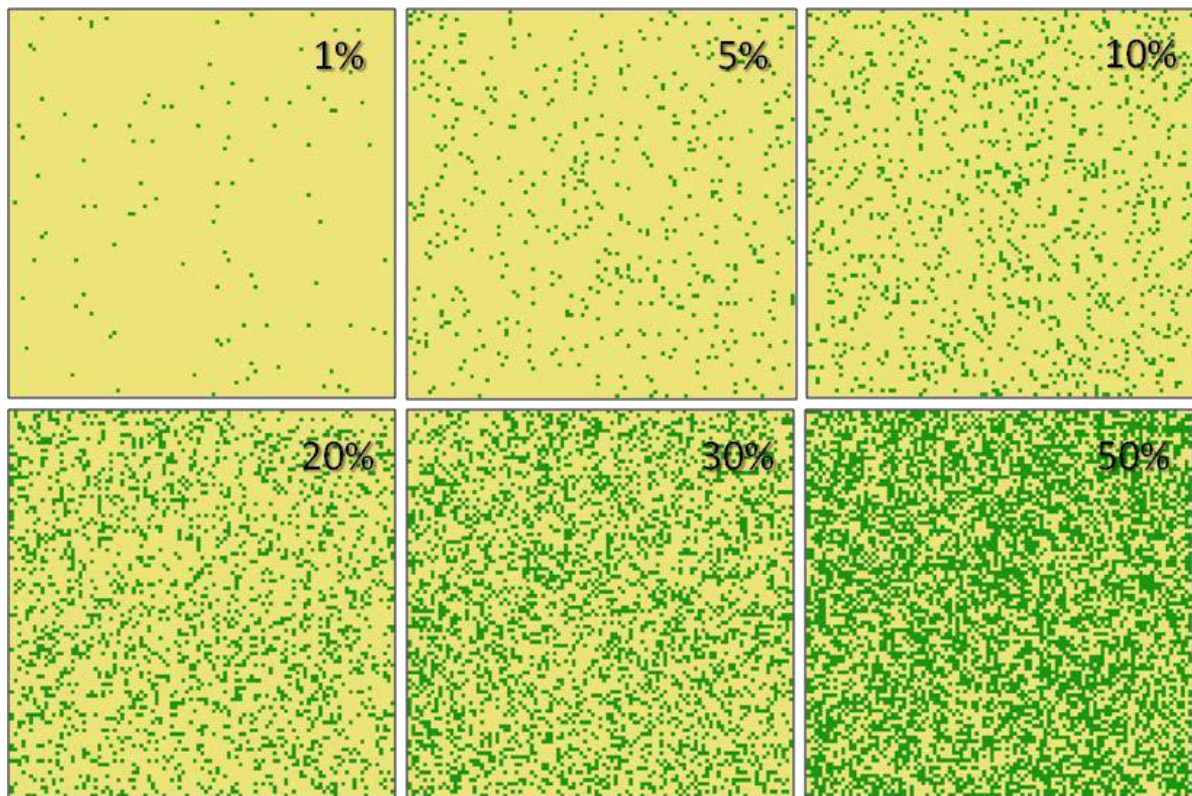
Figure 16 Seagrass cover calibration images.

2.3 Autonomous Underwater Vehicle

The usefulness of Autonomous Underwater Vehicles (AUVs) for measurement and mapping of seagrass in Port Curtis was explored as part of the project, using the Starbug-X. The fully aluminium hull of the Starbug-X AUV is made of two 152 mm diameter tubes fitted with streamlined nose cones and tail fairings (Figure 17). The completed system measures less than 1 m long and 0.6 m wide with an in air weight of 26 kg when fully configured with sensors. The system is light enough that it can be lifted and deployed by one person from a very small vessel, and for transport, can be packed into two small transport cases. A small vertical tail houses the GPS unit as well as a radio antenna. Although Starbug-X was chiefly designed to operate in shallow water from the shore/surface to 50 m

in depth, an operational depth rating of 100 m increases its reach offshore, and allows for increased mission planning flexibility; such as surveying of coastal shelf habitats.
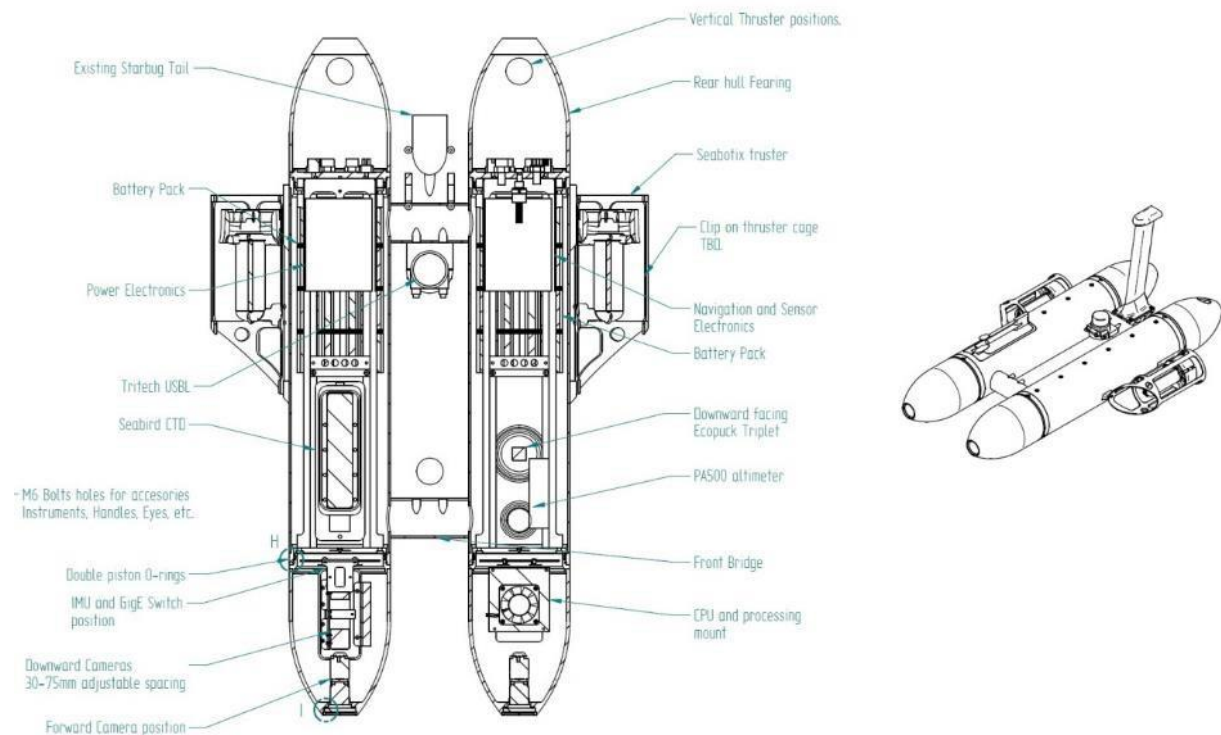
Figure 17 A schematic design of the Starbug-X AUV. Not shown are the front and rear hydrodynamic buoyant fairings and launch/retrieve handles and vertical thrusters.

Unlike autonomous underwater gliders, Starbug-X is actively propelled through the use of thrusters for increased mission planning flexibility. Each of the five thrusters (Seabotix BTD150) are capable of providing up to 3 kg of bollard thrust. There are no active control planes, therefore, surge and yaw control is achieved from the two horizontally mounted thrusters, with roll, pitch and vertical depth control achieved from three vertically mounted thrusters. The lateral motion of the AUV is not actively controlled.

In Starbug a pair of downward facing cameras housed in the starboard nose cone are nominally separated by 40 mm but can be adjusted with a separation ranging from 30-70 mm. These downward facing cameras provide the primary imaging information for habitat mapping as well as vision-based odometry. The cameras are high-definition Point Grey Flea 3 FL3-GE-20S4C-C models, allowing for improved images of the benthic environment. This provides the capability to not only characterise the seafloor, but also identify benthic species such as seagrass or corals in the images. The cameras are fitted with 8 mm lenses operated with a fixed f-stop to allow for maximum shutter speed and better exposure control. Each camera is triggered and synchronised with an external hardware clock. The use of Gigabit Ethernet allows for images to be broadcast through a small Ethernet switch contained inside the hull. As the entire vision system is connected via Ethernet, it is possible to view each video stream live when at the surface using either wifi, or by connecting the external Ethernet port to a computer. If needed, Starbug-X can be tethered via a cable to act in a pseudo ROV (Remote Operated Vehicle) mode by streaming images live to the surface.

Figure 18 The Starbug-X AUV returning from a mission at Pelican Banks, Port Curtis. A GoPro camera is mounted on the tail to provide independent horizontal image recording capability.

Primary global position information is provided via a GPS module embedded in the tail of Starbug-X. The GPS module is activated at the surface to provide corrections to the odometric and dead reckoning system (Figure 18). In addition to vision-based navigation, a Micro-Strain IMU (3DM-GX3-25) and pressure sensor (GE NovaSensor NPI-19B-200AV) was also fitted to aid in navigation. Bottom tracking is achieved using an acoustic altimeter (Tritech PA500) which provides system altitude with a 1 mm resolution at a distance of 0.1 m from the bottom. This was fed back to the control system to allow Starbug-X to maintain a desired altitude for imaging typically around 400–900 mm. A short range infrared proximity sensor was also fitted to allow for near collision detection with the bottom in the 0-0.1 m range or to aid in bottom landing manoeuvres. To reduce long-term navigational error associated with dead reckoning and maintain transect linearity in shallow water, a surface towed GPS was integrated into the navigation system.

The system was powered by a two 30Ah rechargeable lithium ion battery packs connected in parallel providing a nominal pack voltage at 25.9VDC. Currently, the endurance of the AUV at typical survey speeds of 0.5 m/s is approximately 12 hours, which reduces to 4 hours at a cruise speed of 1 m/s.

Starbug-X was deployed at the pre-programmed start point of each transect and picked up at the programmed end point. Position was determined by fusing on-board dead reckoning and real time information from the surface-towed GPS. Height above substratum was determined through fusion of acoustic profiling (sonar) and mean altitude, determined by the on-board downward stereo camera system.

At the completion of each mission the data were downloaded from the Starbug-X to a laptop computer for later analysis. Analysis was completed by visual cover estimates of the digital images. Visual estimates were calibrated against a set of standardised seagrass images (Figure 16). When selecting the images for scoring, every 25th image was selected as the central sampling point and that image plus five images on either side of that point were scored, in order to provide a sample

equivalent to the short transect scored for presence/absence with the towed drop camera (see Section 2.2.3 above). Given the sampling rate of the camera and the speed of the AUV (0.2-0.45 m/s) this equates to 1-2 images per linear meter.

3 Results

3.1 Seagrass depth-range surveys 2012 & 2013

3.1.1 YEAR 1: 20–27 NOVEMBER 2012

<u>Seagrass biomass</u>

The sites sampled for seagrass biomass are summarized in Table 3.1. The results indicate highest prevalence of seagrass at Pelican Banks with a mean overall above ground dry weight of 24.86 gDW·m^{-2} at Pelican Banks north and 22.33 gDW·m^{-2} at Pelican Banks south. *Zostera muelleri* was by far the most abundant species, although mixed beds with *Halophila ovalis* were found in the southern portion of the banks (Figure 19, Table 3.1). Further south, relatively high biomasses of seagrass (mainly *Zostera muelleri*) were found at South Trees 2 (Figure 13 and Figure 19). Similar biomasses were found by TropWater in November 2012 although there were some discrepancies at sites with low biomass (e.g. Wiggins Island) and in terms of species composition (e.g. Pelican Banks south) (Figure 19, Table 3.1).
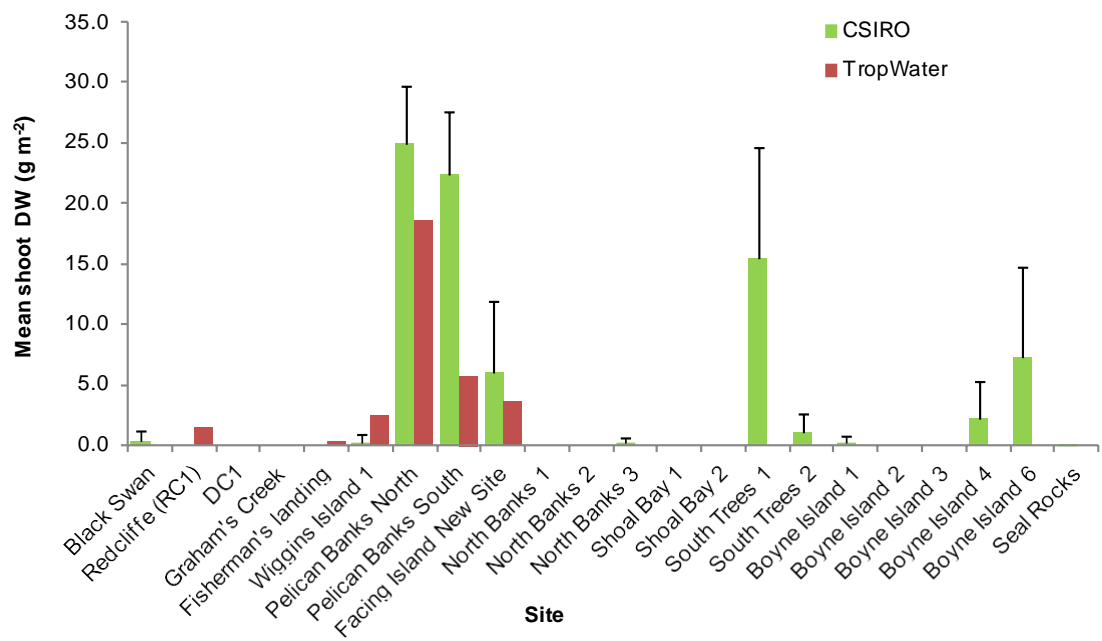
Figure 19 Mean shoot dry weight (DW, g·m^{-2}) (+ S.D.) of total seagrass at the sites in Gladstone Harbour sampled in November 2012, with an indication of the biomass obtained by TropWater (Davies et al. 2012) in the same month.

Overall the middle portion of the harbour had by far the highest seagrass biomass, followed by the lower part and finally the upper harbour where very low biomasses or no seagrass were found at all sampled sites (Figure 19, Figure 20 and Table 3.1).

The mean above and below ground dry weights of each species at each site are reported in Table 3.2.

Table 3.1 Shoot dry weight (mean ±SD) of seagrass at 20 sites in Gladstone Harbour (November 2012), with information on the position, date, depth and height above datum (Ht) of sampling sites, the gear used, as well as the mean percentage species composition of samples. The numbers in *italics* refer to the results obtained by TropWater (Davies et al. 2012) at the same sites in November 2012. Notes: Zc = *Zostera muelleri*, Ho = *Halophila ovalis*, Hd = *Halophila decipiens*, Hu = *Halodule uninervis*.

CSIRO Site	Lat.	Lon.	Date – time	Depth (m)	Ht (m)	Gear	Biomass DW (g Wm^{-2})		Mean species composition (%)			
							Mean	S.D.	Zc	Ho	Hd	Hu
Black Swan	-23.68	151.13	21/11/2012 8:57	0.6	0.882	Corer	0.43	0.85	97 *(78)*	0 *(22)*	3	0
Redcliffe (RC1)	-23.70	151.14	21/11/2012 10:01	0.8	0.397	Corer	*(1.57)*	-	*(78)*	*(22)*		
Duff Creek (DC1)	-23.72	151.16	21/11/2012 11:37	0.4	1.533	Grab	0.00	0.00	0	*(100)*	0	0
Graham's Creek	-23.72	151.22	21/11/2012 12:35	1.5	0.923	Corer	0.00	0.00	0 *(20)*	0 *(80)*	0	0
Fisherman's landing	-23.74	151.16	21/11/2012 13:30	1.3	1.573	Grab	*(0.35)*	-	*(40)*	*(60)*		
Wiggins Island 1	-23.81	151.21	21/11/2012 14:05	1.4	1.473	Corer	0.32 *(2.52)*	0.64	90 *(25)*	10 *(75)*	0	0
Pelican Banks North	-23.77	151.30	20/11/2012 10:00	0.7	1.35	Corer	24.86 *(18.57)*	4.89	100 *(98)*	0 *(2)*	0	0
Pelican Banks South	-23.79	151.30	23/11/2012 13:26	0.8	0.482	Grab	22.33 *(5.71)*	5.25	62 *(93)*	34 *(7)*	0	4
Facing Island New Site	-23.79	151.31	23/11/2012 14:12	1	0.793	Grab	6.01 *(3.65)*	5.89	57 *(58)*	36 *(42)*	0	7
North Banks 1	-23.80	151.29	23/11/2012 15:00	2.3	0.025	Grab	0.00	0.00				
North Banks 2	-23.81	151.30	25/11/2012 8:40	3.1	-0.194	Grab	0.00	0.00				
North Banks 3	-23.81	151.29	25/11/2012 8:08	2.6	0.818	Grab	0.19	0.51	0	0	0	100
Shoal Bay 1	-23.83	151.34	25/11/2012 11:28	0.9	0.726	Grab	0.00	0.00				
Shoal Bay 2	-23.83	151.34	25/11/2012 12:00		1.126	Grab	0.00	0.00				
South Trees 1	-23.87	151.32	22/11/2012 13:02	0.5	1.332	Corer	15.51	9.18	97	0	0	3
South Trees 2	-23.87	151.32	22/11/2012 12:39	0.5	1.332	Corer	1.14	1.49	100	0	0	0
Boyne Island 1	-23.88	151.33	22/11/2012 14:05	1.4	0.943	Corer	0.30	0.45	0	0	0	100
Boyne Island 2	-23.89	151.33	25/11/2012 13:04	0.7	0.119	Grab	0.00	0.00				
Boyne Island 3	-23.89	151.33	25/11/2012 13:55	1.6	-0.712	Grab	0.00	0.00				
Boyne Island 4	-23.90	151.33	25/11/2012 14:32	1.7	-0.346	Grab	2.19	3.09	0	0	0	100
Boyne Island 6	-23.91	151.34	25/11/2012 15:35	2.5	-0.562	Grab	7.26	7.47	0	0	0	100
Seal Rocks	-23.96	151.48	26/11/2012 13:41	1.7	-0.981	Grab	0.04	0.11	0	0	100	0
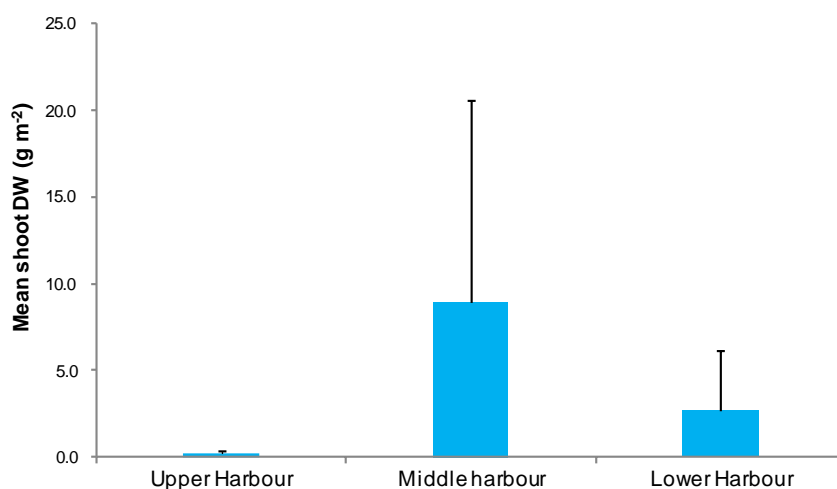
Figure 20 Shoot dry weight (DW, g·m⁻²) (mean + S.D.) of total seagrass in the Upper, Middle and Lower reaches of Gladstone Harbour in November 2012. For sites included in each reach of the harbour refer to Table 2.1.

Table 3.2 Above and Below Ground seagrass biomass. Dry weight of seagrass (mean + S.D.) at 20 sites in Gladstone Harbour (November 2012). BG; below ground (root) and AG; above ground (shoot) values per species.

Site	Species	BG biomass (gDW m⁻²)		AG biomass (gDW m⁻²)	
		mean	S.D.	mean	S.D.
Black Swan	*Halodule uninervis*	0.000	0.000	0.000	0.000
	Halophila decipiens	0.191	0.505	0.015	0.039
	Halophila ovalis	0.000	0.000	0.000	0.000
	Zostera muelleri	1.019	1.846	0.412	0.847
DC1	*Halodule uninervis*	0.000	0.000	0.000	0.000
	Halophila decipiens	0.000	0.000	0.000	0.000
	Halophila ovalis	0.000	0.000	0.000	0.000
	Zostera muelleri	0.000	0.000	0.000	0.000
Grahams Creek	*Halodule uninervis*	0.000	0.000	0.000	0.000
	Halophila decipiens	0.000	0.000	0.000	0.000
	Halophila ovalis	0.000	0.000	0.000	0.000
	Zostera muelleri	0.000	0.000	0.000	0.000
Wiggins Island 1	*Halodule uninervis*	0.000	0.000	0.000	0.000
	Halophila decipiens	0.000	0.000	0.000	0.000
	Halophila ovalis	0.015	0.041	0.032	0.086
	Zostera muelleri	0.398	0.996	0.283	0.650
Pelican Banks North	*Halodule uninervis*	0.000	0.000	0.000	0.000
	Halophila decipiens	0.000	0.000	0.000	0.000
	Halophila ovalis	0.078	0.140	0.090	0.153
	Zostera muelleri	107.257	19.752	24.772	4.864

Pelican Banks South	*Halodule uninervis*	2.616	4.145	0.918	1.423
	Halophila decipiens	0.000	0.000	0.000	0.000
	Halophila ovalis	8.824	6.989	7.492	5.901
	Zostera muelleri	46.471	17.869	13.917	5.911
Facing Is New Site	*Halodule uninervis*	0.594	0.838	0.402	0.493
	Halophila decipiens	0.000	0.000	0.000	0.000
	Halophila ovalis	2.783	2.500	2.172	1.605
	Zostera muelleri	3.561	3.778	3.436	4.732
NorthB3	*Halodule uninervis*	0.364	0.963	0.192	0.509
	Halophila decipiens	0.000	0.000	0.000	0.000
	Halophila ovalis	0.000	0.000	0.000	0.000
	Zostera muelleri	0.000	0.000	0.000	0.000
Seal Rocks	*Halodule uninervis*	0.000	0.000	0.000	0.000
	Halophila decipiens	0.032	0.086	0.042	0.111
	Halophila ovalis	0.000	0.000	0.000	0.000
	Zostera muelleri	0.000	0.000	0.000	0.000
South Trees 1	*Halodule uninervis*	2.720	3.548	0.454	0.460
	Halophila decipiens	0.000	0.000	0.000	0.000
	Halophila ovalis	0.000	0.000	0.000	0.000
	Zostera muelleri	52.644	35.906	15.053	9.328
South Trees 2	*Halodule uninervis*	0.000	0.000	0.000	0.000
	Halophila decipiens	0.000	0.000	0.000	0.000
	Halophila ovalis	0.000	0.000	0.000	0.000
	Zostera muelleri	1.454	2.346	1.141	1.493
Boyne Island 1	*Halodule uninervis*	1.440	2.185	0.305	0.454
	Halophila decipiens	0.000	0.000	0.000	0.000
	Halophila ovalis	0.000	0.000	0.000	0.000
	Zostera muelleri	0.000	0.000	0.000	0.000
Boyne Island 4	*Halodule uninervis*	2.781	4.408	2.193	3.086
	Halophila decipiens	0.000	0.000	0.000	0.000
	Halophila ovalis	0.000	0.000	0.000	0.000
	Zostera muelleri	0.000	0.000	0.000	0.000
Boyne Island 6	*Halodule uninervis*	4.991	10.629	7.260	7.467
	Halophila decipiens	0.000	0.000	0.000	0.000
	Halophila ovalis	0.000	0.000	0.000	0.000
	Zostera muelleri	0.000	0.000	0.000	0.000

Leaf length and surface area statistics for each seagrass species at each site showed that Pelican Banks not only had the highest biomass in November 2012 but also highest surface area in terms of both *Zostera muelleri* and *Halodule uninervis* (Figure 21a). The longest leaves, on the other hand, were found at South Trees (Figure 21b).
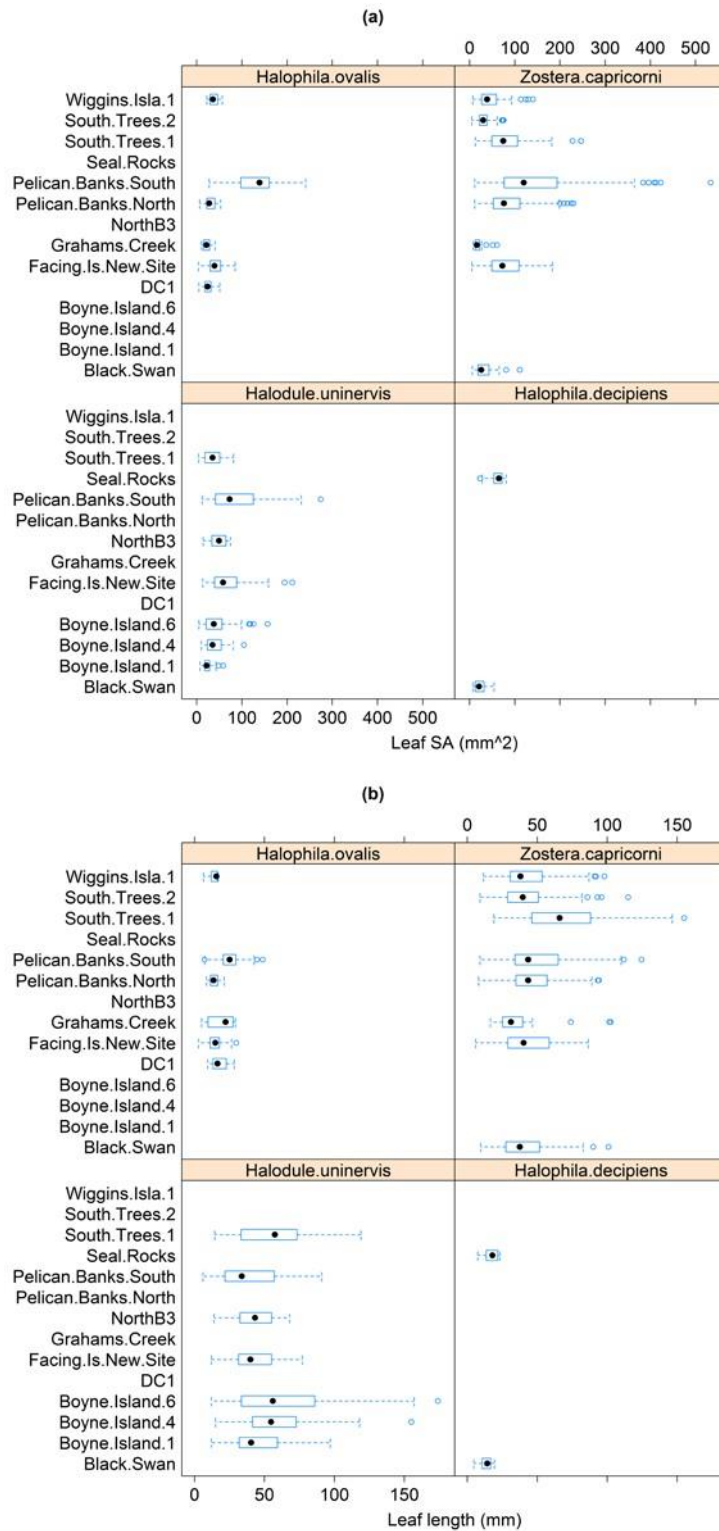
Figure 21 Box and whisker plots of (a) leaf surface area (mm²) and (b) leaf length (mm) by species and sampled site in Gladstone Harbour for November 2012. The dot represents the median, the upper and lower margins of the box represent the 1st and 3rd quantiles respectively, and the lower and upper whiskers represent the minimum and maximum values, respectively.
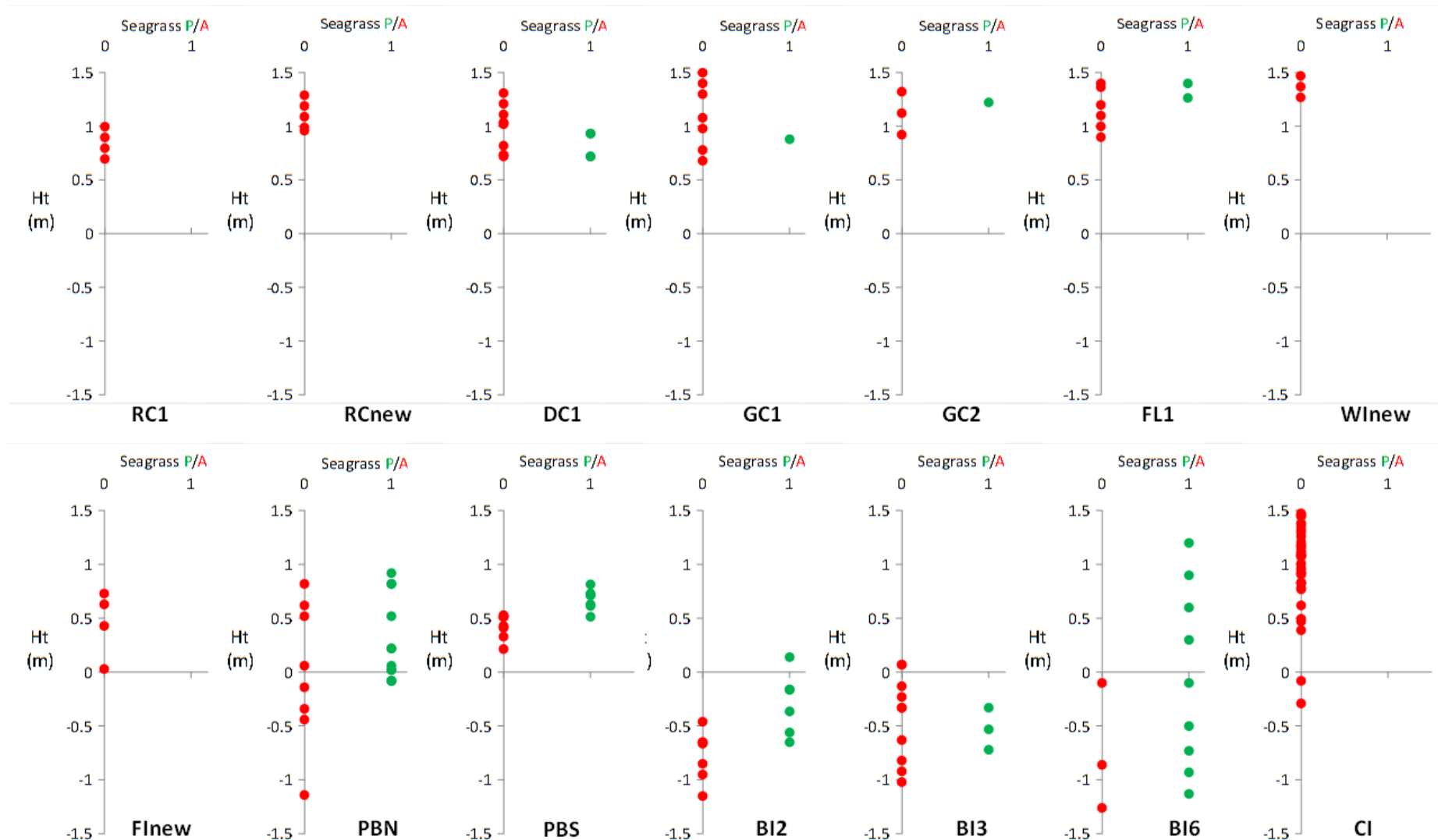
Figure 22 Summary of the depth ranges of seagrass in November 2012 in Gladstone Harbour showing presence (P, green) or absence (A, red) at each sampled depth, converted to height with respect to datum (Ht). For site name abbreviations refer to Table 2.1 Details of the 26 sites sampled for seagrass in November 2012 with an indication of their location within the harbour and the type of sampling carried out. Notes: B = biomass sampling, DR = depth range sampling, T/C = temperature and conductivity, + = sampled, - = not sampled.. Notes: seagrass was present at one sampling location around Compigne Island (-23.78387, 151.25509), at a Ht of 1.996 m.

Seagrass depth ranges

Depth range sampling revealed four sites with no seagrass: Redcliffe 1 (RC1), Redcliffe new (RCnew), Wiggins Island new (WInew) and Facing Island new (FInew). At five sites (Fl1, PBN, PBS, BI2 and BI6), seagrass was found in shallower waters, whilst no clear patterns emerged for the remaining sites (Figure 22). At Pelican Banks North it was possible to directly compare the depth ranges of seagrass with the depth profiles of Photosynthetically Active Radiation (PAR1 and PAR2) (Figure 23).
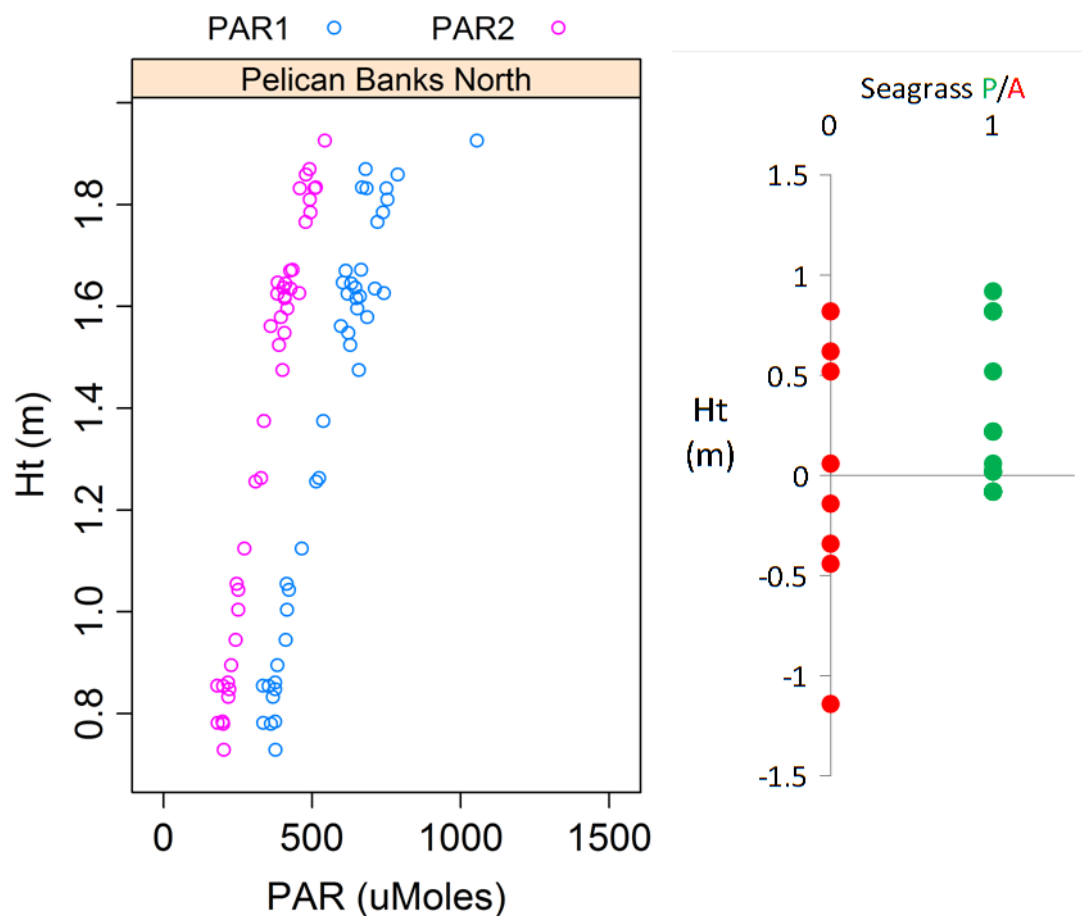
Figure 23 Photosynthetically Active Radiation (PAR1 and PAR2) profiles (on the left) and seagrass depth range (on the right) for Pelican Banks North in November 2012.

3.1.2 YEAR 2: 12–19 SEPTEMBER 2013; 9 NOVEMBER 2013

<u>Seagrass depth ranges</u>

Of the 684 stations sampled with a drop camera in 17 areas in 2013, 654 stations were valid (e.g. visibility was good enough to sample) with 149 of these having seagrass (Table 3.3). The results in terms of minimum and maximum depths of seagrass presence are summarized in Table 3.3 and mapped in Figure 24-Figure 32.

Table 3.3 Summary by area of the depth range sampling for seagrass at valid stations in Gladstone Harbour in 2013, with an indication of the number of stations sampled, the number of stations and percentage with seagrass present and the minimum and maximum height with respect to datum (Ht) at which seagrass was present.

Site	No. stations sampled	No. stations w seagrass	% stations w seagrass	Min seagrass Ht (m)	Max seagrass Ht (m)
Black Swan	8	3	37.5	-0.40	0.97
Redcliffe	18	1	5.6	0.52	0.52
Duff Creek	10	1	10.0	0.87	0.87
Graham's Creek	42	4	9.5	-0.76	1.04
Fisherman's Landing	10	0	0.0		
Wiggins Is	29	1	3.4	1.42	1.42
Compigne Is	35	1	2.9	0.66	0.66
Chinaman Hill	9	3	33.3	0.64	1.13
Pelican Banks North	63	42	66.7	-0.22	2.28
Pelican Banks South	32	12	35.3	-1.76	1.38
North Banks	51	25	49.0	0.25	1.52
Facing Is	31	11	35.5	0.29	1.69
Facing Is Offshore*	46	2	4.3	-19.46	-19.16
South Trees	21	7	33.3	1.32	2.37
Boyne Is	71	25	35.2	-1.26	1.52
Seal Rocks	27	2	7.4	-3.39	-0.48
Rodds Bay	149	9	6.0	-1.32	0.85
TOTAL	**654**	**149**			

* Maximum depth range not sampled; beyond range of surveys.

A clear relationship emerged between maximum depth of the seagrass bed and Secchi depth ($R^2 = 0.5084$), with greater depths reached at sites with lower levels of light attenuation (Figure 33). Light attenuation coefficients ranged from 0.85 (Boyne Island) to 4.25 (South Trees and Wiggins Island). This is equivalent to seagrass beds displaying a maximum depth limit such that the lower edge of the bed receives approximately 13% (±2.99 SE) of incident surface PAR at Mean Low Water Neap Tides, as estimated using Secchi derived attenuation coefficients and average MLWN tide level of 1.555 m in Gladstone Harbour.
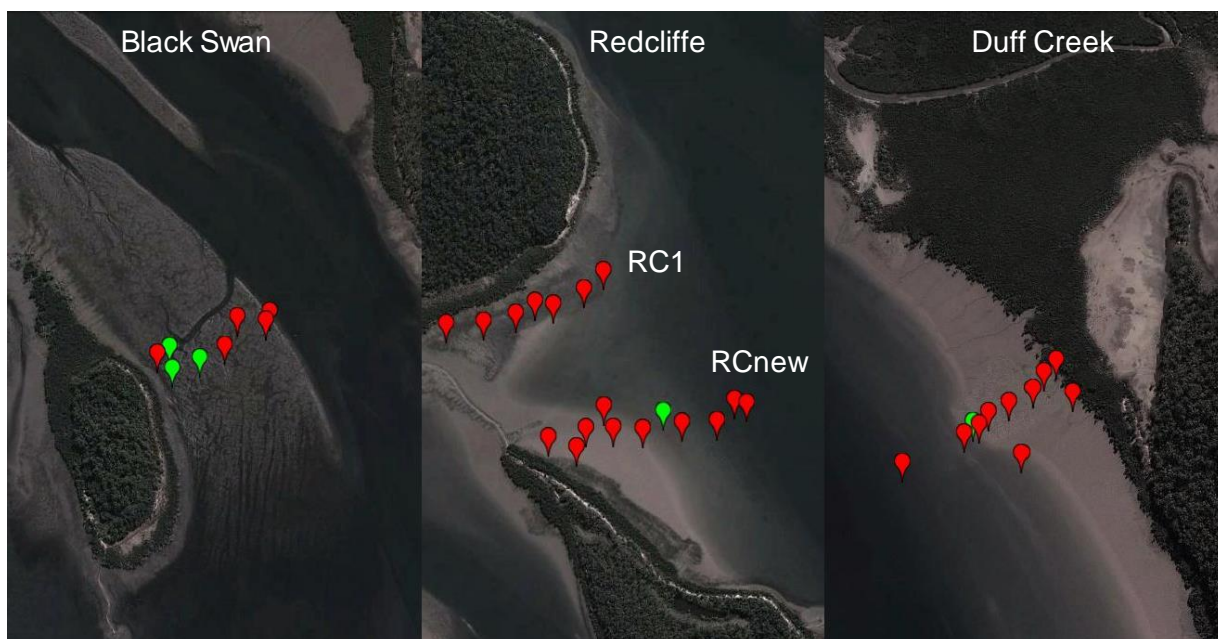
Figure 24 Seagrass depth ranges sampled at the Narrows in September 2013 (green = presence, red = absence).
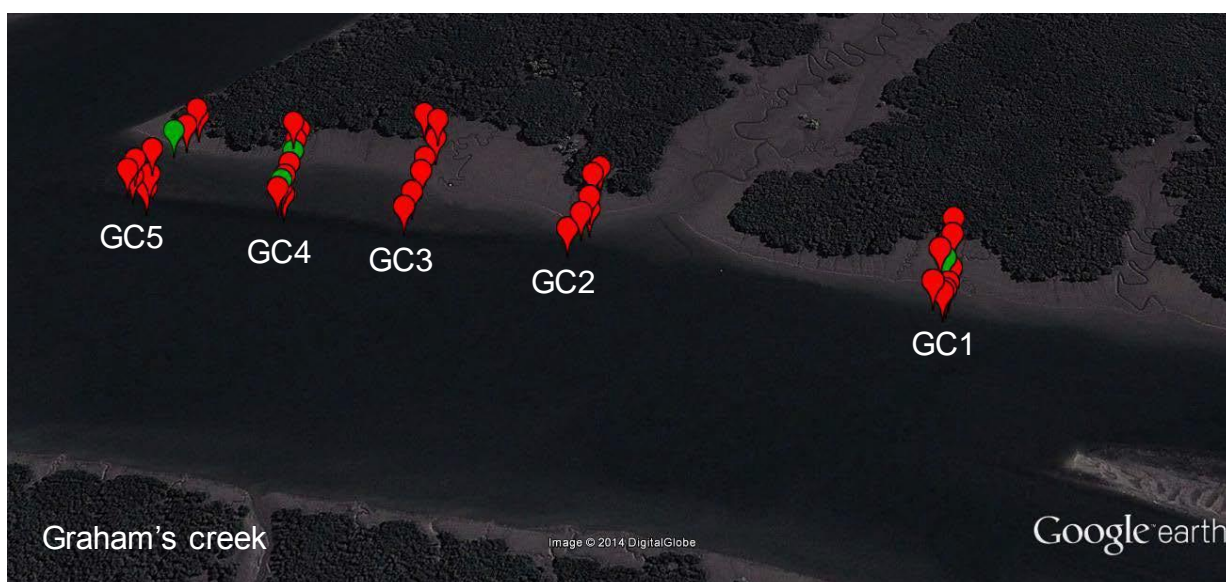
Figure 25 Seagrass depth ranges sampled in Graham's Creek in September 2013 (green = presence, red = absence).

Figure 26 Seagrass depth ranges sampled at Fisherman's Landing in September 2013 (green = presence, red = absence).

Figure 27 Seagrass depth ranges sampled at Wiggins Island in September 2013 (green = presence, red = absence).
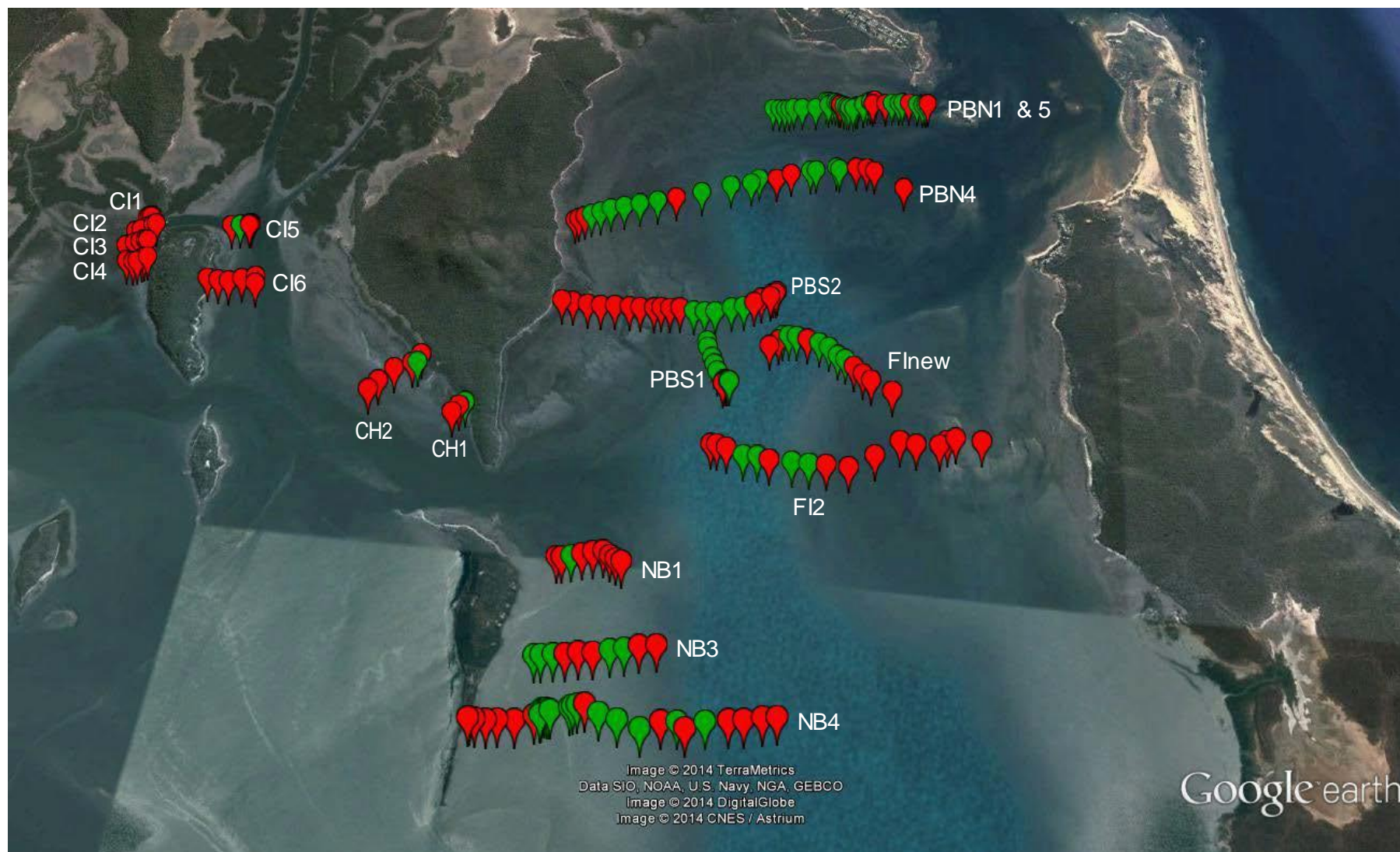
Figure 28 Seagrass depth ranges sampled in the central harbour in September 2013 (green = presence, red = absence). For abbreviations refer to Table 2.2.

Figure 29 Seagrass depth ranges sampled offshore Facing Island in September 2013 (green = presence, red = absence).

Figure 30 Seagrass depth ranges sampled at Seal Rocks in September 2013 (green = presence, red = absence).
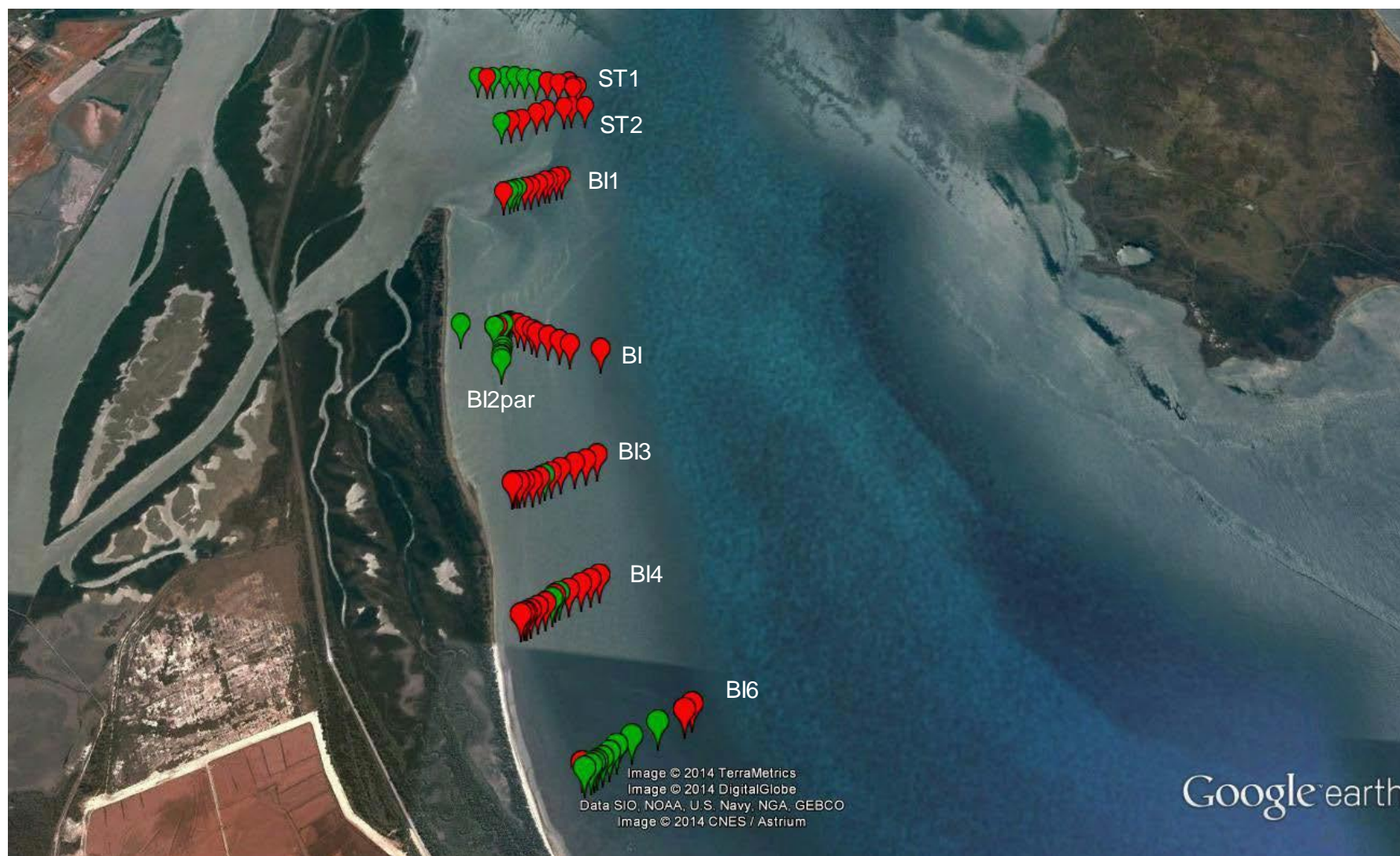
Figure 31 Seagrass depth ranges sampled at South Trees and Boyne Island in September 2013 (green = presence, red = absence). For abbreviations refer to Table 2.2.

Figure 32 Seagrass depth ranges sampled at Rodds Bay in September (RB1A – RB6) and in November (RB7) 2013 (green = presence, red = absence). For abbreviations refer to Table 2.2.
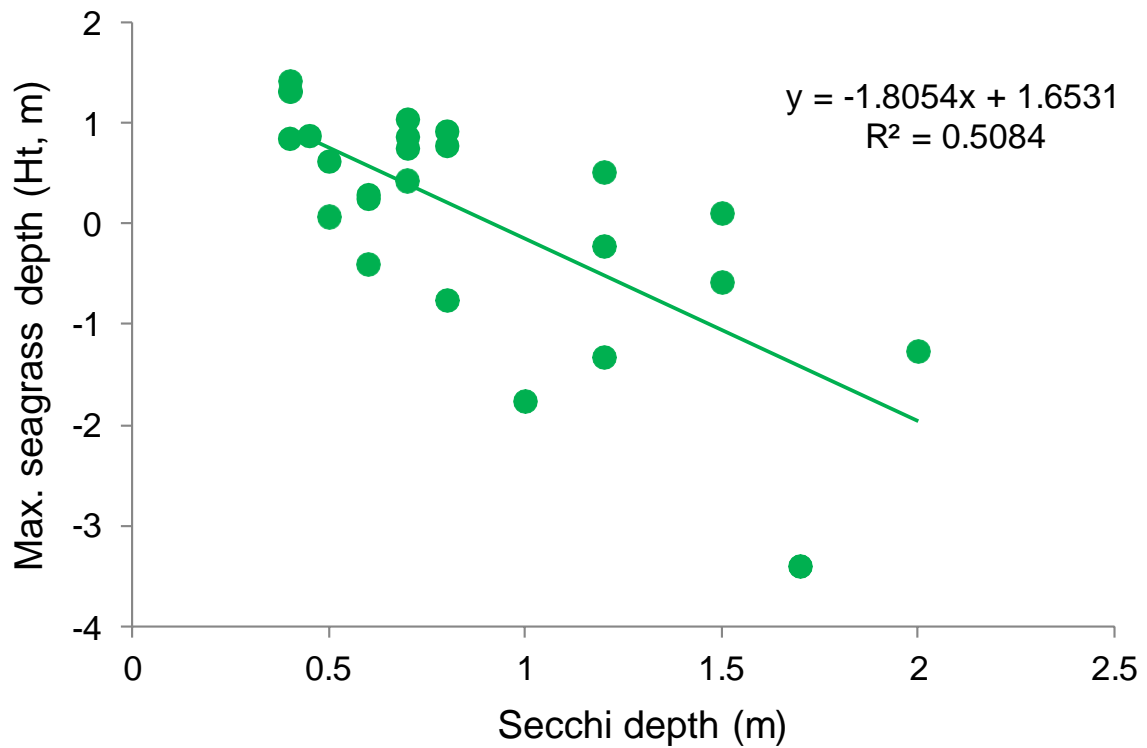
Figure 33 Relationship between the maximum seagrass depth at each site (with respect to datum) and the Secchi disk depth at each site derived from depth range sampling in September 2013.

3.2 Seagrass fine-scale distribution 2014

During the first day of sampling it was evident that it would not be possible to sample all 532 sites within the time available (3 days) and so we decided to sample only every second site, except in the vicinity of the area described as a 'hot spot' for turtles where all sites were sampled. This gave a total of 346 sites.
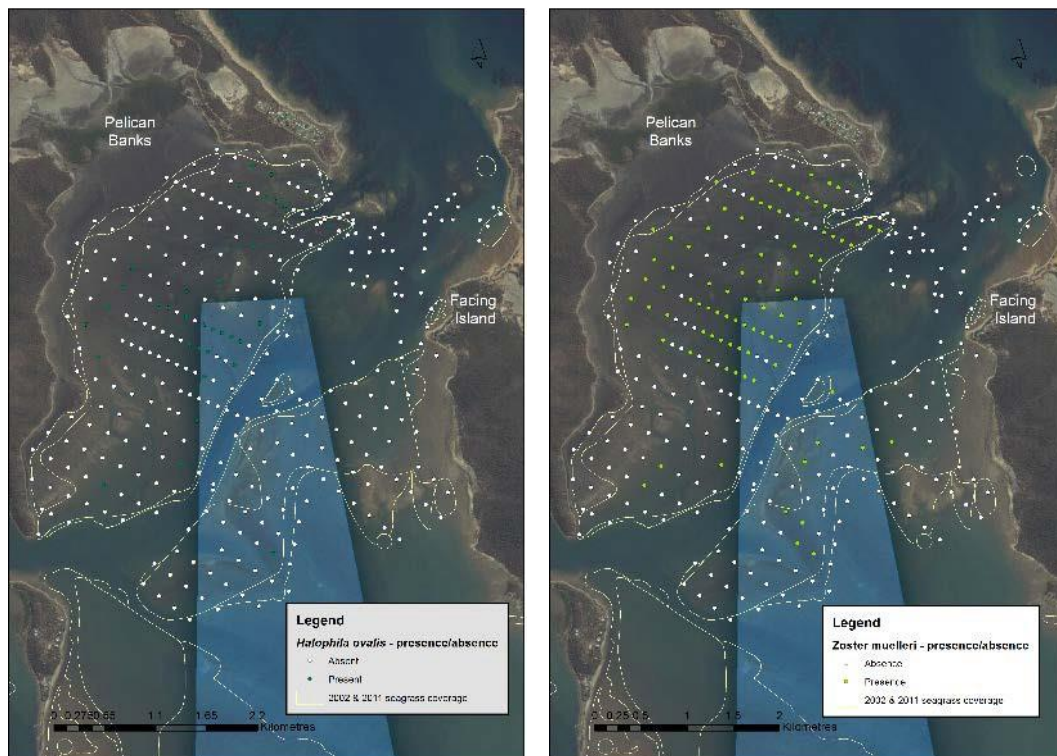
Figure 34 Presence/absence of seagrass, *Halophila ovalis* (left) and *Zostera muelleri* (right), at 346 sites on Pelican Banks and to the west of Facing Island.

Seagrass was found at 95 of the 346 sites (Figure 34), principally on the northern half of Pelican Banks; very little seagrass was found on the banks to the west of Facing Island. Percentage cover of seagrass ranged from 0 to 70% with the highest cover at the north-eastern and central western edges of Pelican Banks (Figure 35 and Figure 37), leaving a central area running from north-east to south-west of the main seagrass bed where seagrass was either absent or present in relatively low levels. *Zostera muelleri* dominated total seagrass composition in terms of cover and biomass, and while *Halophila ovalis* was a relatively minor component of total seagrass cover, its distribution was very similar to that of *Z. muelleri*. Values for biomass (Figure 36) were in the range of those predicted by the GISERA seagrass growth model (Chapter III).

Digital images collected at points within the Pelican Banks seagrass bed represented a range of seagrass densities, and were used to develop a relationship between the seagrass cover and shoot biomass (above ground dwt g m^{-2}) of *Zostera muelleri* (Figure 38) that could be used in the development of the seagrass biogeochemical model (Chapter III).
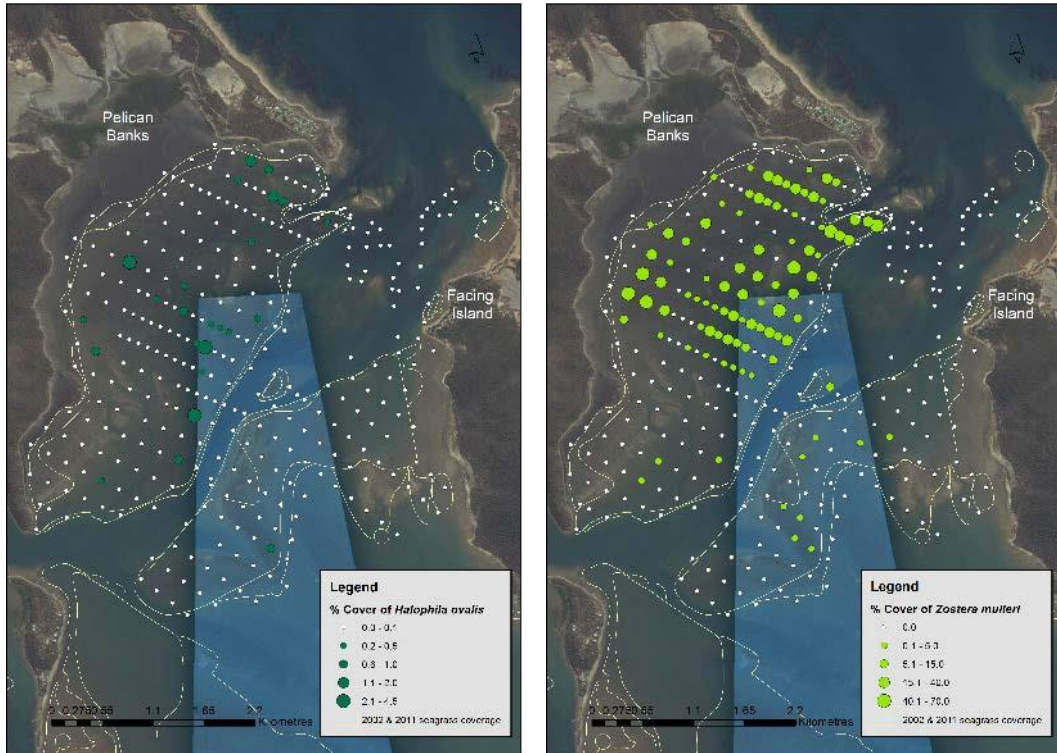
Figure 35 Bubble plot of the estimated percentage cover of seagrass, *Halophila ovalis* (left) and *Zostera muelleri* (right), at Pelican Banks and to the west of Facing Island.
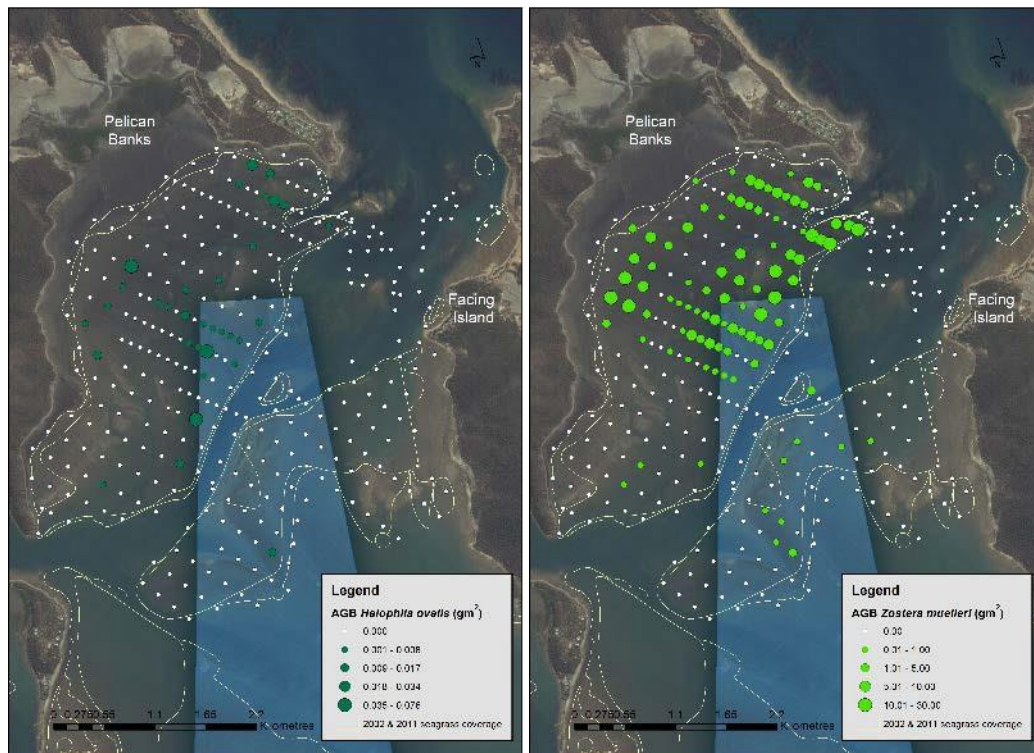
Figure 36 Bubble plot of the estimated biomass (above ground biomass AGB dwt g.m^{-2}) of *Halophila ovalis* (left) and *Zostera muelleri* (right), at Pelican Banks and to the west of Facing Island.
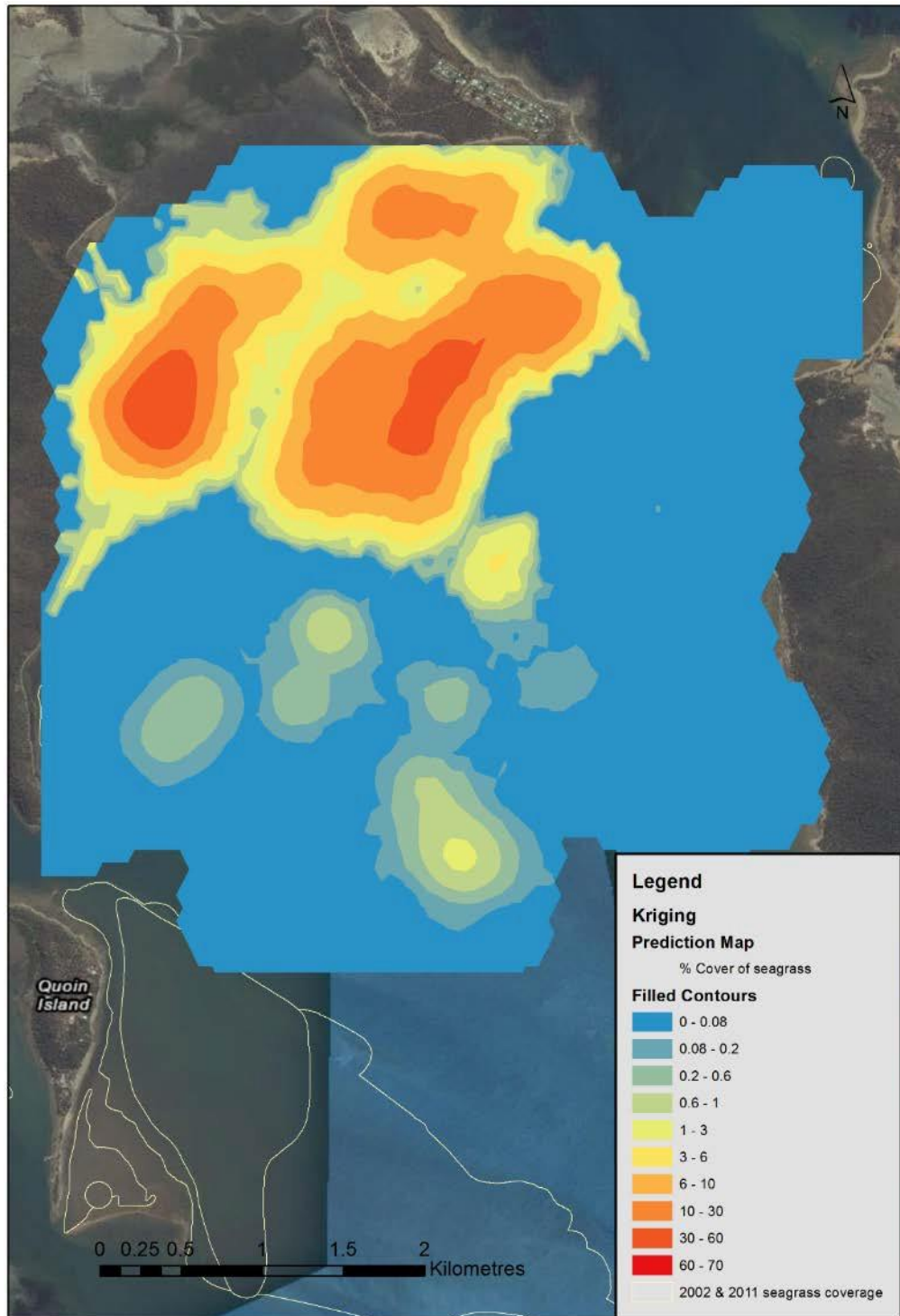
Figure 37 Map of predicted % cover of seagrass at Pelican Banks and to the west of Facing Island produced by krigging the data obtained from the benthic photographs.
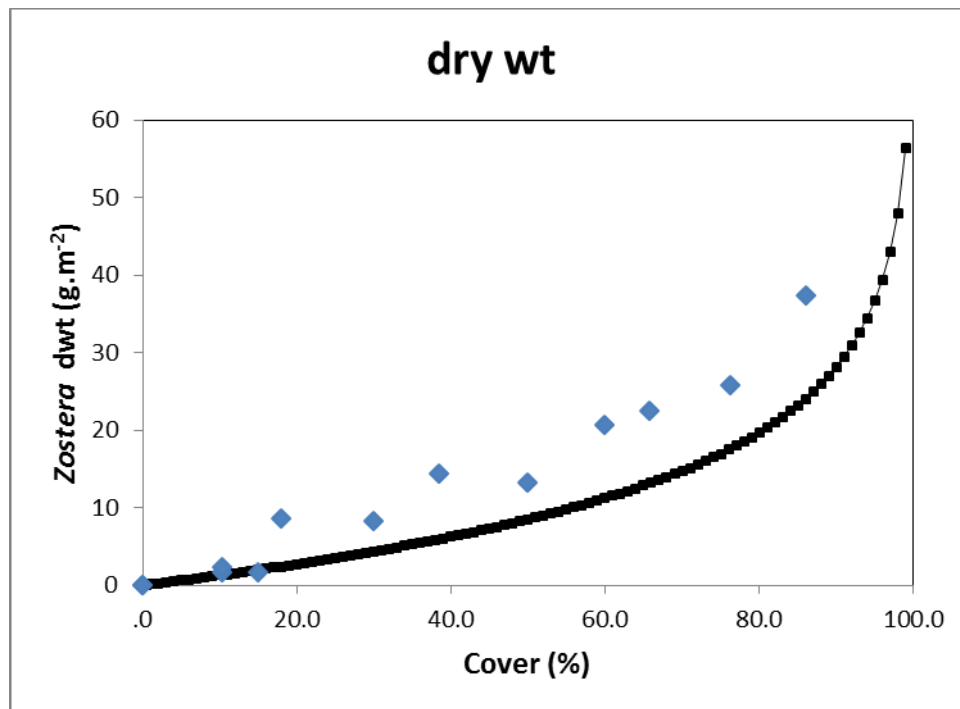
Figure 38 Relationships between seagrass (*Zostera muelleri*) percent cover and biomass (dry weight) determined at Pelican Banks. Black symbols indicate the relationship used in Chapter III (seagrass biogeochemical model) equation A8 for translating leaf surface area A_{eff} to seagrass biomass.

3.3 Autonomous Underwater Vehicle

Eight AUV missions were completed (Figure 39), to assess seagrass depth range, comprising transects run across depth contours at Pelican Banks (1), Quoin Island (2), Rodds Bay (4), and Seal Rocks (1). While the mission execution and navigation by Starbug were up to expectation, the conditions during many of the transect runs were too turbid to allow useable photographs to be obtained, largely due to wave action near the bottom creating a layer of suspended sediment. The most useable data was obtained at Pelican Banks where multiple depth range transects were completed crossing in and out of seagrass beds during a single mission. Other missions where visibility was sufficient for quantifying cover did not record any seagrass (Table 3.4) and so were not informative in terms of providing data that would improve model performance.

Figure 39 Port Curtis and Rodds Bay AUV seagrass transects completed in 2013.

Table 3.4 AUV missions completed at Gladstone during the 2013 surveys.

Location	Date/Time	Distance	Mission Name	Mission Goal
Pelican Banks North	13/9/2013 11:41	Na	Image.mission	Starbug Seagrass Biomass Calibration
Pelican Banks North	13/9/2013 12:45	Na	Image2.mission	Starbug Seagrass Biomass Calibration
Pelican Banks North	13/9/2013 15:00	920m	PBN_Grid1a.mission	Seagrass depth range mapping
Quoin Is North Banks 1	13/9/2013 15:30	900m	NB1_Grid2a.mission	Seagrass depth range mapping
Rodd's Bay	14/9/2013 08:00	575m	RB_4.mission	Seagrass depth range mapping
Rodd's Bay*	14/9/2013 09:20		RB_7.mission	Aborted due to pitch oscillation
Rodd's Bay	14/9/2013 09:28	810m	RB_7a.mission	Seagrass Mapping
Rodd's Bay*	14/9/2013 10:54	180m	RB_2.mission	Seagrass Mapping (image capture failure)
Rodd's Bay	14/9/2013 11:38	380m	RB_8.mission	Seagrass Mapping
Rodd's Bay	14/9/2013 13:27	180m	RB_2a.mission	Seagrass Mapping (no surface GPS)
Seal Rocks	15/9/2013 13:31	215m	SR_test.mission	Testing Starbug Imaging Capabilities in Deeper Water
Quoin Island	18/9/2013 07:19	100m	QI_test.mission	Seagrass Mapping
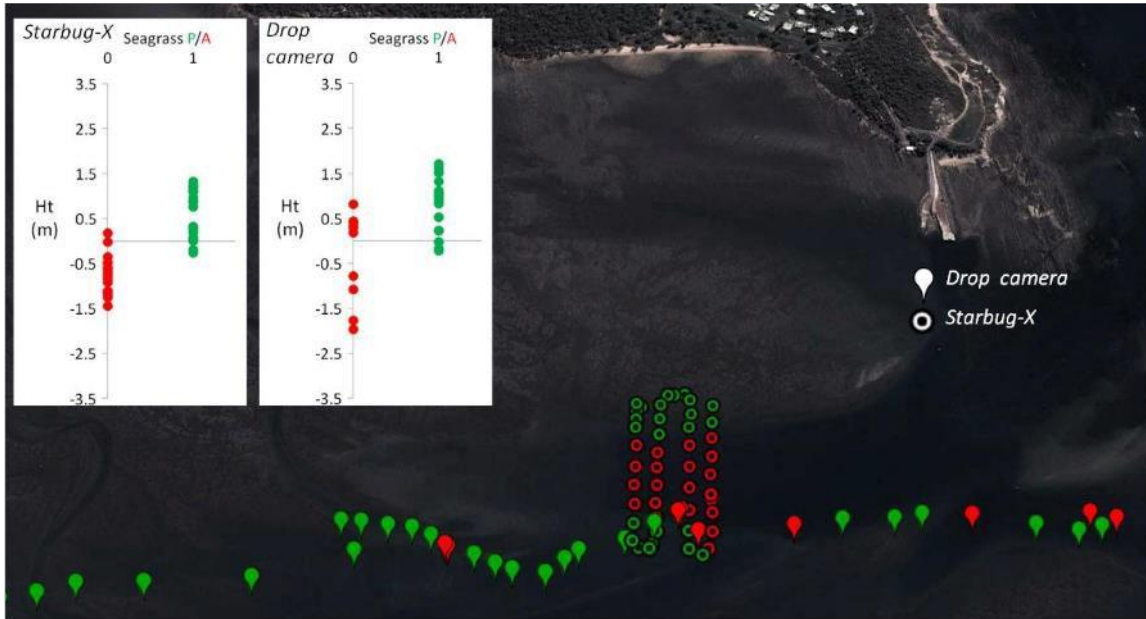
Figure 40 Comparison between the results obtained with the drop camera and the AUV Starbug-X at Pelican Banks North in September 2013 (green = presence, red = absence).

There was quite close agreement between the results obtained with the Starbug-X AUV and those of the drop camera (Figure 40). Visual comparison of the AUV tracks and the small boat track with the drop camera is also instructive. The vessel track is irregular and does not follow a straight line, while the track of the AUV is quite regular, despite the complex mission that followed a series of parallel transects.

Depth range estimates from the two methods also compare quite well with the two approaches producing maximum depth of seagrass distribution ranging between 0.23 m (drop camera) and 0.26 m (Starbug-X).

4 Discussion

4.1 Seagrass Distribution

One of the main aims of the seagrass sampling programs was to obtain estimates of maximum seagrass depth range that would provide a means of assessing the effectiveness of the seagrass biogeochemical model (Chapter III). Thus, we undertook sampling with a range of independent methods (grab, sledge, drop camera and AUV) as well as ensuring our results were appropriately comparable to those obtained by other independent seagrass studies in the area (e.g. Davies et al. 2012, Bryant 2014).

Sampling for seagrass depth range data in 2012 and 2013 confirmed the patchy nature of what remained of seagrass bed through most of the harbour area during this period. Many areas where seagrass beds had been described had cover and biomass values so low and/or so patchy that in some cases it was not possible to sample them. Wiggins Island stood out in this respect, and very little seagrass was found there in both 2012 and 2013 and even a change in sampling gear (from van Veen grab to naturalist dredge) was not effective at sampling these extremely patchy "beds". Similar challenges were faced by other groups sampling the seagrasses of the harbour at this time (e.g. Davies et al. 2012) who were in some cases (e.g. Wiggins Is.) required to establish new sites in order to obtain samples. Comparisons of our sampling in 2012 with samples at Pelican Banks obtained by Davies et al. (2012) showed similar values, where the sample sites coincided. This included sites such as those at the Pelican Banks which sustained much higher levels of seagrass biomass than almost all other sites in Gladstone Harbour. These sites are subjected to lower levels of turbidity than sites closer to the central harbour due to reduced tidal velocities and lower levels of sediment re-suspension, as well as benefitting from regular flushing with clearer, offshore waters entering through the passage between Curtis and Facing Islands. Another area of high seagrass cover and biomass was in the outer estuary of the Boyne River at South Trees, where *Zostera* biomass was equivalent at some sites to that found at Pelican Banks. This location is largely protected by a sand bar, reducing re-suspension due to wave action and mixing with turbid waters from the nearby harbour approaches. Despite the reasonable agreement of our sampling results with those from independent sampling carried out at approximately the same time (Davies et al. 2012) we were concerned that the effectiveness of the method of sampling we had employed, grab sampling in particular, had the potential to be affected by this patchiness.

Sampling in September 2013 employed a naturalist dredge in areas too turbid for image based sampling and occurred two months before the regular sampling conducted as part of long-term sampling in the Port Curtis and Rodds Bay area (Bryant et al. 2014). The method appeared to be quite effective in determining the presence or absence of seagrass as it showed close agreement with independent helicopter based visual sampling at low tide (Bryant et al. 2014). We recorded seagrass at all sites in the Narrows where Bryant et al. (2014) had reported seagrass, and at one site where it was not found (Redcliffe New). At sites in Fishermans Landing North and South, dredge sampling recorded seagrass at only one site whereas helicopter surveys reported extensive, though sparse, beds. At Compigne Island dredge sampling and subsequent inspections on-foot at low tide revealed seagrass was present only at Compigne East (bed 80; site C15 in this work) and not at bed 152 on the western side of Compigne Island.

Depth range sampling in 2013 revealed an area of moderate seagrass cover at the southeast of Quoin Island (North Banks 3 and 4)Throughout the rest of the harbour, including sites to the east of Facing Island and at sites in Rodds Bay, results were also in broad agreement between GISERA and independent sampling (Bryant et al. 2014).

Finally, the results of drop camera and AUV sampling of seagrass depth range at Pelican Banks showed very close agreement, to within a few centimetres. The use of AUVs shows promise as a means of surveying seagrass but was not viable in areas of high turbidity and/or high current flow such as prevail in much of Gladstone Harbour. It was effective in other areas such as Pelican Banks, Seal Rocks and, during suitable conditions, in parts of outer Rodds Bay.

4.2   Seagrass Depth Ranges

Maximum depths of seagrass beds throughout the harbour varied as expected with water quality, extending deeper where light penetration was greater. The greatest depths at which seagrasses were encountered were at sites offshore from Facing Island, where *Halophila spinulosa* was recorded at depths of over 20 m. However, since the maximum extent of these beds was not determined, these could not be included in the depth range analysis which was therefore restricted to seagrass beds within Gladstone Harbour. Interestingly, the shallowest margin of these offshore seagrasses appears to have receded into deeper water over the past decade (Bryant et al. 2014) and is now approximately two or more kilometres further offshore than in 2002. There is no consistent water quality/light attenuation data available for this area over the entire period but it would be interesting to assess regional trends in light penetration that might influence the growth of seagrass in this part of the region. Maximum depth of seagrass beds within the harbour ranged from -3.39 m to 1.42 m above datum. This depth range, when measured across the range of sites, corresponded to light levels of around 13% (±2.99 SE) of available surface PAR at Mean Low Water Neap Tide. Generally speaking seagrasses require an average of approximately 11% of surface irradiance (Duarte 1991) in order to survive. The levels we observed were very similar to this and also correspond almost exactly with the minimum levels needed to sustain *Zostera muelleri* in Gladstone Harbour (Chartrand et al. 2012). Periods of more than two weeks at less than 4.5-12 Mol PAR $m^{-2}.d^{-1}$ (Chartrand et al. 2012) were found to result in net reduction in seagrass cover and biomass. At the latitude of Gladstone, these values are between 13% and 36% of available surface PAR (~ 33 mol $m^{-2} d^{-1}$; Frouin and Murukami 2007) at MLWN, once again corresponding well with our observations. These critical light values are in a range similar to those for *Halodule uninervis* recorded on the GBR (Collier et al. 2012).

4.3   Seagrass distribution in relation to turtle habitat use

Distribution of seagrass biomass on Pelican Banks is concentrated largely in two areas of the northern Pelican Bank, one area being on the north-western shore, the other on the north-east of the bank along the top of a sandbank running parallel to the main channel between Curtis and Facing islands. South Pelican Bank supports considerably lower biomass of seagrass. The high cover/high biomass areas are shallower and dominated by *Zostera muelleri*. Distribution of both *Z. muelleris* and *H. ovalis* was similar which was somewhat unexpected in that *H. ovalis* is reported to have greater depth limits than *Z. muelleris* (Duarte 1991, Abal and Dennison 1996)

and has the ability to adapt its photo-physiology to facilitate growth in deeper, lower light habitats (Campbell et al 2007). *Zostera* also competes with *Halophila* and may overshade it at higher densities.

The northern Pelican Banks area of Gladstone Harbour likely supports higher densities of green turtles (*Chelonia mydas*) than any other part of the harbour (C Limpus pers. comm. 2012) and the centre of their habitat use is focused not on the areas of highest seagrass cover but on the slightly deeper adjacent areas to the south (Chapter IV) where *Zostera* and *Halophila* cover declines. The low cover or lack of seagrass in the centre of this area may be due to the slightly greater depth, but may also be due to the grazing activity of the turtles themselves (Lal et al. 2010).

4.4 Summary

The seagrass component of GISERA Marine was designed to complement existing seagrass monitoring of the cover, biomass and spatial extent of seagrass beds conducted through the Western Basin Project and as part of the Gladstone Port's long term seagrass monitoring objectives. In 2012 and 2013 the emphasis was placed on estimating biomass and depth ranges at a number of sites within and around Port Curtis (17 – 26 sites). Van veen grabs, naturalist dredges, a drop camera and an AUV were used to obtain these data.

Sampling for seagrass depth range data in 2012 and 2013 confirmed the patchy nature of what remained of seagrass beds through most of the harbour area during this period. Many areas where seagrass beds had been described had cover and biomass values so low and/or so patchy that in some cases it was not possible to sample them; Wiggins Island stood out in this respect. Other areas, where cover was greater (e.g. Pelican Banks), had comparable cover and biomass to those previously recorded. Areas of high seagrass cover included Pelican Banks and Boyne River at South Trees; both dominated by *Zostera muelleri*. Depth range sampling in 2013 revealed an area of moderate seagrass cover at the southeast of Quoin Island. Seagrass biomass measurements provided essential data for parameterization of the seagrass growth model (Chapter III).

Maximum depths of seagrass beds throughout the harbour varied with water quality, extending deeper where light penetration was greater. A clear relationship emerged between maximum depth of the seagrass beds and Secchi depth. Maximum depth of seagrass beds within the harbour ranged from -3.39 m to 1.42 m above datum. This depth range, when measured across the range of sites, corresponded to light levels of around 13% (±2.99 SE) of available surface PAR at Mean Low Water Neap Tide. These levels correspond almost exactly with the minimum levels needed to sustain *Zostera muelleri* in Gladstone Harbour. The depth range measurements were used to validate the seagrass growth model, with model results and observations showing substantial agreement.

There was a close agreement between the results obtained with the Starbug-X AUV and those of the drop camera. The use of AUVs shows promise as a means of surveying seagrass but was not viable in areas of high turbidity and/or high current flow.

In 2014, the focus was on one area, the Pelican Banks, which corresponded to high utilization by green turtles. A grid of parallel transects was adopted and seagrass % cover was quantified using underwater still photography within a 0.5 x 0.5 m quadrat. The higher cover/higher

biomass areas at Pelican banks are shallower and dominated by *Zostera muelleri*. Distribution of both *Z. muelleri* and *Halophila ovalis* was similar.

The northern Pelican Banks area likely supports higher densities of green turtles than any other part of the harbour and the centre of their overall habitat use is focused not on the areas of highest seagrass cover but on the slightly deeper adjacent areas to the south where *Zostera* and *Halophila* cover declines. However habitat use at high tide shifted to high cover areas of the Pelican banks, thus the seagrass measurements enabled us to explain this tidal variation.

Chapter III Port Curtis Biogeochemical and Seagrass Growth Model

Mark Baird, Russ Babcock, Kadija Oubelkheir, Matthew Adams, Kate O'Brien, Karen   Wild-Allen

CSIRO

1 Introduction

Mathematical modelling is an essential tool for assessing how different environmental impacts affect important coastal habitats, and for effectively guiding investment in resource management. Seagrass ecosystems are economically and ecologically valuable, and are threatened by stressors such as water quality decline that act across a range of scales (Orth et al. 2006; Grech et al. 2012). The reason seagrasses provide so many valuable ecosystem services is that they act as ecosystem engineers, creating structures and modifying environmental conditions which support a wide range of trophic processes and different species (Hastings et al. 2007).

Strong feedbacks between seagrass processes and environmental conditions (including water column nutrients, water clarity and sediment resuspension) mean that incorporating seagrass in ecosystem models may be important for accurate water quality predictions in shallow-water coastal ecosystems (Webster and Harris 2004). Conversely, modelling seagrass in isolation without accounting for interactions with water quality and sediment resuspension, may fail to capture important remote forcing of seagrass communities (van der Heide et al. 2007).

Availability of photosynthetically active radiation is a key requirement for seagrass growth, and a limiting resource in many seagrass habitats (Ralph et al. 2007; Collier et al. 2012). Seagrass photosynthesis responds to light following a saturating curve, and this process has been modelled by fitting empirical data to various mathematical configurations, e.g. hyperbolic tangent function, adjusted to account for carrying capacity (Burd and Dunton 2001), Monod function (Elkalay et al. 2003), or an asymptotic exponential function (Newell and Koch 2004; Zimmerman et al. 1995). However, photosynthesis-irradiance curves are strongly affected by preceding environmental conditions, such as long and short term light history, and temperature (Kehoe et al. 2015; O'Brien et al. 2009). Some phytoplankton photosynthesis models use measurable mechanistic parameters (Han 2002) or allometric relationships to address this challenge (Baird and Suthers 2007). There is a strong need for such mechanistic relationship in seagrass models (Baird et al. 2003; Macreadie et al. 2014).

The motivation of the seagrass model developed here is twofold: firstly to develop a mechanistic formulation for seagrass response to light, which depends on measurable, transferable parameters, and overcomes some of the limitations of standard photosynthesis-irradiance formulations. Secondly, to represent seagrass processes as they impact on ecosystem function in shallow-water coastal environments, in a complex ecosystem model that also quantifies other water column (phytoplankton), benthic (macroalgae, corals) and sediment (microphytobenthos) primary producers. Where differences exist in the supply of nutrients and light between different primary producers, these differences are given greater attention in the model parameterisation (Baird et al. 2003; CSIRO Coastal Environmental Modelling Team 2014). Thus, the seagrass model component investigated here has nutrient uptake from multiple sediment layers (to distinguish it from macroalgae), geometric calculations of light

uptake that consider the 2 dimensionality of leaves (to distinguish it from 3 dimensional microalgae (Baird and Middleton 2004)), and non-Redfield stoichiometries. However many other details, such as light scattering within a seagrass canopy (Zimmerman 2003) or details of photo-physiology, that are justifiable in a model of a single-species seagrass meadow, have not been included in order to keep the complexity of the ecosystem model manageable.

Seagrass communities are often split into shallow and a deep water species, with deeper water seagrass species recovering faster from disturbance than those present in shallow water (Rasheed et al. 2014). As this dynamic may be important in Gladstone Harbour, we have configured the model with two seagrass species, with the contrasting behaviour of the two species providing insights into the model behaviour.

In this chapter, a two-species seagrass model is derived which introduces new parameterisations including constraints of leaf geometry, as well as root morphology and is forced by spectrally-resolved downwelling light. The model is applied in a highly-impacted estuarine environment with strong tides in which light is the most common limiting factor to seagrass growth. The model is assessed against spatially-resolved biomass and percent coverage maps of the two seagrass species. Finally, analytical calculations are undertaken to understand the behaviour of the new model parameterisations.

2 Methods

2.1 Study site and observations

Gladstone Harbour is a macro-tidal, sub-tropical estuary with large barotropic tides of amplitudes approaching 2 m (Herzfeld et al. 2015). The tides undergo a neap-spring cycle with a period of approximately 14 days, with a spring tide range of 4 m and neap tide range of 1 m, with maximum currents of 2 m s^{-1}). Fresh water flows may propagate through the Narrows as a result of flooding from the nearby Fitzroy River to the north, and the Calliope River which discharges into the estuary through Gladstone. The large tides ensure that the water column is vertically well mixed most of the time, and are also responsible for significant resuspension of fine sediment, resulting in a generally turbid water column. The region is characterized by extensive areas of tidal flats that become exposed at low tide and large areas of mangroves fringing the estuary.

Seagrass distribution in Gladstone Harbour has been intensively monitored and studied (Petrou et al. 2013; Rasheed et al. 2013; Chartrand et al. 2012; Petus et al. submitted). Seagrass distribution data is available from monitoring performed between 2002 and 2013 inclusive as part of the long-term monitoring in Gladstone Harbour and Rodds Bay (Rasheed et al. 2005; Taylor et al. 2007; Rasheed et al. 2006, 2008b; Chartrand et al. 2009; Thomas et al. 2010; Davies et al. 2013; Rasheed et al. 2014). These data, always collected in October to December, consists of biomass estimates (g DW m^{-2}) for the species *Zostera muelleri, Halophila ovalis, Halophila decipiens, Halophila spinulosa* and *Halodule uninervis* (wide and thin morphologies), and qualitative description of sediment type (e.g. fine sand, sand, mud, shell or a combination thereof), from seagrass meadows named Wiggins Island, South Fishermans Landing, North Fishermans Landing, Pelican Banks, Quoin Island, South Trees, Rodds Bay, Black Swan and Channel Islands. The monitoring also looked for the species *Cymodocea rotundata*, but it was never observed.

In addition to these observations, this chapter details observations during the GISERA project (Chapter II).

2.2 Seagrass model

The CSIRO Environmental Modelling Suite is used in this paper to model the biogeochemical processes in Gladstone Harbour, and is described in detail elsewhere (Wild-Allen et al. 2010; CSIRO Coastal Environmental Modelling Team 2014). Here we will only describe the seagrass processes, quantifying their local rates of change on water column, epibenthic and sedimentary state variables (Table 2.1).

Table 2.1 State and derived variables for the seagrass model. For simplicity in the equations all dissolved constituents are given in grams, although elsewhere they are shown in milligrams. The bottom water column thickness varies is spatially-variable, depending on bathymetry. The 4 sediment layers have nominal thicknesses of 0.005, 0.02, 0.08, 0.295 m, which are altered through the simulation by deposition and resuspension.

Variable	Symbol	Units
Downwelling irradiance	E_d	W m^{-2}
Porewater DIN concentration	N_s	g N m^{-3}
Porewater DIP concentration	P_s	g P m^{-3}
Water column DIC concentration	DIC	g C m^{-3}
Water column oxygen concentration	$[O_2]$	g O m^{-3}
Above-ground seagrass biomass	SG_A	g N m^{-2}
Below-ground seagrass biomass	SG_B	g N m^{-2}
Detritus at 550:30:1 in sediment	$D_{Atk,sed}$	g N m^{-3}
Effective projected area of seagrass	A_{eff}	m^2 m^{-2}
Bottom stress	τ	N m^{-2}
Thickness of sediment layer l	$h_{s,l}$	m
Bottom water layer thickness	h_{wc}	m
Wavelength	λ	nm
Translocation rate	Υ	g N m^{-2} s^{-1}
Porosity	ϕ	-

Seagrass biomass is quantified in g N per m^2 with a constant, non-Redfield stoichiometry (C:N:P = 550:30:1) for both above-ground, SG_A, and below- ground, SG_B, biomass, and can translocate organic matter at this constant stoichiometry between the two stores of biomass. Growth, which we define as the input of carbon, nutrient and phosphorus resources into the seagrass biomass from the environment, occurs only in the above-ground biomass, but losses (grazing, decay, etc.) occur in both. Two seagrass varieties, nominally *Zostera* and *Halophila*, are represented in the model. For both seagrass species considered, the equations used are identical but the parameters vary to reflect their individual growth patterns/behaviours. The general equations for the dynamics of above-ground and below-ground biomass are:

$$\frac{\partial SG_A}{\partial t} = + \text{ growth } - \text{ loss } +/- \text{ translocation} \tag{1}$$

$$\frac{\partial SG_B}{\partial t} = - \text{ loss } -/+ \text{ translocation} \tag{2}$$

All these rates are in units of g N m^{-2} d^{-1}. In the following sections, we define the rates for growth, loss and translocation.

Table 2.2 Equations for the seagrass model. Other constants and parameters are defined in Table 2.3. The equation for organic matter formation gives the stoichiometric constants; 14 g N mol N^{-1};12 g C mol C^{-1}; 31 g P mol P^{-1}; 32 g O mol O^{-1}.

$$\frac{\partial N_{s,l}}{\partial t} = -f_{N,l}/\left(h_{s,l}\phi_l\right) \tag{15}$$

$$\frac{\partial P_{s,l}}{\partial t} = -f_{P,l}\frac{1}{30}\frac{31}{14}/\left(h_{s,l}\phi_l\right) \tag{16}$$

$$\frac{\partial DIC}{\partial t} = -\frac{550}{30}\frac{12}{14}\left(\mu_{SG_A}SG_A\right)/h_{wc} \tag{17}$$

$$\frac{\partial [O_2]}{\partial t} = \frac{716}{30}\frac{32}{14}\left(\mu_{SG_A}SG_A\right)/h_{wc} \tag{18}$$

$$\frac{\partial SG_A}{\partial t} = \mu_{SG_A}SG_A - \zeta_{SG_A}\left(SG_A - \frac{f_{seed}}{\Omega_{SG}}(1-f_{below})\right) - \Upsilon \tag{19}$$

$$\frac{\partial SG_B}{\partial t} = -\zeta_{SG_B}\left(SG_B - \frac{f_{seed}}{\Omega_{SG}}f_{below}\right) + \Upsilon \tag{20}$$

$$\frac{\partial D_{Atk,sed}}{\partial t} = \frac{\zeta_{SG_A}\left(SG_A - \frac{f_{seed}}{\Omega_{SG}}(1-f_{below})\right) + \zeta_{SG_B}\left(SG_B - \frac{f_{seed}}{\Omega_{SG}}f_{below}\right)}{h_{sed}\phi} \tag{21}$$

$$\tag{22}$$

$$\mu_{SG_A} = \min\left[\frac{\mu_{SG}^{max}\overline{N_s}}{K_{SG,N}+\overline{N_s}}, \frac{\mu_{SG}^{max}\overline{P_s}}{K_{SG,P}+\overline{P_s}}, \frac{30}{5500}14\frac{\max(0,k_I-k_{resp})}{SG_A}\right] \tag{23}$$

$$\overline{N_s} = \frac{\sum_{l=1}^{L}N_{s,l}h_{s,l}\phi_l}{\sum_{l=1}^{L}h_{s,l}\phi_l} \tag{24}$$

$$\overline{P_s} = \frac{\sum_{l=1}^{L}P_{s,l}h_{s,l}\phi_l}{\sum_{l=1}^{L}h_{s,l}\phi_l} \tag{25}$$

$$f_{N,l} = \frac{N_{s,l}h_{s,l}\phi_l}{\sum_{l=1}^{L}N_{s,l}h_{s,l}\phi_l}\mu_{SG}SG_A \tag{26}$$

$$f_{P,l} = \frac{P_{s,l}h_{s,l}\phi_l}{\sum_{l=1}^{L}P_{s,l}h_{s,l}\phi_l}\mu_{SG}SG_A \tag{27}$$

$$k_I = \frac{(10^9 hc)^{-1}}{A_V}\int E_{d,\lambda}\left(1-\exp\left(-A_{L,\lambda}\Omega_{SG}SG_A\sin\beta_{blade}\right)\right)\lambda d\lambda \tag{28}$$

$$k_{resp} = 2\left(E_{comp}A_L\Omega_{SG}\sin\beta_{blade} - \frac{5500}{30}\frac{1}{14}\zeta_{SG_A}\right)SG_A \tag{29}$$

$$\Upsilon = \left(f_{below} - \frac{SG_B}{SG_B+SG_A}\right)(SG_A+SG_B)\tau_{tran} \tag{30}$$

$$550CO_2 + 30NO_3^- + PO_4^{3-} + 792H_2O \tag{31}$$
$$\xrightarrow{5500 \text{ photons}} (CH_2O)_{550}(NH_3)_{30}H_3PO_4 + 716O_2 + 391H^+$$
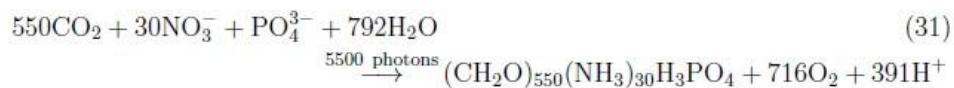
The realised seagrass growth rate, μ, is represented using a law of the minimum formulation (Table 2.2, Eq. 23), limited by either by nitrogen, phosphorus, light availability or the maximum growth rate. We first derive the individual uptake rates for each of these factors, before determining which is the most limiting factor, and then use this factor to calculate the realised growth rate, and therefore the realised nutrient uptake rates. But before looking at the individual rates, we need to consider the area on the bottom taken up by the seagrass biomass, as this impacts on light capture.

Relationship between biomass and percent coverage

At low biomass, the seagrass community is composed of a few specimens spread over a small fraction of the bottom, with no interaction between the nutrient and energy acquisition of individual specimens. Thus, at low biomass the areal fluxes are a linear function of the biomass.

As biomass increases, the individuals begin to cover a significant fraction of the bottom. For nutrient and light fluxes that are constant per unit area, such as downwelling irradiance and sediment releases, the flux per unit biomass decreases with increasing biomass. Some processes, such as photosynthesis in a thick seagrass meadow become independent of biomass (Atkinson 1992) as the bottom becomes completely covered. To capture the non-linear effect of biomass on benthic processes, we use an effective projected area fraction, A_{eff}:

$$A_{eff} = 1 - \exp(-\Omega_{SG}\ SG_A) \qquad (3)$$

where A_{eff} is the effective projected area fraction of the benthic community ($m^2\ m^{-2}$), SG_A is the above ground seagrass biomass present as nitrogen (g N m^{-2}), and Ω_{SG} is the nitrogen-specific leaf area coefficient (m^2 g N^{-1}). For a derivation of Eq. 3, and a comparison to data from Chapter II, see Appendix C.

The parameter Ω_{SG} is critical: it provides a means of converting between biomass and fractions of the bottom covered, and is used in calculating the absorption cross-section of the leaf. That Ω_{SG} has a simple physical explanation, and can be determined from commonly undertaken morphological measurement (Cambridge and Lambers 1998), gives us confidence in its use.

Nutrient uptake

Dissolved inorganic nutrients are taken up by the root system following a Michaelis-Menton form:

$$k_N = \frac{\mu_{SG}^{\max} N_s}{K_{SG,N} + N_s} \qquad (4)$$

where μ_{SG}^{max} is the maximum growth rate of the above-ground seagrass biomass, N_s is the concentration of dissolved inorganic nitrogen in the sediment pore waters of porosity ϕ, and $K_{SG,N}$ is the concentration at which nutrient uptake is half the maximum.

Nutrients are taken from the sediment porewaters to a depth of z_{root}. The nutrient concentration used in Eq. 4 is weighted by the volume of porewater in each of L layers:

$$\overline{N_s} = \frac{\sum_{l=1}^{L} N_{s,l} h_{s,l} \phi_l}{\sum_{l=1}^{L} h_{s,l} \phi_l} \tag{5}$$

where $h_{s,l}$ and ϕ_l are the thickness and porosity of sediment layer l.

As a further caveat, ammonia is preferentially absorbed relative to nitrate, up to the maximum absorption rate defined by the initial slope of the up-take versus concentration curve (for further information, see CSIRO Coastal Environmental Modelling Team (2014)).

The nutrient taken up from each layer, as a fraction of the total growth rate, $\mu_{SG}SG_A$, also matches this weighting. Thus the nutrient uptake from layer l is given by:

$$f_{N,l} = \frac{N_{s,l} h_{s,l} \phi_l}{\sum_{l=1}^{L} N_{s,l} h_{s,l} \phi_l} \mu_{SG} SG_A \tag{6}$$

A similar set of equations to those listed above for nitrogen are also used for phosphorus uptake (Table 2.2).

Light capture

The spectrally-resolved leaf absorbance, $A_{L,\lambda}$, of two common Australian seagrass species, *Zostera muelleri* and *Halophila ovalis*, are given in Figure 41. It is assumed that when co-existing *Z. muelleri* shades *H. ovalis*.
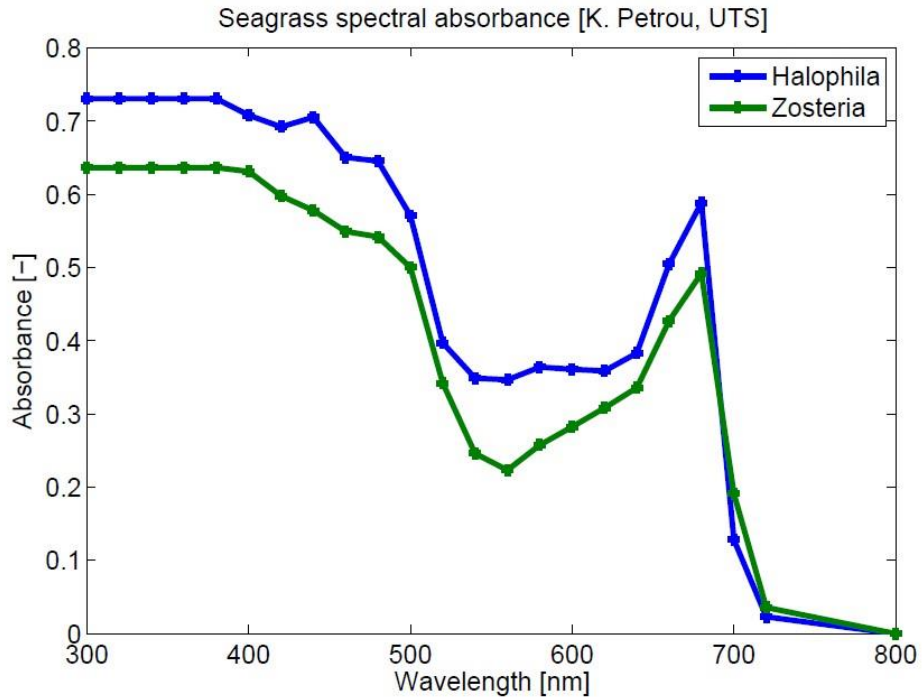
Figure 41 The spectrally-resolved leaf absorbance, $A_{L,\lambda}$, of two common Australian seagrass species from Gladstone Harbour (Petrou et al. 2013).

The light below successive seagrass canopies is given by:

$$E_{d,below,\lambda} = E_{d,above,\lambda} e^{-A_\lambda \Omega_{SG} SG_A \sin \beta_{blade}} \qquad (7)$$

where $E_{d,above,\lambda}$ is the downwelling light above the canopy, $E_{d,below,\lambda}$ is the downwelling irradiance below the canopy, A_λ is the absorbance of the leaf, Ω_{SG} is the nitrogen-specific leaf area, SG_A is the leaf nitrogen biomass, and $\sin \beta_{blade}$ is the sine of the nadir bending angle of the leaf. This formulation captures the phenomena that seagrass biomass cannot be infinitely spread on the bottom, but must be in leaves that shade a fraction of the bottom, while the remaining light passes through the canopy without attenuation.

If we consider a spectrally-resolved light field, with light specified as a flux per nm, the rate of photon capture by seagrass is given by:

$$k_I = \frac{(10^9 hc)^{-1}}{A_V} \int E_{d,\lambda} \left(1 - \exp\left(-A_{L,\lambda} \Omega_{SG} SG_A \sin \beta_{blade}\right)\right) \lambda d\lambda \qquad (8)$$

Where inside the integrand: $E_{d,\lambda}$ (W nm^{-1} m^{-2}) is the incident light at depth d within the wavelength band $d\lambda$ (nm), $A_{L,\lambda}$ (no units) is the spectrally-resolved absorbance of the seagrass leaf (see Figure 41) and λ is the light wavelength (nm). The light captured by seagrass is integrated over all photosynthetically-active wavelengths (W m^{-2}) and is then multiplied by $(1/(10^9 hcA_V))$. The factor $(1/(10^9 hcA_V))$ contains 10^9 nm m^{-1} (which accounts for the typical representation of wavelength λ in nm) as well as the fundamental constants $h = 6.626 \times 10^{-34}$ J s, $c = 2.998 \times 10^8$ m s^{-1}, $A_V = 6.02 \times 10^{23}$ mol^{-1}, in order to convert the light capture to units of mol photon m^{-2} s^{-1}.

A further factor (30 × 14/5500) converts mol photon m^{-2} s^{-1} to g N m^{-2} s^{-1}: according to Eq. (31), 5500 mol photon are required to fix 30 mol N, and the molar mass of nitrogen is 14 g N mol N^{-1}.

As shown in Eq. 3, the term $1 - \exp(-\Omega_{SG} SG_A)$ gives the effective projected area fraction of the community (see also Appendix C). In the case of light absorption of seagrass, the exponent is multiplied by the leaf absorbance, $A_{L,\lambda}$, to account for the transparency of the leaves, and sin β_{blade} to account for the orientation of the leaf. At low seagrass biomass, absorption at wavelength λ is equal to the $E_{d,\lambda} A_{L,\lambda} \Omega_{SG} SG_A \sin \beta_{blade}$, initially increasing linearly with biomass as all leaves are exposed to full light (i.e. there is no self-shading). As biomass increases, the absorption by the community asymptotes to $E_{d,\lambda}$, at which point increasing biomass does not increase the absorption as all light is already absorbed. These end points arise for the same reasons as given in Eq. 3 for A_{eff}.

Respiration

The seagrass model does not consider internal reserves of energy and nutrients, and therefore cannot respire using energy from reserves like in the representation of microalgae in the biogeochemical model (CSIRO Coastal Environmental Modelling Team 2014). Thus growth is represented as net production, not gross production. Given growth timescales of many days, this is a reasonable approximation for the purposes of estimating seagrass biomass, and daily

fluxes of metabolites. To include respiration in the model the concept of a minimum light requirement is used.

Critical thresholds for seagrass growth/decline are typically defined as "minimum light requirements" (MLR), expressed as either percentage of surface irradiance (e.g. Duarte (1991)) or in daily dose in mol photon $m^{-2} d^{-1}$ (recently reviewed in Table 2.2 of York and Smith (2013)). The latter is more helpful as it can be generalised to seagrass ecosystems outside of the study area of interest. The daily dose measurements (MLR) are used in the model as the term E_{comp} (mol photon $m^{-2} d^{-1}$).

Minimum light requirements should only affect seagrass growth when light is the limiting factor. Recent experimental work has suggested that daytime respiration may be significantly larger than night time respiration (Rheuban et al. 2014). Hence we include the MLR in the model as a reduction of the photosynthesis rate. We will later assume (in Section 3.6) that the mortality of above-ground seagrass nitrogen mass occurs approximately at a rate of $\zeta_{SGA} SG_A$ (ignoring the minor adjustment of this mortality rate due to the viable seedbank), and this rate is assumed to be an order of magnitude larger than the below-ground loss (see parameters in Table 2.3). We choose the daytime respiration rate k_{resp} to balance light-limited growth and the mortality rate when the daily light is equal to E_{comp}. Observations from Gladstone Harbour suggest that *Zostera* is unable to survive at less than 4.5 mol photon $m^{-2} d^{-1}$ (Petrou et al. 2013). Presuming this is for a leaf without self-shading (i.e. absorption given by $A_L \Omega_{SG} SG_A \sin \beta_{blade}$), the loss rate of photons through respiration is given by:

$$k_{resp} = 2 \left(E_{comp} A_L \Omega_{SG} \sin \beta_{blade} - \frac{5500}{30} \frac{1}{14} \zeta_{SGA} \right) SG_A \qquad (9)$$

The respiration rate, k_{resp}, is subtracted from the rate of absorption, k_I, to give the growth rate at a particular light intensity. If k_{resp} exceeds k_I, then no growth occurs (Table 2.2). The factor of two accounts for mortality occurring throughout a 24 period, but being only included in the respiration calculations during daylight hours.

Finally, it is worth noting that the limiting terms for nutrient uptake have units of one over time, so that to compare rates of light limitation in mol photon $m^{-2} s^{-1}$, we need to divide by the seagrass biomass (Eq. 23).

Translocation between above- and below-ground biomass

Translocation has been shown experimentally to occur both upwards (Wetzel and Penhale 1979; Penhale and Thayer 1980) and downwards (Moriarty et al. 1986; Zimmerman and Alberte 1996; Kaldy et al. 2013). Translocation is modelled as a rate, Υ, with a time constant, τ_{tran}, at which the above and below ground biomasses approach a steady state, specified by a fraction of below ground biomass, f_{below}.

$$\Upsilon = \left(f_{below} - \frac{SG_B}{SG_B + SG_A} \right) (SG_A + SG_B) \tau_{tran}$$

This formulation, unlike previous ones used in seagrass models, allows translocation in both directions rather than just downwards (Burd and Dunton 2001; Carr et al. 2012).

Table 2.3 Constants and parameter values used to model seagrass. [a] ×2 for nighttime ×2 for roots; [b] *Zostera* - calculated from leaf characteristics in (Kemp et al. 1987;Hansen et al. 2000), *Halophia ovalis* - calculated from leaf dimensions in Vermaat et al. (1995) - Ω_{SG} can also be determined from specific leaf area such as determined in Cambridge and Lambers (1998) for 9 Australian seagrass species; [c] Spectrally-re-solved values in Figure 41; [d] Chapter II; [e] loosely based on Kaldy et al. (2013); [f] *Thalassia testudinum* Gras et al. (2003); [g] *Thalassia testudinum* (Lee and Dunton 1999); [h] Chartrand et al. (2012); Longstaff (2003); [i] Roberts (1993).

	Symbol	*Zostera muelleri*	*Halophila ovalis*	Units
Parameters				
[a]Maximum growth rate of seagrass	μ_{SG}^{max}	0.4	0.4	d^{-1}
[b]Nitrogen-specific area of seagrass	Ω_{SG}	1.5	1.9	$(g\ N\ m^{-2})^{-1}$
[c]Leaf absorbance	$A_{L,\lambda}$	~ 0.7	~ 0.7	-
[d]Fraction biomass below ground	f_{below}	0.75	0.5	-
[e]Translocation rate	τ_{tran}	0.033	0.033	d^{-1}
[f]Half-saturation P uptake	$K_{SG,P}$	96	96	$mg\ P\ m^{-3}$
[g]Half-saturation N uptake	$K_{SG,N}$	420	420	$mg\ N\ m^{-3}$
[h]Compensation scalar PAR irradiance	E_{comp}	4.5	2.8	$mol\ photon\ m^{-2}\ d^{-1}$
[h]Leaf loss rate	ζ_{SG_A}	0.03	0.06	d^{-1}
[h]Root loss rate	ζ_{SG_B}	0.004	0.004	d^{-1}
Seed biomass as a fraction of 63 % cover	f_{seed}	0.01	0.01	-
[i]Seagrass root depth	z_{root}	0.15	0.08	m
Sine of nadir canopy bending angle	$\sin \beta_{blade}$	0.5	1.0	-

Mortality

A linear mortality rate is defined for above ground biomass, ζ_{SGA}, transforming above ground seagrass biomass into labile detritus at the Atkinson ratio. Additionally, seeds are represented as a component of the seagrass biomass that are unaffected by mortality. The fraction of the total seagrass nitrogen biomass at $1/\Omega_{SG}$ that is seeds is given by f_{seed}. Thus, the above ground mortality is:

$$\frac{\partial SG_A}{\partial t} = -\zeta_{SG_A}\left(SG_A - \frac{f_{seed}}{\Omega_{SG}}(1-f_{below})\right) \qquad (10)$$

The inclusion of the terms indicating seed fractions f_{seed} in the above equation effectively introduces a minimum of $f_{seed}\Omega_{SG}$ for seagrass biomass in the model. This minimum represents the seedbank, which is assumed to be always viable over the timescales of the simulations performed here.

The below ground mortality becomes:

$$\frac{\partial SG_B}{\partial t} = -\zeta_{SG_B}\left(SG_B - \frac{f_{seed}}{\Omega_{SG}}f_{below}\right) \qquad (11)$$

In equations (10) and (11), the factors $(1 - f_{below})$ and f_{below} respectively are included so that the steady state for seagrass areas that have reduced to only their seedbank possesses a fraction of below-ground biomass equal to f_{below}.

Temperature dependence

Seagrass maximum growth rate and mortality rate, as well other biogeochemical process rates such as remineralisation rates, have a temperature dependence that is determined from:

$$r_T = r_{Tref}Q_{10}^{(T-T_{ref})/10} \qquad (12)$$

where r_T is the physiological rate parameter at temperature T, T_{ref} is the reference temperature (nominally 20∘C), *Q10* is the Q10 temperature coefficient and represents the rate of change of a biological rate as a result of increasing temperature by 10°C.

2.3 Model configuration

The CSIRO Environmental Modelling Suite (EMS) has been developed over 20 years to model coupled physical, optical, sediment and biogeochemical processes in marine and estuarine environments (Wild-Allen et al. 2010; CSIRO Coastal Environmental Modelling Team 2014). The hydrodynamic model is a fully three-dimensional finite-difference baroclinic model based on the three dimensional equations of momentum, continuity and conservation of heat and salt, employing the hydrostatic and Boussinesq assumptions (Herzfeld 2006; Schiller et al. 2014). The equations of motion are discretized on a finite difference stencil corresponding to the Arakawa C grid. In the vertical z-coordinate scheme, there are 20 fixed z-levels. The atmospheric forcing products (wind, pressure, heat fluxes) are supplied by the Bureau of Meteorology (BOM) reanalysis products. The local grid open boundary was forced with temperature, salinity and velocity (with local flux adjustment) derived from the regional grid. A semi-Lagrangian advection scheme is used to transport biogeochemical tracers. The sediment model (Margvelashvili 2009) represents the processes of resuspension, sinking and flocculation of 4 particle sizes.

The biogeochemical model is organised into 3 zones: pelagic, epibenthic and sediment. The epibenthic zone overlaps with the lowest pelagic layer and the top sediment layer, sharing the same dissolved and suspended particulate material fields. The sediment is modelled in multiple layers with a thin layer of easily resuspendable material overlying thicker layers of more consolidated sediment. Dissolved and particulate biogeochemical tracers are advected and diffused throughout the model domain in an identical fashion to temperature and salinity. Additionally, biogeochemical particulate substances sink and are resuspended in the same way

as sediment particles. Biogeochemical processes are organized into pelagic processes of phytoplankton and zooplankton growth and mortality, detritus remineralisation and fluxes of dissolved oxygen, nitrogen and phosphorus; epibenthic processes of growth and mortality of macroalgae and seagrass, and sediment based processes of phytoplankton mortality, microphytobenthos growth, detrital remineralisation and fluxes of dissolved substances.

The biogeochemical model considers four groups of microalgae (small and large phytoplankton, trichodesmium and microphytobenthos) and three macrophyte types (seagrass species *Zostera* and *Halophila*, macroalgae). Photosynthetic growth is determined by concentrations of dissolved nutrients (nitrogen and phosphate) and photosynthetically active radiation. Autotrophs take up dissolved ammonium, nitrate, phosphate and inorganic carbon. Microalgae incorporate carbon (C), nitrogen (N) and phosphorus (P) at the Redfield ratio (106C:16N:1P) while macrophytes do so at the Atkinson ratio (550C:30N:1P). Microalgae contain two pigments (chlorophyll a and an accessory pigment), and have variable carbon:pigment ratios determined using a photoadaptation model.

Micro- and meso-zooplankton graze on small and large phytoplankton respectively, at rates determined by particle encounter rates and maximum ingestion rates. Half of grazed material is released as dissolved and particulate carbon, nitrogen and phosphate, with the remainder forming detritus. Additional detritus accumulates by mortality. Detritus and dissolved organic substances are remineralised into inorganic carbon, nitrogen and phosphate with labile detritus transformed most rapidly (days), refractory detritus slower (months) and dissolved organic material transformed over the longest timescales (years). The production (by photosynthesis) and consumption (by respiration and remineralisation) of dissolved oxygen is also included in the model and, depending on prevailing concentrations, facilitates or inhibits the oxidation of ammonia to nitrate and its subsequent denitrification to di-nitrogen gas which is then lost from the system. The optical model considers the processes of absorption and scattering by clear water, coloured dissolved organic matter (CDOM), non-algal particulates (NAP) and phytoplankton cells. First the inherent optical properties (IOPs), such as total phytoplankton absorption at a specific wavelength, are calculated from the model state variables (e.g. phytoplankton chlorophyll biomass) and model parameters (e.g. cell radius). The optical model then solves for the apparent optical properties (AOPs), such as the spectrally-resolved scalar irradiance, from the surface downwelling light field and the IOPs. The optical model is solved at 23 wavelengths (CSIRO Coastal Environmental Modelling Team 2014).

The Gladstone Harbour hydrodynamic model configuration is based on Herzfeld et al. (2004), with the inclusion the Calliope and Boyne Rivers to the top of their tidal limits (Herzfeld et al. 2015). The model has two boundaries, an ocean boundary and flow from the north through the Narrows. Two rivers are represented as point sources of water and catchment loads (Table 2.4). The ocean boundary conditions are space and time varying for hydrodynamic and biogeochemical quantities was supplied from the 4 km resolution eReefs model (Schiller et al. 2014).

The simulation was run from 1 September 2010 through to 1 September 2012. The initial conditions for the water column and sediment properties were downscaled from the eReefs model initial conditions for 1 September 2012. Initial seagrass distributions for *Zostera* were

0.01 / Ω_{SG}, representing 1% of seagrass coverage, in areas identified in the Mackenzie seagrass database as having seagrass in the last 20 years. In contrast *Halophila* was given a biomass of 0.01/ Ω_{SGH} everywhere. The below ground fraction was initialised as $SG_B = f_{below}\,SG_A$ for both species.

Table 2.4 River boundary conditions based on Gladstone Harbour and Tributaries Comparison of Current and Historical Water Quality October 2011, and setting from "dry tropical" rivers in eReefs.

Constituent	Symbol	Calliope	Boyne
Diss. Inorganic Carbon [mg m^{-3}]	DIC	6000	6000
Diss. Inorganic Phosphorus [mg m^{-3}]	P	4.2	4.2
Ammonia [mg m^{-3}]	$[NH_4]$	0.1	0.1
Nitrate [mg m^{-3}]	$[NO_3]$	171	171
Total Alkalinity [mmol m^{-3}]	A_T	900.0	900.0
Dissolved Oxygen [mg m^{-3}]	$[O_2]$	5854	5854
Labile Detritus Red [mg m^{-3}]	D_{Red}	43.5	43.5
Labile Detritus Atk [mg m^{-3}]	D_{Atk}	0	0
Ref. Det. Carbon [mg m^{-3}]	D_C	670	670
Ref. Det. Nitrogen [mg m^{-3}]	D_N	101.5	101.5
Ref. Det. Phosphorus [mg m^{-3}]	D_P	22.4	22.4
Diss. Organic Carbon [mg m^{-3}]	O_C	528	528
Diss. Organic Nitrogen [mg m^{-3}]	O_N	80	80
Diss. Organic Phosphorus [mg m^{-3}]	O_P	5.8	5.8

3 Results and Discussion

3.1 Brief summary of circulation, optical properties and biogeochemistry

The effect of circulation on water quality can be summarised by the mean duration a parcel of water spends in the estuary. A spatially-resolved age tracers (Mongin and Baird 2014; CSIRO Coastal Environmental Modelling Team 2014) shows that the longest 'residence' time of water in the estuary was during winter and spring, suggesting that during these times ocean flushing is less likely to improve water quality, with autumn being the period of most ocean influence (Figure 42).
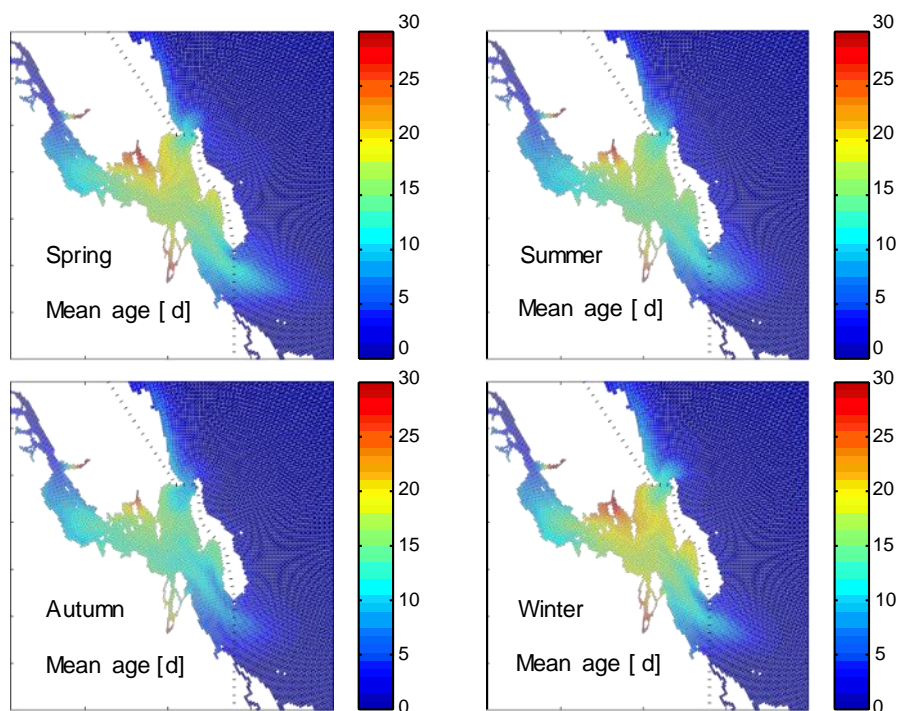
Figure 42 Spatially- and seasonally- resolved age of the water within Gladstone Harbour.

The in-water light field in Gladstone Harbour is dominated by the tides. The large tides (up to ±3 m), and the intermittent and often extremely low freshwater input, provide the major source of suspended particles to the water column. The settling time for particles is longer than the slack period between flood and ebb tides in the semi-diurnal signal. Thus, the dominant determinant of the vertical attenuation of light is the point in the neap-spring tidal cycle, and the amount of total suspended solids that are resuspended.

3.2 Modelled seagrass distributions

The spatial distributions of biomass of *Zostera* (Figure 43) and *Halophila* (Figure 44) at the conclusion of the 2 year run are shown. The intention of this chapter is to illustrate reasonable behaviour of the two species implementation of the model, rather than an exhaustive model assessment. A more detailed comparison will require including more realistic forcing, and in particular the poorly-quantified dredge plume sources of total suspended solids.

The model predicts high *Zostera* biomass in shallow waters of Pelican Banks with some viable meadows off Quoin Island (and also Wiggins Island - data not shown). In the deeper waters of Pelican Banks, as well as off Facing Island, Qu0in Island and Wiggins Island *Halophila* biomass has stabilised. Generally *Zostera* dominates shallow waters, and has a higher above ground biomass than *Halophila*. Observations of *Zostera* biomass in 2014 at Pelican Banks show patterns of distribution similar to those predicted by the model (Chapter II, Figure 36), and the long-term boundaries of the seagrass beds at Pelican Banks (Map 9 in Bryant et al. 2014) show a high level of similarity with model outputs.

Variation in biomass observed across the seagrass bed at northern Pelican Banks (Chapter II, Figure 35) is probably due to small scale variations in the depth of the substratum which is present at spatial scales finer than the resolution of the model. Distribution of *Halophila* was similar to that of *Zostera*, indicating that they co-occurred, rather than *Halophila* being totally outcompeted by *Zostera*. In the field the patchy nature of seagrass growth probably allows for micro scale variations that allow *Halophila* to persist in the presence of *Zostera*. The highest observed cover of *Zostera* on the Pelican banks was 90% but cover was usually much lower (Chapter II).

The observed maximum depth of seagrass on Pelican Banks South was -1.76 m relative to the datum (Chapter II, Table 3.3). This is similar to the ~2 m limit seen in the model within the northern section of the harbour (compare distributions in Figure 43 and Figure 44, with bathymetry in Figure 46). Noting there are uncertainties in model bathymetry resolved on a 200 m grid, and in fact the model is based on mean sea level relative to the datum itself, this is a reasonable model performance. Note that the seagrass depth range is an emergent property of the model, a result of the balance between (generally) light-limited growth and mortality. Thus depth range is a good integrated metric of model skill, and on this metric the model has good skill.

There is a general agreement over prediction of both *Halophila* and *Zostera* biomass. Observations have a maximum shoot dry weight biomass of 25 ± 5 g DW m^{-2} (Chapter II, Table 3.1), while the model can reach 50 g DW m^{-2}. This will be partly due to the model not containing some port activities that reduce water transparency, and therefore bottom light. It should also be noted that some of the regions were heavily grazed by turtles (see Chapter IV), and that the observed seagrasses have a lower aboveground to belowground biomass ratio (Chapter II), perhaps also an indication of grazing. While mortality is included in the model, it may be under predicted. The predicted biomass is closer to the mean of the 2002-2012 observations described above.

Model Zostera biomass [g DW m^{-2}]
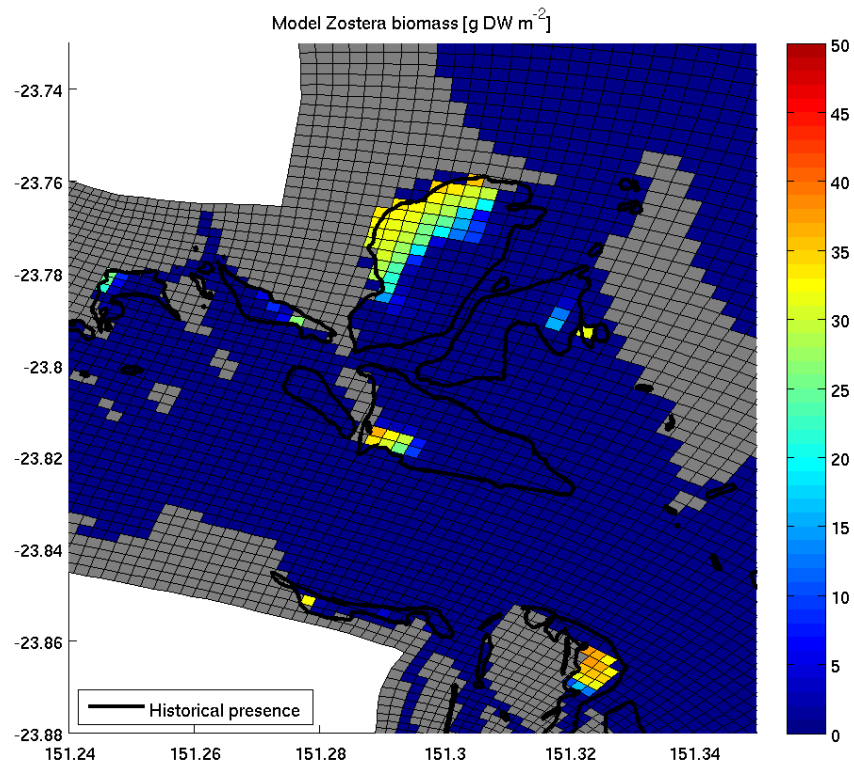
Figure 43 Modelled biomass of _Zostera_ at the conclusion of the 2 year run. Grey is land.

Model Halophila biomass [g DW m^{-2}]
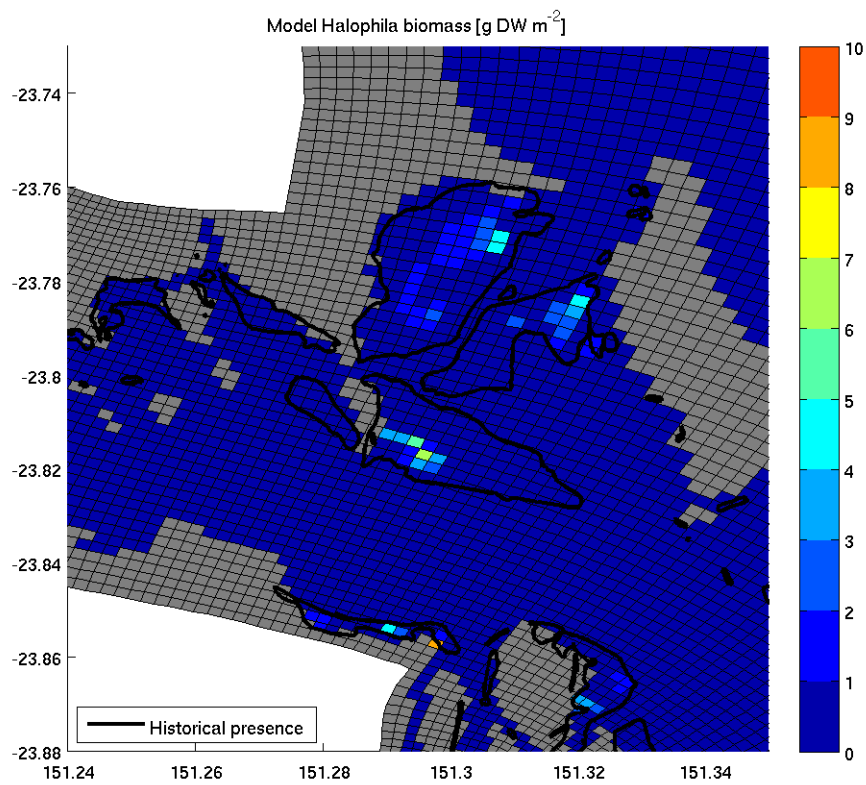
Figure 44 Modelled biomass of _Halophila_ at the conclusion of the 2 year run. Grey is land.

To investigate the dynamics of seagrass, Figure 45 plots model output from 00:00 8 Aug 2012 to 00:00 12 Aug 2012. The PAR radiation just below the surface is relatively high as a result of clear skies typical of August. The daily peak on the four days shown is nearly identical (thin blue line, Figure 45). In contrast the daily cycle of light at the top of the seagrass canopy varies significantly between days, a result of changing water column vertical attenuation, $K_{d,490}$ (green line), and water column depth (black line). At Pelican Banks, where the low tide during the 4 days corresponds with approximately zero water depth, and low tide occurs in the early daylight hours, the light at the bottom is equal to the light at the surface. As the tide rises, the fraction of light reaching the bottom reduces. At the deeper Facing Island meadow, the impact of varying $K_{d,490}$ is more pronounced. A further complication arises because the highest levels of vertical attenuation are associated with low tide, particular at Pelican Banks, due to greater resuspension in shallow waters.

The contrasting light levels above the seagrass canopies has resulted in *Zostera* dominating at Pelican Banks, and *Halophila* at Facing Island. Over the 4 days shown, the mean daily dose of photons is approximately 8.7 and 1.8 mol m^{-2} at Pelican Banks and Facing Island meadows respectively. At Pelican Banks bottom light is well above the minimum light requirement of both species (4.5 and 2.8 mol m^{-2} respectively), and so *Zostera* is able to thrive. At a biomass of 1.6 g N m^{-2}, *Zostera* covers $1 - \exp(-\Omega SG_A) = 0.91$ of the bottom. The light remaining after passing through *Zostera*, $\sim 8.7 \times 0.09 = 0.78$ mol m^{-2} d^{-1} is insufficient for *Halophila* to survive, and hence its biomass has decreased to zero.
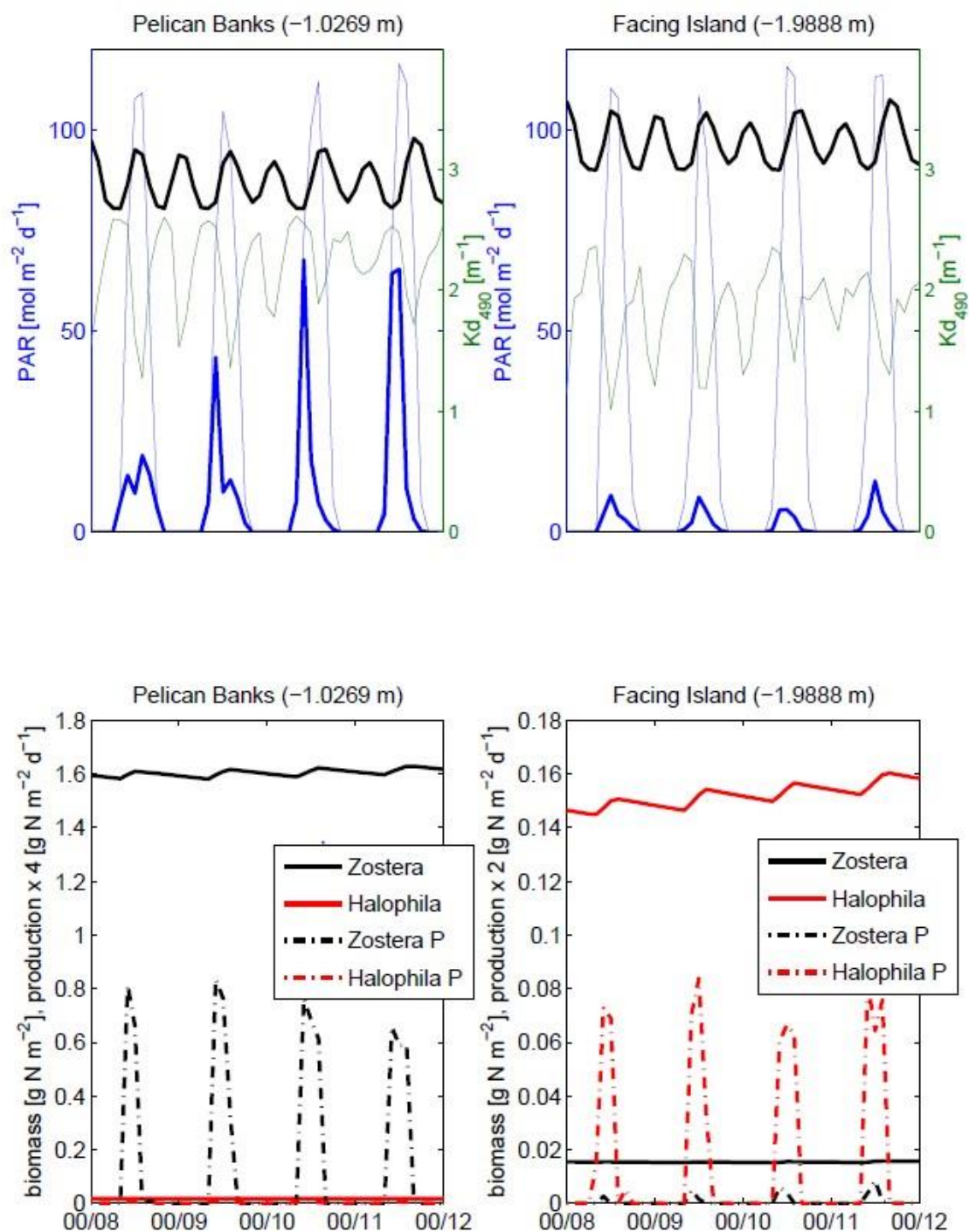
Figure 45 Model output at a site on Pelican Banks (left) with a total depth of 1.03 m below mean sea level, and a site on Facing Island meadow that is 1.99 m below mean sea level (right). Top panels show PAR just below the water surface (thin blue line) and at the top of the seagrass canopy (thick blue line), vertical attenuation at 490 nm (green) and the sea level (black line, amplitude ~ 2 m). Bottom panels show biomass (lines) and production (dash-dot) for *Zostera* (black) and *Halophila* (red).

At Facing Island, the bottom light during these four days is well below that required for *Zostera*, and therefore *Zostera*'s biomass is decreasing. In contrast with no shading by *Zostera*, *Halophila* has been able to grow. The estimated mean bottom light level is slightly below the minimum light parameter for *Halophila*, but it has been able to increase slightly biomass through the 4 day period. The two-hourly estimate of bottom light level, combined with processes such as translocation, have affected the growth calculation. Generally in the model *Halophila* cannot grow much below 2 m (compare range in Figure 44 with Figure 46) in the relatively turbid waters inside the harbour. These results for Zostera are in accordance with observations which show lower biomass on Facing Island than at Pelican Banks (Chapter II).
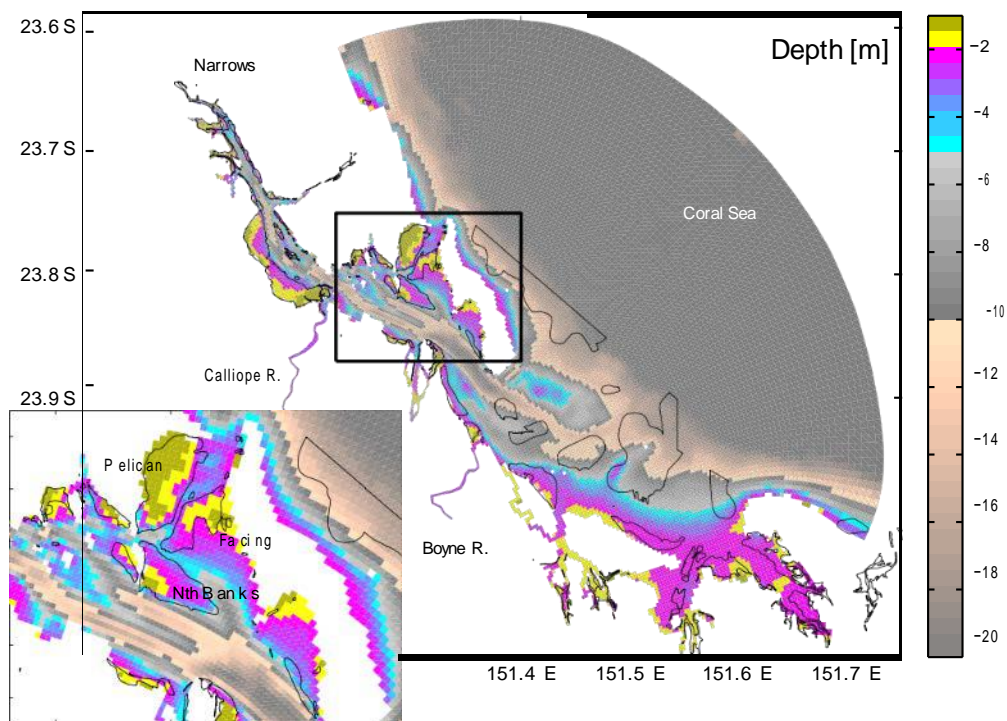
Figure 46 Model grid, showing model bathymetry resolved to 50 cm intervals by the colour map, meadow sites used in the model-observation comparison, and black line contours showing the local in which seagrasses have been observed historically (McKenzie et al. 2014). Pelican - Pelican Banks; Facing - meadow east of Facing Island; North Banks - meadow extended east from Quoin Island

3.3 Parameter uncertainty

In terms of the technical aspects of model development, the goal of the GISERA seagrass modelling effort was to develop a new seagrass model that provides a relatively detailed process-based model of seagrass, but that did not add unnecessary uncertainty to an already complex 60 state variable shallow-water biogeochemical model. The model contains two state variables, above- and below-ground biomass, and 13 new parameters (Table 2.3). Of these 13 parameters, four have clear physical interpretations (Ω_{SG}, $A_{L,\lambda}$, $\sin \beta_{blade}$, z_{root}), and can be considered well-constrained for a particular species. The remaining nine parameters represent physiological rates, with species-specific data available for the four (μ_{SG}^{max}, f_{below}, E_{comp}, ζ_{SGA}). The remaining five parameters are constrained by values common across seagrass species (τ_{tran}, $K_{SG,P}$, $K_{SG,N}$) or are unsupported estimates (f_{seed}, ζ_{SGB}).

The most important parameter for the prediction of seagrass biomass is the nitrogen-specific leaf area, Ω, as this parameter relates biomass to both fraction of the bottom covered and light capture. In some cases in the literature this parameter has been determined as a carbon-specific, or dry weight specific leaf area (Cambridge and Lambers 1998). We use a nitrogen-specific value because the biogeochemical model has nitrogen as its main currency, but the two are interchangeable using 550 mol C: 30 mol N. Observations show seagrass C:N:P ratios vary from 550:30:1 with nutrient status, although the carbon-specific leaf area index is unlikely to be a function of nutrient status. If C:N ratios do vary significantly from 550:30:1, it is most appropriate to use the carbon-specific leaf area, and convert to nitrogen-specific using 550:30.

Nitrogen-specific leaf area varies across species by up to an order of magnitude, but is well constrained for an individual species (Cambridge and Lambers 1998). If the parameter represents the dominant species, or as in this report by two dominant species, then errors due to specification of Ω are small. Like-wise the other physical variables, if specified for a particular species, are well constrained.

The physiological variables have varying uncertainty, with multiple estimates in the literature of μ^{max}, f_{below} and E_{comp}. The size of the seed bank, f_{seed}, although poorly known only affects the model at low seagrass biomass. The largest errors introduced in this application were due to the uncertainty in mortality of above and below ground biomass. The model was calibrated by varying these mortality parameters to obtain the best fit to observed data. The parameter values obtained seem to represent reasonable values for a parameter that represents many processes (grazing by animals, shoot displacement, etc.). Thus, based on the practicality of applying the seagrass model, and its performance in Gladstone Harbour, we find this model has struck a workable balance between model representation and model complexity.

3.4 Analytical results

In the model, the light-limited net production of seagrass is a balance between growth, respiration and mortality. To undertake an analysis of the model behaviour, we simplify the calculations by (1) assuming a PAR-integrated light field, (2) excluding translocation, (3) setting seed fractions to zero, (4) assuming growth is not limited by nutrients, (5) averaging the seagrass biomass dynamics over

greater than daily timescales, and (6) considering one spatial location. Using these assumptions, together with Eqs. 19, 23, 28 and 29, we can approximate the rate of change in above-ground biomass by:

$$\frac{\mathrm{d}SG_A}{\mathrm{d}t} = \min\Big[\big(\mu_{SG}^{\max} - \zeta_{SG_A}\big) SG_A,$$
$$\frac{30 \times 14}{5500}\Big(E_{PAR}\big(1 - e^{-A_L \Omega_{SG} SG_A \sin\beta_{blade}}\big)$$
$$- E_{comp}A_L\Omega_{SG}SG_A\sin\beta_{blade}\Big)\Big], \quad (13)$$

where E_{PAR} (mol m^{-2} d^{-1}) is the downwelling PAR at the top of the seagrass canopy.
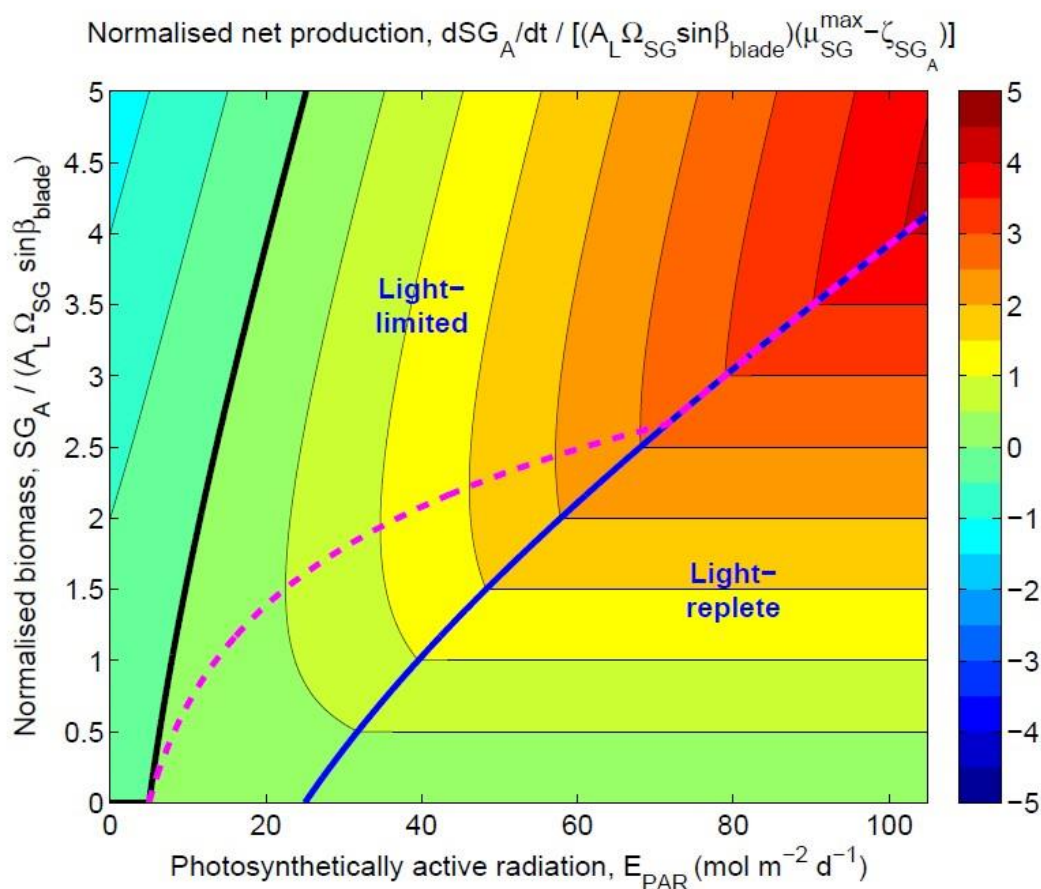
Figure 47 Numerical solution to the light-limited normalised (by (A$_L\Omega_{SG}$ sinβ$_{blade}$)(μ$_{SG}^{\max}$- ξ$_{SGA}$)) net production, dSG$_A$/dt, as a function of the above-ground seagrass biomass SG$_A$ and photosynthetically active radiation, E_{PAR}. The above-ground seagrass biomass, SG_A, is normalised by the wavelength-averaged leaf absorbance, A_L, nitrogen-specific leaf area, Ω, and the sine of the leaf bending angle β_{blade}. Three analytical solutions are shown: the line of zero net production (black, Eq.~B.3~and~B.4), the line of minimum biomass at which biomass production is light-limited (blue, Eq.B.5), and the line of maximum net production (magenta, Eq. B.6).

Figure 47 characterises the behaviour of seagrass dynamics predicted by Eq. 13. In this contour plot, the net production dSG$_A$/dt is expressed as a function of downwelling PAR (x-axis) and above-ground biomass SG$_A$ (y-axis). To explain the relationship between biomass production, biomass and light, three additional lines are plotted, representing: stable biomass (black line), maximum net production (dashed magenta line) and the boundary (blue line) between production limited by

available light ("light-limited" region) and production limited by the maximum growth rate, μ_{SG}^{max}, ("light-replete" region). The line of stable biomass (black line) indicates that seagrass decline is predicted when E_{PAR} is below the minimum light requirements E_{comp}, here assumed to be 5 mol m^{-2} d^{-1}. This line also shows that seagrass growth is predicted when $E_{PAR} > E_{comp}$, and the stable seagrass biomass increases with light availability.

The boundary between light-replete and light-limited regions (blue line) indicates that seagrass growth is unhindered by light only when both (1) light availability is sufficiently high and (2) biomass is sufficiently low so that biomass production is not significantly reduced by self-shading. In the light-replete region, the contours of dSG_A/dt = 0 are horizontal because biomass production is independent of light availability; physically this indicates that seagrass growth is only limited by the maximum growth rate of seagrass.

Maximum net production (dashed magenta line) occurs at a biomass larger than zero but less than the stable biomass value (black line). Maximum net production occurs at an optimal biomass that is sufficiently high for growth but sufficiently low so that mortality does significantly reduce net production. In the "light-limited" region, the contours of constant dSG_A/dt tend towards a linear relationship between biomass and PAR at high biomass because this represents the physical situation where seagrass has reached 100% coverage, and hence production then becomes linearly related to PAR (in the absence of other physiological limitations).

In summary, Figure 47 can be used to interpret the effect of a two dimensional light field on the net production of an exponentially-saturating bottom coverage with a biomass-dependent loss terms the fundamental geometric characteristics on which the seagrass model developed here has been formulated.

3.5 Parameterisation of physiological adaptations of seagrass to light limitation

Under low light conditions, a number of factors in the seagrass model determine the relative rates of survival of the *Zostera*, *Z*, and *Halophila*, *H* :

1) Access to light. *Zostera* is assumed to grow taller than *Halophila*. As a result, it grows based on the downwelling irradiance at the bottom of the water column. *Halophila* grows based on the downwelling irradiance after it has passed through *Zostera*. Thus *Zostera* is at a competitive advantage, which can be quantified under light-limiting conditions as the ratio of the absorbed light per unit area, *R*:

$$\mathcal{R} = \int \frac{E_{d,wc,\lambda} A_{Z,\lambda} Z \left(1 - \exp(-\Omega_Z Z)\right) \; d\lambda}{(1 - E_{d,wc,\lambda} A_{H,\lambda} Z(1 - \exp(-\Omega_Z Z)) \, A_{H,\lambda} H \left(1 - \exp(-\Omega_H H)\right)} \tag{14}$$

At low biomass of *Zostera* and *Halophila*, $R \to Z A_Z / (H A_H)$. Thus at low biomass, the competitive advantage is partly due to the ratio of absorbance of the leaves, *A*, although these are likely to be similar, and the relative biomass of the two species. That is, under exponential growth, starting with a higher initial biomass is a competitive advantage. At high biomass of *Z*, irrespective of the biomass of *H*, $R \to \infty$. At low biomass of *Z* but intermediate

to high values of *Halophila*, $R \rightarrow A_Z Z / (H\, A_H\, (1 - \exp(-\Omega_H H)))$. Thus the competitive advantage of *Halophila* diminishes as it self-shades itself.

2) Leaf to root fraction. The light absorbed by each species is used to synthesise organic matter. If that energy is used to increase leaf area, then the net photosynthesis may increase, while if it is assigned to roots, photosynthesis is not increased. *Halophila* is assumed to have a greater ratio of above ground biomass to below ground biomass, making it better adapted to low light, nutrient replete conditions.

3) Energy requirement to synthesise leaf area. One over the nitrogen-specific leaf area, $1/\Omega$, quantifies the nitrogen required to create a leaf of 1 m^2, assuming no losses. Thus, the photons required to create a 1 m^2 leaf is given by $(5500/30)(1/14)(1/\Omega)$. Under low-light, low biomass conditions, a high Ω creates a bigger surface area per incident photon, more quickly increasing the leaf area favouring *Halophila* over *Zostera*. At high biomass, where coverage approaches 100 %, a large Ω is of no benefit.

4) Seed fraction. A higher seed fraction allows the biomass to reach full coverage quicker than a low seed fraction. In the model both have the same fraction.

5) Mortality. A low mortality rate is useful especially at high coverage, as mortality is a function of biomass while energy supply is not. *Halophila* has a higher mortality rate for above ground biomass.

6) Leaf orientation. A leaf oriented towards the light ($\sin \beta_{blade} = 1$) will more effectively capture light. At low biomass, a seagrass meadow will absorb more light with a larger value of $\sin \beta_{blade}$, although as biomass increases, the light captured becomes less depended on leaf orientation as self-shading becomes important. *Halophila* has value of $\sin \beta_{blade} = 1$, while *Zostera* has a value of 0.5. Thus, at low biomass *Halophila* is better adapted to low light.

3.6 Summary

In summary, we have developed a new model of seagrass growth and loss that has detailed physical representations of the limiting processes of light and nutrient availability, but has a relatively simple representation of physiological processes. This balance was chosen due to the need to use the seagrass model in a complex estuarine biogeochemical model. When applied, the model provides reasonable estimates of seagrass biomass in Gladstone Harbour. Further, analytical results are used in a schematic diagram to illustrate the impact of light levels and canopy density on net production. The most interesting aspect of the model for modellers of benthic communities is the use of the for $1 - \exp(-\Omega S G_A)$ to relate biomass to percent coverage. The form is derived from first principles, and is applied successfully using geometric, not empirical, means to determine the value of Ω. As such, it offers both theoretical and practical advantages over empirical carry-capacity style formulations commonly used.

The seagrass model developed in this chapter, when coupled to the spectrally-resolved optical model detailed in CEM (2014), provides a new ability to capture well-known, but previously unmodelled, processes that impact seagrass communities. These include:

- Seagrass growth depending on the spectral quality of the light reaching the bottom.
- The modelling of multiple species types.

- The representation of above-ground and below-ground biomass, and translocation between the two.
- The representation of spectrally-resolved multiple sources of water column scattering and absorption.
- The inclusion of nutrient uptake from multiple depths of the sediments.

These new advances, in combination with a comparison of modelled and observed seagrass biomass, provides confidence that the seagrass model developed here can represent processes important for predicting the impact of environmental stressors on seagrass communities. This confidence is critical in the application of the seagrass model developed here in the eReefs marine modelling system, and in the Gladstone Healthy Harbours Partnership.

Chapter IV Port Curtis Turtle Movement and habitat use

Richard Pillans, Gary Fry, Russ Babcock, Wayne Rochester, Toby Patterson, Col Limpus

1 Introduction

The green turtle (*Chelonia mydas*) is found worldwide in tropical and sub-tropical coastal regions of the world (Bowen et al. 1992). It is classified as vulnerable under the Australian Environment Protection and Biodiversity Conservation Act (1999) and endangered under the IUCN (2014) Red List.

The green turtle is a large, long-lived, herbivorous reptile that grazes on seagrass and selected marine macroalgae in shallow tropical and temperate waters throughout the world (Bjorndal et al. 1997). Green turtles undertake significant migrations as juveniles and adults. During their oceanic phase, juveniles can move at an ocean basin scale while adults have been recorded moving thousands of kilometres between feeding and breeding grounds (Limpus et al. 1992). Several studies have found that aggregations of turtles at a feeding ground are derived from several genetically distinct breeding populations (Lahanas et al. 1998; Bass and Witzell 2000; Luke et al. 2004; Dethmers et al. 2010) with each foraging population referred to as a 'mixed stock'. Within Australia, Dethmers et al. (2010) identified 7 distinct breeding populations, of which the Southern GBR population represents a genetically distinct stock.

Female green turtles reproduce at intervals of three years or greater (Limpus et al., 1994b) whereas males are recorded at nesting sites on average every two years (Limpus, 1993a). Mating commences in mid-September, peaks in October and ceases by about mid-November (Limpus, 1993). Nesting commences in mid to late October, peaks in late December–early January and ends in late March early April (Bustard, 1972). Hatchlings begin to emerge from late December until May with a peak in February–March.

There is a large degree of variation in the extent of dispersal between feeding and breeding grounds with individuals at a breeding ground coming from feeding grounds as close as 8 km away to greater than 2000 km away (Limpus et al. 1992). Individual females have been shown to faithfully migrate between their breeding areas and resident feeding areas (Limpus et al. 1992; Balazs 1994; Troeng et al. 2005).

As a result of this life history strategy, anthropogenic mortality on feeding grounds has the potential to impact multiple populations with Dethmers et al. (2006) identifying 17 genetically distinct breeding populations within the Indo Pacific, including seven within Australia.

Immature and adult green turtles forage in tidal and sub-tidal coral and rocky reefs, seagrass meadows, and sand and mudflats primarily for seagrass, algae, mangrove leaves and fruit, and occasionally on jellyfish, egg masses, dead fish and small crustaceans (Limpus 2008). Arthur et al. (2008) showed that adult and large immature turtles had similar isotopic signatures and were both significantly enriched in δ13C when compared with hatchlings and small immature turtles supporting observations that juveniles consume more algae than seagrass. Immature green turtles in Moreton Bay have ben show to feed on both seagrass and algae, with most feeding selectively on algae (Brand-Gardner et al. 1999, Brand et al. 1999), primarily *Gracilaria* which was the most frequently selected food item even though it was not abundant within the study area. The seagrass, *Zostera muelleri*, was the most abundant potential food item within the study area but was one of the least selected. Similarly, Read and Limpus (2002) examined diet of juvenile green turtles at Moreton

Banks and demonstrated that although turtles foraged on seagrass, they demonstrated a preference for *Halophila ovalis* and red algae (*Gracilaria cylindrica* and *Hypnea spinella*).

Green turtles at Shoalwater Bay fed primarily on seagrass (mainly *Zostera muelleri* and *Halodule* sp.) but also consumed red algae, filamentous cyanobacteria and small amounts of animal material. Some studies have shown no difference in the diet of males and females and diet of juveniles, subadults and adults were similar (e.g. Arthur et al. 2009). More detailed studies of turtle habitat use in western Shoalwater Bay have shown, however, that different age classes of turtles are utilising different habitats. Small immature individuals occur mostly in the upper intertidal mangrove forest and rocky habitat, and in drainage gutters across the flats. Adults and large immature turtles are more frequently encountered in the mid intertidal to subtidal waters (Limpus et al. 2005).

In addition to these ontogenetic shifts in diet and habitat use, diet may vary seasonally and among years. Diet composition was found to differ between subsequent sampling years primarily due to the quantity of seagrass (mainly *Halodule* sp.) in the diet and the presence of *Lyngbya majuscula*. Inter-annual variation was attributed to changes in seagrass density (Arthur et al. 2009). The diet of juvenile green turtles in Hervey Bay was shown to vary seasonally with samples taken in autumn and winter (Cameron 2007). Hazel (2009) demonstrated that green turtles utilised different day and night areas, and depth at night was greater than during the day. These short term data were consistent with intermittent observation (visual — Bjorndal 1980; and acoustic — Mendonca 1983; Renaud et al. 1994; Taquet et al. 2006) and from short-term records of diving behaviour (Hazel et al. 2009; Makowski et al. 2006; Seminoff et al. 2001) and support the theory that green turtles prefer to travel and forage by day and then rest much of the night. Alternating bands of seagrass and mangrove material in the alimentary tract has led some authors to suggest that for turtles inhabiting intertidal areas adjacent to mangroves, turtles move into the mangroves at high tide to feed on mangrove propagules and leaves (Arthur et al. 2009; Limpus and Limpus 2000). In the future data collected from acoustic telemetry may enable us to determine the extent of diel differences in habitat use.

Thousands of green turtles have been tagged along the Queensland coast since the 1970's. Although recaptures of tagged animals can demonstrate long term fidelity of juvenile and adult green turtles (Limpus and Read 1985; Hirth et al. 1992; Limpus et al. 1992) as well extensive breeding movements and return to foraging areas at the end of breeding migrations (Limpus et al. 1992), they do not provide data on the extent of habitat use and movement between recaptures. Active acoustic telemetry has been successfully used to obtain short term (days to weeks) (Renaud et al. 1994; Whiting and Miller 1998; Seminoff et al. 2002; Makowski et al. 2006) as well as medium term (<12 months.-.MacDonald et al. 2012; Hazel et al. 2013) data on movement and habitat use. The majority of acoustic telemetry studies conducted to date are limited to a few individuals monitored for short time periods that do not encompass seasonal or annual variability. Satellite telemetry has also successfully been used to investigate breeding migration (Spring and Pike, 1998) and habitat use in green turtles (Gredzens et al. 2014), however there are surprisingly few published papers within Australia.

Marine turtles are threatened by a range of anthropogenic factors including habitat loss, increased mortality associated with boat strike, entanglement in fishing gear, disease and pathogens (Lutcavage et al. 1997). With intensifying coastal development occurring along the eastern coast of

Australia, there are many habitats including seagrass beds and coral reefs, which are becoming increasingly vulnerable to anthropogenic change (Duarte 2002; Erftemeijer and Lewis 2006).

The port of Gladstone supports a wide range of coastal marine habitats, including rocky and coral reefs, tidal and sub-tidal seagrass meadows, mangroves and soft-bottom habitats, which provide habitat for a number of threatened species including not only the green turtle (*Chelonia mydas*) but also loggerhead (*Caretta caretta*), hawksbill (*Eretmochelys imbricata*), olive ridley (*Lepidochelys olivacea*) and flatback (*Natator depressus*) turtles as well as dugong (*Dugong dugon*). In addition to Moreton Bay and Shoalwater Bay, the Port Curtis region has been recognised as an important feeding ground of the southern Great Barrier Reef genetic stock of green turtles (Limpus 2008).

Gladstone Harbour is the largest industrial port in Queensland and has received considerable media attention with respect to water quality, habitat modification and reduced health of fish, crabs and turtles. Seagrass cover within Port Curtis has declined significantly in recent years which have been attributed to the cumulative influence of increased rainfall (McCormack et al. 2013).

The health of turtles within Gladstone Harbour has been a source of particular concern in Gladstone following high rainfall years in 2010 and 2011. A strong La Niña event on the south-western Pacific Ocean with associated cyclone activity brought heavy, prolonged rainfall to most of coastal eastern Queensland during December 2010 and January 2011, producing the wettest summer on record for Queensland (BOM 2012). This resulted in extreme flooding of a number of rivers along the Queensland coast, including the Fitzroy, Calliope and Boyne Rivers, and had significant impacts on the local coastal environment. Reductions in biomass of seagrass beds in the Gladstone area were partly attributed to increased turbidity and settling of silt on seagrass meadows (McCormack et al. 2013) which are important feeding grounds for resident populations of green turtles and dugongs.

Immature green turtles from Gladstone were in poorer body condition when compared with immature green turtles from other Queensland coastal regions in 2011 (Limpus et al. 2012). Stranding records between 1996 and 2011 showed that during 2011 there was an increase in the number of turtle strandings along the Queensland coast with proportionally more records from Gladstone Harbour, where 323 turtle strandings were recorded (Meager and Limpus 2012). Increased mortality in 2011 was attributed to the disturbance of seagrass meadows by extreme weather events in 2010 and 2011, however more than 10% of strandings in Gladstone region were due to boat strike (Meager and Limpus 2012). Within the Gladstone region, the number of turtle mortalities attributed to boat strike in 2011 was more than seven times greater than previous years and coincided with both increased port development (traffic) and reduced food availability. Flooding in 2011 which resulted in the overtopping of Awoonga dam on the Boyne River also resulted in a large number of mature barramundi (*Lates calcarifer*) entering coastal systems in Gladstone Harbour. These fish were targeted by commercial net fishers with an increased level of fishing activity also potentially impacting on weakened turtles (C Limpus pers. comm.).

Flint et al. (2014) examined the health of 56 live turtles and 11 stranded turtles from Gladstone Harbour in 2011 and showed live animals were twice as likely to present in an unhealthy state compared to animals from Moreton Bay or Shoalwater Bay. Flint et al. (2014) suggest that there was an underlying environmental process that predisposed animals to acute or secondary pathologies following environmental stressors (e.g. flooding and resulting decline in seagrass). Flint et al. concluded that the cumulative natural and anthropogenic disturbances (in Queensland largest industrial port) may have been significant contributors to the increased strandings. This was

supported by a study on metal levels in the same 56 turtles. Gaus et al. (2012) found levels of arsenic, cadmium, cobalt, mercury, nickel, selenium, and vanadium were present at levels well above those reported for green turtles and other marine megafauna species from other locations. The levels reported were near or above acute tissue based effect concentrations reported across various vertebrate taxa (Gaus et al. 2012).

The increased risk of vessel strike during construction of the LNG loading facilities, as well as during the operational phase of LNG export, has been identified as a threatening process to green turtles (http://www.westernbasinportdevelopment.com.au/marine-megafauna-plant-life-turtles). The main issues were direct impacts on marine mammals and/or turtles from vessel transport, leading to injury or mortality as well as changes in behaviour (avoidance–migration, foraging, breeding) (Australia Pacific LNG Project Appendix I - Marine Mammal and Turtles Management Plan LNG Facility).

The objectives of the research described in this chapter are to better understand the risk of boat strike from commercial vessels operating in Gladstone Harbour the habitat use, home range, depth range and site fidelity of green turtles were investigated using a combination of acoustic and satellite telemetry. Knowledge of habitat usage is essential for conservation planning, and areas of high animal density and/or increased mortality risk to populations should be considered for future regulations and zone protection. These data, in combination with data on habitat distribution and shipping patterns, also form one of the key bases for risk modelling (Chapter V) of green turtle populations in relation to shipping movements in Gladstone harbour and as such are vital to informing any potential management decisions in relation to risk minimization.

Concerns were also held for dugong (*Dugong dugon*) in Gladstone Harbour, similar to those for green turtles. It was decided not to extend GISERA program to dugong in Gladstone harbour since at the time the study started dugong were rare in the harbour and there concerns that they may be under stress due to a range of factors including recent flooding, low seagrass cover and increased shipping activity. However GISERA was involved in trial dugong tagging in a proof-of-concept study in Moreton Bay (Zeh et al. 2014) which showed that acoustic tracking of dugong was not only feasible but that it was highly successful (Appendix D). In the future this knowledge may prove useful in Gladstone for the ongoing monitoring of dugong.

2 Methods

2.1 Study areas and acoustic receiver array

Acoustic receivers (Vemco VR2Ws) were deployed in Gladstone Harbour to monitor the movement of tagged turtles around Pelican Banks and Wiggins Island (Figure 48, Appendix E). Pelican Banks was selected as an example of comparatively optimal habitat for turtles as it has relatively high seagrass cover on the northern side of the channel and extensive, intertidal and subtidal sand flats with subtidal channels up to 6 m deep (Figure 49). Vessel traffic outside the main channel at Pelican Banks is primarily recreational craft (4–7 m in length) usually travelling at high speed (in excess of 15 knots) either outside or within the channel. A vehicle ferry and smaller (<20 m in length) commercial vessels utilise the channel on a daily basis and operate at lower speeds (<10 knots).

The Wiggins Island area provided an example of a location more heavily influenced by port activities as it is adjacent to LNG loading facilities on Curtis Island as well as the Wiggins Island Coal Loading terminal. This area had very little seagrass at the time of our study and was predominantly bare sand/mud with some rocky reef/rubble areas adjacent to Wiggins Island and access to intertidal Mangroves via narrow channels. There is a shipping channel between Curtis Island and the sand/mud flats adjacent to the mainland with water depth greater than 20 m (Figure 50). At Wiggins Island, traffic over the intertidal areas at high tide is restricted to smaller vessels (<6 m) generally travelling at high speed. Along the edge of the channel and the shipping channels, boat traffic is high. The majority of this traffic is of a commercial nature with high speed transport, barges, tugs and bulk tankers using the shipping channel.

The array of receivers consisted of 21 receivers at Pelican Banks and 25 at Wiggins Island. Receivers were spaced 600–800 m apart and attached to subsurface moorings made of railway track in water depth >5 m or on screw anchors in water <5 m. Receivers were held above the substrate by subsurface floats and were between 1-3 m above the substrate depending on the depth. Permission to deploy temporary moorings within Port Curtis was obtained from Maritime Safety Queensland. Dredging and high traffic adjacent to the LNG processing wharf on Curtis Island prevented us from placing receivers on the northern side of the shipping channel adjacent to this area. Similarly, construction of the Wiggins Island Coal loading facility prevented us from deploying receivers immediately to the north and north east of Wiggins Island.

Figure 48 Map of Gladstone Harbour and acoustic receiver arrays. Location of acoustic receivers (red dots) shown at Wiggins Island and Pelican Banks.
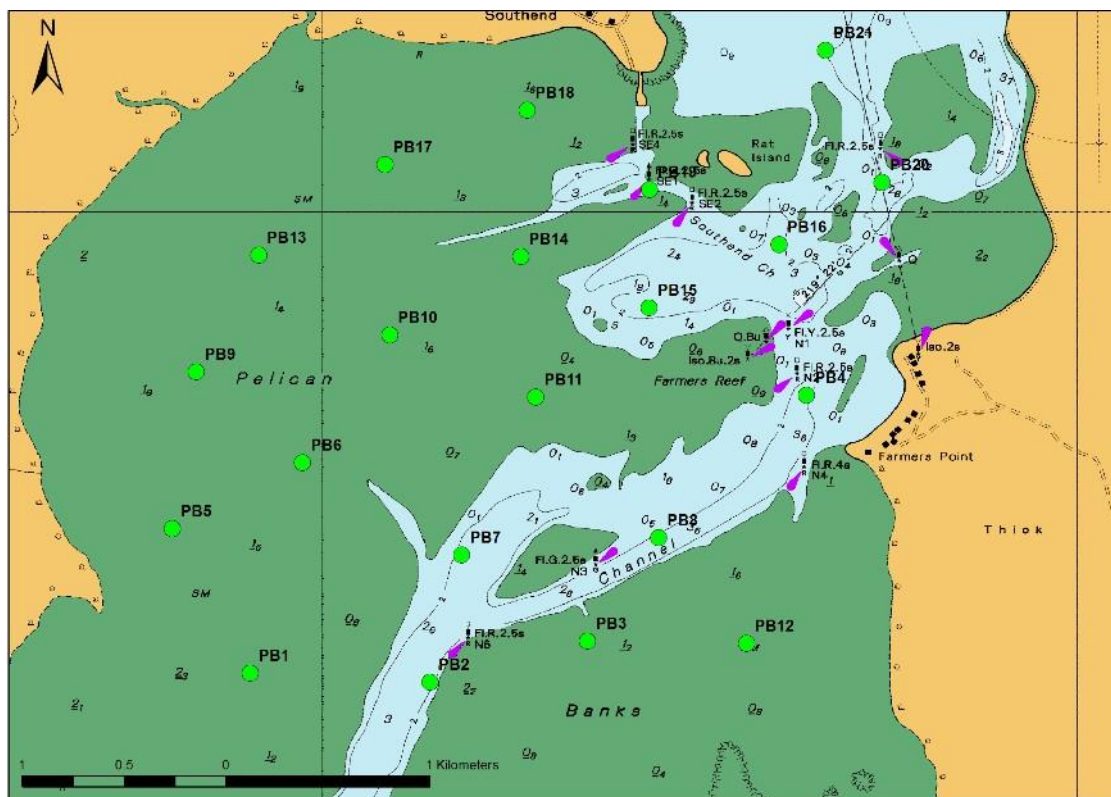
Figure 49 Map of Pelican Banks showing the location of acoustic receivers (green circles).
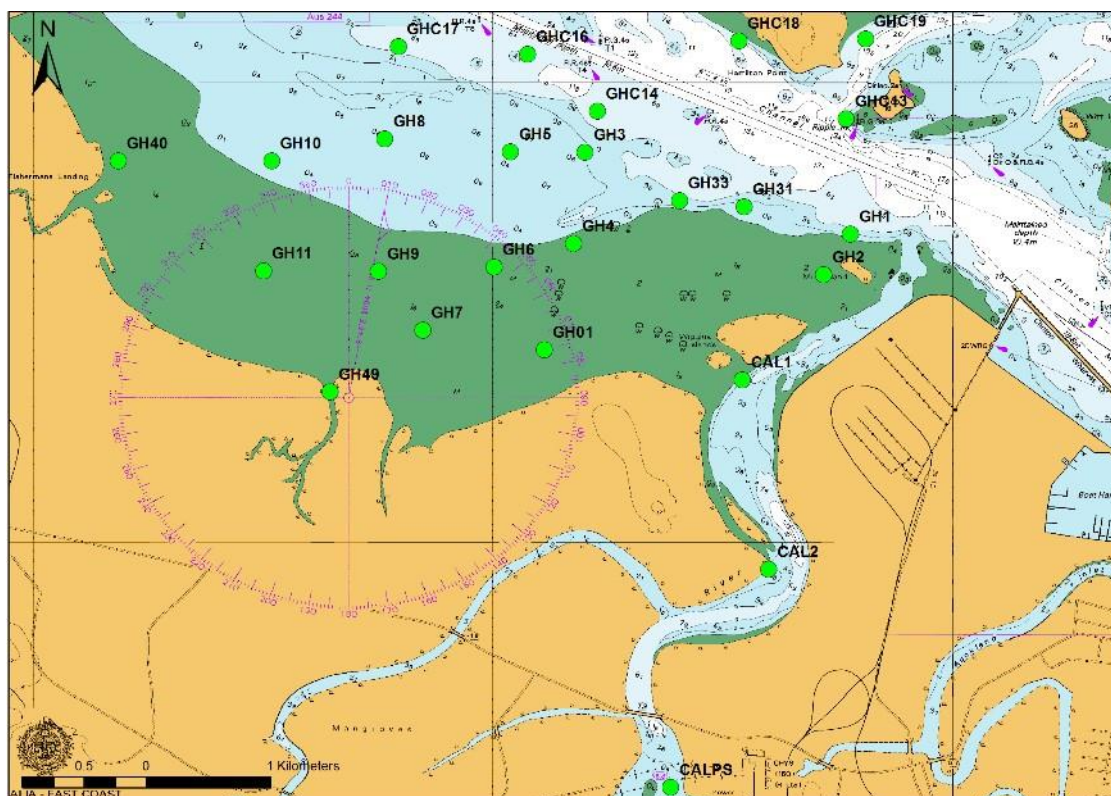
Figure 50 Map showing receiver locations (green circles) adjacent to Wiggins Island

2.2 Turtle capture and handling

Green Turtles (*Chelonia* mydas) were captured around Wiggins Island and Pelican Banks in May and November 2013. Turtles adjacent to Pelican Banks were captured by EHP (Queensland Department of Environment and Heritage Protection) staff and volunteers by jumping on them from moving vessels over intertidal and subtidal flats (rodeo method; as described in Limpus and Walter 1980). Around Wiggins Island, the low visibility precluded this standard method as a viable means to capture turtles. Fifteen turtles around Wiggins Island were captured in gillnets with a mesh size of 22 cm set across mangrove drains on the ebb tide. Nets were monitored continuously and as soon as a turtle became entangled in the net, the animal was removed. One additional turtle was captured in a 300 m seine net adjacent to Wiggins Island at high tide.

Captured turtles were taken back to shore and processed in the Queensland Parks and Wildlife precinct in Gladstone. All captured turtles were double tagged with titanium flipper tags, measured for midline curved carapace length (CCL, ± 0.1 cm) and weighed on a spring balance (± 0.5 kg, if over 30 kg) or on an electric balance (± 0.01 kg, if under 30 kg). Turtles captured in May 2013 were examined by laparoscopy (carried out by Colin Limpus) to determine the sex, maturity and breeding status. Changes to regulations precluded the use of laparoscopy on the turtles captured in November 2013, resulting in immature turtles not being sexed and breeding condition not evaluated for these turtles. Blood and skin samples were taken from all turtles for isotope, toxicology and parasitological research being conducted at CSIRO, James Cook University and University of Queensland.

2.3 Tagging

All tagging was conducted as part of a collaborative project with EHP and functioned within an approved EHP research project led by Dr Col Limpus.

2.3.1 ACOUSTIC TAGGING

Once turtles were restrained, the post marginal scutes above the back flipper were cleaned with cloth soaked in Hexawash surgical wash ((10 ml Hexacon, 90 ml distilled H_2O and 900 ml EtOH). Following cleaning, an acoustic tag was attached to the post marginal scutes by drilling either one or two 3 mm diameter holes through the carapace (see Figure 51). All acoustic tags were coated in International Ultra (high strength hard antifouling paint) before being attached. The antifouling paint was allowed to dry for 24 h before the tags were applied. The post-marginal scutes were chosen as the attachment site to minimize the instrument's hydrodynamic impact on the turtle and to ensure eventual detachment by natural outgrowth should we fail to recapture the turtle for device-recovery (van Dam and Diez, 1996). Attachment of transmitters by drilling holes through the post marginal scutes of turtles is routinely employed by turtle researchers (see Mendonca 1983; van Dam and Diez, 1996; Addison et al 2002; Seminoff et al. 2002; Doody et al., 2009) and our methods have been adapted from these studies. Location of transmitters has been shown to not interfere with flipper movements of turtles (Seminoff et al. 2002; Doody et al., 2009). Drilling through carapace scutes has also been used to attach satellite transmitters to leatherback turtles (Byrne et al., 2009). Holes were

drilled using a battery operated drill and a 3 mm drill bit that has been sterilised by soaking in a Hexacon surgical wash (10 ml Hexacon, 90 ml distilled H_2O and 900 ml EtOH).
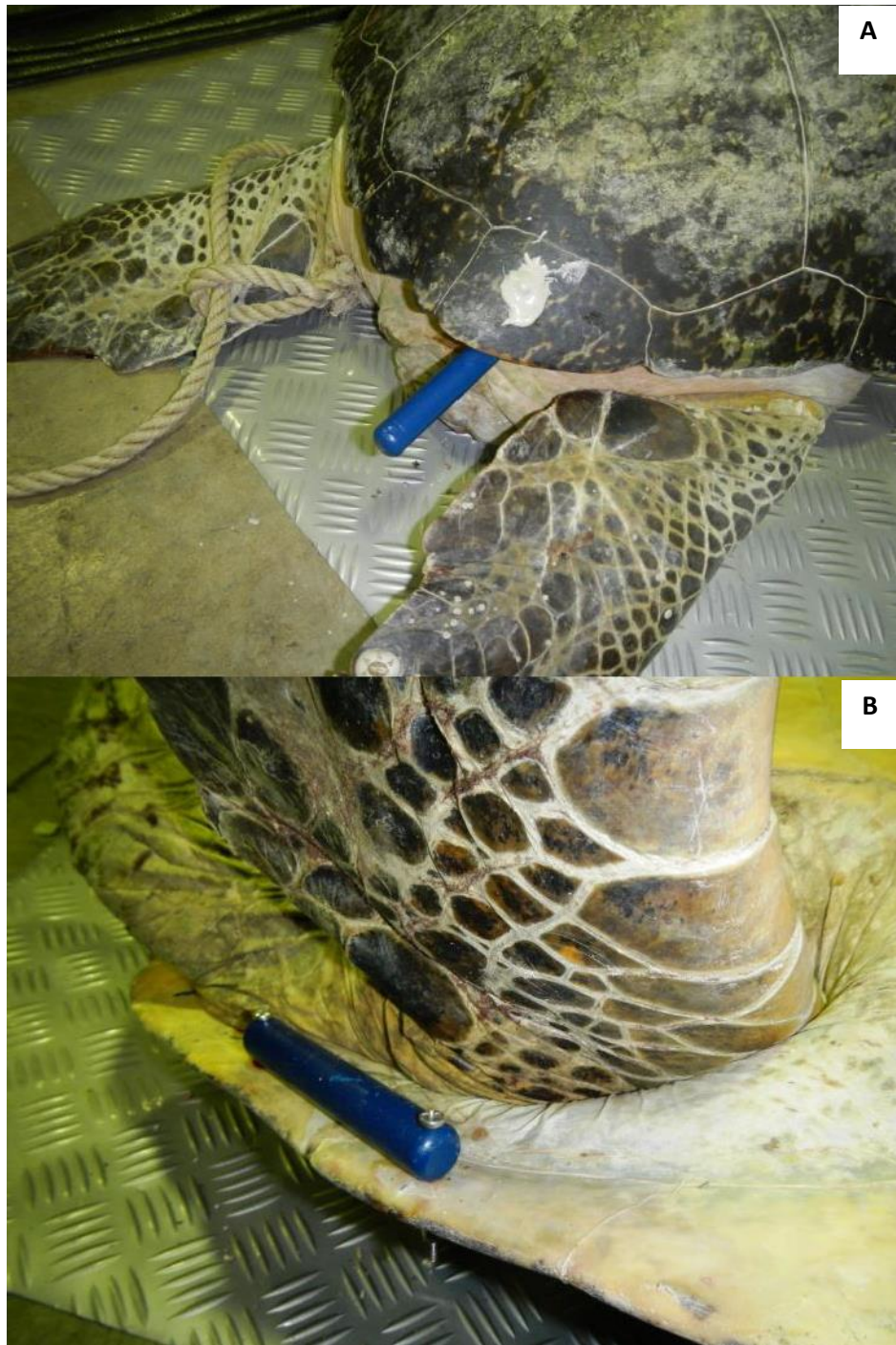
Figure 51 Image of acoustic tag attached with one bolt (A) and two bolts (B)

Acoustic tags were secured by either one (Figure 51A) or two (Figure 51B) 3 mm stainless steel bolts soaked in Hexacon surgical wash. A large stainless steel washer was placed over the bolts on the dorsal surface and secured with Nyloc bolts. The protruding ends of the bolts were cut off and a two-part epoxy resin (Sika AnchorFix®-3+, Sika Australia Pty Ltd) placed over the bolts to smooth their profile.

The two types of tag attachments were chosen to test whether tags protruding from the carapace (Figure 51A) had better detection rates than tags secured under the carapace (Figure 51B). During the second deployment in November 2013, the acoustic tags did not have holes at each end and were glued inside a PVC sleeve with more than half the tag remaining exposed (Figure 52). A hole drilled though the sleeve allowed the tags to be bolted to the post marginal scutes (Figure 52).

Depending on turtle size, individuals were tagged with a V13-1L, V16-4H or V16-6H Vemco coded transmitter (tag). These transmitters range in length from 36–98 mm and weighed between 11-37 g in air. The pulse rate of transmitters varied from 30-180 s and battery life varied from 1090-3650 d depending on the frequency of each ping and the power output of the tag. Each successfully decoded pulse train was recorded as a single detection in the memory of the individual VR2 as the transmitter's identification number, date and time. Receivers were downloaded every six months throughout the study, and the batteries were changed at least every six months.

Figure 52 Photograph showing a V13 acoustic tag sitting within a PCV sleeve bolted through the post marginal scutes of a juvenile Green Turtle.

2.3.2 SATELLITE TAGGING

SPLASH10-F-296A and SPLASH10-F-296C Wildlife Computer tags with Argos, fastloc, temperature and depth receivers were used. Tags were programmed to transmit 254 times per day with position estimates having priority over depth and temperature.

Satellite tags were attached to the first two vertebral scutes immediately posterior to the nuchal scute using a two-part epoxy resin (Sika AnchorFix®-3+, Sika Australia Pty Ltd) (Figure 53). Prior to attachment, a paint scraper was used to remove any flaking scute material. This was followed by gently sanding the area with wet and dry sandpaper. The area was then wiped with 100% ethanol

and allowed to dry before attaching the tag. Once the epoxy resin had set, the tag was coated with antifoul paint (International Ultra high strength hard antifouling paint) and allowed to dry overnight. Tagged animals were released close to their capture site the day after capture.

Figure 53 Position of satellite and "one bolt" acoustic tag on a green turtle. Note: BluTack covering wet/dry sensors during antifouling had not yet been removed on this image.

2.4 Range testing of acoustic monitoring system

Detections of satellite and acoustic tags within 1-5 minutes of each other served as a means of range testing with these data illustrating that the greatest degree of temporal overlap in tag detections was when satellite tags and acoustic receivers were separated by less than 400 m, with highest overlap at distances between 200–400 m (Figure 54).
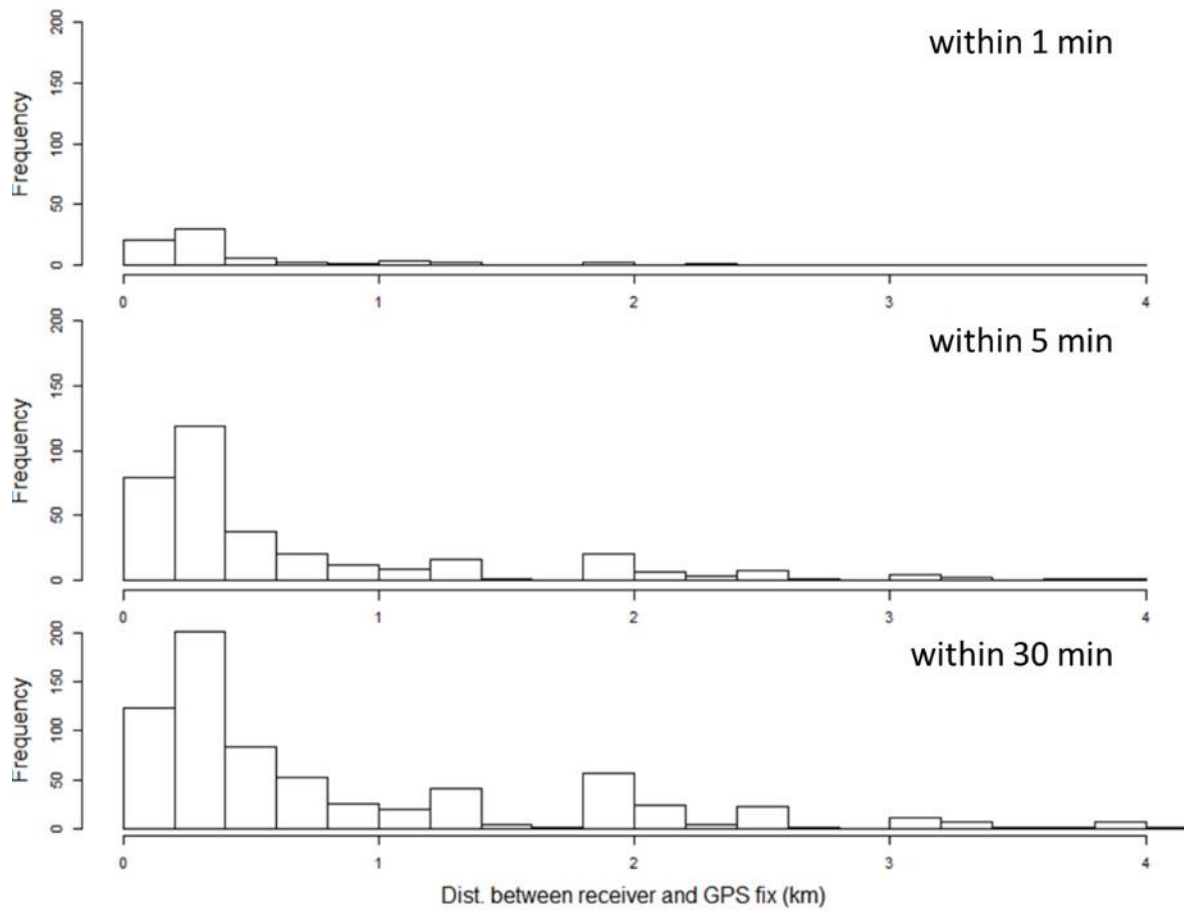
Figure 54 Distribution of the distances in space between GPS fixes and the receiver station that detected the closest (in time) ping for individual animals. Upper panel represents the distribution of distances between GPS fixes and receiver stations when the time differences between those detections was less than 1 minute; the middle and bottom panels are just distributions of distances when the maximum time difference was increased to 5 and 30 min respectively, (x-axis truncated at 4 km; acoustic-GPS fix matches occurred up to 10 km in distance for the 'within 30 min' category).

2.5   Analysis of acoustic tag detection data

For acoustic tags, the detection span of each individual was calculated as the date from first detection to last detection whereas days detected was the total number of days on which each individual was detected. The percentage of days detected was calculated by dividing detection span by days detected multiplied by 100. The number of receivers each tag was detected by is represented as "number of receivers detected on".

The number of daily detections over time for each individual were plotted to provide an overview of detection span and detection frequency for animals tagged at Pelican Banks and Wiggins Island.

To examine the influence of tide on animal position within the array, each receiver was assigned to a habitat type based on their depth and proximity to the channel. For Pelican Banks, receivers were classified as being in the following habitat types: intertidal flat, subtidal flat or channel based on the high tide depth of 0.70–1.50 m, 1.51–3.0 m and 3.10–10.0 m. At Wiggins Island, the classification of intertidal and subtidal flat was identical to Pelican Banks; however there was an expansive area

between intertidal flat and the channel, therefore an additional habitat of "channel edge" was included. For Wiggins Island, receivers were classified as follows: intertidal flat (0.70–1.50 m), subtidal flat (1.51–3.0 m), channel edge (3.1–5.0 m), channel (5.1–15.0 m) based on the depth at mean high water. In addition, narrow drains into the mangroves were classified as "mangrove drains" (GH49 and GH7 in Figure 3) and the channels between the small Islands around Wiggins Islands were classified as "Wiggins channel" (GH01 and GH2 in Figure 50).

Kernel distribution was calculated for those animals that were detected for more than 30 days and on at least one receiver. Area utilisation was estimated using the utilisation distribution (van Winkle 1975) and its estimates with kernel techniques (Worton 1989). Utilisation distribution is a probability density function that quantifies an individual's relative use of space (Kernohan et al. 2001). It depicts the probability of an animal occurring at a location within its home range as a function of relocation points (data obtained from receiver detections) (White & Garrot 1990). Kernel utilisation distribution has been widely used to investigate animal movement from acoustic telemetry of a range of species ranging from marine turtles (Makowski et al. 2006; MacDonald et al. 2012), dugongs (Zeh et al. 2014), crocodiles (Dwyer et al. 2014) and fish (Pillans et al. 2014). The bandwidth (or smoothing parameter = h) can greatly influence the shape and size of the kernel (Wand and Jones 1995; Gitzen et al. 2006; Pillans et al. 2014). There is no single *a priori* method for determining the most appropriate bandwidth. Choice of a bandwidth method may vary depending on the study goals, sample size, and patterns of space use by the study species (Worton 1989, Gitzen et al. 2006). We therefore tested the two most commonly used methods: the reference smoothing parameter function (h_{ref}; Worton 1989) and the least squares cross validation function (h_{lscv}; Silverman 1986) and found the reference smoothing parameter (h_{ref}) provided the most realistic representation of space use, with h_{lscv} tending to produce unrealistic multiple kernels that were fragmented and clustered around receivers, excluding important areas occupied by turtles.

Kernel utilisation distribution (50 and 95%) was calculated using the adehabitatHR package in R (Calenge 2006). Passive acoustic detections resulted in thousands to hundreds of thousands of detections of individuals on each receiver with identical X and Y coordinates. To alleviate this issue, we randomly assigned acoustic detections within a 200 m radius of each receiver. This radius was chosen based on range test data from turtles tagged with both satellite and acoustic tags as well stationery tags within the array.

Behaviour at the individual level was characterised by the 50 and 95% kernel densities which were calculated for all months combined, as well as for each month-year combination that the animal was detected. To determine the influence of tide on movement and habitat use, 50 and 95% KUDs of individuals and all turtles combined were calculated during the period one hour each side of high and low tide for each month/year and for the entire monitoring period. This was achieved by calculating the time difference from each detection to the nearest high and low tide. Within the detection database, a row with time to high tide and a row with time to low tide were created for each detection.

The proportion of animals of known sex (and those where sex could not be determined) remaining within the array after tagging was calculated using the detection span of each individual. When an animal was not detected within the array for more than one week, it was classified as having left the array. Animals that left the array and then returned were incorporated into the calculation at each time period.

2.5.1 COMPARING ACOUSTIC AND SATELLITE TAG DATA

Raw GPS data (Fastloc) from Argos were used to investigate the movement of individual turtles and compare home range estimates from satellite and acoustic telemetry. The satellite fixes were plotted to enable visual estimation of long distance movements and home range estimates (50 and 95% KUD's) were obtained using the adhabitateHR package in R. There were insufficient GPS fixes to examine the influence of tide on movement using GPS data. The number of GPS fixes and acoustic detections from animals tagged with both tag types as well KUD size and shape were used to compare estimates obtained from the two types of tags.

3 Results

3.1 Tagged turtles

A total of 98 green turtles were captured during two collaborative field trips in May and November 2013. Within the array of receivers at Pelican Banks, 33 turtles were tagged with acoustic tags with five of these animals also tagged with satellite tags (Figure 55). At the Wiggins Island array of receivers, 16 turtles were tagged with acoustic tags with five of these also tagged with satellite tags (Figure 56). The acoustic tag identification code (Tag ID), satellite tag serial number, sex, curved carapace length (CCL (cm)) and mass (kg) of individuals are provided for animals tagged at Pelican Banks and Wiggins Island (Table 3.1 and Table 3.2, respectively). Animals tagged at Pelican Banks ranged from 43–114 cm CCL, whereas those at Wiggins Island ranged from 46-60 cm CCL (Figure 57).
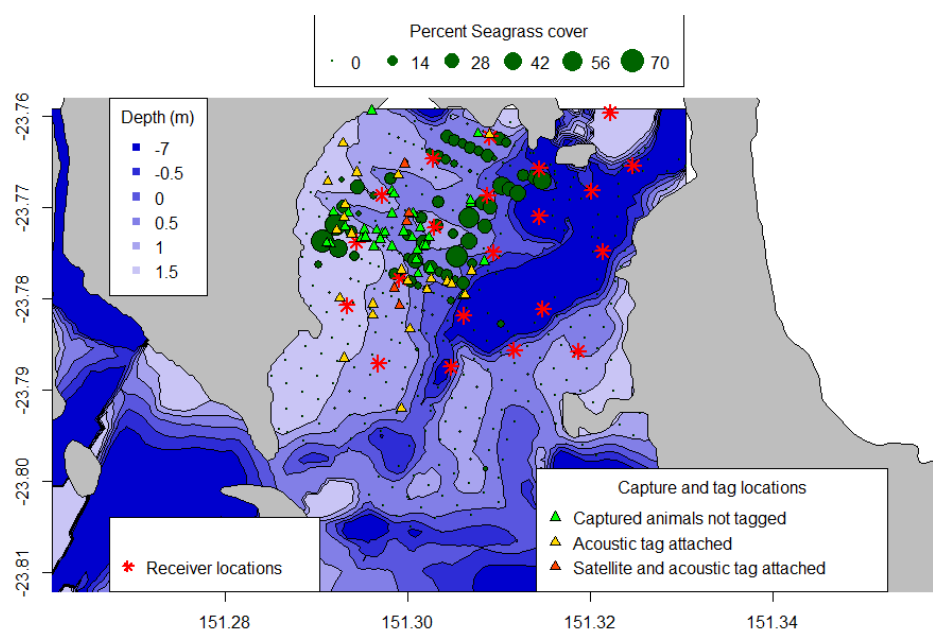
Figure 55 Pelican Banks receiver array showing the seagrass density, receiver locations, low tide depth contours and capture location of all turtles. Of the turtles captured, those tagged with both acoustic and satellite tags as well as those only tagged with acoustic tags are also shown.

3.2 Acoustic detections

From the 49 turtles tagged in this study, tags were detected 1,385,100 times by the 46 acoustic receivers within Gladstone Harbour between 1 May 2013 and 16 September 2014. There were 706,362 detection of the 33 turtles tagged with acoustic tags around Pelican Banks; with individuals detected between 2 – 62,751 times on 1 – 36 receivers for 1 – 495 days after tagging. Of the 16 turtles tagged with acoustic tags at Wiggins Island, there were 678,738 detections with individuals detected between 425 – 127,137 times on 5 – 18 receivers for 181 – 502 days after tagging. The mean proportion of days detected for turtles at Pelican Banks was (75.5 ± 4.7 SE) and Wiggins Island (85.3 ± 3.9 SE) was not significantly different (one sample t-test, p = 0.12). Overall, turtles at Wiggins

Island were detected on significantly more days following release (295.4 ± 35.5 SE) than turtles at Pelican Banks (180.8 ± 25.9) (one sample t-test, p = 0.01).
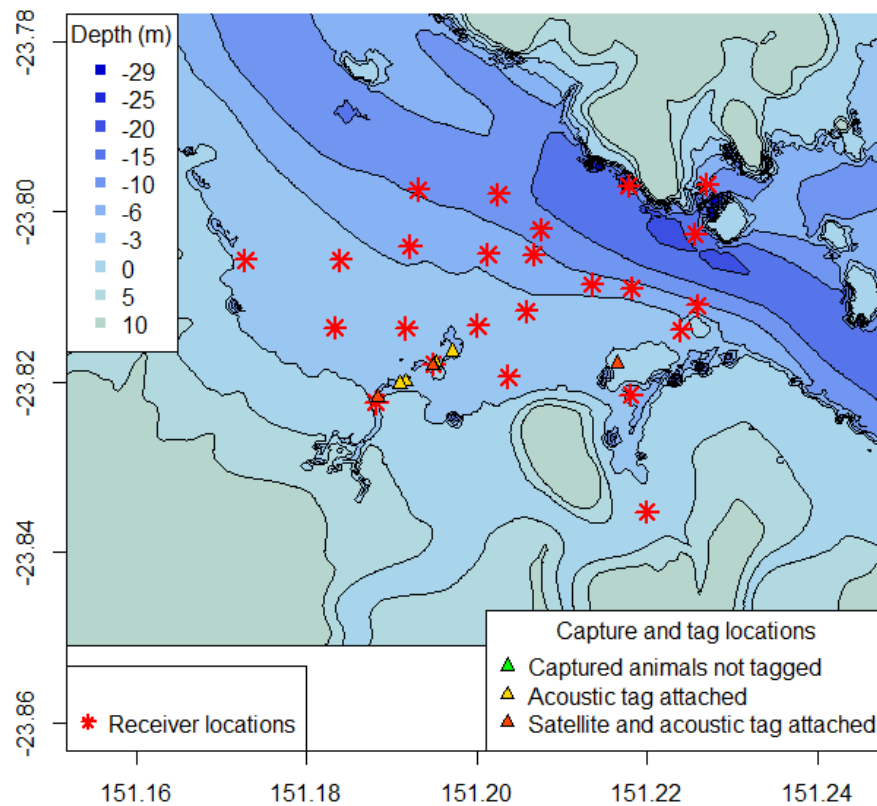
Figure 56 Wiggins Island receiver array showing the receiver locations, low tide depth contours and capture location of all turtles. All captured turtles were tagged with acoustic tags and five individuals were tagged with both satellite and acoustic tags.
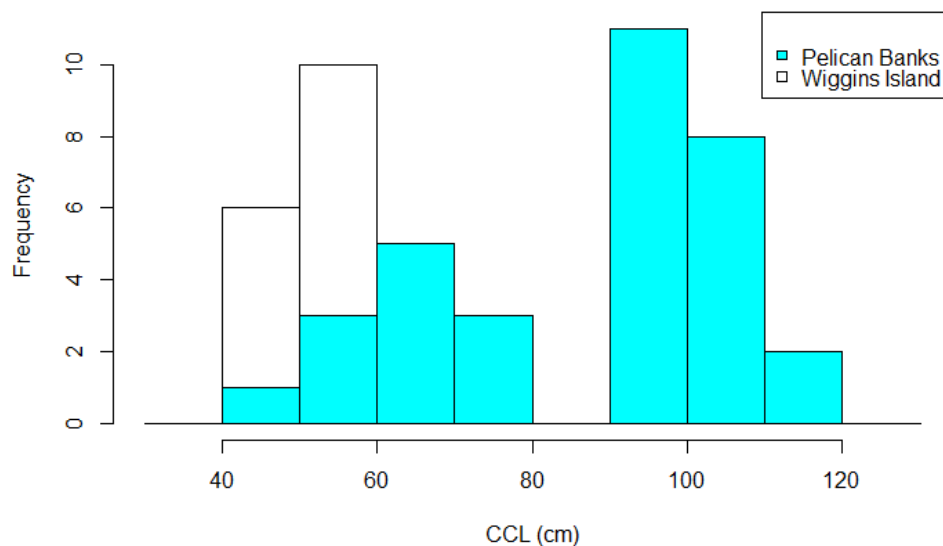
Figure 57 Curved carapace length (CCL (cm)) of turtles tagged with acoustic and satellite tags at Pelican Banks and Wiggins Island.

3.3 Influence of acoustic tag attachment method

Acoustic tags were attached with either one bolt or two with an assumption that having the tag tucked under the back of the carapace may result in fewer detections than a tag that was protruding. For turtles at Pelican Banks tagged with acoustic tags attached with either one or two bolts, there was no difference in the number of daily detections (t-test, p > 0.5) with the mean number of daily detections of 138 (± 122.8 SD) and 187 (± 155.3 SD) for one and two bolts, respectively (Figure 58).
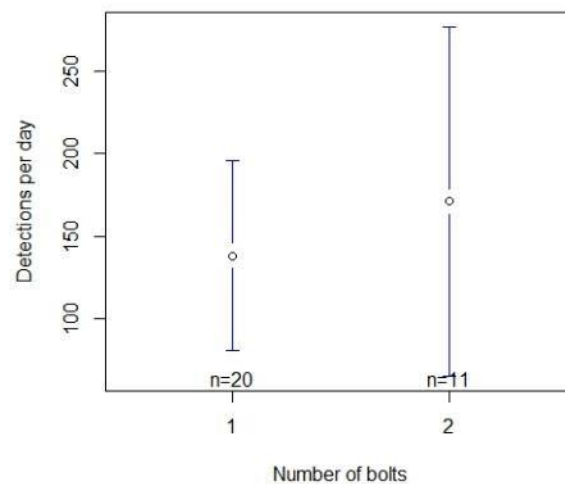
Figure 58 Mean (± 95 % CI) of acoustic tag detections per day from turtles at Pelican Banks with 1 and 2 bolts holding the tag in place.

For animals at Pelican Banks, the influence of a sleeve was significant (t-test, p < 0.001) with the mean number of detections of tags attached with a sleeve (39.9 ± 27.1 SE) significantly lower than mean without a sleeve (212.3 ± 128.4) (Figure 59A).

For animals at Wiggins Island, tags that were attached with one bolt were also those that were within a sleeve, with the influence of bolt type confounded by sleeve but tags with a sleeve (and one bolt) were detected significantly less (39.9 ± 27 SD per day) than tags with no sleeve (212.4 ± 128) (Figure 59B).
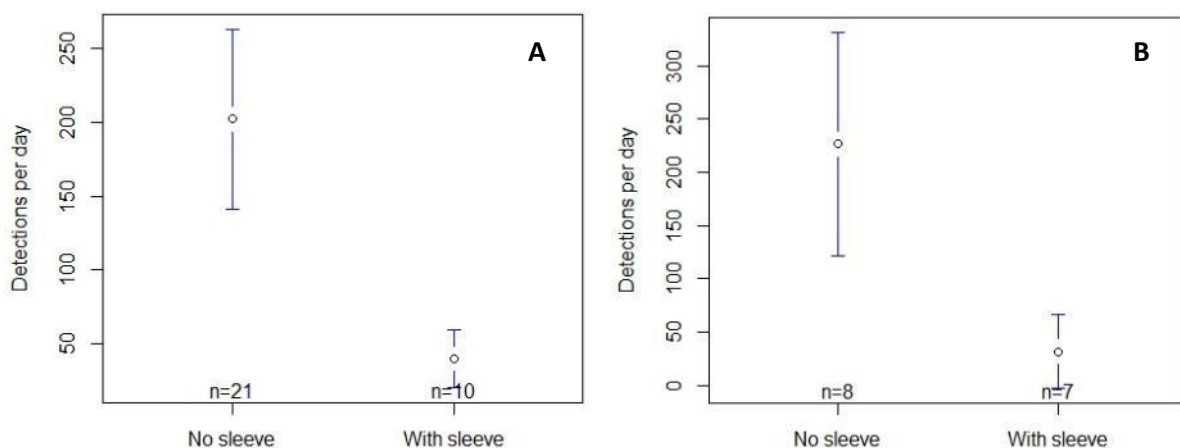
Figure 59 Acoustic tag detections per day (mean ± 95 % CI) of from turtles at Pelican Banks (A) and Wiggins Island (B) without and with a PVC sleeve around the acoustic tag.

Table 3.1 Turtles tagged at Pelican Banks: acoustic tag number, satellite tag number, date tagged, sex, age class, curved carapace length (CCL) and mass of turtles tagged with acoustic tags. The detection span, number of days each individual was detected and the percentage of days detected (detection span/days detected since tagged multiplied by 100) as well as the number of receivers each individual was detected by for all turtles tagged with acoustic tags in Gladstone Harbour. Age class abbreviations: A = adult (known sexually mature), AT = Adult (defined from carapace and tail measurements), SP = Pubescent immature (gonads and ducts differenciating from that of a young immature), SA = Prepubescent immature (defined from carapace measurements), J = Juvenile

Tag ID	Satellite tag	Date tagged	Sex	Age class	CCL (cm)	Detection span	Days detected since tagged	Percentage of days detected	Number of Receivers detected on
27949	126272	01-May-13	F	A	106.2	499	495	99	18
27928		01-May-13	F	A	101.1	500	273	55	17
27948	126274	02-May-13	F	A	113.8	98	4	4	14
27952		02-May-13	M	AT	98.8	149	136	91	27
27924		02-May-13	M	AT	96.7	236	172	73	37
27926	126273	02-May-13	F	SP	101.6	15	15	100	20
27944		03-May-13	F	A	110	63	63	100	18
27935		03-May-13	F	A	98.3	256	246	96	19
27945		03-May-13	M	AT	95.7	4	4	100	14
27934		03-May-13	M	AT	93.5	5	5	100	8
27942		03-May-13	M	AT	94.8	400	186	47	19
27936		03-May-13	M	AT	100.3	437	321	73	20
27933		03-May-13	M	J	57.9	21	15	71	11
27927		03-May-13	F	J	61.1	497	344	69	36
27938		03-May-13	F	SA	67.8	146	52	36	16
27940		03-May-13	F	SA	67.9	189	189	100	30

Tag ID	Satellite tag	Date tagged	Sex	Age class	CCL (cm)	Detection span	Days detected since tagged	Percentage of days detected	Number of Receivers detected on
27929		03-May-13	F	SA	69.7	414	371	90	15
27930		03-May-13	F	SA	71	483	272	56	18
27923		03-May-13	F	SA	70.7	495	417	84	19
27925		03-May-13	F	SA	74.5	498	411	83	20
27939		03-May-13	F	SA	65.2	498	425	85	23
26572	133769†	05-Nov-13	F	A	107.4	291	185	64	16
26575	133764†	05-Nov-13	F	A	111	306	217	71	24
27980	133765†	05-Nov-13	M	AT	96.5	314	258	82	20
26571	133766†	07-Nov-13	F	A	105.6	7	7	100	12
28352	133768†	07-Nov-13	M	A	93.6	137	131	96	17
26573	133767†	07-Nov-13	F	A	105.8	146	137	94	18
26568	131868	07-Nov-13	M	A	97.7	229	192	84	31
16229	131869	07-Nov-13	F	AT	96.2	77	4	5	6
26576		07-Nov-13	F	AT	99.5	224	212	95	15
27663		08-Nov-13	I	J	56	51	15	29	5
27657		08-Nov-13	I	J	59.8	306	205	67	14
27661	133758†	09-Nov-13	I	J	43.6	1	1	100	1

† satellite tags deployed by EHP (data not provided to CSIRO)

Table 3.2 Turtles tagged at Wiggins Island: acoustic tag number, satellite tag number, date tagged, sex, age class, curved carapace length (CCL) and mass of turtles tagged with acoustic tags. The detection span, number of days each individual was detected and the percentage of days detected (detection span/days detected since tagged multiplied by 100) as well as the number of receivers each individual was detected by for all turtles tagged with acoustic tags in Gladstone Harbour.

Tag ID	Satellite tag	Date tagged	Sex	Age class	CCL (cm)	Detection span	Days detected since tagged	Percentage of days detected	Number of Receivers detected on
27951		02-May-13	F	J	51.8	502	458	91	17
27947	126275	02-May-13	M	J	58.8	502	413	82	12
27950	126276	02-May-13	M	J	54.6	500	448	90	18
27931		03-May-13	F	J	51.5	248	248	100	13
27932		03-May-13	F	J	50.6	211	199	94	15
27941		03-May-13	F	J	48.2	256	237	93	17
27937		03-May-13	M	J	56.1	500	475	95	17
27946		03-May-13	M	J	46.4	500	490	98	13
27943	133761†	05-Nov-13	F	J	46.1	500	485	97	18
27622	133760†	05-Nov-13	I	J	46	199	156	78	14
27629	131871*	05-Nov-13	I	J	60	313	308	98	10
31598	131862	05-Nov-13	I	J	52.1	313	219	70	11
27662	133762†	06-Nov-13	I	J	49.1	180	180	100	13
29771	131872	07-Nov-13	I	J	52.7	222	118	53	5
27656		08-Nov-13	I	J	48.2	200	107	54	5
27658		08-Nov-13	I	J	52.7	258	186	72	9

* satellite tag failed (no Fastloc data); † satellite tags deployed by EHP (data not provided to CSIRO)

3.4   Turtle detection span

The average detection span for all turtles was 273 (± 19 SE) days with turtles at Wiggins Island having a greater detection span (337 ± 34 days) than turtles at Pelican Bank (242 ± 31 days). The average number of days on which turtles were detected was 218 (± 20) with turtles at Wiggins Island being detected on more days (295 ± 34 days) than turtles at Pelican Bank (181 ± 25 days).

For juveniles and subadults tagged at Pelican Banks in May 2013, 75% of females and 0% of males (n=7) remained in the array after six months. Sex of immature turtles was not determined in November 2013 so comparisons were not possible (Figure 60). For adult animals at Pelican Banks, 50% of males and females tagged in May 2013 were still being detected within the array after 6 months. For adults tagged in November 2013, after six months 100% of males and 66% of females were still being detected by the array suggesting that more adult turtles departed the array during 2013 than 2014 (Figure 61).

At Wiggins Island, for both males and females tagged in May 2013, 100% were still being detected within the array after six months. Sex of animals was not determined in November 2013, however of those tagged during that time, 100% were still being detected within the array after six months (Figure 62).
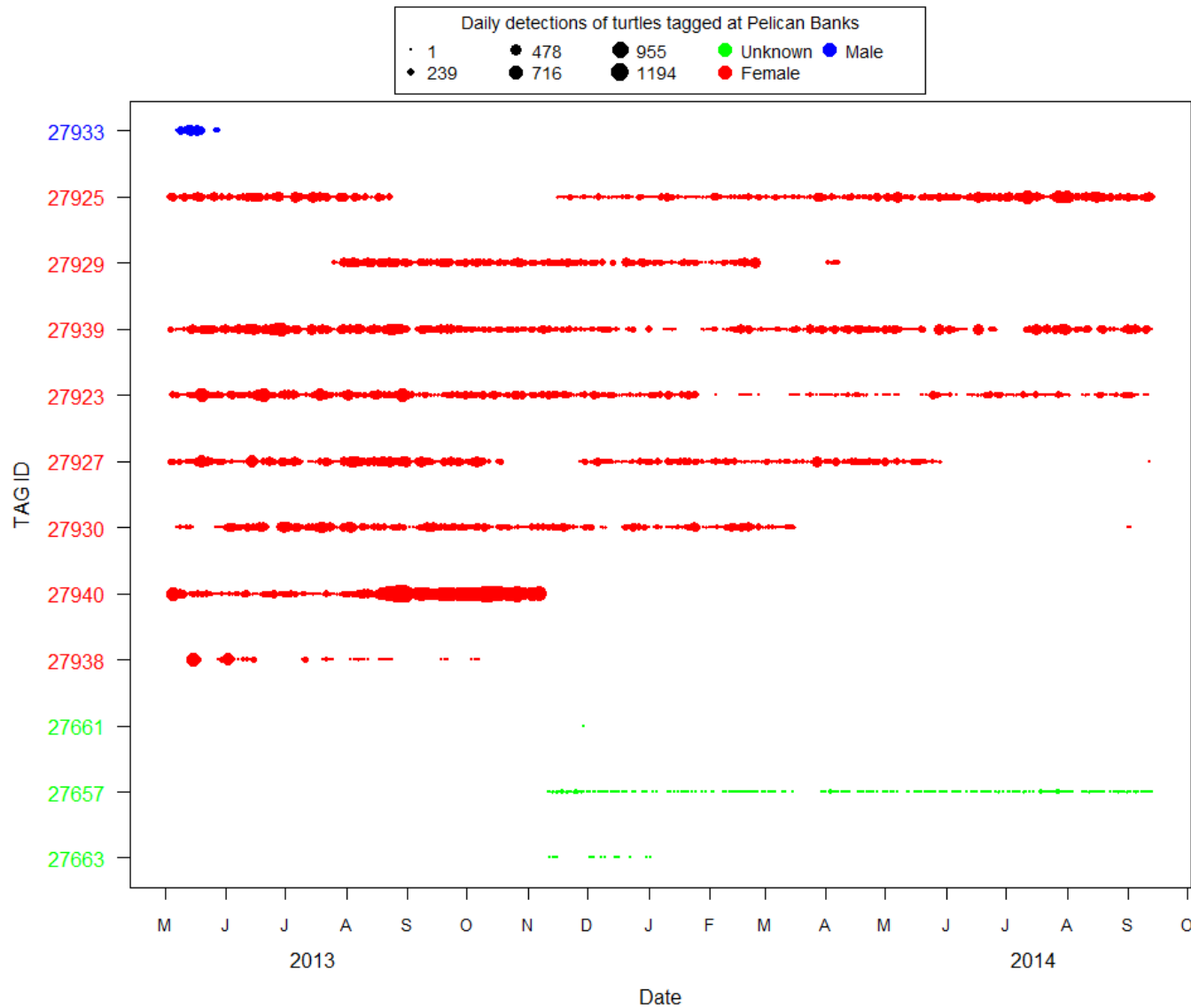
Figure 60 Number of daily detection for each individual juvenile and subadult turtles tagged at Pelican Banks (n = 12). Males, females and individuals of unknown sex are shown in different colours. The acoustic tag ID of individuals are shown on the y-axis with the size of the bubbles representative of the number of detections on each day between 1 May 2013 – 16 September 2014
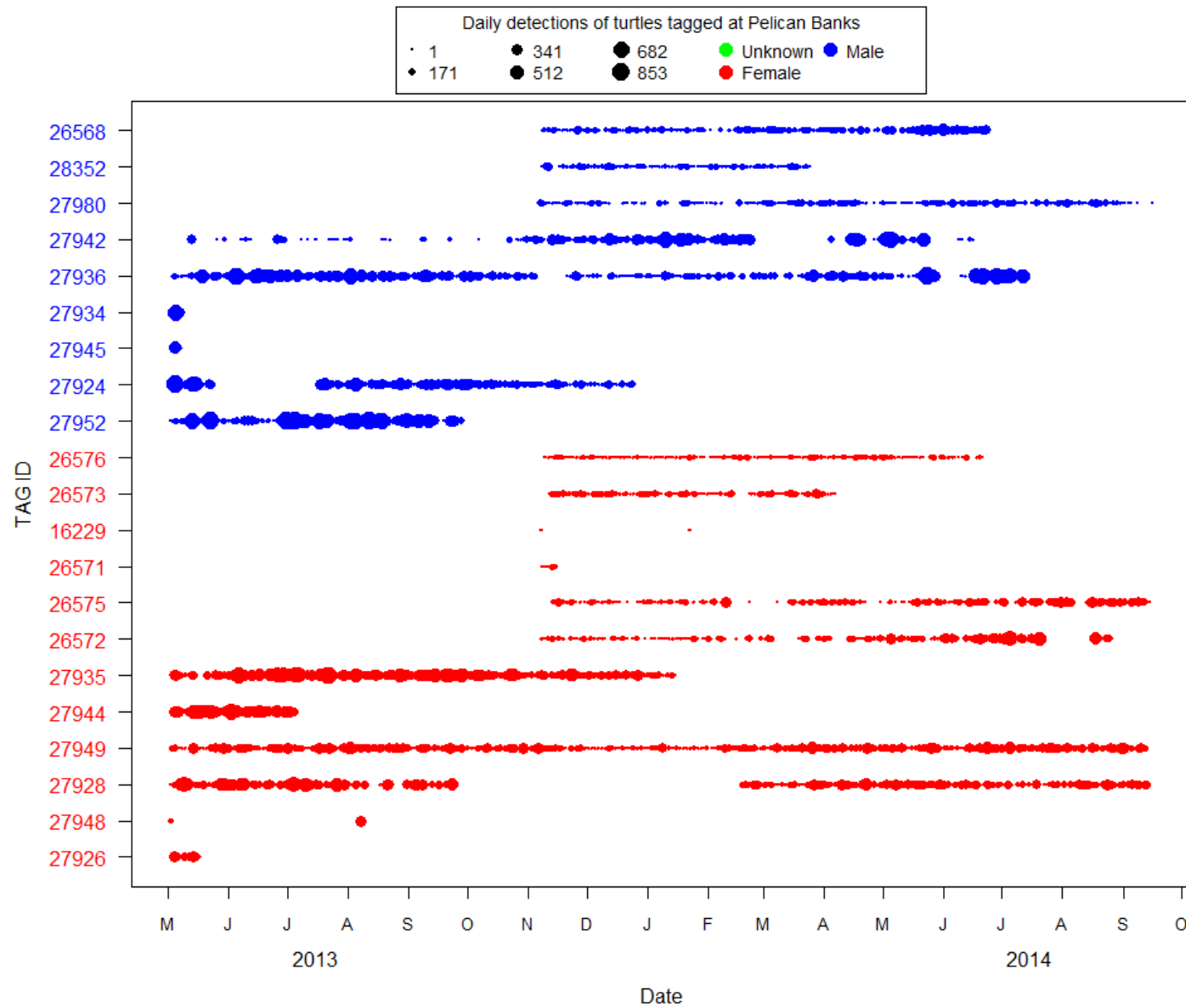
Figure 61 Number of daily detections for each individual adult turtle tagged at Pelican Banks (n = 21). The acoustic tag ID of individuals is shown on the y-axis with the size of the bubbles representative of the number of detections on each day between 1 May 2013 – 16 September 2014
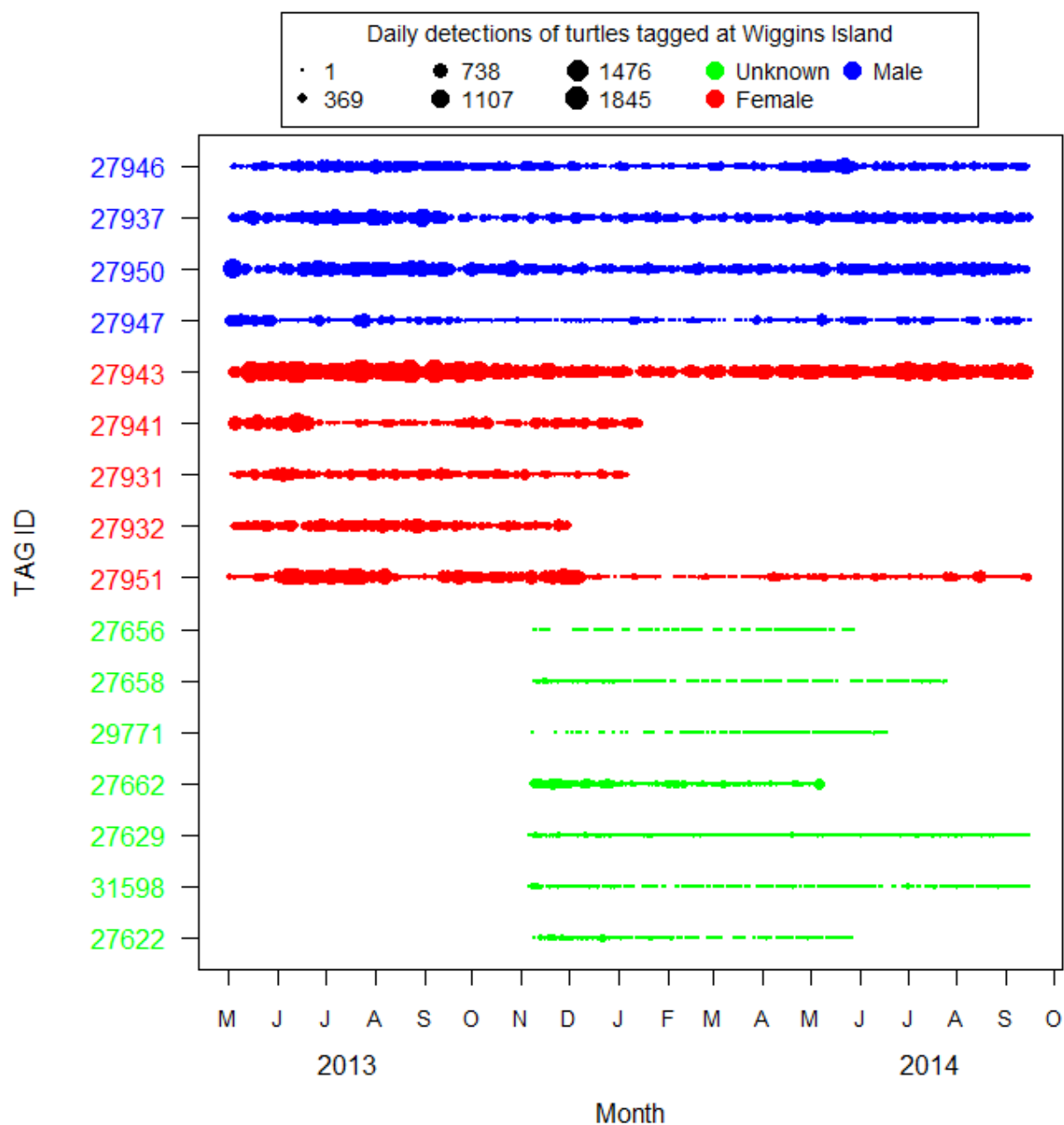
Figure 62 Number of daily detection for each individual turtle tagged at Wiggins Island (n = 16). Males, females and individuals of unknown sex are shown in different colours. The acoustic tag ID of individuals are shown on the y-axis with the size of the bubbles representative of the number of detections on each day between 1 May 2013 – 16 September 2014

3.5 Cumulative home range

The 50 and 95% KUDs of individuals tagged at Pelican Banks and Wiggins Island are shown in Table 3.3 and Table 3.4, respectively. Estimates of average (± SE) cumulative (total home range over the duration that individuals were detected) home range of green turtles within Gladstone Harbour was 1.3 ± 0.2 km^2 and 6.7 ± 0.8 km^2 for 50 and 95% KUD, respectively. For those animals tagged at Pelican Banks, six individuals were also detected at some time at Wiggins Island. The average 50 and 95% KUD of these animals was 2.2 ± 0.7 km^2 and 14.7 ± 3.5 km^2, respectively and was significantly larger (t-test, $p < 0.01$) than the home range of animals that remained at either Pelican Banks or Wiggins Island. Excluding these animals that moved, the average 50 and 95% KUD of animals at Pelican Banks was 1.4 ± 0.2 km^2 and 6.7 ± 0.9 km^2, respectively which was significantly greater (t-test, $p < 0.01$) than animals at Wiggins Island (0.7 ± 0.1 km^2 and 3.8 ± 0.4 km^2, respectively).

There was significant individual monthly variation in KUD size and shape as shown in the 50 and 95% KUD per month of the year from May 2013–September 2014 for animals tagged at Pelican Banks and Wiggins Island (Table 3.5 and Table 3.6). Large differences in home range between months were primarily due to animals moving from Pelican Banks to Wiggins Island and in some cases back to Pelican Banks (Table 3.5). However, even for animals that had small and persistent home ranges and remained within the area where they were tagged, there were subtle variations in the monthly size and shape of the area used over the duration of the monitoring period. At Pelican Banks, over a 17 month period a mature female turtle (106 cm CCL, tag ID 27949) had a 50% KUD of 0.95 km^2 and a 95% KUD of 4.11 km^2 with Figure 63 demonstrating that home range was smallest in June-July 2013 and October 2013 (50% KUD = 0.58-0.77 km^2) before increasing in December-January 2014 (50% KUD = 1.17 and 1.35 km^2, respectively). For the remainder of 2014, the average home range size then declined slightly in March before increasing in April-July before shrinking again in August-September.

Table 3.3 Turtle home range size at Pelican Banks. The 50 and 95% KUD (km^2) for individuals turtles that were tagged at Pelican Banks and detected for more than 30 days on 2 or more receivers (n = 26).

TagID	50% KUD (km^2)	95% KUD (km^2)
26568 *	4.6	25.2
26572	0.9	4.0
26573	1.8	6.9
26575	2.0	13.8
26575 *	2.0	13.8
26576	1.0	4.4
27657	1.6	6.0
27923	2.0	8.5
27924 *	4.2	25.4
27925	0.9	5.0
27926	2.2	9.2
27927	1.7	6.8
27928	0.7	3.6
27929	0.6	3.7
27930	1.0	5.5
27935	0.5	3.9
27936	0.8	4.5
27938	1.0	5.0
27939	1.0	3.7
27940 *	0.5	6.3
27942	1.2	5.1
27944	1.2	6.1
27949	1.0	4.1
27952 *	1.0	8.0
27980 *	1.0	9.2
28352	1.5	6.1

* individuals that were tagged at Pelican Banks but also detected at the Wiggins Island array.

Table 3.4 Turtle home range at Wiggins Island. The 50 and 95% KUD (km^2) for individuals turtles that were tagged at Wiggins Island and detected for more than 30 days on 2 or more receivers (n = 16).

TagID	50% KUD (km^2)	95% KUD (km^2)
27622	0.4	2.3
27629	0.6	3.1
27656	0.4	2.0
27658	0.5	2.7
27662	0.3	2.1
27931	0.8	4.1
27932	1.0	4.8
27937	0.8	5.1
27941	1.1	6.3
27943	0.3	2.0
27946	0.5	2.0
27947	0.5	2.7
27950	1.1	5.8
27951	1.3	6.7
29771	0.6	3.6
31598	1.3	4.8

Table 3.5 Turtle home range size at Pelican Banks. Monthly 50 and 95% KUD (in parenthesis) for all animals were detected for more than 30 days on two or more receivers. Monthly KUD's were only calculated when there were more than 5 detections in a month. * indicates animals that moved from Pelican Banks to Wiggins Island.

TAG_ID	May-13	Jun-13	Jul-13	Aug-13	Sep-13	Oct-13	Nov-13	Dec-13	Jan-14	Feb-14	Mar-14	Apr-14	May-14	Jun-14	Jul-14	Aug-14	Sep-14
26568 *							8.48(53.3)	16.7(70.1)	0.79(3.57)	0.62(4.94)	1.64(8.41)	1.97(9.28)	0.93(5.45)	0.88(4.7)			
26572							1.18(4.93)	0.99(4.17)	1.19(5.06)	1.58(5.66)	1.09(4.06)	0.85(3.48)	0.91(3.96)	0.90(3.79)	0.84(3.55)	1.18(4.25)	
26573							1.37(6.24)	1.32(5.91)	2.31(8.42)	2.17(7.53)	0.97(6.11)	1.93(7.64)					
26575 *							1.28(4.66)	5.35(31.9)	1.95(11.2)	1.36(7.43)	0.34(1.64)	0.44(2.48)	0.37(1.78)	0.52(2.24)	0.52(2.17)	0.52(1.98)	0.34(1.94)
26576							0.79(4.13)	0.74(3.9)	0.58(3.14)	1.26(5.17)	1.23(4.6)	1.11(4.3)	1.11(5.41)	1.24(6.55)			
27657							0.61(5.04)	1.44(6.13)	1.82(6.54)	1.5(6.69)	1.7(6.84)	0.68(3.92)	0.89(4.06)	1(4.24)	0.89(3.97)	1.1(5.29)	1.66(7.29)
27923	2.0(8.24)	1.79(7.24)	1.58(6.95)	2.49(9.14)	0.90(5.34)	1.8(7.55)	0.45(2.28)	0.53(4.33)	1.3(6.7)	0.19(0.81)	0.20(0.9)	0.21(0.98)	0.38(1.43)	0.21(0.95)	0.23(1.09)	0.21(0.93)	0.21(0.97)
27924 *	7.7(45.9)		1.37(6.54)	1.59(5.84)	1.04(4.41)	0.77(4.17)	6.24(43.1)	0.55(2.9)									
27925	1.61(6.04)	1.59(6.36)	1.49(6.87)	1.59(6.44)			0.73(4.64)	1.22(5.01)	0.91(4.88)	0.57(4.27)	1.36(5.69)	1.22(5.33)	1.02(5.1)	0.64(4.18)	0.74(4.21)	0.29(2.45)	0.27(1.84)
27926	2.19(9.24)																
27927	1.18(5.56)	1.18(4.75)	1.4(5.69)	1.23(6.05)	1.40(5.6)	4.79(33.7)	0.79(3.73)	1.32(5.29)	1.48(5.88)	0.75(4.07)	1.42(5.07)	0.76(3.97)	1.04(4.57)				
27928	0.60(2.8)	0.71(2.95)	0.53(2.38)	0.84(3.97)	1.07(3.87)					0.87(3.82)	1.01(4.06)	0.38(2.62)	0.30(2.43)	1.15(4.08)	0.75(3.74)	0.57(3.45)	1.05(4.74)
27929			0.66(3.39)	0.77(3.87)	0.81(3.69)	0.43(3.09)	0.39(2.51)	0.54(3.4)	0.63(3.14)	0.57(3.06)		0.49(2.39)					
27930	0.79(4.43)	0.75(4.11)	0.53(3.37)	0.83(4.87)	0.43(3.32)	0.59(3.45)	0.50(2.76)	0.62(3.6)	1.25(4.89)	0.65(2.51)	0.67(2.77)						0.11(0.43)
27935	1.50(7.72)	0.70(4.53)	0.58(3.6)	0.63(3.76)	0.34(2.71)	0.38(2.79)	0.42(3.46)	0.41(2.99)	0.79(4.58)								
27936	1(3.83)	0.87(4.15)	0.85(4.39)	0.99(4.08)	0.85(3.56)	0.70(3.44)	0.75(3.24)	0.72(3.56)	1.19(5.83)	1.05(6.88)	0.78(4.21)	0.72(2.96)	0.77(3.22)	0.77(3.63)	0.77(3.34)		
27938	0.43(2.65)	1.40(8.38)	0.26(1.44)	0.19(0.88)	0.22(1.05)	0.25(1.25)											
27939	1.30(8.93)	0.79(3.49)	0.62(3.82)	0.69(3.57)	0.94(4)	0.69(3.32)	0.80(3.25)	1.03(3.9)	0.72(3.25)	0.83(3.47)	0.52(2.46)	0.83(3.27)	0.73(2.81)	0.66(2.88)	0.55(2.66)	0.53(2.64)	0.48(1.97)
27940 *	11.1(47.3)	0.70(3.43)	1.11(4.36)	0.34(3.73)	0.20(0.87)	0.20(0.87)	0.20(0.89)										
27942	0.29(1.61)	0.35(2.18)	0.22(0.88)	0.23(1)	0.22(0.92)	1.89(5.97)	1.08(4.71)	0.59(3.54)	0.68(3.64)	1.18(4.26)		0.91(4.54)	0.94(4.03)	2.27(11.4)			
27944	0.83(3.92)	1.41(6.28)	1.12(4.44)														
27949	1.08(4.62)	0.76(3.78)	0.76(3.53)	0.88(4.01)	1(4.81)	0.58(3.91)	0.86(3.88)	1.17(4.56)	1.35(4.69)	1.07(4.35)	0.71(3.58)	1.15(3.98)	1.2(4.39)	1.03(3.9)	1.0(4.66)	0.43(2.25)	0.71(3.42)
27952 *	4.92(18.1)	1.08(5.03)	0.77(5.13)	0.5(3.49)	0.97(6.17)												
27980 *							0.87(4.62)	2.83(20.5)	7.13(39.1)	14.2(64.9)	0.36(2.74)	0.39(2.77)	0.30(1.7)	0.31(1.47)	0.35(1.63)	0.27(1.38)	0.25(1.07)
28352							1.91(9.64)	0.96(4.33)	0.74(4.32)	1.62(6.69)	1.77(6.69)						

Table 3.6 Turtle home range at Wiggins Island. Monthly 50 and 95% KUD (in parenthesis) for all animals detected for more than 30 days on two or more receivers. Monthly KUD's were only calculated when there were more than five detections in a month.

TAG_ID	May-13	Jun-13	Jul-13	Aug-13	Sep-13	Oct-13	Nov-13	Dec-13	Jan-14	Feb-14	Mar-14	Apr-14	May-14	Jun-14	Jul-14	Aug-14	Sep-14
27622							0.52(3.34)	0.42(2.15)	0.30(2.02)	0.25(1.37)	0.25(1.01)	0.23(1.08)	0.37(2.11)				
27629							0.94(3.96)	0.41(2.09)	0.28(1.41)	0.29(1.59)	0.62(2.76)	0.67(3.36)	0.69(3.59)	0.65(2.42)	0.62(2.55)	0.71(2.88)	0.58(2.16)
27656							0.69(4.01)	0.42(1.74)	0.40(1.55)	0.35(2.07)	0.43(1.54)	0.29(1.28)	0.22(1.04)				
27658							0.50(2.63)	0.49(2.78)	1.11(3.5)	0.4(1.99)	0.73(3.14)	0.68(2.48)	0.42(2.07)	0.32(1.77)	0.28(1.63)		
27662							0.38(2.25)	0.44(2.46)	0.46(2.35)	0.27(1.75)	0.25(1.58)	0.36(2.3)	0.29(1.99)				
27931	0.92(4.52)	1(4.39)	0.36(1.94)	0.37(2.17)	0.32(2.07)	1.07(4.04)	0.98(3.98)	0.68(4.05)	1.09(5.29)								
27932	0.86(4.86)	1.06(5.1)	0.97(4.94)	0.94(4.94)	1.02(3.94)	1.04(4.08)	1.08(4.28)										
27937	0.65(3.93)	1.05(5.65)	1.09(5.7)	1.21(5.88)	1.37(6.02)	0.71(3.15)	0.65(2.89)	0.52(2.85)	0.44(2.45)	0.58(2.63)	0.62(3.6)	0.55(3.07)	0.52(2.99)	0.88(3.86)	0.92(4.46)	0.49(2.88)	0.66(3.6)
27941	0.74(3.58)	1.19(8.28)	0.28(1.56)	0.35(1.75)	0.99(6.43)	0.94(4.69)	0.6(3.71)	0.79(4.36)	0.70(3.77)								
27943	0.72(5.53)	0.54(3.2)	0.45(1.91)	0.45(1.95)	0.45(1.78)	0.46(2)	0.32(2.74)	0.23(1.13)	0.23(1.3)	0.2(0.91)	0.25(1.39)	0.22(1.06)	0.23(1.11)	0.22(1.15)	0.24(1.19)	0.22(1.1)	0.21(0.92)
27946	0.46(2.9)	0.50(2.23)	0.48(2.1)	0.43(1.73)	0.45(1.96)	0.37(1.59)	0.42(1.78)	0.44(2.08)	0.43(2.03)	0.6(2.18)	0.66(2.34)	0.52(2.09)	0.44(2.02)	0.2(0.89)	0.21(0.88)	0.2(0.9)	0.2(0.88)
27947	0.28(1.95)	0.39(3.07)	0.50(2.43)	0.50(2.71)	0.62(2.83)	0.92(3.4)	0.54(2.74)	0.49(2.48)	0.40(2.36)	0.36(2.31)	0.57(4.03)	0.66(2.93)	0.72(2.88)	0.4(2.41)	0.56(2.68)	0.28(1.85)	0.29(1.91)
27950	1.93(7.75)	1.35(5.99)	0.6(2.74)	0.58(3.02)	0.65(3.83)	0.37(3.25)	0.53(5.43)	1(4.3)	0.79(5.08)	0.90(4.84)	0.95(5.27)	1.12(5.6)	1.09(5.28)	0.54(5.01)	0.81(4.85)	0.81(4.01)	0.94(4.6)
27951	2.33(11.4)	0.57(3.16)	0.64(3.48)	1.09(4.63)	0.73(3.71)	0.58(3.17)	0.67(4.67)	0.69(5.7)	0.22(0.96)	0.23(1.02)	0.18(0.86)	0.21(0.89)	0.20(0.9)	0.21(0.9)	0.21(0.88)	0.20(0.93)	0.21(0.92)
29771							0.23(0.9)	1.19(5.29)	0.86(2.92)	0.75(2.67)	0.69(2.57)	0.99(4.43)	0.85(5.53)	0.38(2.65)			
31598							0.69(4.34)	1.22(4.69)	0.87(3.27)	0.76(2.87)	0.73(2.88)	0.40(2.15)	0.85(3.34)	0.76(3.83)	0.65(2.78)	0.77(3.38)	1.10(5.55)
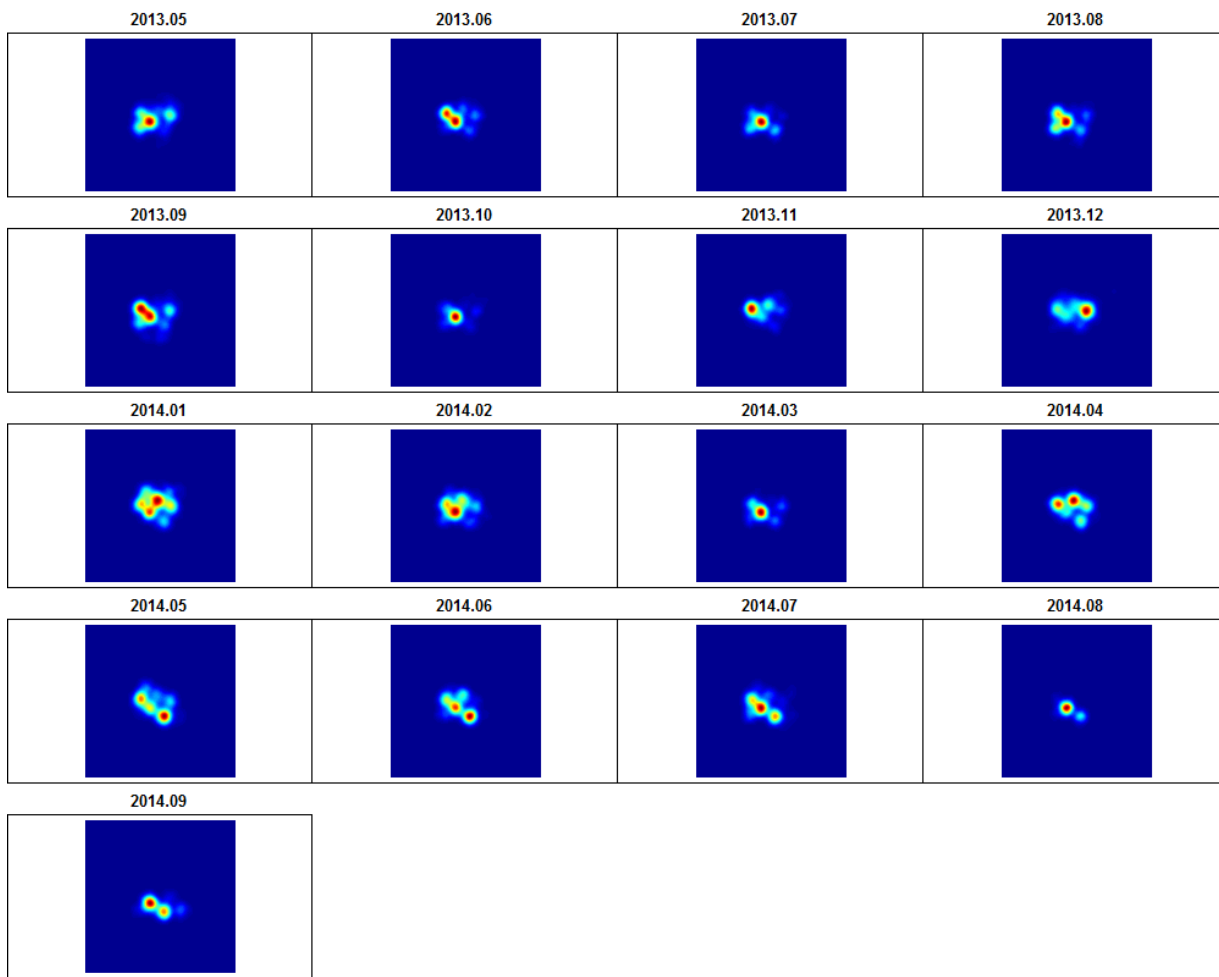
Figure 63 Monthly home range variation of a mature female turtle at Pelican Banks. Kernel utilisation distribution of a female turtle (106 cm CCL tag ID 27949) monthly from May 2013 – September 2014. Orientation of each month of the year is the same with high use areas shown as red/orange/yellow (50% KUD) with a gradient through to turquiose (95% KUD).

Similarly, and also at Pelican Banks, a mature male turtle (94.8 mm CCL, tag ID 27942) had a 50% KUD of 1.2 km^2 and a 95% KUD of 5.1 km^2 over a 13 month period with Figure 64 demonstrating that area used was smallest in May–September 2013 (50% KUD between 0.22–0.35 km^2) when this animal was primarily detected on only one receivers and largest in October 2013 and June 2014 (50% KUD = 1.89 and 2.27 km^2, respectively) when it was moving between 4-5 receivers.
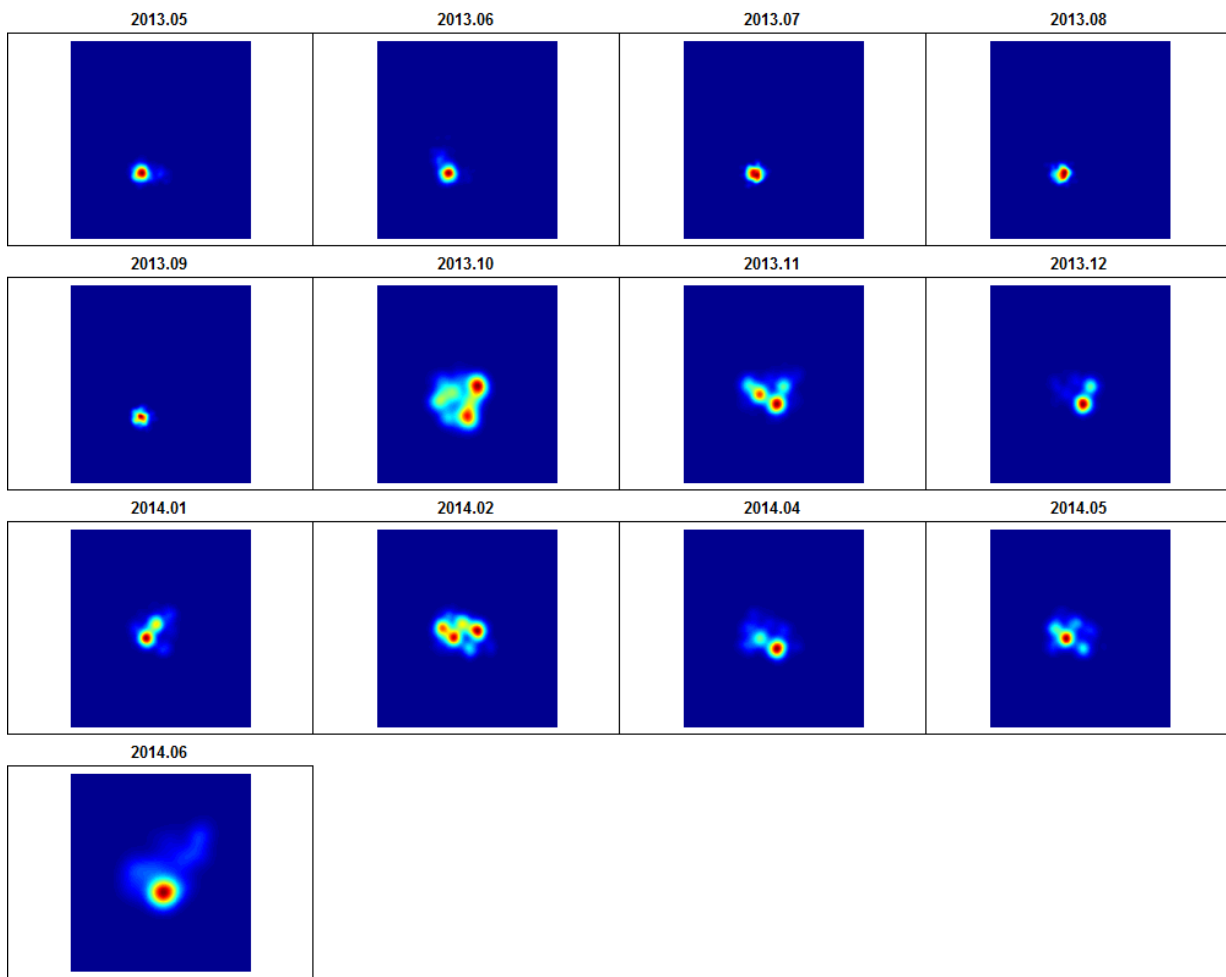
Figure 64 Monthly home range variation of a mature female turtle at Pelican Banks. Kernel utilisation distribution of a female turtle (94.8 cm CCL tag ID 27942) monthly from May 2013 – September 2014. Orientation of each month of the year is the same with high use areas shown as red/orange/yellow (50% KUD) with a gradient through to turquiose (95% KUD).

At Wiggins Island, over a 17month period, a juvenile male turtle (46.4 cm CCL, tag ID 27946) had a 50% KUD of 0.5 km^2 and a 95% KUD of 2.0 km^2, with Figure 65 and Table 3.6 demonstrating that area used was largest in February-March 2014 (50% KUD between 0.6–0.66 km^2) and smallest in June-September 2014 (50% KUD = 0.2–0.2). The decrease in size was primarily due to the animal moving around three receivers in February–March and then primarily being detected by one receiver in June –September 2014.
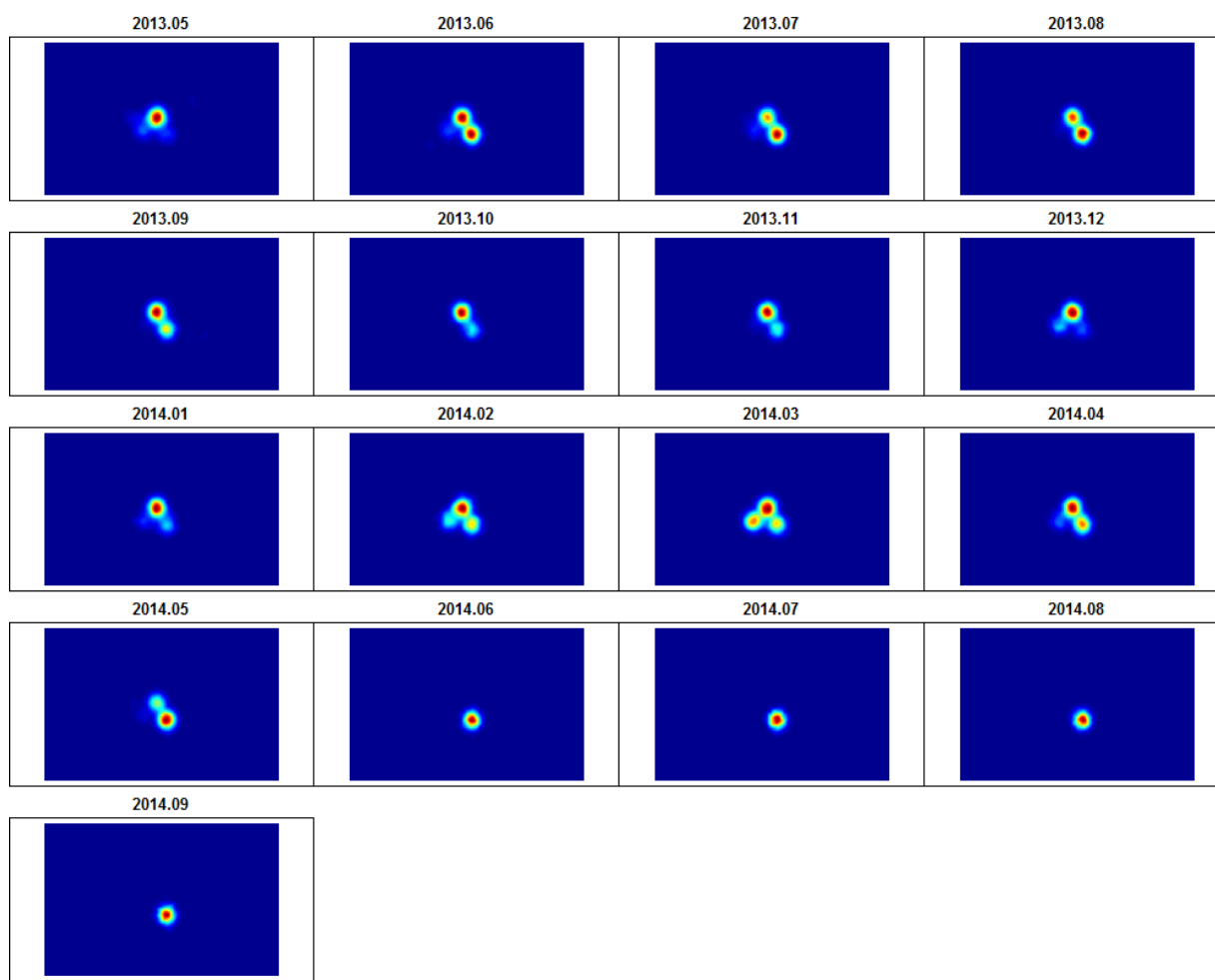
Figure 65 Monthly home range variation of amature female turtle at Pelican Banks. Kernel utilisation distribution of a female turtle (46.4 cm CCL, tag ID 27946) monthly from May 2013 – September 2014. Orientation of each month of the year is the same with high use areas shown as red/orange/yellow (50% KUD) with a gradient through to turquiose (95% KUD).

At Wiggins Island, over a 17month period, a juvenile male turtle (54.6 cm CCL, tag ID 27950) had a 50% KUD of 1.1 km^2 and a 95% KUD of 5.8 km^2 with Figure 66 and Table 3.6 demonstrating that area used was largest in May 2013 (50% KUD 1.93 km^2) and smallest in October 2013 and June 2014 (50% KUD = 0.37 and 0.54 km^2, respectively). The decrease in size was primarily due to the animal being detected by 4-6 receivers in May-June 2013 and only 1-2 receivers in October 2013.
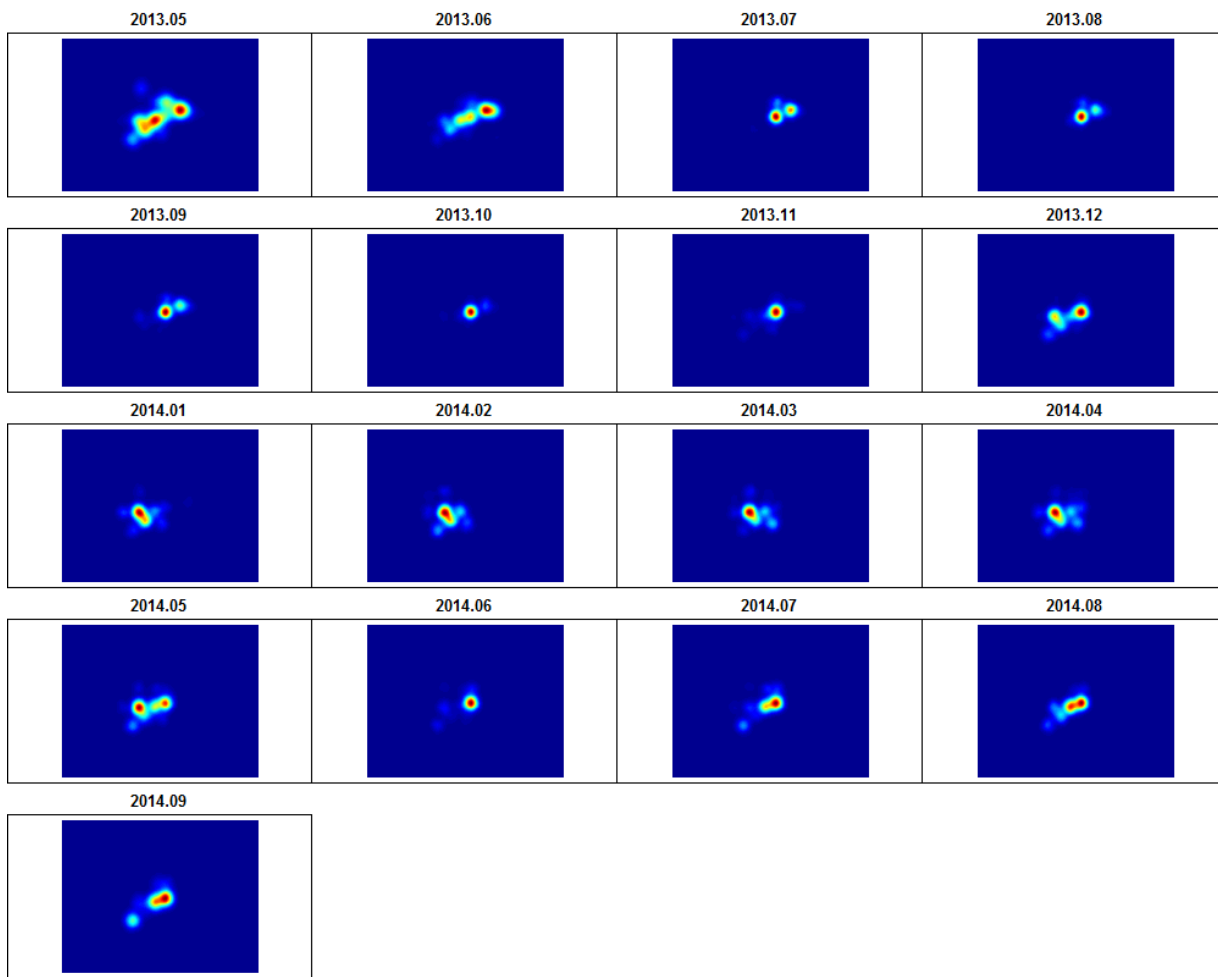
Figure 66 Monthly home range variation of amature female turtle at Pelican Banks. Kernel utilisation distribution of a female turtle (54.6 cm CCL tag ID 27950 monthly from May 2013 – September 2014. Orientation of each month of the year is the same with high use areas shown as red/orange/yellow (50% KUD) with a gradient through to turquiose (95% KUD).

3.6   Population level monthly variation in turtle home range size

There was a significant interaction between KUD area and year-month for turtles captured at Wiggins Island (ANOVA, p < 0.01) but not for those captured at Pelican Banks (ANOVA, p = 0.14). A Tukeys HSD test between months showed that for animals at Wiggins Island, the large KUD area in May 2013 was responsible for the significant difference between months with 50% KUD in May 2013 significanly greater than all months between January–September 2014 (Table 3.7) with no other months being significanlty different from another. For Wiggins Island, the difference between months was driven largely by high KUD in May 2013 and for both areas there was an observable declining trend in 50% KUD area over time (Figure 67) with KUDs on average 80-300% smaller at the end of the period of tracking (Table 3.6).
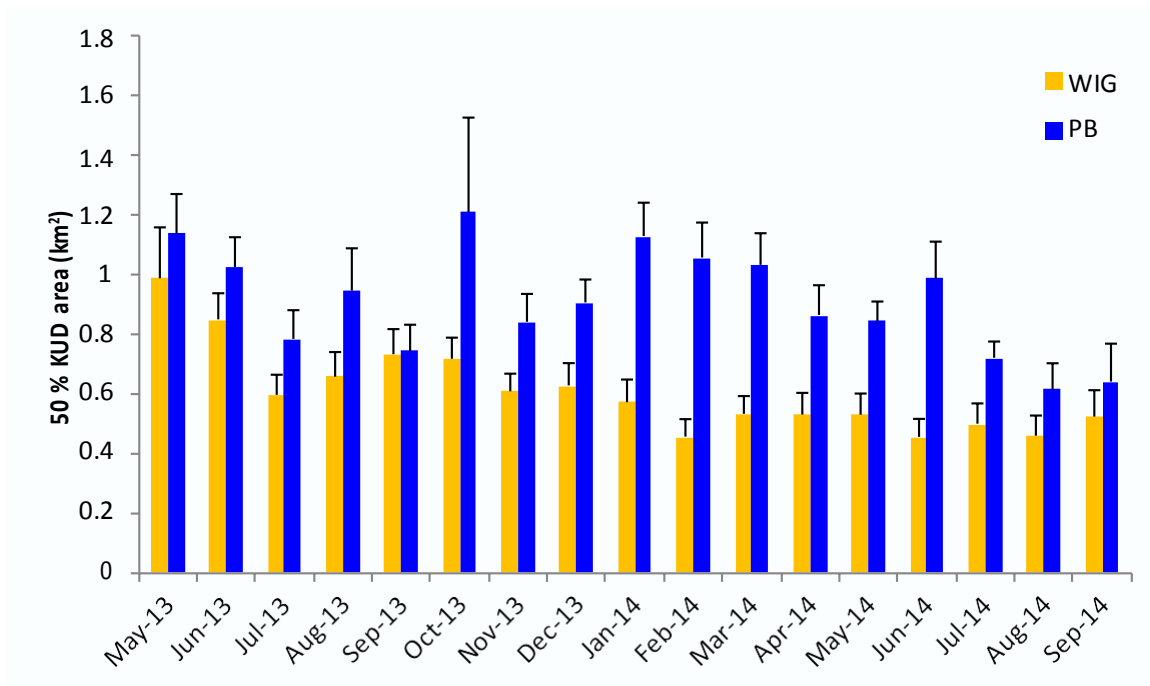
Figure 67 Plot of mean monthly 50% KUD area (+ SE) of green turtles tagged at Pelican Banks (PB, n = 19) and Wiggins Island (WIG, n = 16) including only those animals at Pelican Banks that did not move between the two areas.

Table 3.7 Analysis of monthly variation in turtle home range size at Wiggins Island. Results of Tukeys HSD test monthly 50% KUD area (km^2) for turtles tagged at Wiggins Island. Significant differences ($p < 0.05$) between month-year combinations are denoted by an asterisk.

	May-13	Jun-13	Jul-13	Aug-13	Sep-13	Oct-13	Nov-13	Dec-13	Jan-14	Feb-14	Mar-14	Apr-14	May-14	Jun-14	Jul-14	Aug-14	Sep-14
May-13		0.999	0.129	0.378	0.808	0.729	0.055	0.103	0.022*	0.001*	0.010*	0.009*	0.009*	0.002*	0.012*	0.006*	0.033*
Jun-13	0.999		0.813	0.979	1.000	1.000	0.713	0.839	0.488	0.057	0.303	0.291	0.287	0.097	0.277	0.166	0.455
Jul-13	0.129	0.813		1.000	1.000	1.000	1.000	1.000	1.000	0.998	1.000	1.000	1.000	0.999	1.000	1.000	1.000
Aug-13	0.378	0.979	1.000		1.000	1.000	1.000	1.000	1.000	0.936	1.000	0.999	0.999	0.959	0.997	0.980	1.000
Sep-13	0.808	1.000	1.000	1.000		1.000	0.999	1.000	0.989	0.550	0.937	0.931	0.929	0.646	0.893	0.755	0.965
Oct-13	0.729	1.000	1.000	1.000	1.000		1.000	1.000	0.996	0.652	0.969	0.965	0.964	0.737	0.937	0.828	0.983
Nov-13	0.055	0.713	1.000	1.000	0.999	1.000		1.000	1.000	0.980	1.000	1.000	1.000	1.000	0.990	1.000	1.000
Dec-13	0.103	0.839	1.000	1.000	1.000	1.000	1.000		1.000	0.946	1.000	1.000	1.000	0.971	0.999	0.988	1.000
Jan-14	0.022*	0.488	1.000	1.000	0.989	0.996	1.000	1.000		0.999	1.000	1.000	1.000	1.000	1.000	1.000	1.000
Feb-14	0.001*	0.057	0.998	0.936	0.550	0.652	0.980	0.946	0.999		1.000	1.000	1.000	1.000	1.000	1.000	1.000
Mar-14	0.010*	0.303	1.000	1.000	0.937	0.969	1.000	1.000	1.000	1.000		1.000	1.000	1.000	1.000	1.000	1.000
Apr-14	0.009*	0.291	1.000	0.999	0.931	0.965	1.000	1.000	1.000	1.000	1.000		1.000	1.000	1.000	1.000	1.000
May-14	0.009*	0.287	1.000	0.999	0.929	0.964	1.000	1.000	1.000	1.000	1.000	1.000		1.000	1.000	1.000	1.000
Jun-14	0.002*	0.097	0.999	0.959	0.646	0.737	0.990	0.971	1.000	1.000	1.000	1.000	1.000		1.000	1.000	1.000
Jul-14	0.012*	0.277	1.000	0.997	0.893	0.937	1.000	0.999	1.000	1.000	1.000	1.000	1.000	1.000		1.000	1.000
Aug-14	0.006*	0.166	1.000	0.980	0.755	0.828	0.996	0.988	1.000	1.000	1.000	1.000	1.000	1.000	1.000		1.000
Sep-14	0.033*	0.455	1.000	1.000	0.965	0.983	1.000	1.000	1.000	1.000	1.000	1.000	1.000	1.000	1.000	1.000	

3.7 Turtle home range characteristics and habitat use

Individual variation in the size and shape of home range area used by turtles is apparent in the shape and location of home ranges (cumulative 50 and 95% KUD contours over the entire study period) plotted on habitat and bathymetry maps (Figure 68). Six individuals tagged at Pelican Banks were also detected by receivers on Wiggins Island resulting in the cumulative 95% KUD area spanning both Wiggins Island and Pelican Banks (Figure 68). The home range of 33 turtles at Pelican Banks was centred on the western side of the Pelican Banks array with the 50 % KUD confined to an area of 2.18 km^2 that overlapped with intertidal and subtidal sand flats between areas of the banks with highest seagrass cover (Figure 69). The 95 % KUD area was 13.4 km^2 and at Pelican Banks completely encompassed the areas of highest seagrass cover.
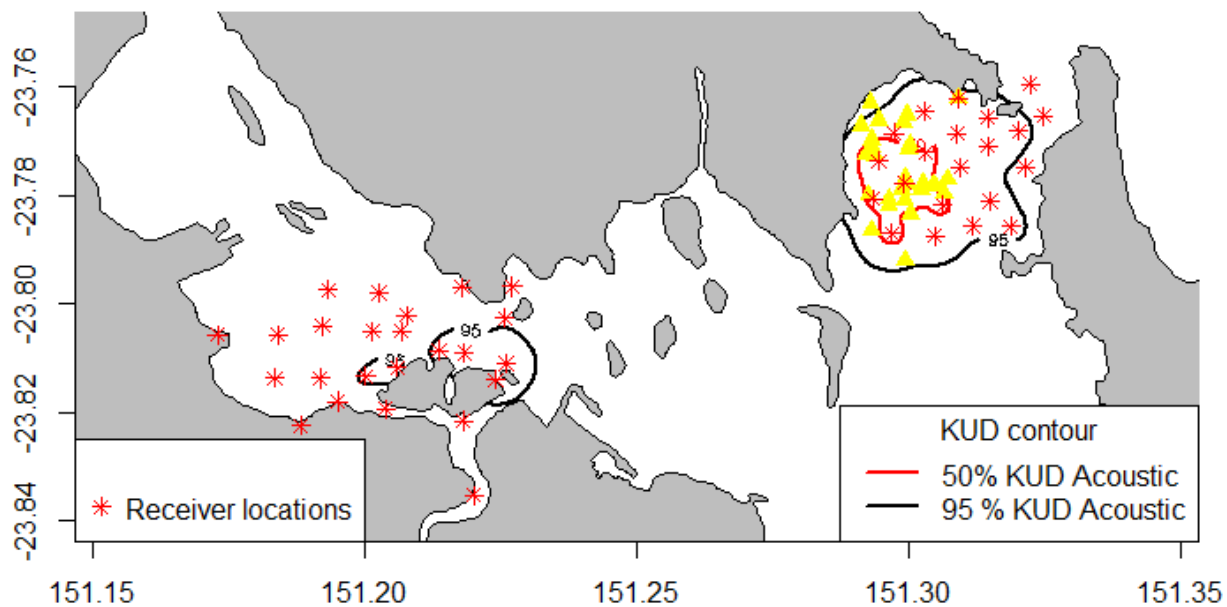
Figure 68 Map of Port Curtis showing the receiver arrays and combined cumulative 50 and 95% KUD area (km^2) for 33 green turtles tagged at Pelican Banks. Capture locations of individuals are shown as yellow triangles.
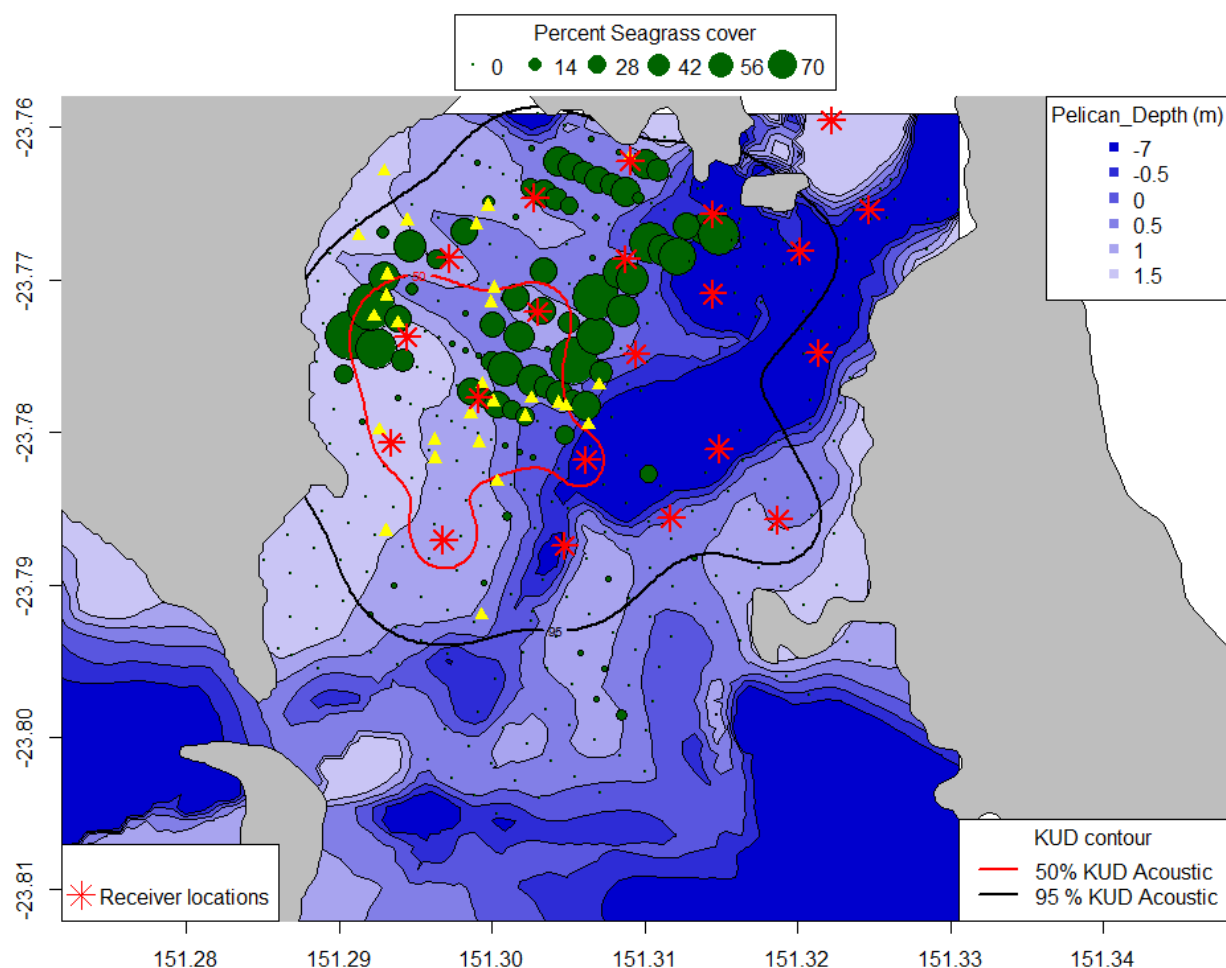
Figure 69 The cumulative 50 and 95% KUD contours for 33 green turtles tagged with acoustic tags at Pelican Banks. Capture locations of individuals are shown as yellow triangles.

Despite the small and stable home range of the Pelican Banks turtles, there was individual variability in home range size and shape. For turtle 27949, a 106 cm CCL adult female turtle detected on 495 days, there were two distinct 50% KUD's that were centred on the southern extent of highest seagrass density in the intertidal and subtidal area as well as the channel. The 95% KUD overlapped with high seagrass density as well the deeper channel (Figure 70A). For turtle 27938, a 101 cm CCL adult female turtle detected on 273 days, there were two distinct 50% KUD's that were centred on the northern extent of highest seagrass density in the intertidal and subtidal area as well as the channel. The 95 % KUD overlapped with high seagrass density in the northern half of Pelican Banks as well the deeper channel (Figure 70B). For turtle 27936, a 100 cm CCL adult male turtle detected on 321 days, the 50% KUD was centred on the southern extent of high seagrass density but also overlapped an area no seagrass cover. The 95% KUD encompassed half of the area of highest seagrass density but also a similar sized area to the south that had no seagrass. For turtle 27923, a 70 cm CCL subadult female turtle detected on 417 days, the 50% KUD had four distinct areas with three of these centred on areas of highest seagrass density on the western side of Pelican Banks and one on the eastern side of Pelican Banks in an area with very little seagrass. This animal had one of the largest 95% KUD's (8.5 km^2) of a resident turtle that didn't move between Pelican Banks and Wiggins Island and the 95% KUD encompassed most of Pelican Banks.

We have related the cumulative home range distribution for turtles at Pelican Banks to seagrass sampled in September 2014, however seagrass biomass varies seasonally, and the seagrass data we collected in September 2014 may not accurately reflect seagrass density at Pelican Banks for the

remainder of the year. To determine if turtle home range in August/September was more closely aligned with seagrass density in September 2014, the 50 and 95% KUD's of all turtles within the Pelican Banks array in August/September 2014 were calculated. The overall pattern of habitat use was very similar with the majority of turtles having at least half of their 50 and 95% KUD's overlapping with areas of highest seagrass density. In most cases, animals continued to utilise the area immediately to the south of the highest seagrass density where seagrass density was low (Figure 71). In August/September 2014, the size, shape and configuration of the 50 and 95% KUD's of turtle 27949 was very similar to that from the entire monitoring period (May 2013–September 2014) (Figure 71A). For turtle 27938, the 50 and 95% KUD's in August/September were much smaller compared to the size during the entire monitoring period (May 2013–September 2014) due to there only being one 50% KUD which had shifted to the south west, overlapping the area with highest seagrass density (Figure 71B). For turtle 27936, the shape of the KUD was similar, however there was an additional 50% KUD to the south in an area with no seagrass cover in August/September 2014 (Figure 71C). For turtle 27923, the shape of the 95% KUD was similar, however the 50% KUD had contracted from four distinct areas to only two which were centred on the west and east side of the channel with the KUD on the west side of the channel overlapping with an area of high seagrass cover (Figure 71D).
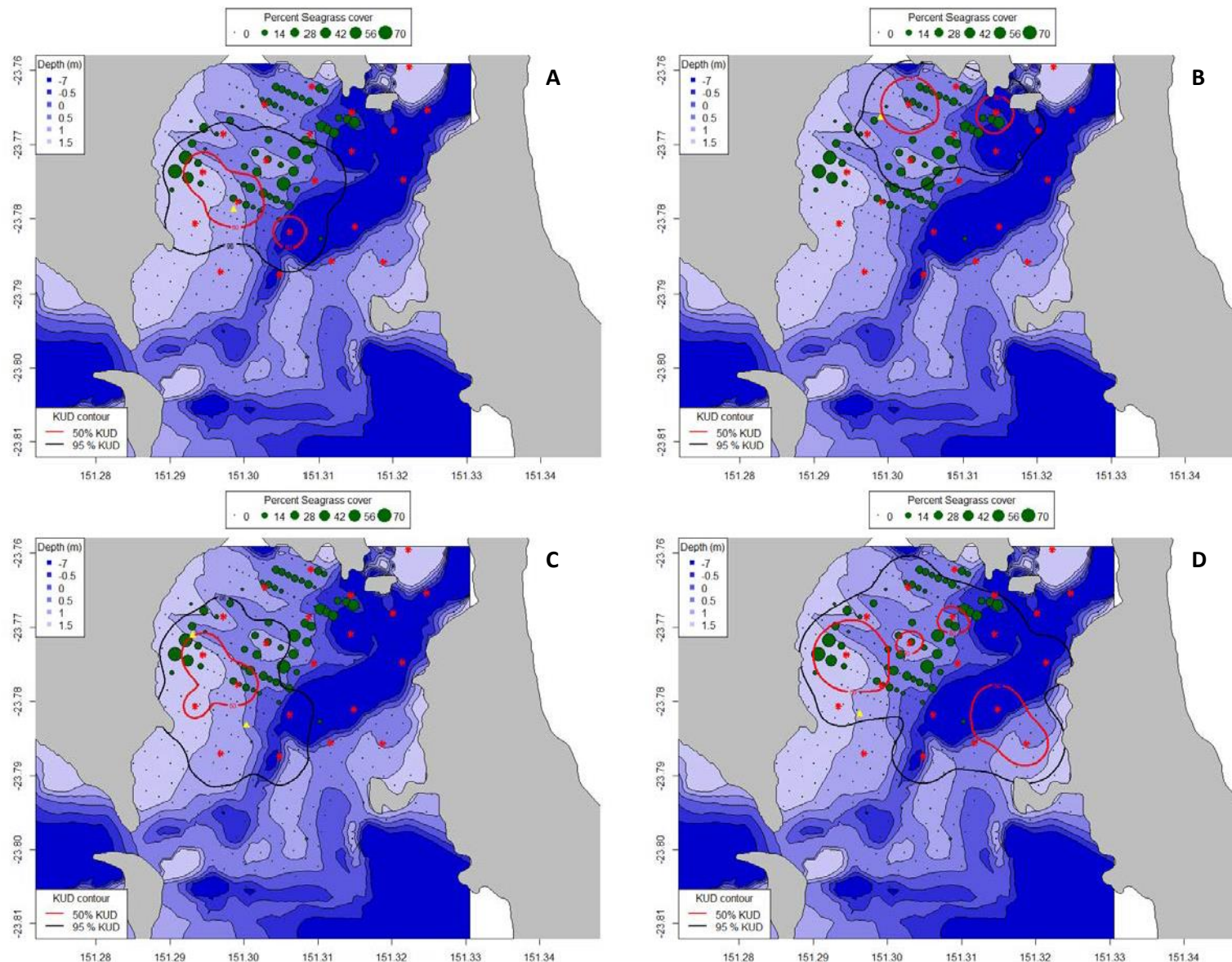
Figure 70 Individual turtle home range and habitat use variation at Pelican Banks over entire study period. Map showing cumulative 50 and 95% KUD contours over the entire study period of turtles 27949 (A), 27938 (B), 27936 (C) and 27923 (D). All turtles were captured and tagged with acoustic transmitters in May 2013. Capture location shown as yellow triangle. Receiver locations are shown as red asterisks. For turtle 27936, the southernmost yellow triangle represents a recapture location in November 2013.
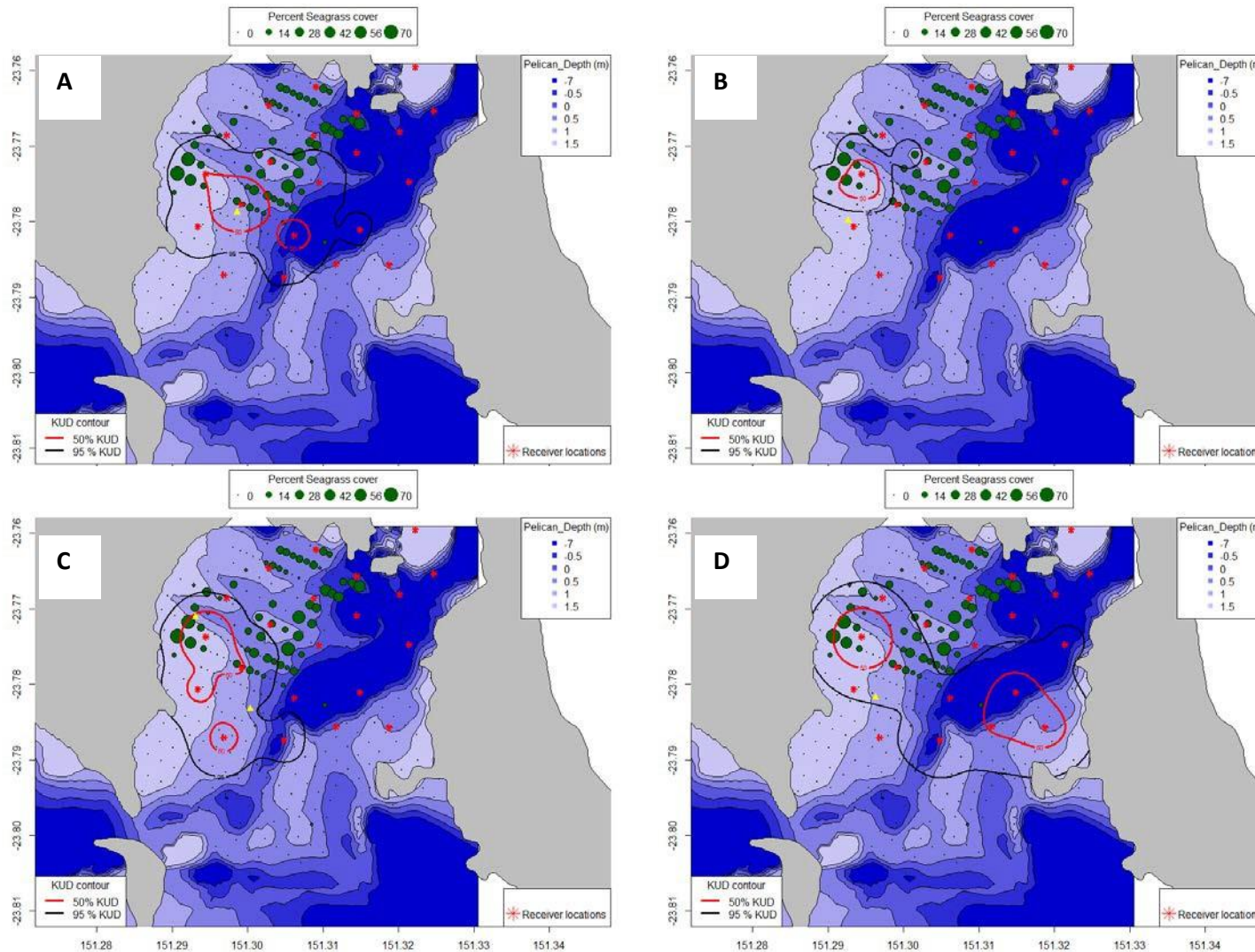
Figure 71 Individual turtle home range and habitat use variation at Pelican Banks August/September 2014. Map showing cumulative 50 and 95% KUD contours over the period August/September 2014 for turtles 27949 (A), 27938 (B), 27936 (C) and 27923 (D). All turtles were captured and tagged with acoustic transmitters in May 2013. Capture location shown as yellow triangle. Receiver locations are shown as red asterisks. For turtle 27936, the southernmost yellow triangle represents a recapture location in November 2013.

The home range of 16 turtles at Wiggins Island was centred on an area to the west of Wiggins Island including southern and northern end of Wiggins Island (Figure 72). For animals tagged at Wiggins Island, the 50% KUD confined to an area of 1.5 km^2 that overlapped with intertidal and subtidal sand flats in the centre of the array (Figure 73B). The 95% KUD area was 7.5 km^2 and had very little overlap with the shipping channel and intertidal and subtidal habitat adjacent to Curtis Island and LNG loading facilities.

Despite the small and stable home range of the Wiggins Island turtles, there was individual variability in home range size and shape. For turtle 27951, a 51.8 cm CCL juvenile female turtle detected on 458 days, there were three distinct 50% KUD's. These were centred on the mangrove drain near were this animal was tagged, on the intertidal flat to the north of this mangrove drain and also in the channel south of Wiggins Island (Figure 73A). The 95% KUD overlapped the intertidal and subtidal flats with little overlap with the deeper shipping channel to the north of Wiggins Island (Figure 73A). Turtle 27951 had a largest 50 and 95 % KUD of all animals tagged at Wiggins Island (1.3 and 6.7 km^2, respectively). For turtle 27950, a 54.6 cm CCL juvenile male turtle detected on 448 days, there were three distinct 50% KUD's that extended along the mangrove drain where it was tagged and north east towards the intertidal and subtidal areas. The 95% KUD overlapped this same area forming a narrow band along the mangrove drain (Figure 73B). For turtle 27947, a 58.0 cm CCL juvenile male turtle detected on 413 days, the 50% KUD were centred on the western end of Wiggins Island near where it was tagged and also around the north east corner of Wiggins Island in a narrow channel between another small mangrove island (Figure 73C). The 95% KUD encompassed both of the Wiggins Islands but did not extent into the deep shipping channel to the north. For turtle 27931, a 51.5 cm CCL juvenile female turtle detected on 248 days, the 50% KUD had two distinct areas that, unlike most other turtles tagged at Wiggins Island, were not centred around the tag location. The 50% KUD of this animal was to the north of Wiggins Island. The 95% KUD encompassed the area around Wiggins Island but did not extend across the shipping channel (Figure 73D).
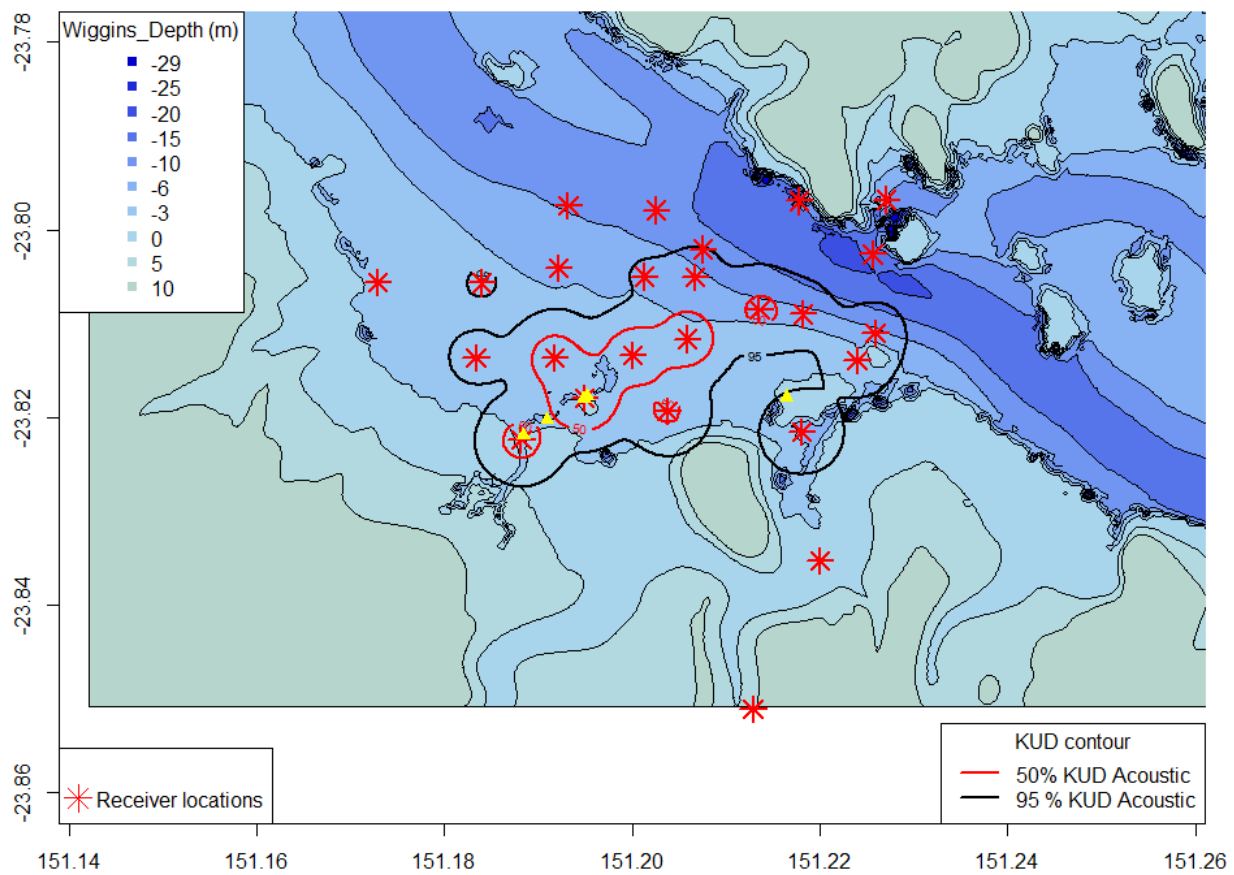
Figure 72 The cumulative 50 and 95% KUD contours for 16 Green Turtles tagged with acoustic tags at Wiggins Island. Capture locations of individuals are shown as yellow triangles.
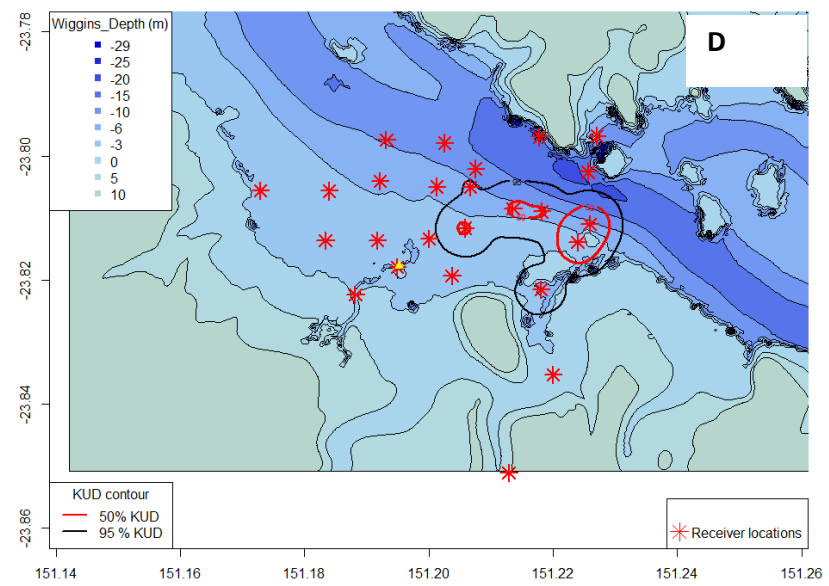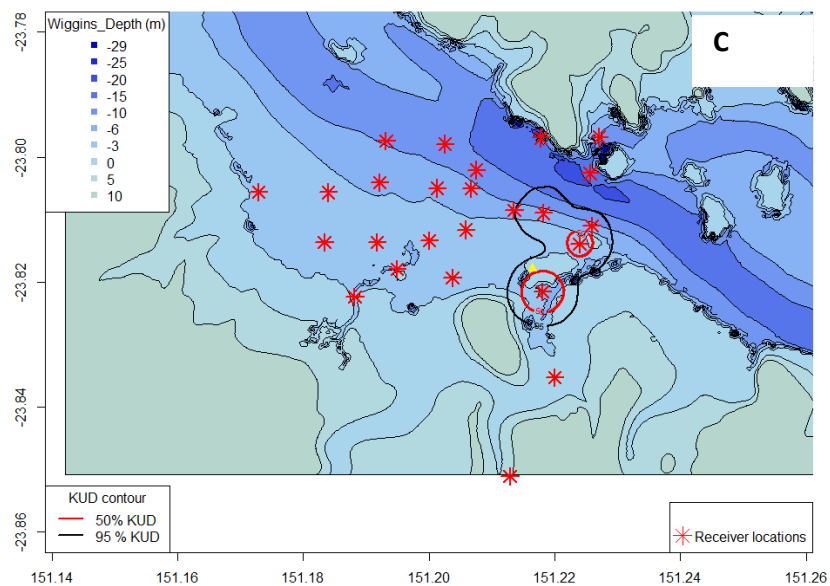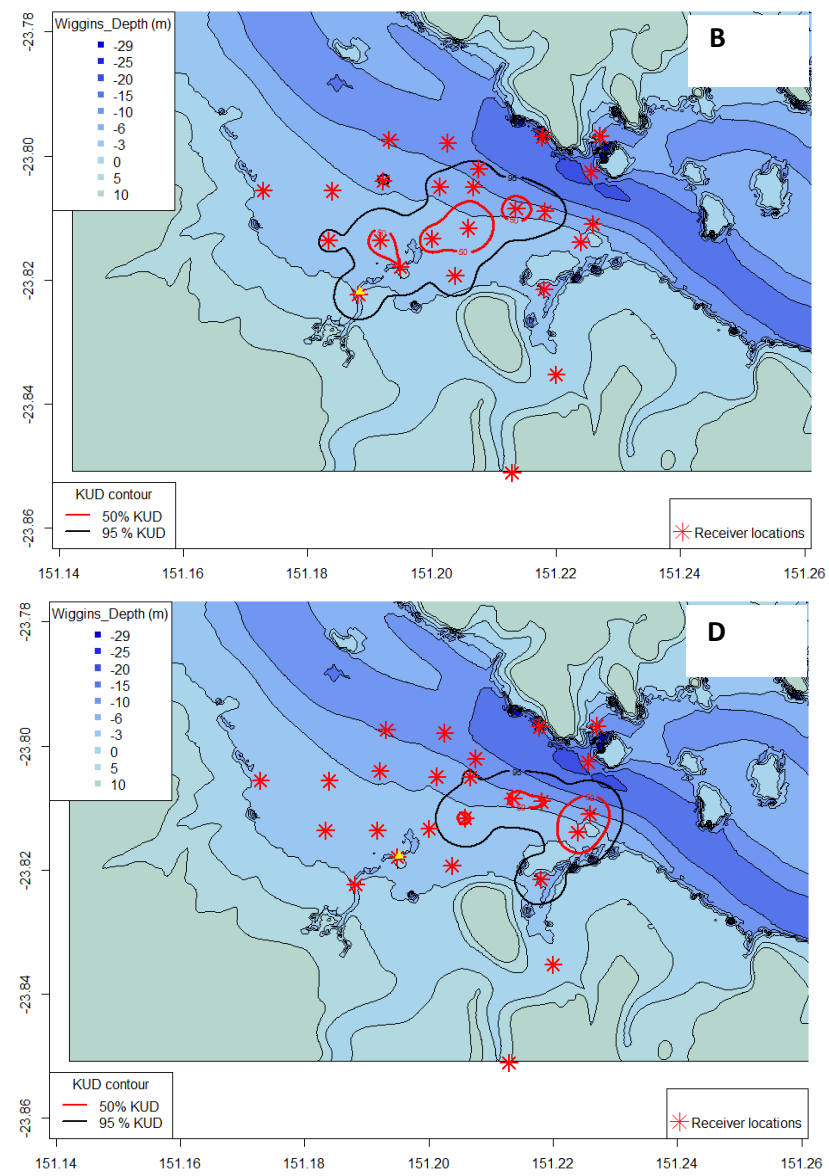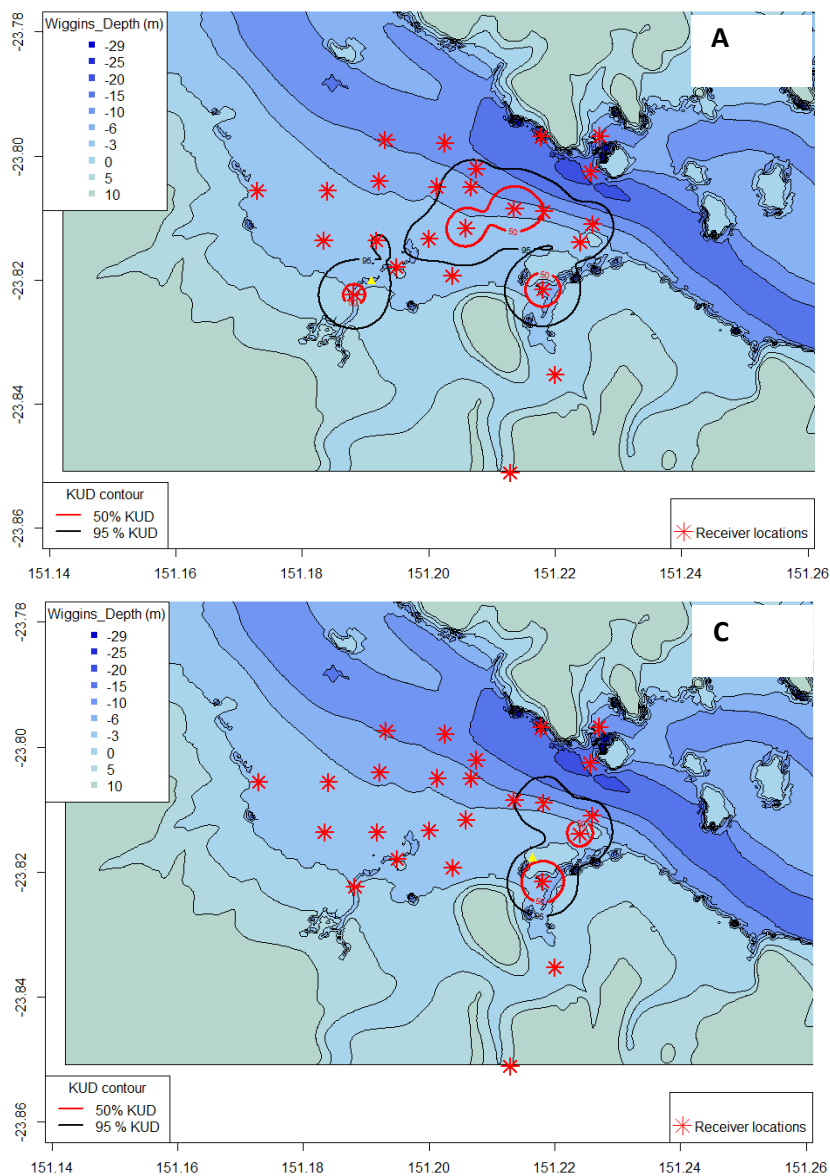
Figure 73 Map showing 50 and 95% KUD contour of turtle 27951 (A), 27950 (B), 27947 (C) and 27931 (D) all with acoustic tags in May 2013 at Wiggins Island. Capture location of individuals shown as yellow triangle.

3.8   Tidal influences on turtle habitat use

Using the Bureau of Meteorology's tide data for Gladstone Harbour, each detection was matched to a tide height using a cosine curve of daily tide height and time. This was used to evaluate the mean number of detections on receivers in different habitat types against tide height for turtles at Pelican Banks (Figure 74 and Figure 75) and Wiggins Island (Figure 76 and Figure 77) for each month of the year from May 2013–September 2014. At Pelican Banks, although there was some monthly variation, it was clear that the majority of detections on receivers in the channel and channel edge occurred when tide height was between 1–2 m, or around low tide. Conversely, detection on receivers located in the intertidal and subtidal flat occurred predominantly when tide height was between 2–4 m (around high tide).

Around Wiggins Island there was a similar pattern (Figure 76 and Figure 77), however detections on receivers in the channel accounted for less than 6% of total detections and were dominated by one or two individuals which meant that overall there was not trend in mean detections with tide height for this habitat. There was however a clear tidal pattern for receivers on the channel edge with the greatest number of detections occurring primarily during water depths between 1–1.5 m (low tide). Detections on the intertidal and subtidal flats occurred predominantly around mid high tide (water depth ~ 2 m). The pattern in the mangrove drain and Wiggins channel habitat were confounded by the fact that some individuals remained within a deep hole at the top of the mangrove drain during low tide (receiver GH49 on Figure 51) and animals could remain in the Wiggins channel at both low and high tide.
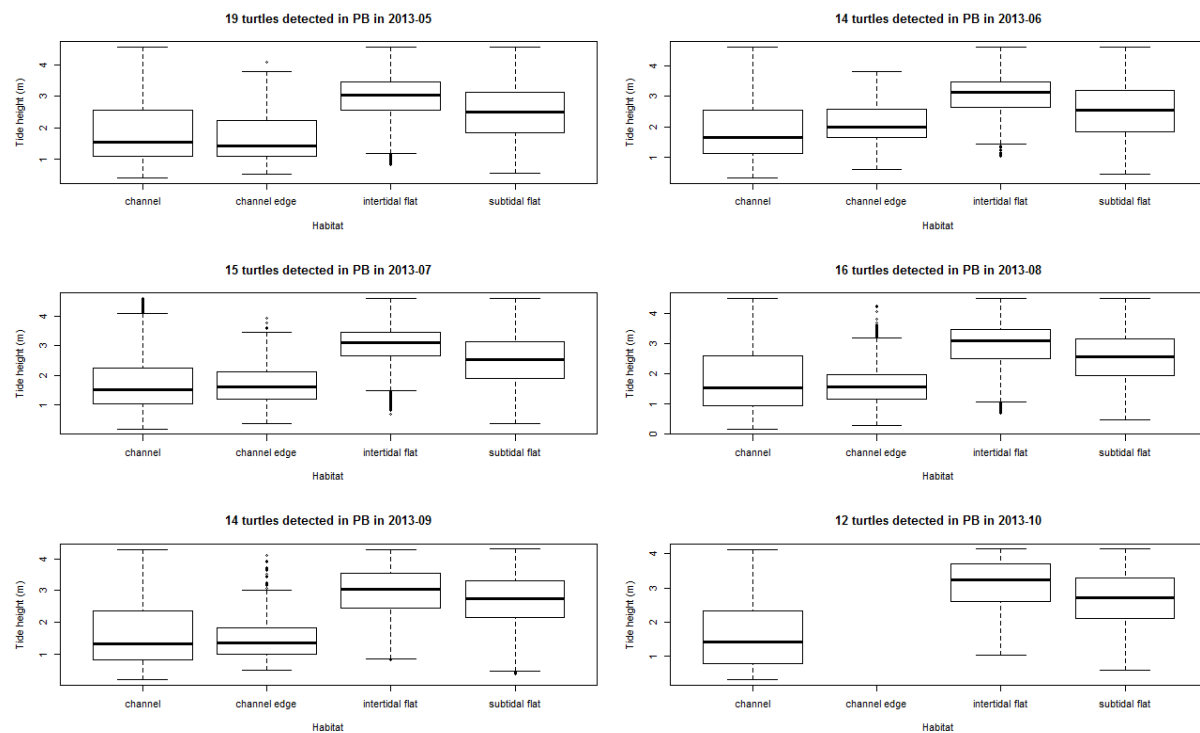
Figure 74 Turtle habitat use and tidal phase Pelican Banks May - October 2013. Box and whisker plot of mean (± 95% CI) number of detections against tide height for receivers in the channel, channel edge, intertidal flat and subtidal flat at Pelican Banks. Each month from May-October 2013 are plotted separately.
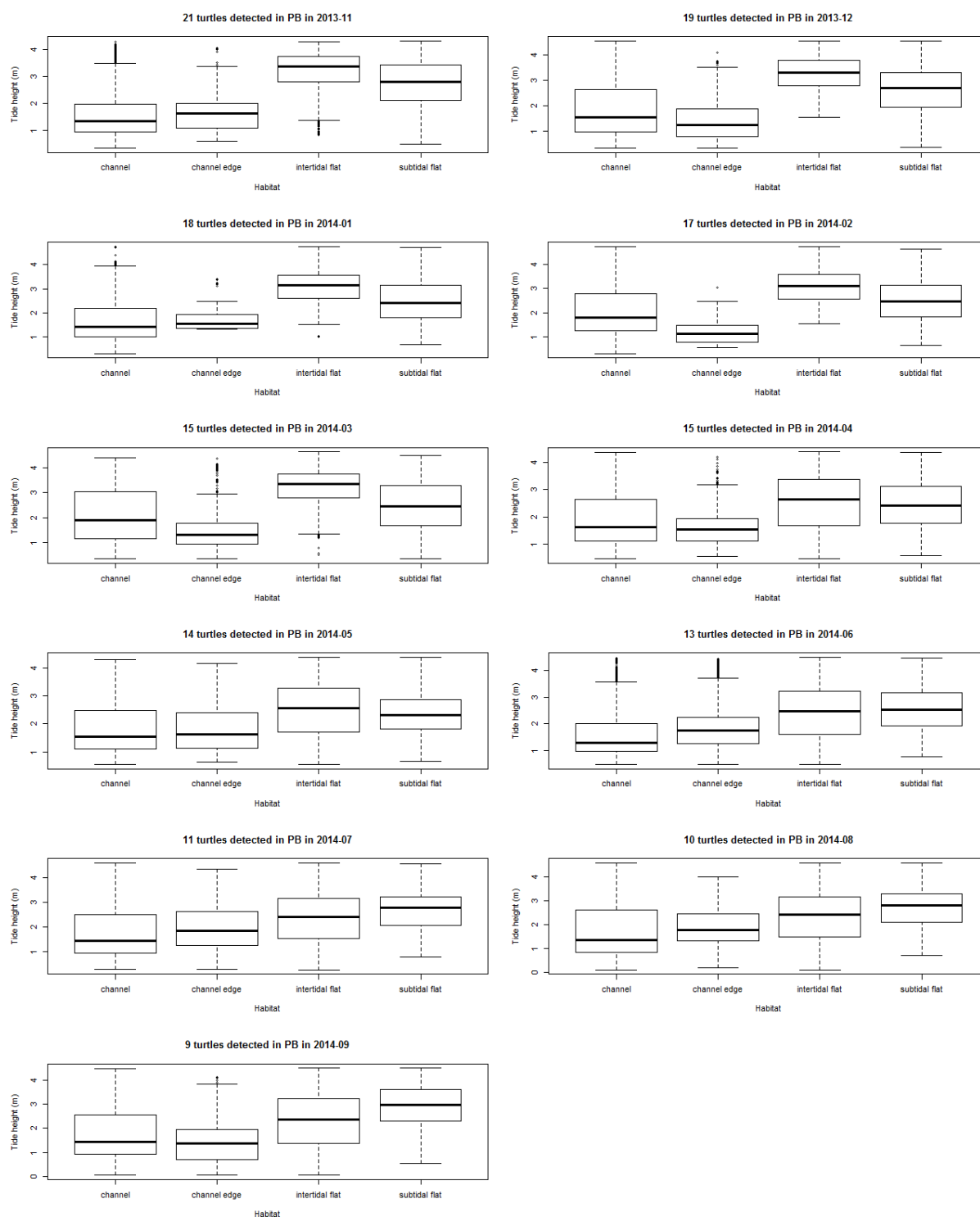
Figure 75 Turtle habitat use and tidal phase Pelican Banks November 2013 – September 2014. Box and whisker plot of mean (±95% CI) number of detections against tide height for receivers in the channel, channel edge, intertidal flat and subtidal flat at Pelican Banks. Each month from November 2013–September 2014 are plotted separately.
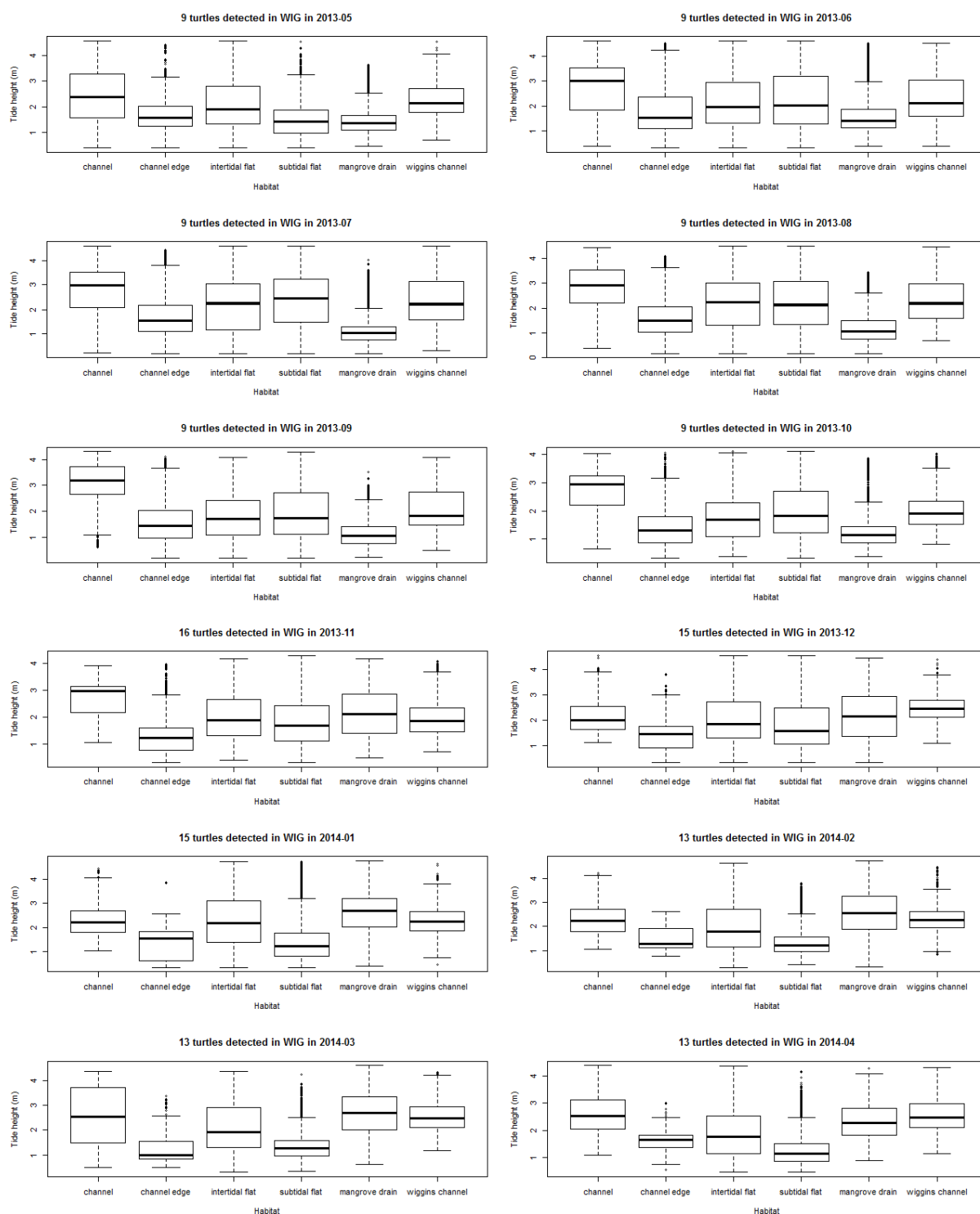
Figure 76 Turtle habitat use and tidal phase Wiggins Island May 2013 – April 2014. Box and whisker plot of mean (± 95% CI) number of detections against tide height for receivers in the channel, channel edge, intertidal flat and subtidal flat, mangrove drain and Wiggins channel at Wiggins Island. Each month from May 2013–April 2014 are plotted separately.
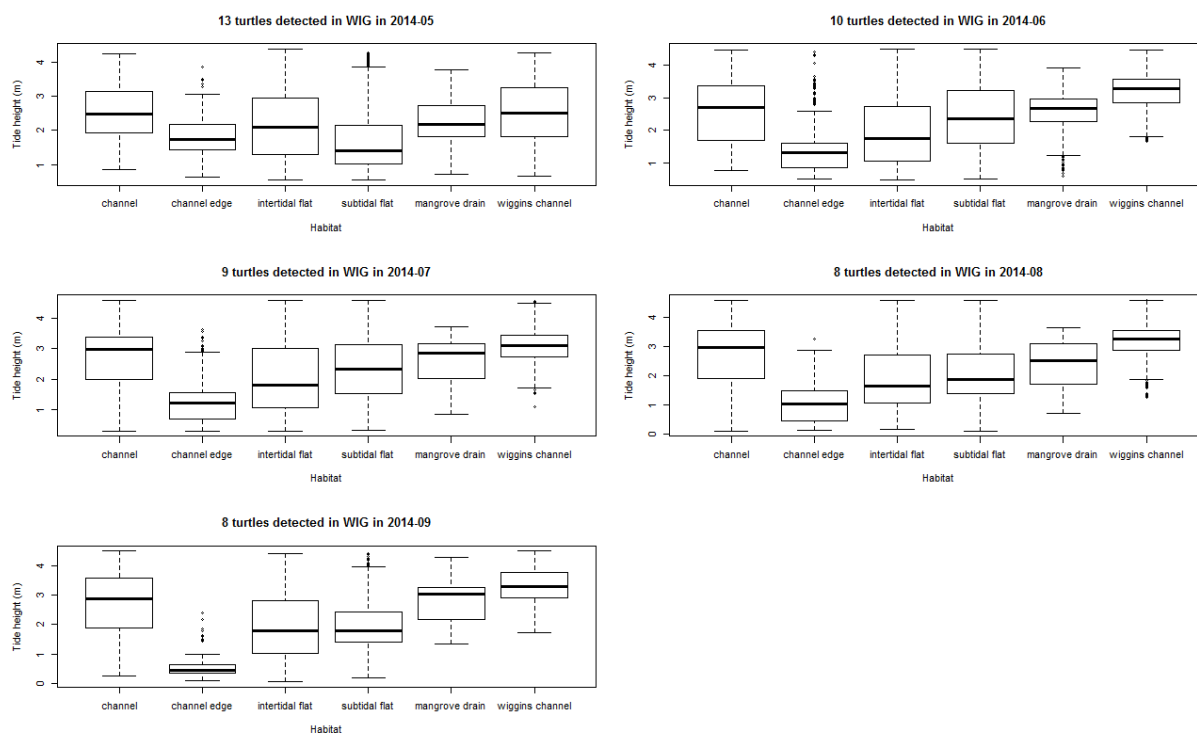
Figure 77 Turtle habitat use and tidal phase Wiggins Island May – September 2014. Box and whisker plot of mean (± 95% CI) number of detections against tide height for receivers in the channel, channel edge, intertidal flat and subtidal flat, mangrove drain and Wiggins channel at Wiggins Island. Each month from May–September 2014 are plotted separately.

To further investigate individual and population level habitat use at high and low tide, 50 and 95% KUD's of animals tagged at Pelican Banks and Wiggins Islands were calculated for the periods one hour before and after low tide and high tide and the contour plotted and area calculated. For animals tagged at Pelican Banks, the cumulative 50% and 95% KUD areas at high tide were 2.1 km^2 and 13.6 km^2, respectively which were smaller than corresponding low tide 50% and 95% KUD areas (3.5 km^2 and 19.3 km^2). At high tide, the 50% KUD was primarily on the intertidal and subtidal flat on the western side of Pelican Banks with little overlap with the channel, however at low tide, the animals moved into deeper water in the centre of Pelican Banks with much greater overlap with the channel (Figure 78). There difference in the habitat encompassed by the 95% KUD contour was less obvious but with the same trend towards a shift towards the east at low tide.
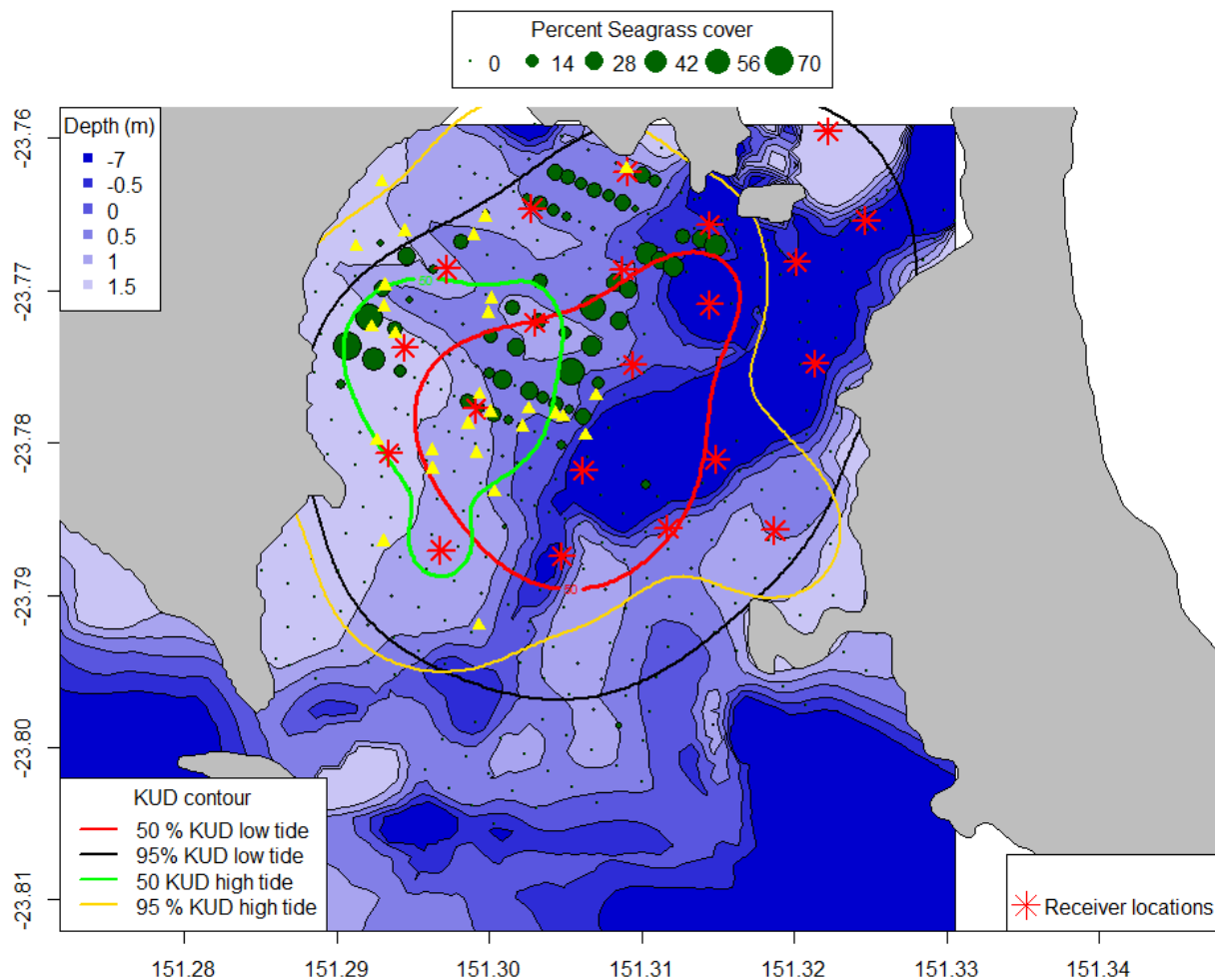
Figure 78 Tidal influence on cumulative habitat use by turtles at Pelican Banks. The 50 and 95% KUD contours of detections from 32 green turtles one hour either side of low tide and high tide at Pelican Banks. Capture locations of individuals are represented as yellow triangles.

For animals tagged at Wiggins Island, the 50 and 95% KUD areas at high tide (1.7 and 7.8 km2, respectively) were slightly bigger than those at low tide (1.1 and 7.1 km2, respectively). At low tide, the 50% KUD was centred on the mangrove drain where the majority of turtles were tagged. This area had a water depth of 1–4 m at low tide whereas the surround flats dried 2-3 h before low tide. At high tide, the 50% KUD extended towards the channel edge and also to the intertidal flat to the northwest of the mangrove drain. The 95% KUD shapes were very similar with slightly more use of the channel edge at low tide (Figure 79). There was no movement across the shipping channel at either high or low tide.
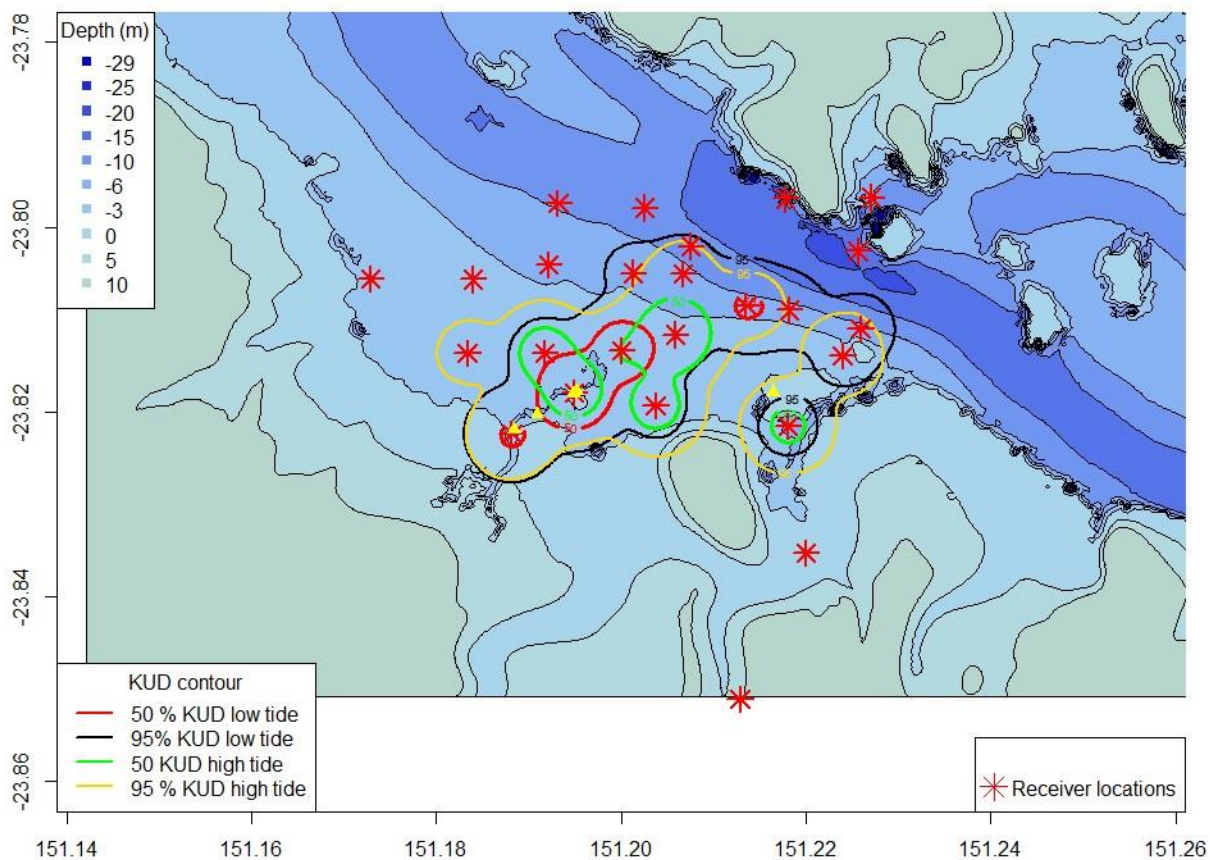
Figure 79 Tidal influence on cumulative habitat use by turtles at Wiggins Island. The 50 and 95% KUD contours of detections from 16 green turtles one hour either side of low tide and high tide at Wiggins Island. Capture locations of individuals are represented as yellow triangles.

Despite the consistent use of intertidal and subtidal habitat at high tide at the population level (Figure 78), there was also individual variation in high and low tide habitat use at Pelican Banks. For turtle 27949, a 106 cm CCL adult female turtle detected on 495 days, there was very little overlap between high and low tide 50% KUD's which were centred on the intertidal and subtidal flats and the channel, respectively with the majority of the high tide detections coming from one receiver in the channel (Figure 80A). Both the 50 and 95% high tide KUD's were significantly larger than the size of the low tide KUD area.

For turtle 27938, a 101 cm CCL adult female turtle detected on 273 days, there were was a distinct separation of the high and low tide 50% KUD that were centred on the intertidal and subtidal area and the channel, respectively. The 50 and 95% high tide KUD's were slightly larger than the low tide KUD (Figure 80B).

Turtle 28352 was a 93.6 cm CCL adult male detected on 131 days with no overlap of 50% high and low tide KUD's. This individual was using the intertidal flats with high seagrass density at high tide and retreated to the channel during low tide (Figure 80C). The 50 high tide KUD was nearly double the size of the 50% high tide KUD whereas the 95% high tide KUD was marginally bigger than the 95% low tide KUD.

Turtle 27928 was a 101 cm CCL adult female detected on 273 days with no overlap of 50% high tide KUD and low tide KUD. Although this animal was clearly using the subtidal flats at high tide, at low tide it moved to the intertidal flat and channel to the north east that had fairly high density of seagrass (Figure 80D). Both the 50 and 95% high and low tide KUD's were of similar size in this individual, with both the high tide KUD's more than double the size of low tide KUD areas.

It is apparent from these four examples that for individuals on the Pelican Banks, there are subtle differences in their high and low tide foraging and or resting areas with some animals spending high tide over dense seagrass beds to the south west, whereas others are spread across gradients of seagrass density.

In contrast to Pelican Banks, high and low tide home ranges of animals tagged at Wiggins Island, were similar in shape, size and habitat at the population level, however, there was individual variation in high and low tide habitat use. For turtle 27951, a 51.8 cm CCL juvenile female turtle captured in the mangrove drain and detected on 458 days, there was very little overlap between high and low tide 50% KUD's which were centred on the intertidal flats and mangrove drain and subtidal flats, respectively, to the west of Wiggins Island. Animals also utilised the area to the south of Wiggins Island at high tide (Figure 81A). At low tide, the 95% KUD extended further into the shipping channel but overall, the 50 and 95 % high tide KUD area were of similar size to low tide KUD area.

For turtle 27950, a 54.6 cm CCL juvenile male turtle captured in the mangrove drain and detected on 448 days, there were was some overlap in the high and low tide 50% KUD subtidal area, with the low tide KUD extending further towards the channel edge (Figure 81B). Overall, the 50% low tide KUD was nearly twice as large as the 50% high tide KUD. As with turtle 27951, at low tide, the 95% KUD extended further into the shipping channel with 95% high tide KUD extending further west up the mangrove drain. Overall, 95% high tide KUD areas were of similar size to 95% low tide KUD area.

Turtle 27947 was a 58 cm CCL juvenile male tagged adjacent to Wiggins Island and detected on 413 days. At high tide, the 50% KUD was exclusively abutting Wiggins Island whereas at low tide, although the animal was also recorded close to Wiggins Island, some of the 50% KUD was also centred on the intertidal flats and channel edge to the north of Wiggins Island resulting in the low tide 50% KUD being nearly double the size of the high tide 50% KUD (Figure 81C). As with the 50% KUD, the 95% high tide KUD was larger and extended further towards the shipping channel than the low tide KUD.

Turtle 27931 was a 51.4 cm CCL juvenile female tagged in the mangrove drain and detected on 273 days (Figure 81D). While the high and low tide 50% KUD's were of similar size, there was no overlap. The 50% high tide KUD was centred on the receiver in a deep (5 m) hole near the upstream limit of the mangrove drain, whereas the 50% low tide KUD was centred on the receiver immediately downstream also within the mangrove drain. The 95% high and low tide KUD's showed a similar pattern, however this animal was also detected adjacent to Wiggins Island at high tide but not at low tide.
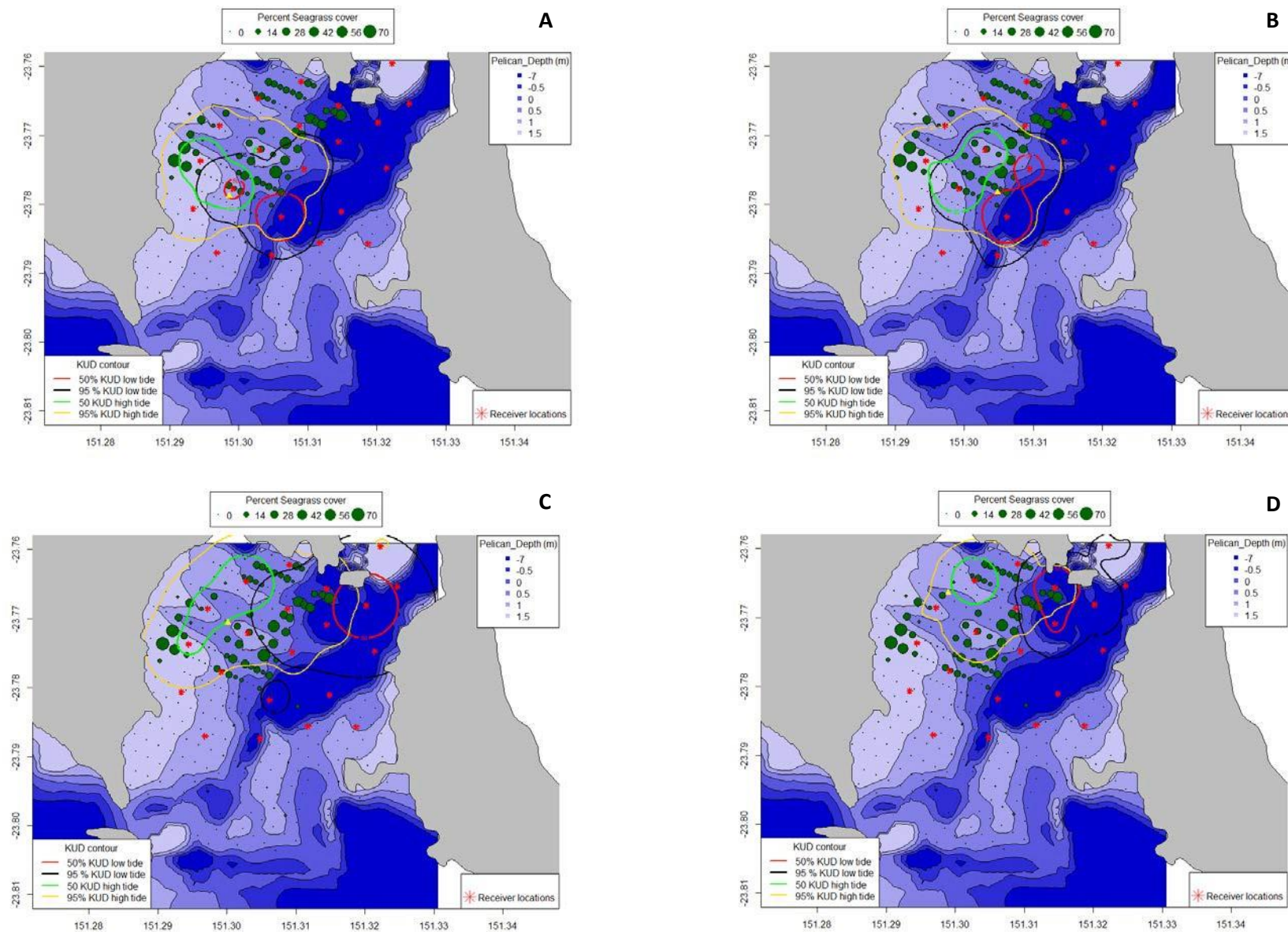
Figure 80 The 50 and 95% KUD high and low tide contours for turtles Pelican Banks May 2013. Calculated from detections one hour either side of low and high tide for individual turtles 27949 (A), 27939 (B), 28352 (C) and 27928 (D) tagged with acoustic tags in May 2013. Capture location shown as yellow triangle.
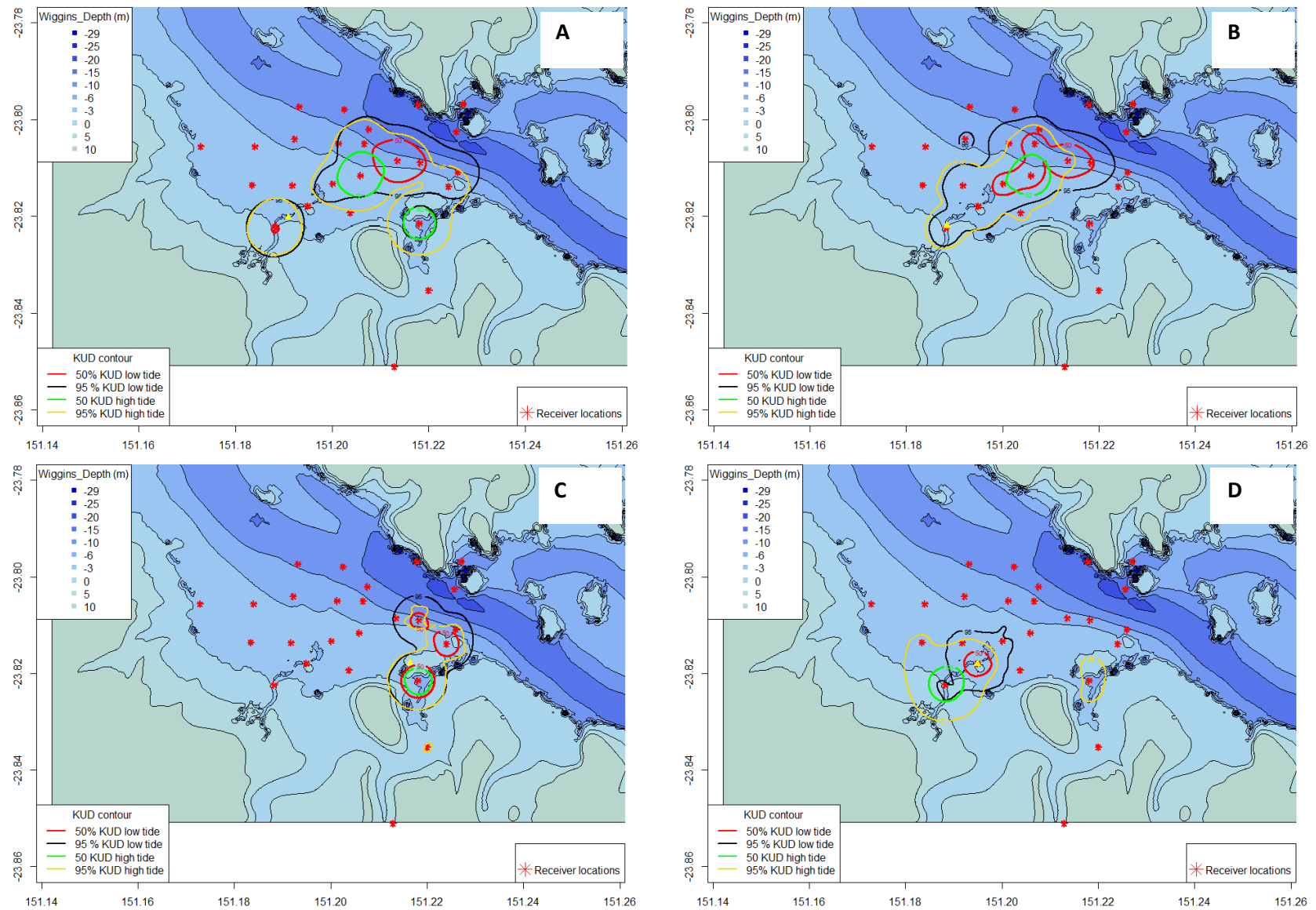
Figure 81 The 50 and 95 % KUD high and low tide contours for turtles Pelican Banks May 2013 (cont.). Calculated from detections one hour either side of low and high tide for individual turtles 27951 (A), 27950 (B), 27947 (C) and 27622 (D) tagged with acoustic tags in May 2013. Capture location shown as yellow triangle.

3.9 Nesting movement

One of the adult females turtles that was captured at Pelican banks in May 2013 and tagged with an acoustic (27928) and flipper tags (QA 34792) was recorded daily within the Pelican Banks array between 2 May-25 September 2013 at which time the animal disappeared from the array for nearly five months. On the 18 February 2014, it was again recorded and thereafter it was detected daily until the last download of acoustic receivers in mid-September 2014. This animal was recorded nesting on Lady Musgrave Island in the Capricorn Bunker Group in December 2013 (C. Limpus pers. comm.) with the acoustic data providing data on when the animal left and returned to its foraging ground between nesting.

3.10 Long term residency

There was a decline in the number of turtles remaining within the Pelican Banks and Wiggins Island array over time with animals tagged at Pelican Banks much more likely to leave the array than animals at Wiggins Island. For adult animals (96–114 cm CCL) tagged at Pelican Banks, after 510 days since the first animals were tagged in May 2013, only 37% of females and 10% of males were still being detected within the 12 km^2 array of receivers at Pelican Banks (Figure 82). For juvenile and sub-adult animals (43-75 cm CCL), after 510 days since the first animals were tagged in May 2013,   only 50% of females, 36% of animals of unknown sex and no males were still being detected within the 12 km^2 array of receivers at Pelican Banks (Figure 83). Of those animals tagged at Wiggins Island in May 2013, after 510 days, 100% of females, 40% of males and 28% of animals of unknown sex were still being detected within the 16 km^2 array of receivers (Figure 84). At both Pelican Banks and Wiggins Island, across all sizes, males were much more likely to depart the array than females, suggesting that males are possibly more transient than females.
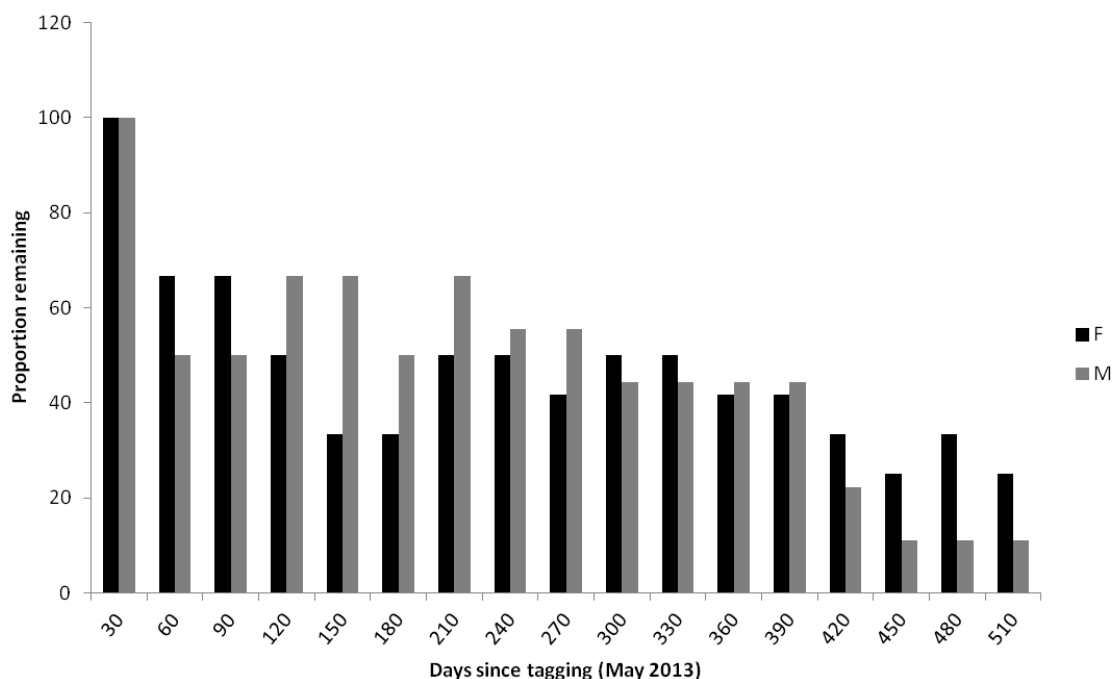
Figure 82 Number of tagged turtles 96–114 cm CCL over the study period. Long term decline in the number of female and male turtles between 96–114 cm CLL remaining at Pelican Banks and Wiggins Island array. Data represent all adult green turtles between 96-114 cm CCL tagged with acoustic tags at Pelican Banks from date of tagging to the last download of receivers on 14 September 2014. For females, six turtles were tagged in May and six in November 2013 (210 days). For males, six were tagged in May and three in November.
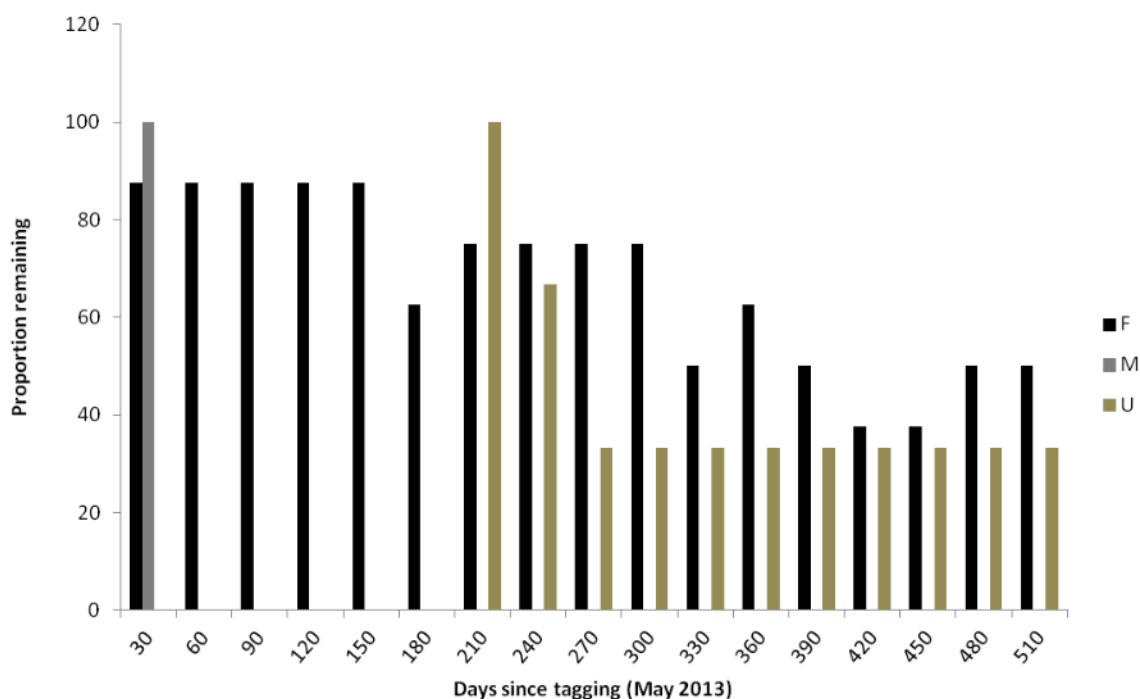
Figure 83 Number of tagged turtles 43–75 cm CCL at Pelican Banks over the study period. Long term decline in the number of female, male and turtles of unknown sex remaining between 43-75 cm CLL remaining at Pelican Banks and Wiggins Island array. Data represent all juvenile and subadult green turtles between 43-75 cm CCL tagged with acoustic tags at Pelican Banks from date of tagging to the last download of receivers on 14 September 2014. For females, 8 turtles were tagged in May 2013. For males, one was tagged in May 2013. The sex of all turtles was known in May 2013, however sex of three turtles was unknown in November 2013.
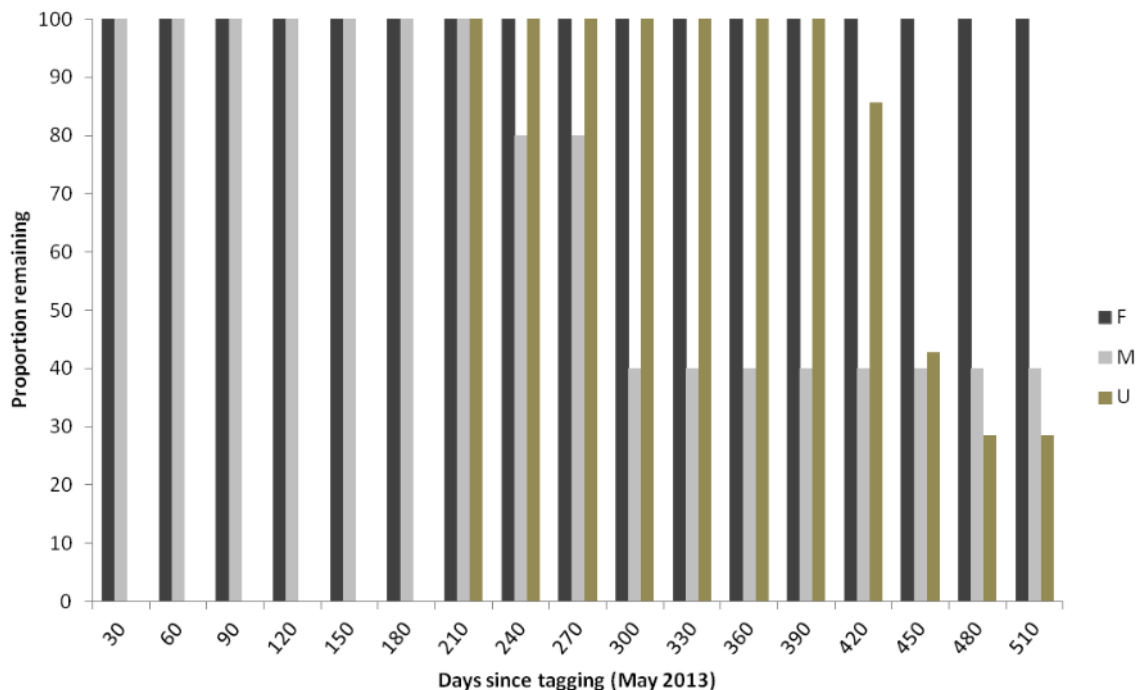
Figure 84 Number of tagged turtles 43–75 cm CCL at Wiggins Island over the study period. Long term decline in the number of female, male and turtles of unknown sex remaining in the Wiggins Island array. Data represent all juvenile green turtles tagged with acoustic tags at Wiggins Island from date of tagging to the last download of receivers on 14 September 2014. For females and males, five and four turtles were tagged in May, respectively. The sex of all turtles was known in May 2013; however sex of all seven turtles tagged in November 2013 was unknown.

3.11 Satellite tag turtle tracking data

Satellite tags were deployed on five turtles at both Pelican Banks and Wiggins Island. At Pelican Banks, only two of the animals with satellite tags remained within the array of receivers in Gladstone Harbour with three individuals moving north and south along the coast shortly after tagging. All animals tagged with satellite tags were also tagged with acoustic tags enabling a comparison between the two tag types. Three animals left the array shortly after tagging with the satellite tags providing information on where these turtles went.

An immature pubescent female turtle of 101.6 cm CCL (satellite tag 126273, acoustic tag ID = 27926) was detected by satellite 1140 times between 1/5/2013 and 4/2/2014 (Figure 85). This individual left Pelican Banks 15 days after it was tagged. Over a period of 15 days it moved 271 km south along the Queensland coast directly to Hervey Bay where it remained within a small area from 31 May–17 December (50% KUD = 0.7–2.76 km^2). On the 18 December, this animal moved ~ 55 km north along the coast and was between Elliot Heads and Woodgate Beach from 26–30 December before moving back to Hervey Bay where it returned to the same small area it had occupied on the 3 January. It remained in this area until February when the tag stopped transmitting (Figure 86).

Diving depth from the satellite tag showed that this animal spent 80% of its time less than 4 m under the surface and approximately 60% of its time less than 2 m under the surface (Figure 87). Between May and September, average daily depth was approximately 5 m, whereas from October 2013–

February 2014, average daily depth was approximately 2.5 m suggesting a slight shift in feeding behaviour and area despite the animal remaining within a small area (Figure 88). The deepest dive was 25 m which occurred when the animal moved between Gladstone and Hervey Bay in May 2013. The second deepest dive was 17 m when the animal moved from Hervey Bay to Elliot Heads in December 2013.

An adult female turtle of 113.8 cm CCL (satellite tag 126274, acoustic tag ID = 27926) was detected 665 times between 1/5/2013 and 15/10/2013 (Figure 89). This individual left Pelican Banks 1 day after it was released and over a period of 5 days moved 182 km directly to West Water, a small inlet north of Byfield National Park, where it remained within a small area from 7 May–23 July (50% KUD = 0.59–0.79 km^2). On the 23 July, this animal moved south along the coast and entered Baffle Creek, 313 km to the south of West Water on 14 August 2013. It remained within Baffle Creek until the 15 October when the tag stopped transmitting and during this time the 50% KUD was between 0.79–1.79 km^2 (Figure 90).

Diving depth from the satellite tag showed that this animal spent 90% of its time less than 4 m under the surface and approximately 60% of its time less than 2 m under the surface (Figure 91). Average daily depth was less than 5 m for the entire track, with the deepest dives to 17 m occurring when the animal moved between Gladstone and Port Clinton in May 2013 (Figure 92). The second deepest dive was 15 m when the animal moved from Port Clinton to Baffle Creek in August 2013. Average water depth was similar in Port Clinton and Baffle Creek.

An adult female of 106.0 cm CCL (satellite tag 131869, acoustic tag ID = 16229) was detected 523 times between 7/11/2013 and 17/2/2014 (Figure 93). This individuals left Pelican Banks 1 day after it was released and over a period of 6 days moved approximately 237 km north directly to Shoalwater Bay, where it remained within a small area from 13 November 2013–17 January 2014 (50% KUD = 1.89 km^2). On the 17 January, this animal moved south along the coast arriving at the area between Elliot Heads and Woodgate on the 28 January 2014, approximately 435 km to the south of Shoalwater Bay. It remained in this area until the 17 February 2014 when the tag stopped (Figure 94).

Diving depth from the satellite tag showed that this animal spent 90% of its time less than 4 m under the surface and approximately 75% of its time less than 2 m under the surface (Figure 95). Average daily depth was less than 5 m until mid-January 2014 with the deepest dives to 25 m occurring when the animal moved from Gladstone to Shoalwater Bay in November 2013 (Figure 96). The second deepest dive was also to 25 m when the animal moved from Shoalwater Bay to Elliot Heads in January 2014. While this animal was between Elliot Head and Woodgate Beach, average water depth was between 5–10 m with dives below 15 recorded on all days that data were recorded.
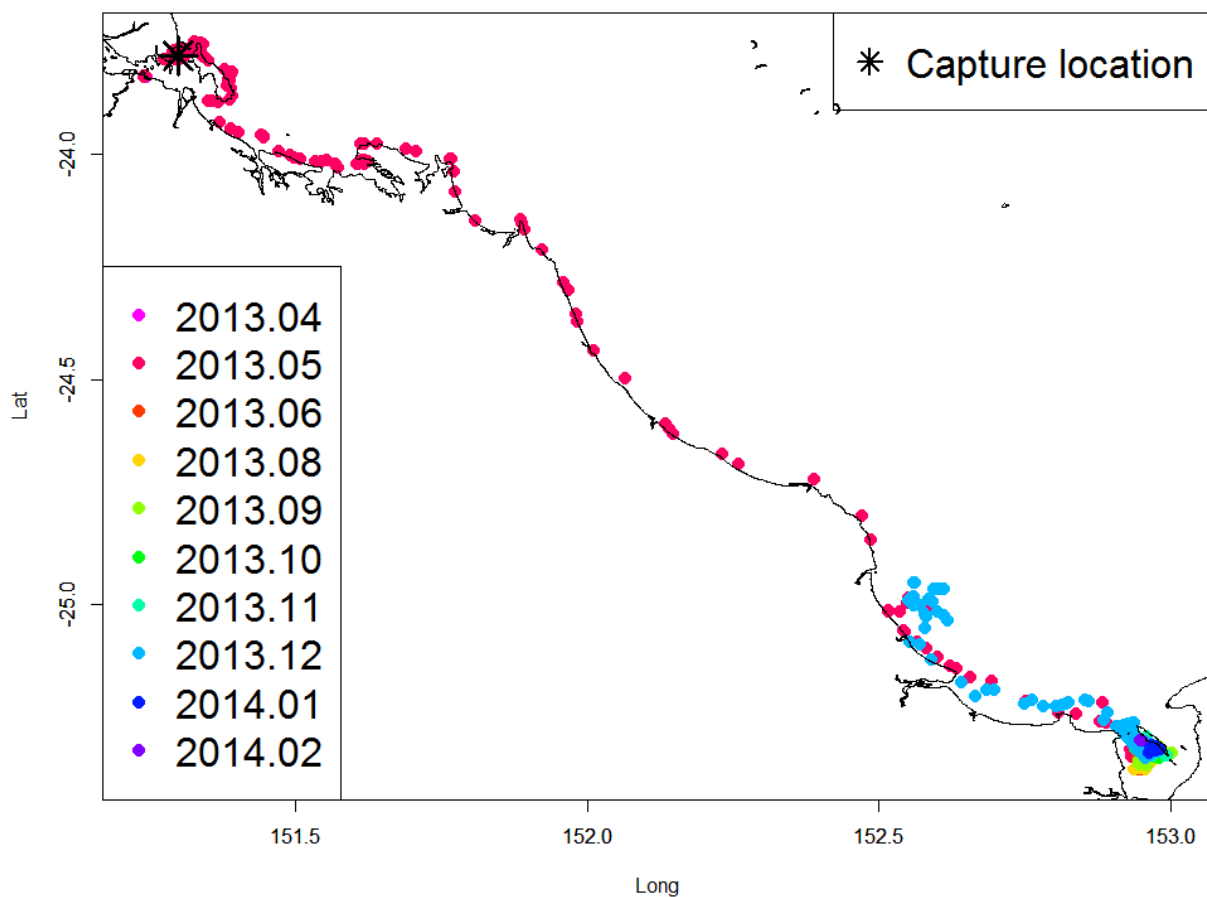
Figure 85 Map of turtle movement (satellite tag PTT = 126273). Track showing monthly GPS (Fastloc) detections of satellite tag (PTT = 126273, Acoustic Tag ID = 27926) from May 2013–February 2014 of a pubescent immature female of 101.6 cm CCL.
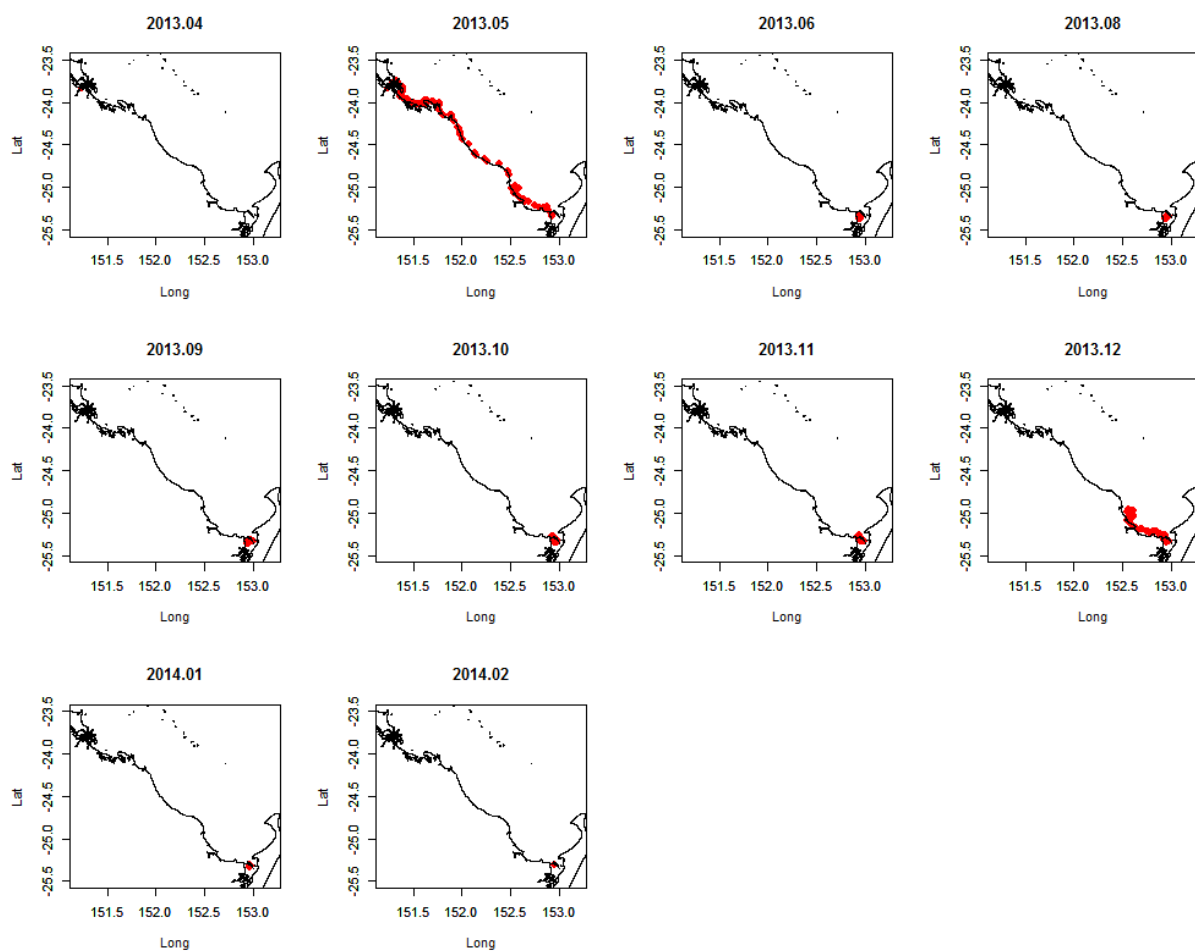
Figure 86 Monthly GPS detections of satellite tag 126273 (pubescent immature female of 101.6 cm CCL) with each panel representing a month. Animal was tagged at Pelican Banks with tag location shown as a black asterisk.
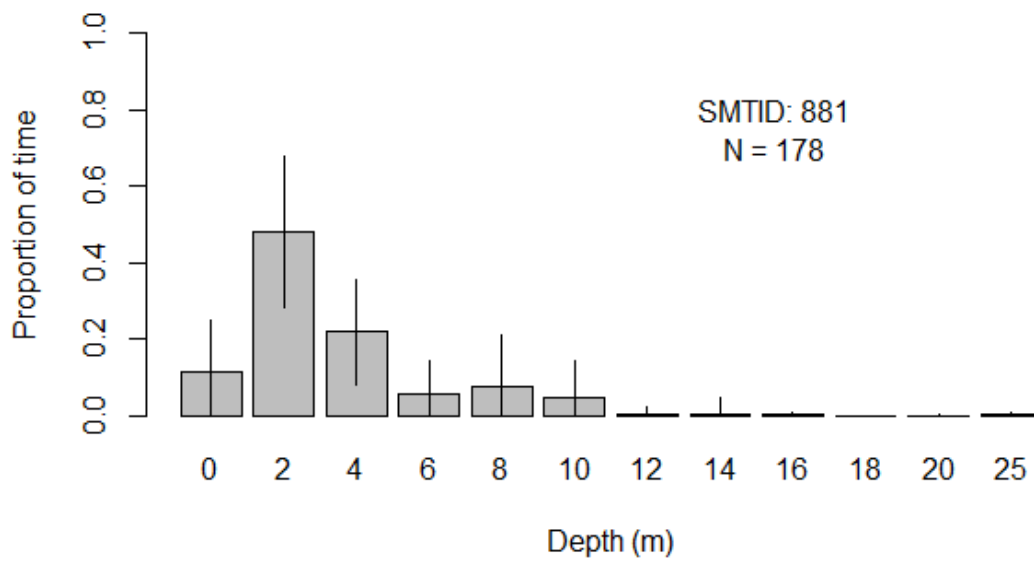
Figure 87 Proportion of time (±SD) spent at depth for a pubescent immature female turtle (tag 126273, 101.6 cm CCL).
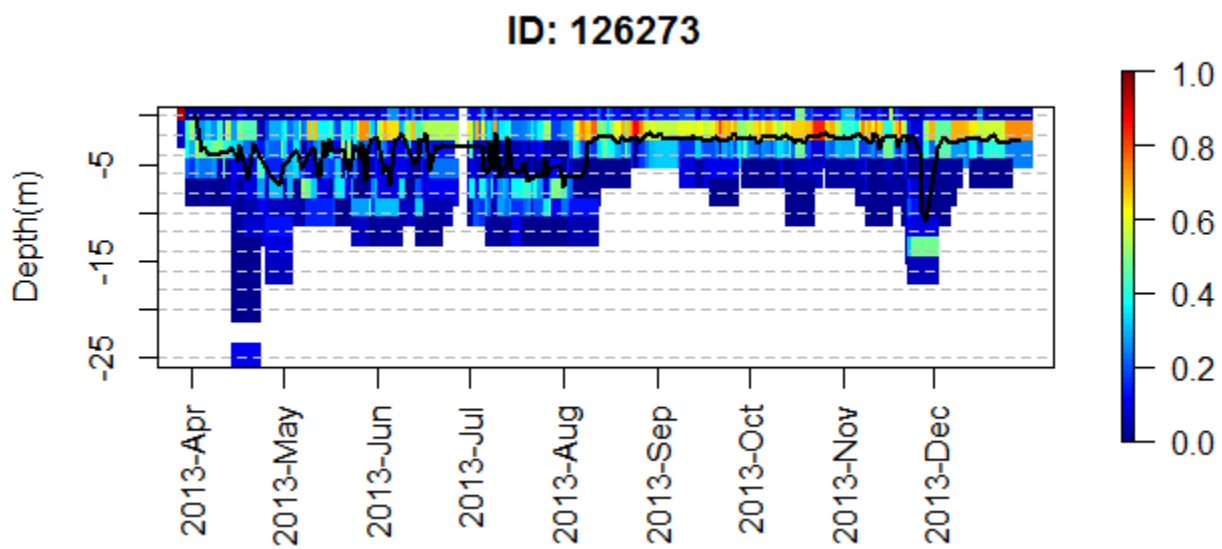
Figure 88 Plot of average time spent at depth per day (black line) for a pubescent immature female (tag 126273, 101.6 cm CCL).
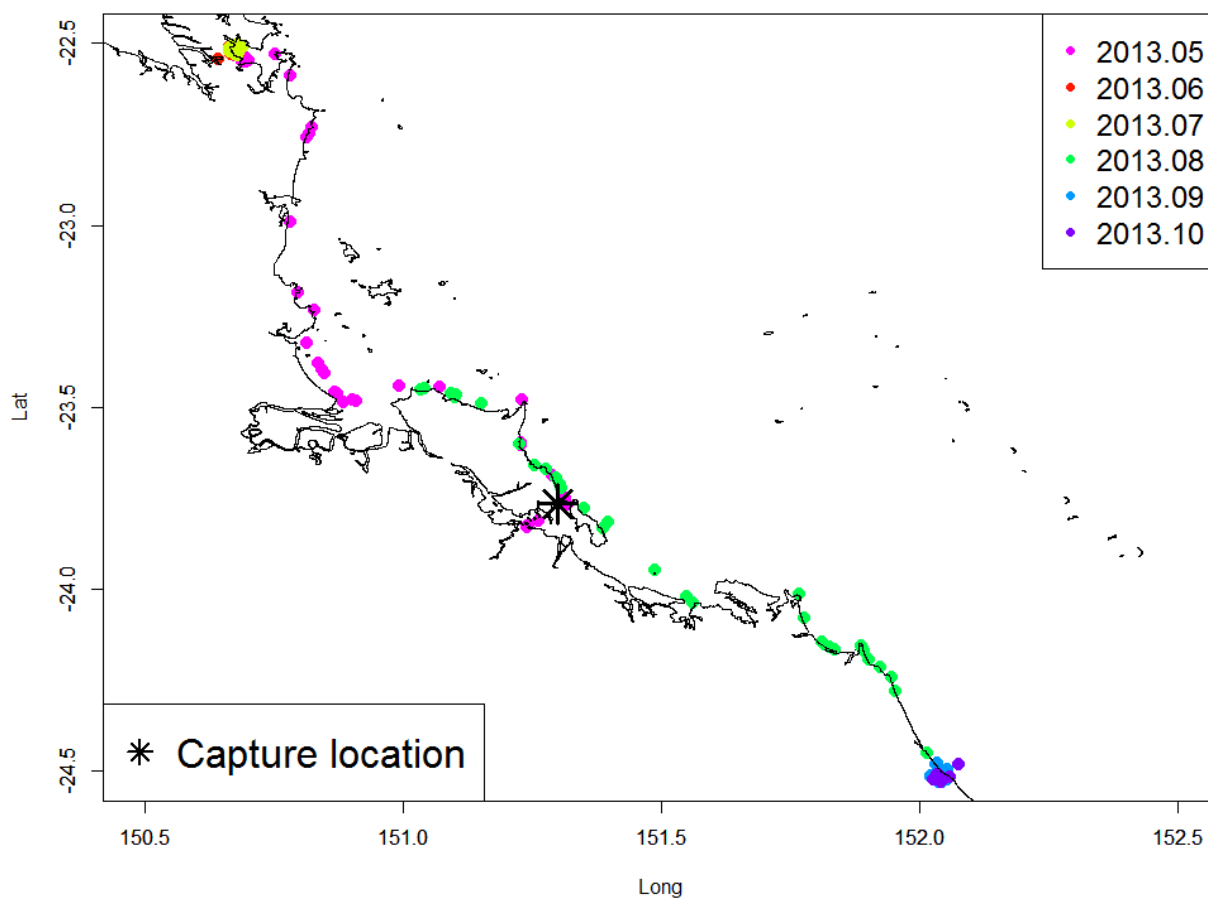
Figure 89 Map of turtle movement (satellite tag PTT = 126274). Monthly GPS (Fastloc) detections of satellite tag (PTT = 126274, Acoustic Tag ID = 27948) from May 2013 – October 2013 of amature female of 113.8 cm CCL.
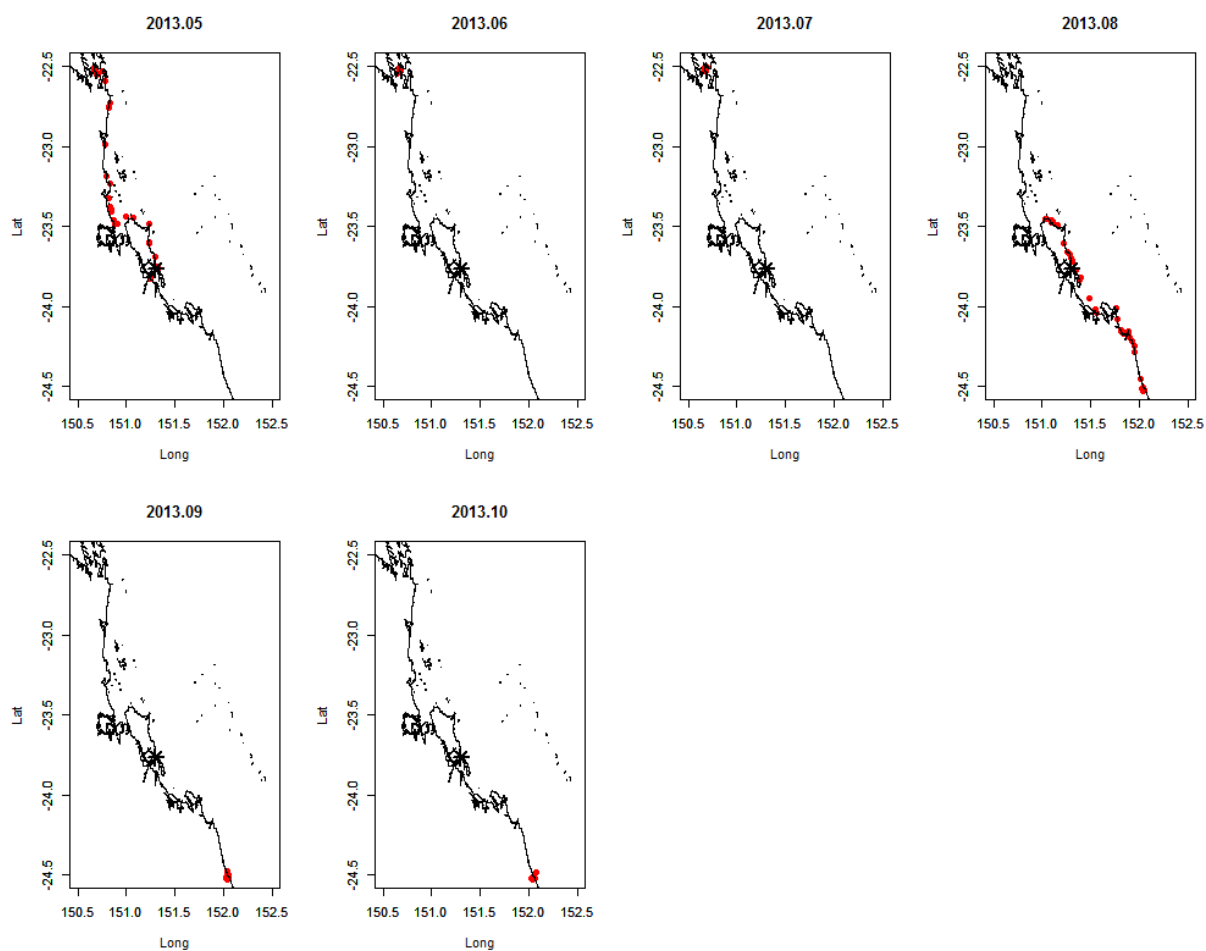
Figure 90 Monthly GPS detections of satellite tag 126274 (mature female of 113.8 cm CCL) with each panel representing a month. Animal was tagged at Pelican Banks with tag location shown as a black asterisk.
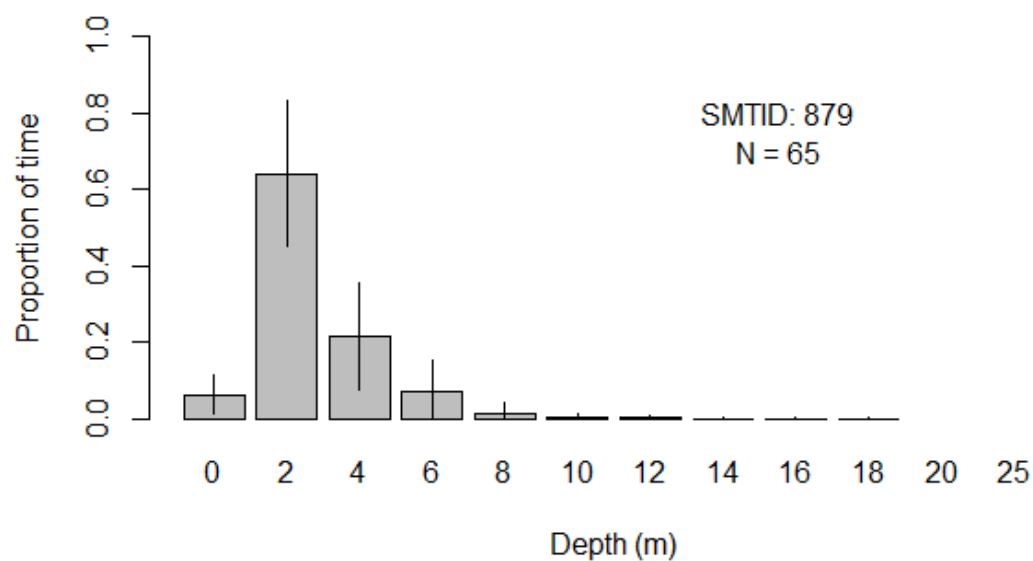
Figure 91 Proportion of time (±SD) spent at depth for a mature female turtle (tag 126274, 113.8 cm CCL).
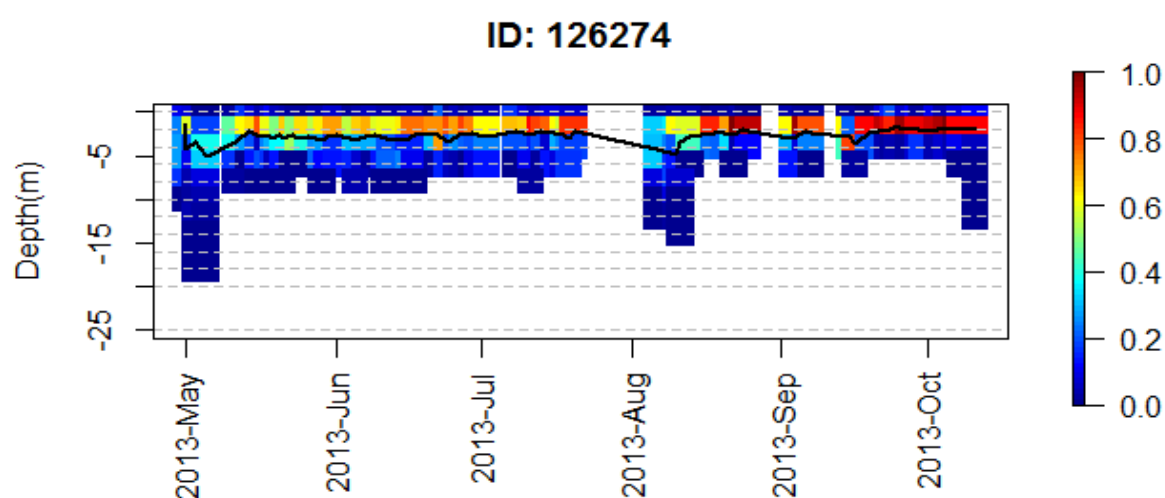
Figure 92 Plot of average time spent at depth per day (black line) for a mature female turtle (tag 126274, 113.8 cm CCL).
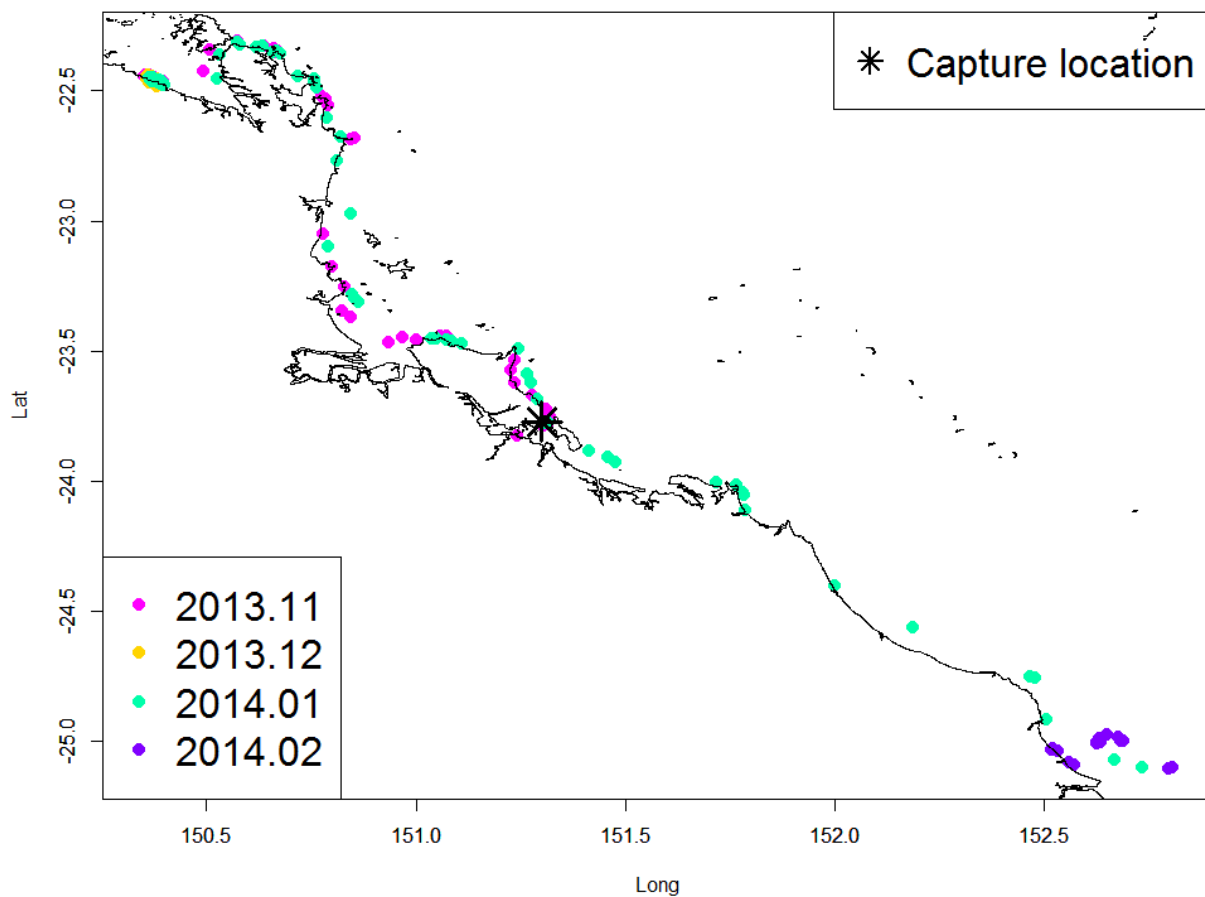
Figure 93 Map of turtle movement (satellite tag PTT = 131869). Monthly GPS (Fastloc) detections of satellite tag (PTT = 131869, Acoustic Tag ID = 16229) from November 2013 – February 2014 of a mature female of 96.2 cm CCL.
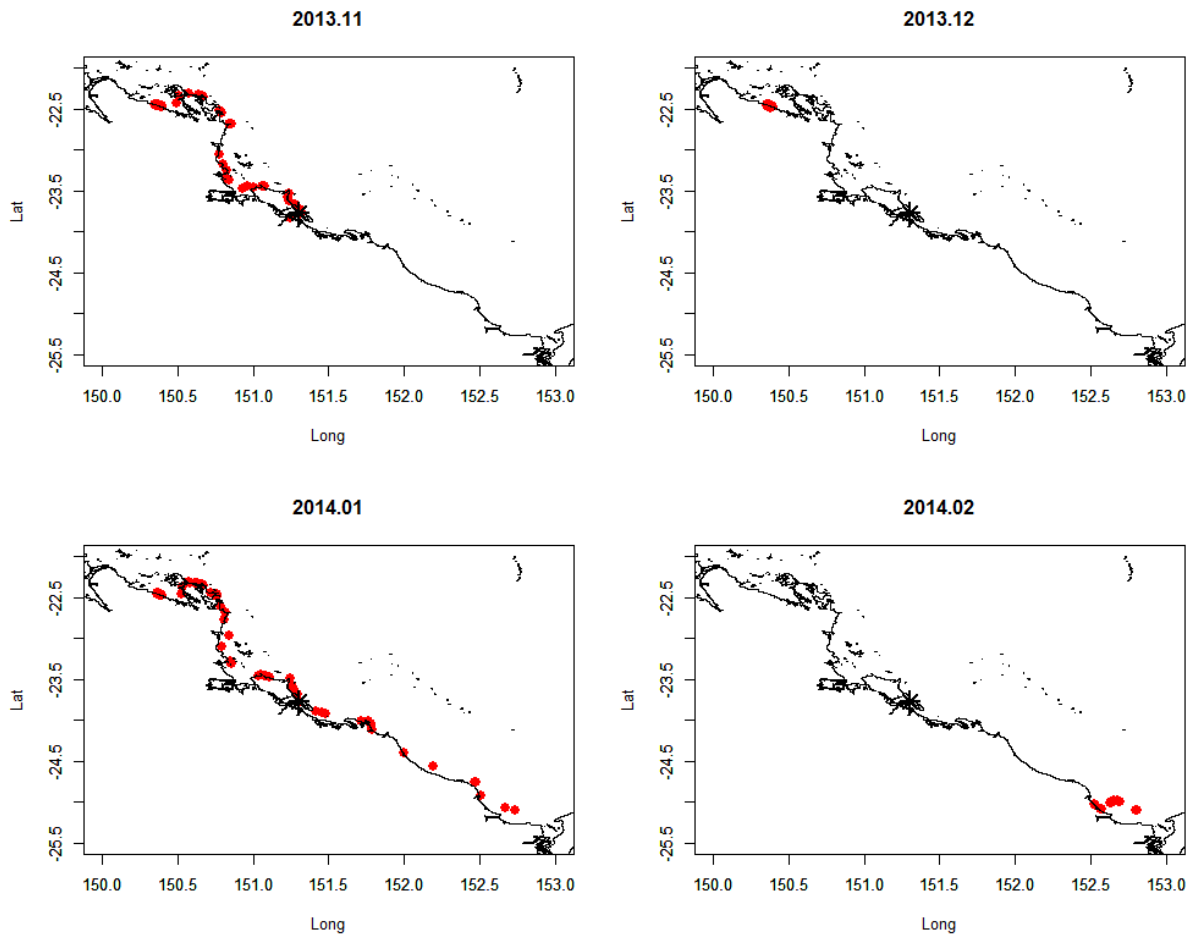
Figure 94 Monthly GPS detections of satellite tag 131869 (mature female of 96.2 cm CCL) with each panel representing a month. Tag location indicated by black asterisk.
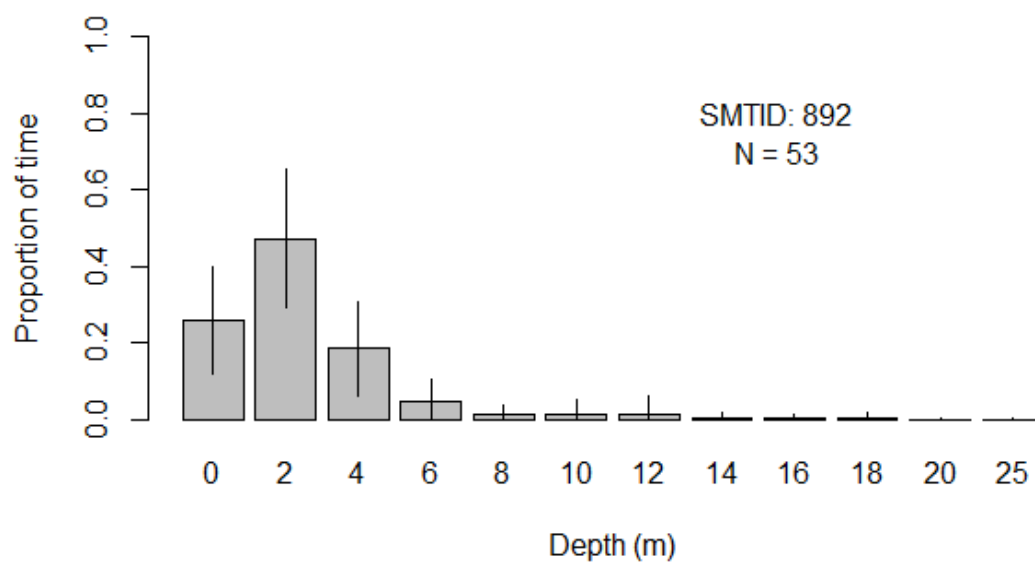
Figure 95 Proportion of time (± SD) spent at depth for amature female turtle (tag 131869, 96.2 cm CCL).
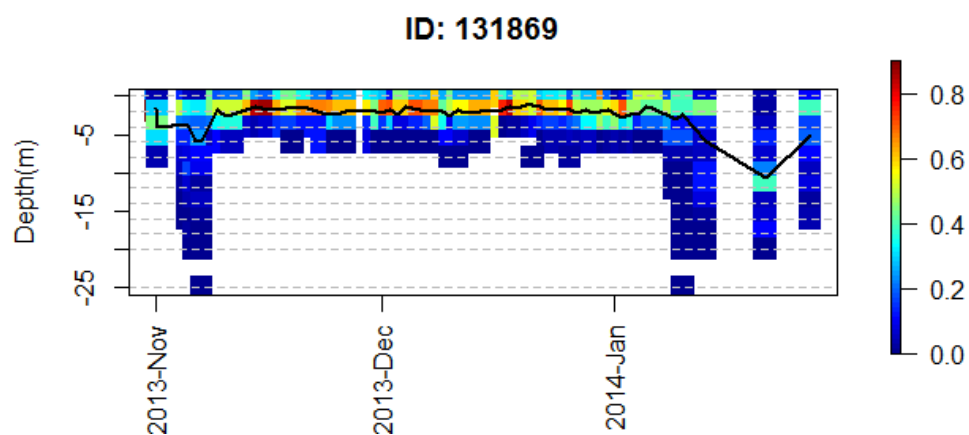
Figure 96 Plot of average time spent at depth per day (black line) for a mature female turtle (tag 131869, 96.2 cm CCL).

Two of the turtles tagged with satellite tags at Pelican Banks remained within Gladstone Harbour. An adult male turtle of 97.7 cm CCL with satellite tag 131868 (acoustic tag ID = 26568) was tagged on the 6/11/13 at Pelican Banks (Figure 97) and its satellite tag was detected on 793 occasion between 7/11/2013–14/6/2014. Following tagging this animal moved as far south as South Trees Island within Gladstone Harbour and moved to the area around Wiggins Island before moving back to Pelican Banks on the 13 November 2013. During December 2013 it moved between Pelican Banks and Wiggins Island with the 50% KUD in November and December between 23–35 km^2 (Figure 98). During January, the majority of time was spent around Pelican Banks (50% KUD = 5.4 km^2) before moving to Wiggins Island in February where it remained until 14 June 2014. During this time the 50% KUD was between 1.14–3.36 km^2. The satellite tag stopped transmitting on the 14 June 2014 while the acoustic tag showed that this animal remained at Wiggins Island until 23 June 2014 with no further detection beyond this date.

Diving depth from the satellite tag showed that this animal spent 85% of its time less than 2 m under the surface (Figure 99). Average daily depth was less than 2.5 m from November 2013–March 2014 with the deepest dives to 25 m occurring when the animal moved between Pelican Banks and South Trees. Dives to 20 m were recorded when the animal moved between Pelican Banks and Wiggins Island in December 2013 (Figure 100). From March–July 2014 while the animal was resident at Wiggins Island, no dives deeper than 6 m were recorded and the average daily depth was approximately 1.5 m which was approximately 1 m shallower than when the animals was resident at Pelican Banks (average depth of 2.5 m).

An adult female turtle with satellite tag 126272 (acoustic tag ID = 27949), was 106 cm CCL and tagged at Pelican Banks on 2/5/2013. The satellite tag on this individual was detected on 793 occasions between 2/5/2013–21/11/2013. This animal remained at Pelican Banks for the entire duration with the 50% KUD between 0.51–1.14 km^2 in the seven months it was detected (Figure 101 and Figure 102).

Diving depth from the satellite tag showed that this animal spent 85% of its time less than 2 m under the surface (Figure 103). Average daily depth was between 1–3 m for the duraction of the monitoring period with regular daily dives to 7 m and occasional dives to 10 m (Figure 104).
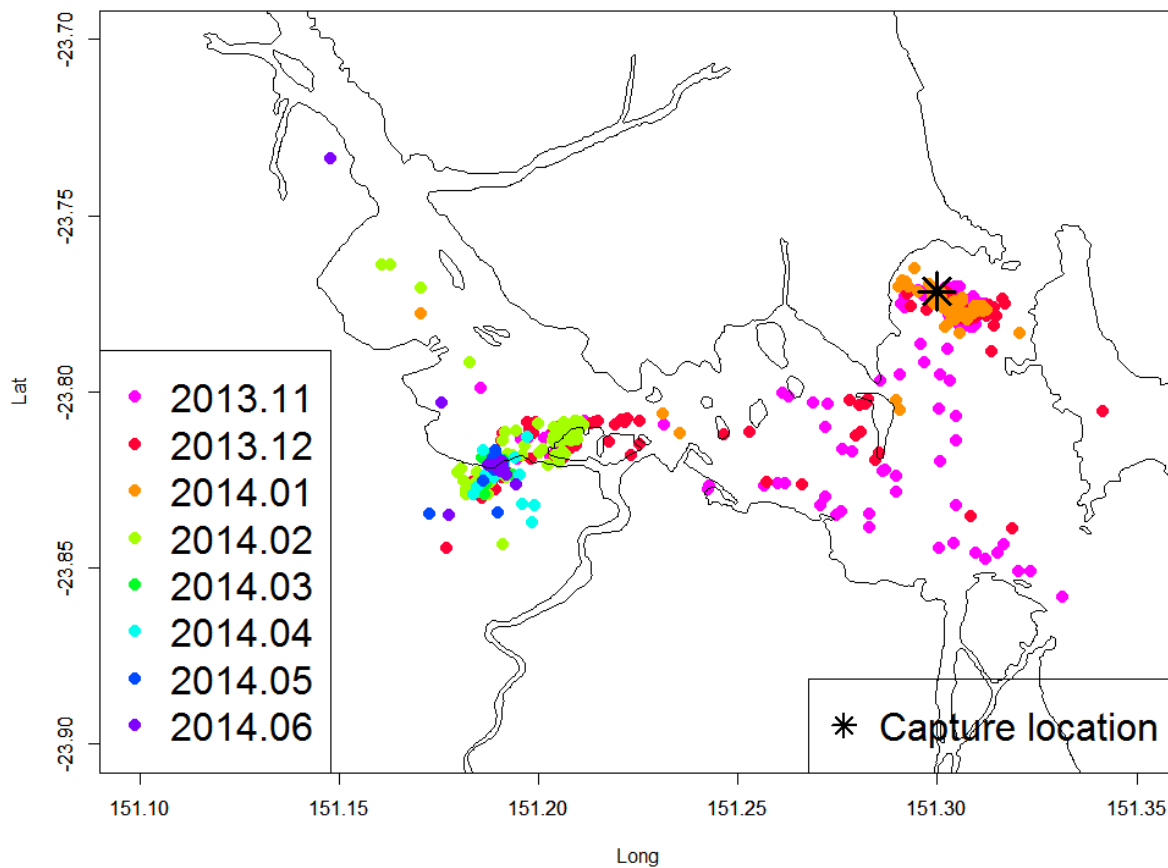
Figure 97 Map of turtle movement (satellite tag PTT = 131868). Monthly GPS (Fastloc) detections of satellite tag (PTT = 131868, Acoustic Tag ID = 26568) from November 2013–June 2014 of a mature male of 97.7 cm CCL.
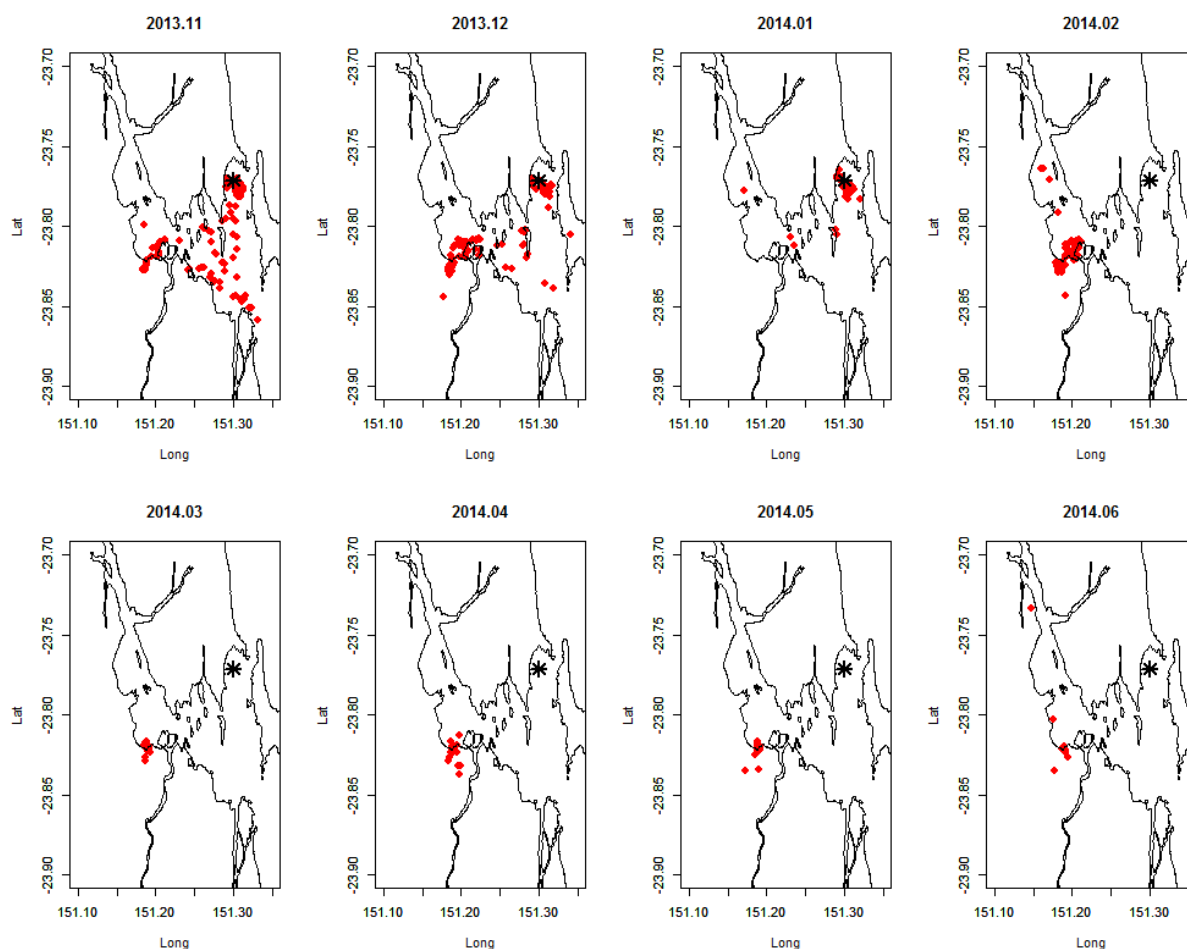
Figure 98 Monthly GPS detections of satellite tag 131868 (mature male of 97.7 cm CCL) with each panel representing a month. Animal was captured at Pelican Banks with capture location shown as a black asterisk.
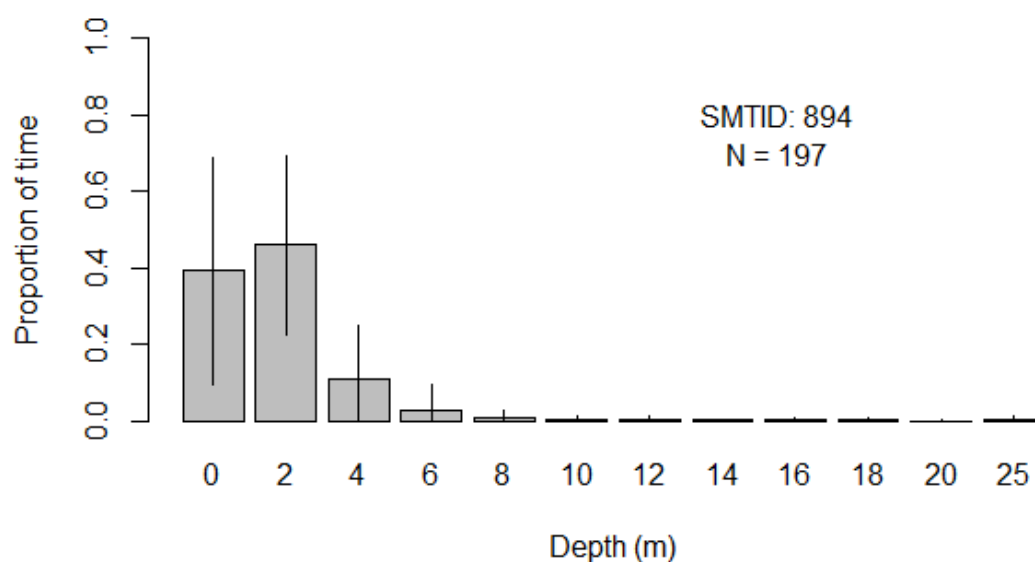
Figure 99 Proportion of time (± SD) spent at depth for a mature male turtle (tag 131868, 97.7 cm CCL) .
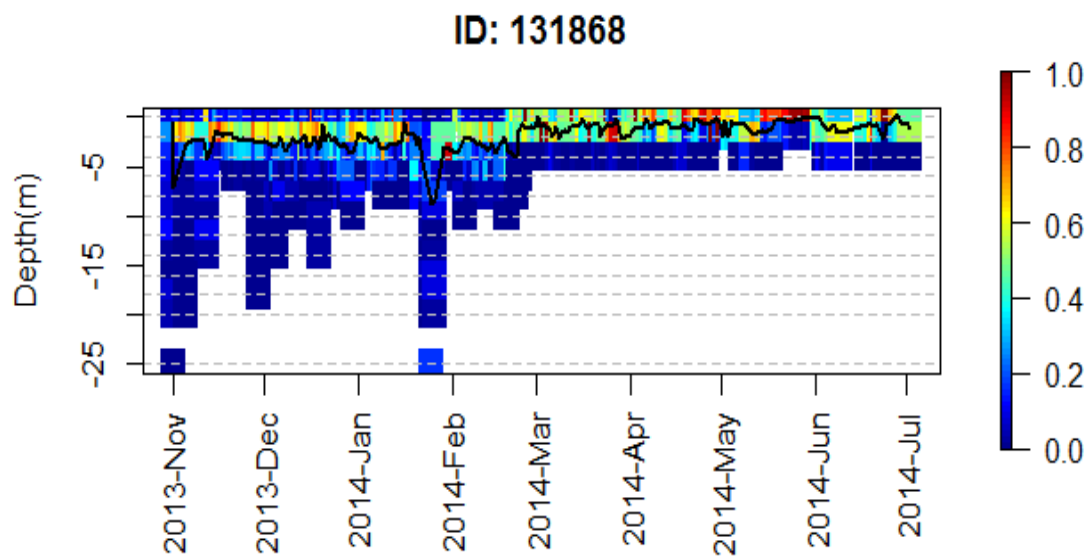
Figure 100 Plot of average time spent at depth per day (black line) for amature male turtle (tag 131868, 97.7 cm CCL).
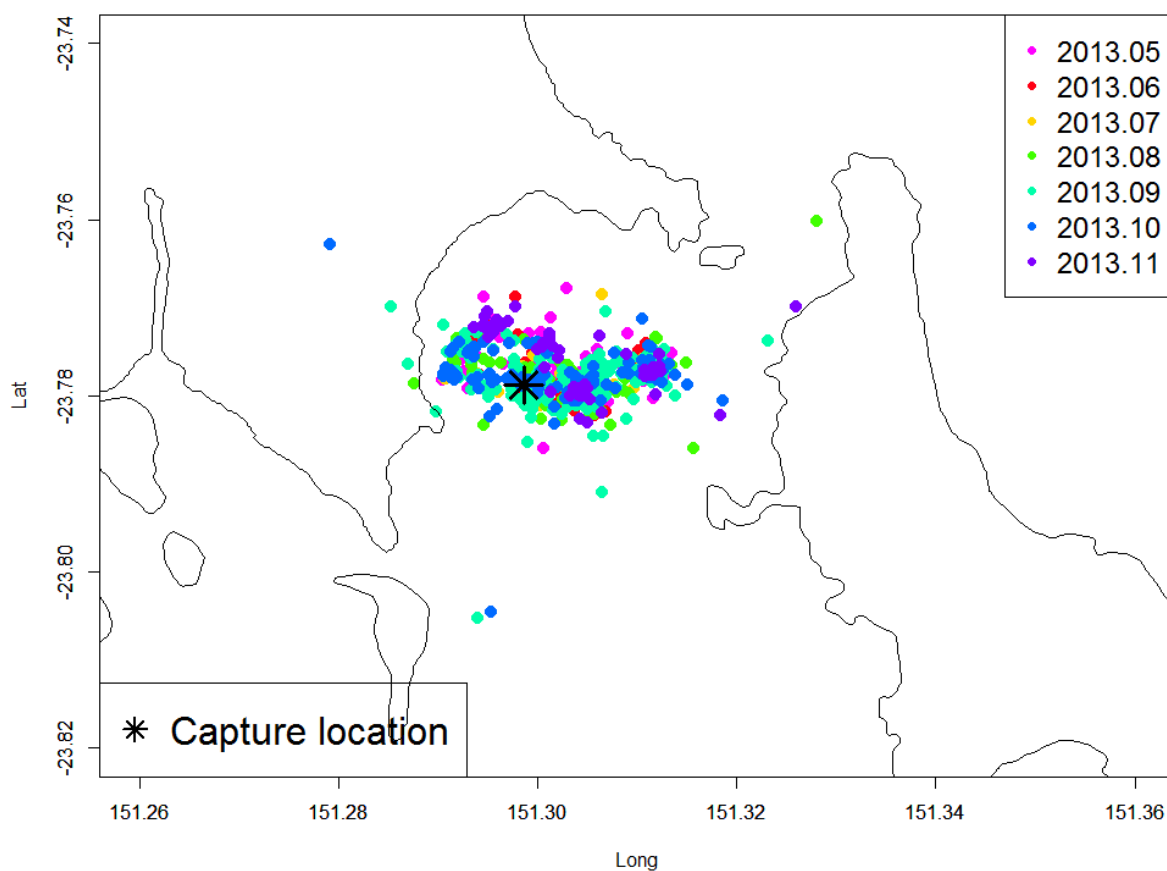
Figure 101 Map of turtle movement (satellite tag PTT = 126272). Monthly GPS (Fastloc) detections of satellite tag (PTT = 126272, Acoustic Tag ID = 27949) from May 2013 – November 2014 of amature female of 106.2 cm CCL.
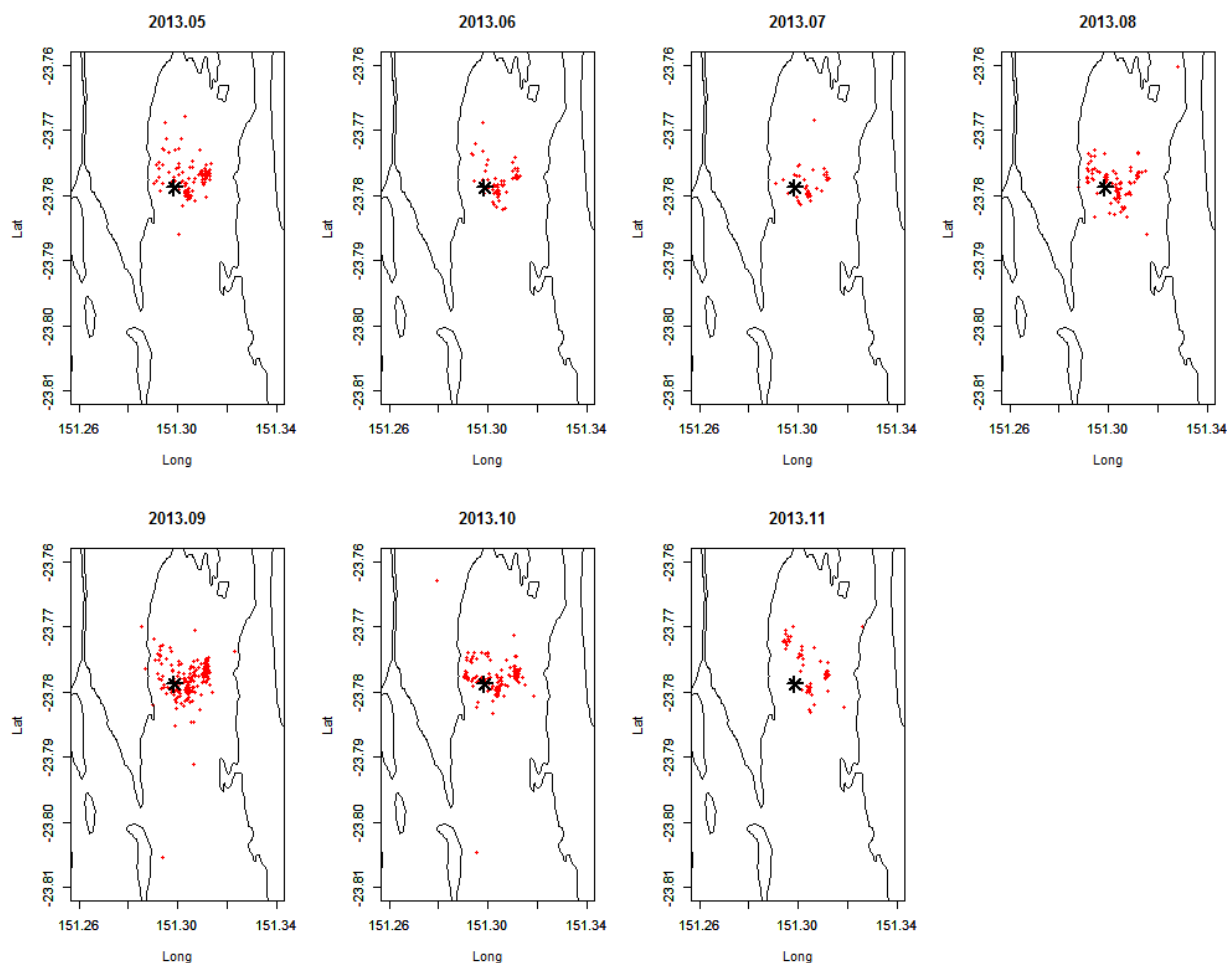
Figure 102 Monthly GPS detections of satellite tag 126272 (mature female of 106.2 cm CCL) with each panel representing a month. Animal was tagged at Pelican Banks with capture location shown as a black asterisk.
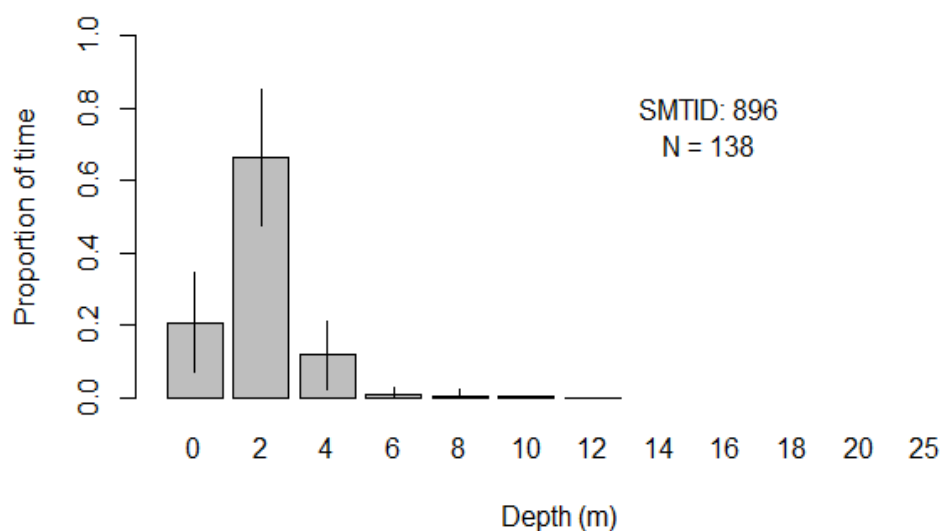
Figure 103 Proportion of time (± SD) spent at depth for a mature female turtle (tag 126272, 106.2 cm CCL).
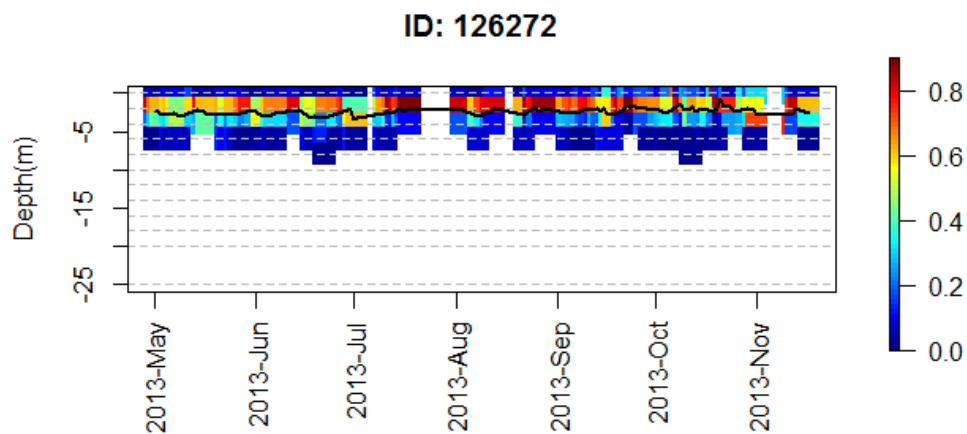
Figure 104 Plot of average time spent at depth per day (black line) for a mature female turtle (tag 126272, CCL 106.2 cm).

Five satellite tags were deployed on juvenile turtles capture at Wiggins Island. One of the satellite tags (satellite tag ID 131871, acoustic tag ID 27629) deployed at Wiggins Island malfunctioned with the GPS antenna not providing any data. From the detection of the acoustic tag, we know this individual remained around Wiggins Island from the time it was tagged in November 2013 until September 2014. The other four individuals remained around Wiggins Island with an average home range of 0.98 km^2.

A juvenile male turtle of 58.8 cm CCL was captured along the north western edge of Wiggins Island (satellite tag ID 126275, acoustic tag ID 27947) and detected 925 times between 1/5/2013 and 4/5/2014 (Figure 105). Average monthly 50% KUD ranged from 0.20–0.63 km^2 with the animal mainly detected around Wiggins Island and the rock wall along the south western bank of the mouth of the Calliope River (Figure 106). From May–September it was detected around Wiggins Island and the mouth of the Calliope and then between October – December only around Wiggins Island. During January and February 2014 it was detected around Wiggins Island the rock wall and then only detected around Wiggins Island from March–May 2014. Figure 107 shows the location of the rock wall and mangrove covered Wiggins Islands.

Diving depth from the satellite tag showed this animal spent 90% of its time less than 2 m under the surface (Figure 107). Average daily depth was less than 2.5 m for the entire monitoring period with deepest dives to 11 m which occurred when the animal moved between Wiggins Island and the rock wall at the mouth of the Calliope River (Figure 108). Regular dives to 7 m were recorded throughout the monitoring period.

The other three animals tagged with satellite and acoustic tags around Wiggins Island were all captured in the mangrove drain and displayed very similar movement patterns with a large proportion of detections occurring within the drain.

A juvenile male turtle of 54.6 cm CCL (satellite tag ID 126267, acoustic tag ID 27950) was detected on 295 occasions between 1/5/13 and 10/11/13 (Figure 109). Average monthly 50% KUD ranged from 1.5–4.0 km^2 with detections in May, June and September predominantly adjacent to the mangrove drain and intertidal and subtidal flats to the northeast of the mangrove drain (Figure 110 and Figure 111). During May this individual was also recorded along the mangrove fringe to the southwest of where it was captured (Figure 110). In July and August, the majority of detections were on intertidal and subtidal flats with few detections within the mangrove drain (Figure 110).

Diving depth from the satellite tag showed this animal spent 85% of its time less than 2 m under the surface (Figure 112). Average daily depth was less than 1.5–3.5 m for the entire monitoring period with the deepest dives up to 12 m and consistent daily dives to 7 m (Figure 113).

A juvenile of 52.1 cm CCL and unknown sex (satellite tag ID 131862, acoustic tag ID 31598) was detected on 1110 occasions between 5/11/13 and 27/2/14 (Figure 114). Average monthly 50% KUD ranged from 0.46–1.03 km^2 with detections in November and December predominantly in the mangrove drain and intertidal and subtidal flats to the northeast of the mangrove drain (Figure 115 and Figure 116). During February, this individual was primarily detected within the mangrove drain (Figure 115). No depth data was obtained from the satellite tag on this animal.

A juvenile turtle of 52.7 cm CCL and unknown sex (satellite tag ID 131872, acoustic tag ID 29771) was detected on 1365 occasions between 7/11/13 and 18/4/14 (Figure 117). Average monthly 50% KUD area ranged from 0.32 0.70 km^2 with detection in November and December predominantly in the mangrove drain as well as the intertidal and subtidal flats to the north-west of the mangrove drain (Figure 118 and Figure 116). In December 2013, and April and May 2014 there were a few detections along the edge of the shipping channel, however the majority of detections occurred along the mangrove drain, and intertidal and subtidal flats (Figure 118 and Figure 119).

Diving depth from the satellite tag showed this animal spent 85% of its time less than 2 m under the surface (Figure 119). Average daily depth was between 0.5–2.5 m for the entire monitoring period with the deepest dives up to 13 m and consistent daily dives to 9 m (Figure 120).
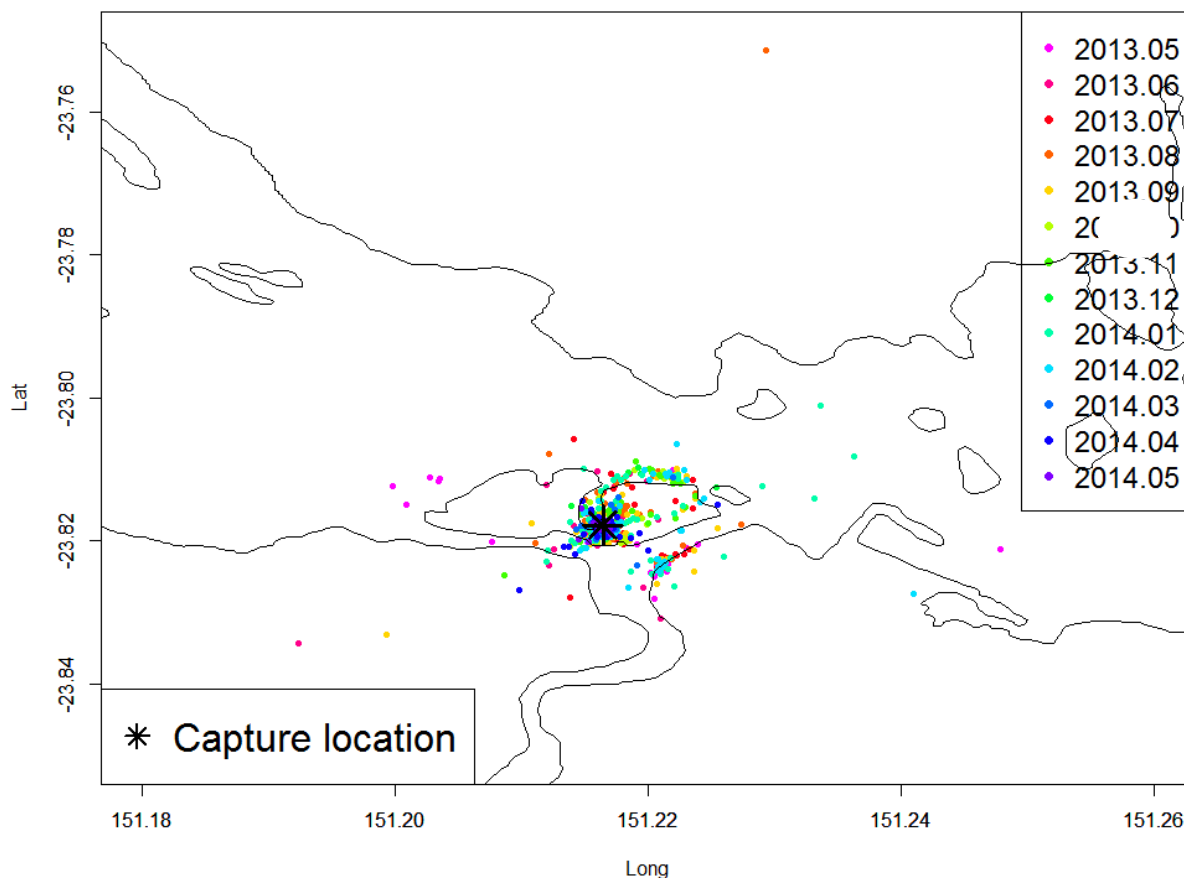
Figure 105 Map of turtle movement (satellite tag PTT = 126275). Monthly GPS (Fastloc) detections of satellite tag (PTT = 126275, Acoustic Tag ID = 27947) from May 2013–May 2014 of a juvenile male of 58.8 cm CCL.
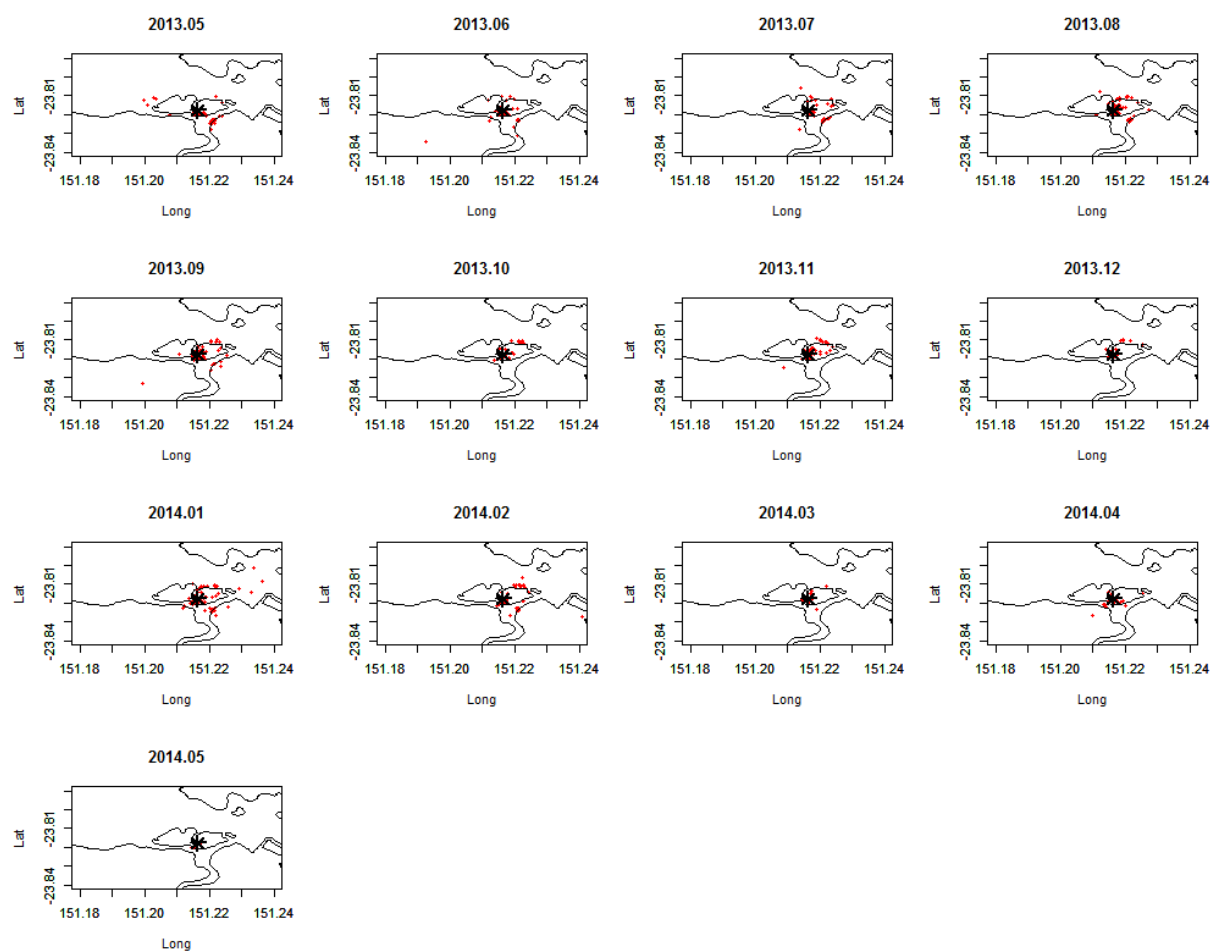
Figure 106 Monthly GPS detections of satellite tag 126275 (juvenile male of 58.8 cm CCL) with each panel representing a month. Capture location indicated by black asterisk.
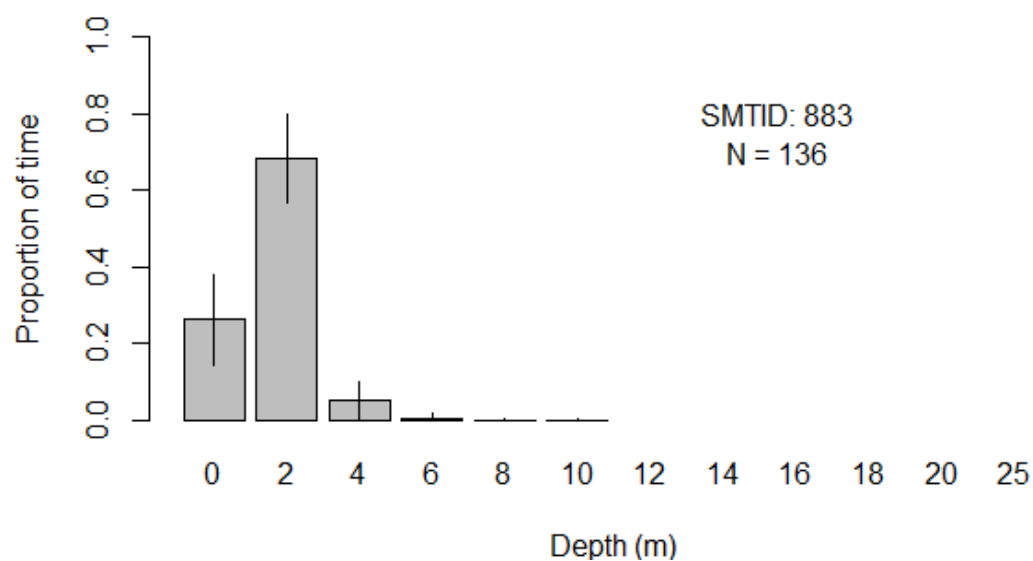
Figure 107 Proportion of time (± SD) spent at depth for a juvenile male turtle (tag 126275, 58.8 cm CCL).
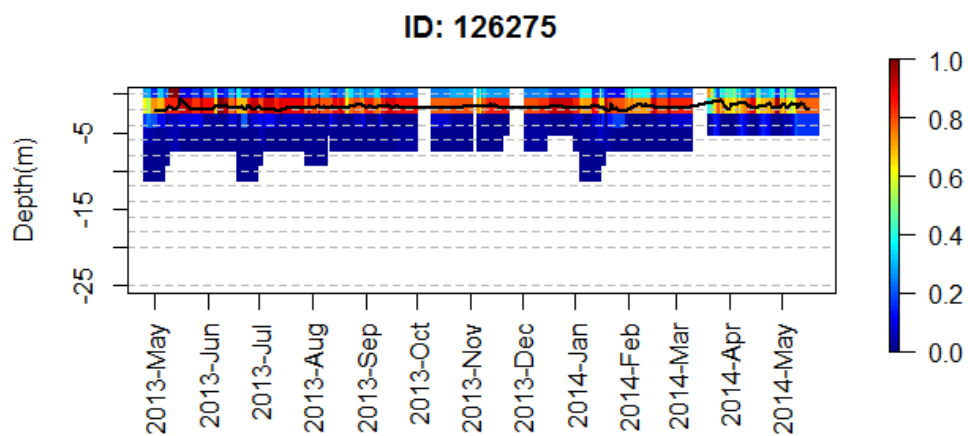
Figure 108 Plot of average time spent at depth per day (black line) for a juvenile male turtle (tag 126275, 58.8 cm CCL).
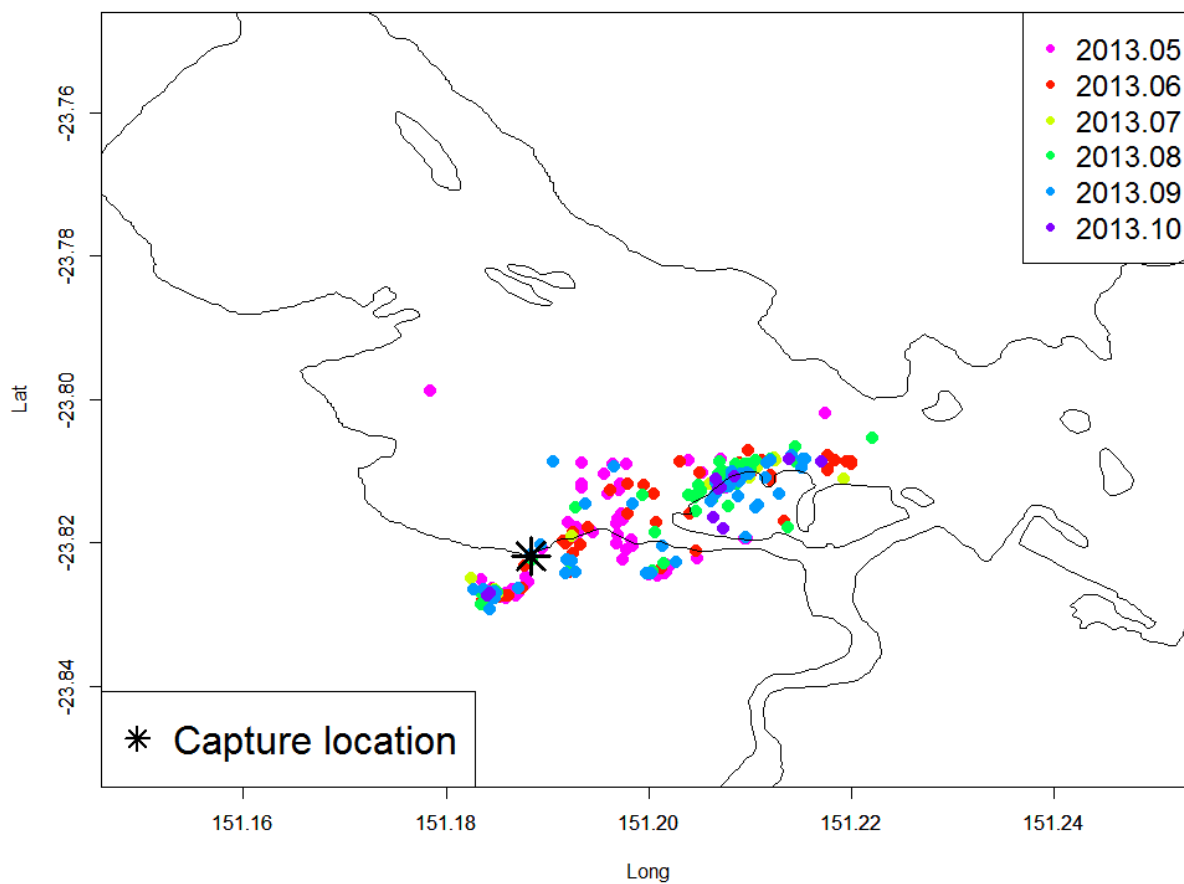
Figure 109 Map of turtle movement (satellite tag PTT = 126273). Monthly GPS (Fastloc) detections of satellite tag (PTT = 126276, Acoustic Tag ID = 27950) from May 2013 – May 2014 of a juvenile male of 54.6 cm CCL.
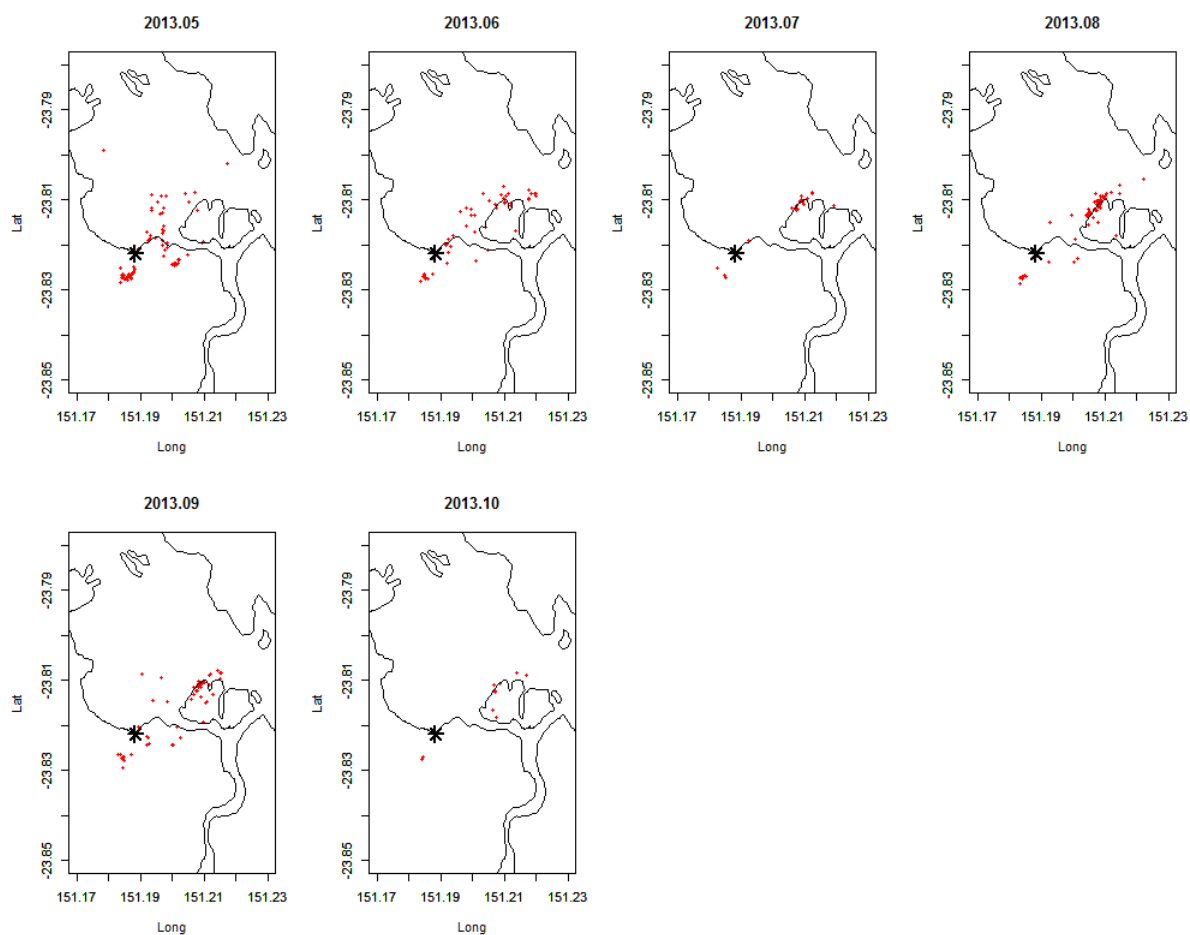
Figure 110 Monthly GPS detections of satellite tag 126276 (juvenile male of 54.6 cm CCL) with each panel representing a month. Tag location indicated by black asterisk.
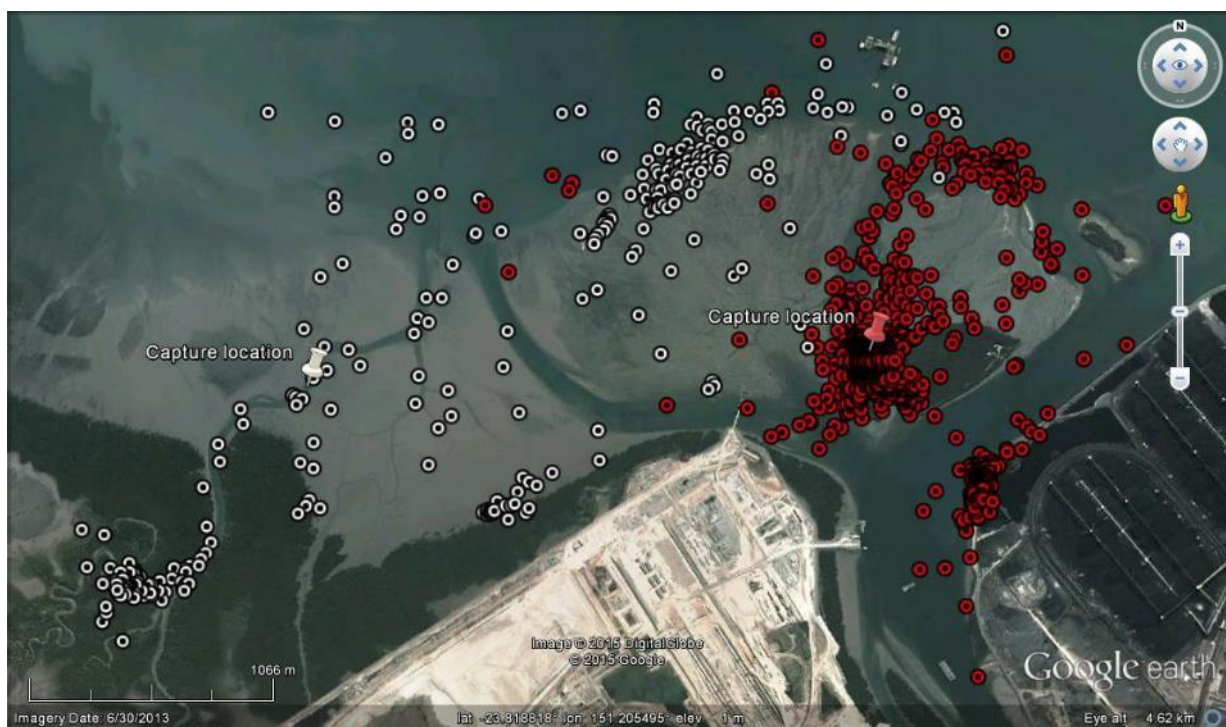
Figure 111 Fastloc detections of satellite tag 126275 (red circles; juvenile male of 58.8 cm CCL) and 126276 (white circles; juvenile male of 54.6 cm CCL) around Wiggins Island and the mangrove drain. Capture location shown by same coloured pin.
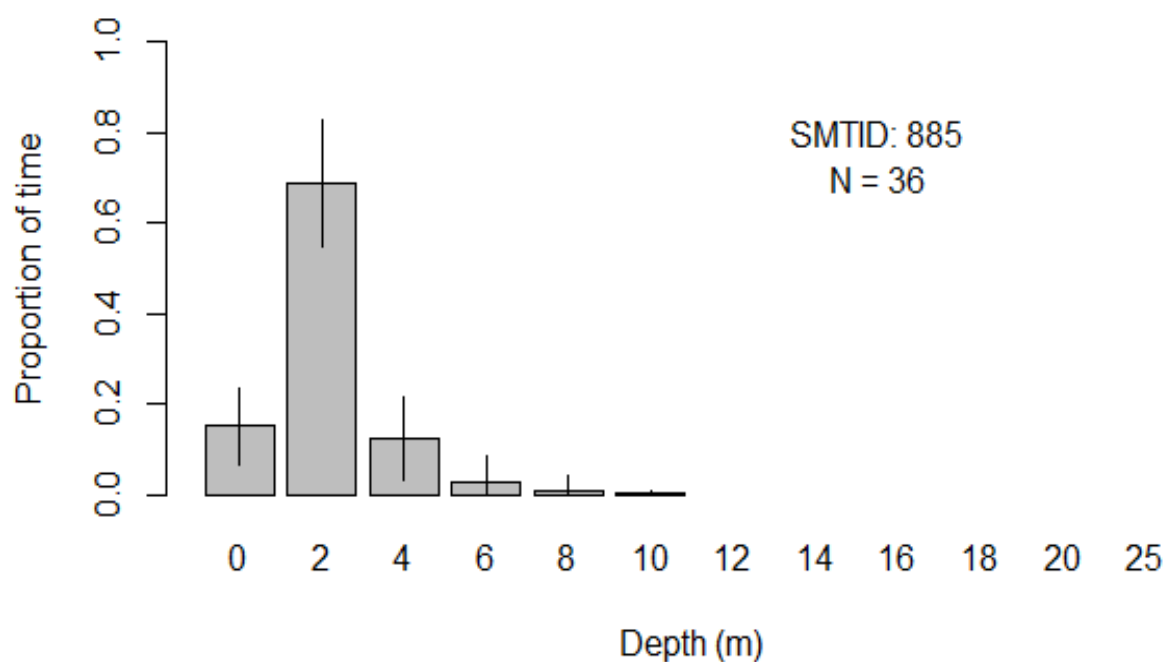
Figure 112 Proportion of time (± SD) spent at depth for a juvenile male turtle (tag 126276, 54.6 cm CCL).
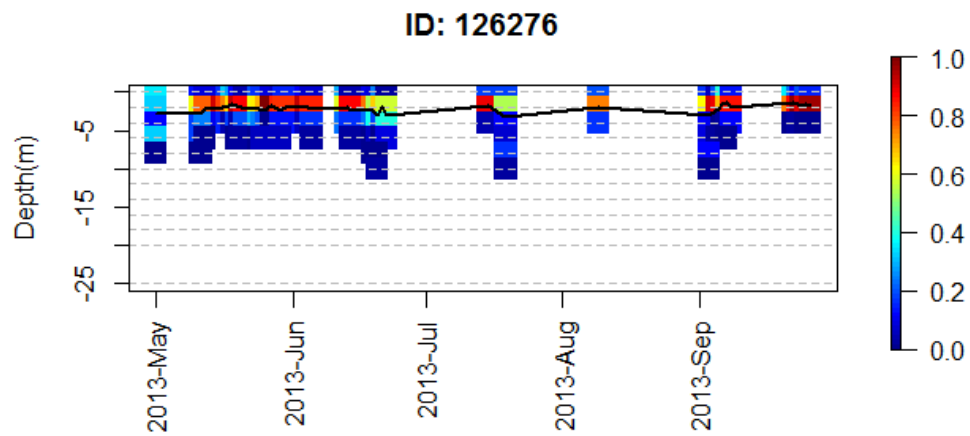
Figure 113 Plot of average time spent at depth per day (black line) for a juvenile male turtle (tag 126276, 54.6 cm CCL).
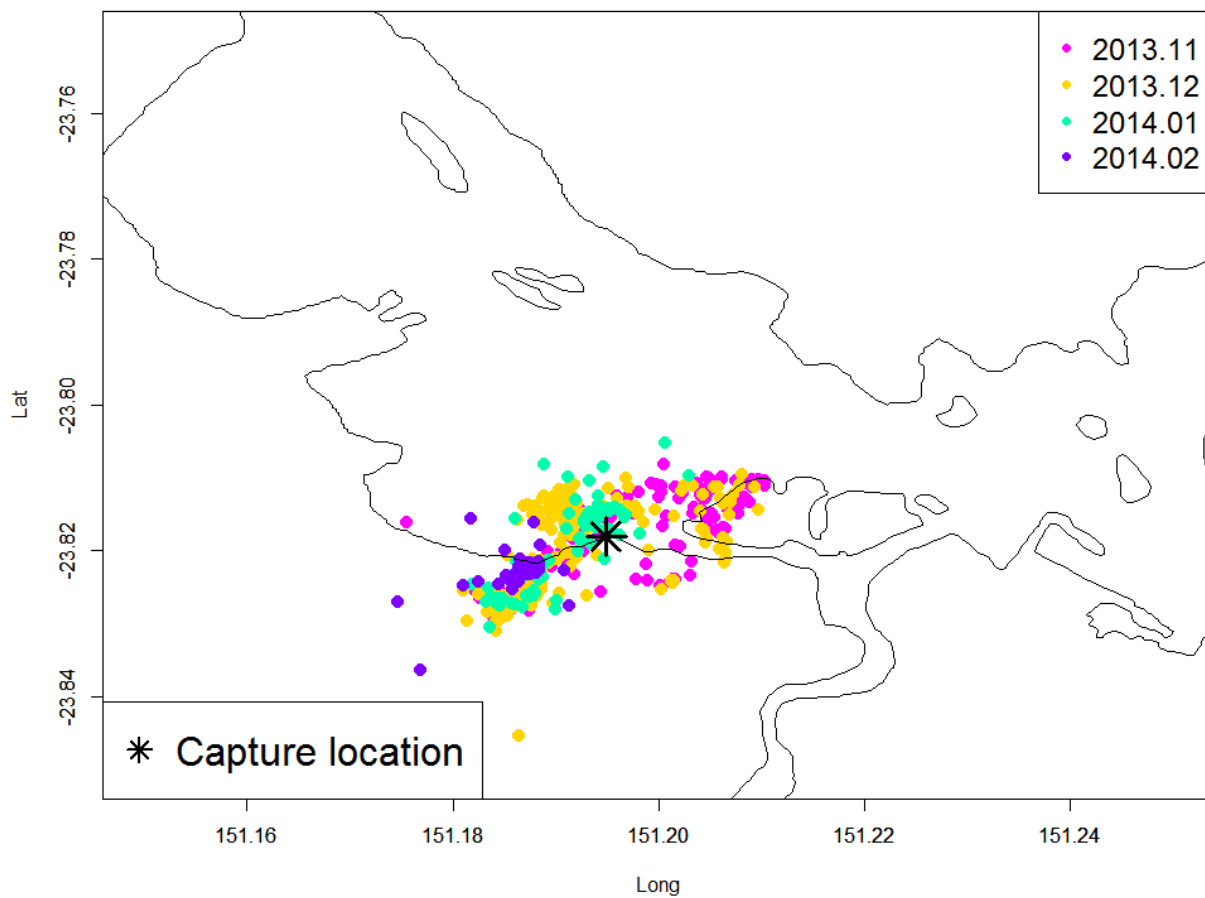
Figure 114 Map of turtle movement (satellite tag PTT = 131862). Monthly GPS (Fastloc) detections of satellite tag (PTT = 131862, Acoustic Tag ID = 31598) from November 2013 – February 2014. Coloured points indicatate detections in each month of a juvenile (unknown sex) of 52.1 cm CCL.
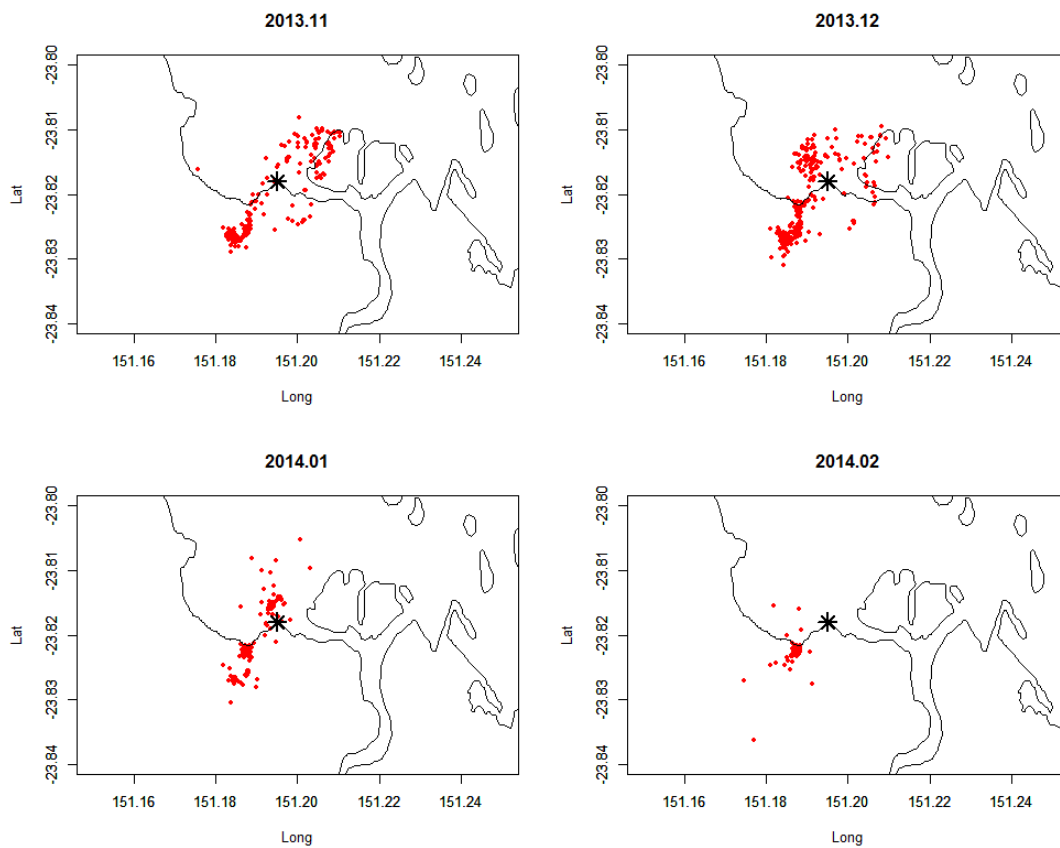
Figure 115 Monthly GPS detections (red points) of satellite tag 131862 (juvenile (unknown sex) of 52.1 cm CCL) with each panel representing a month. Capture location shown as black asterisk.
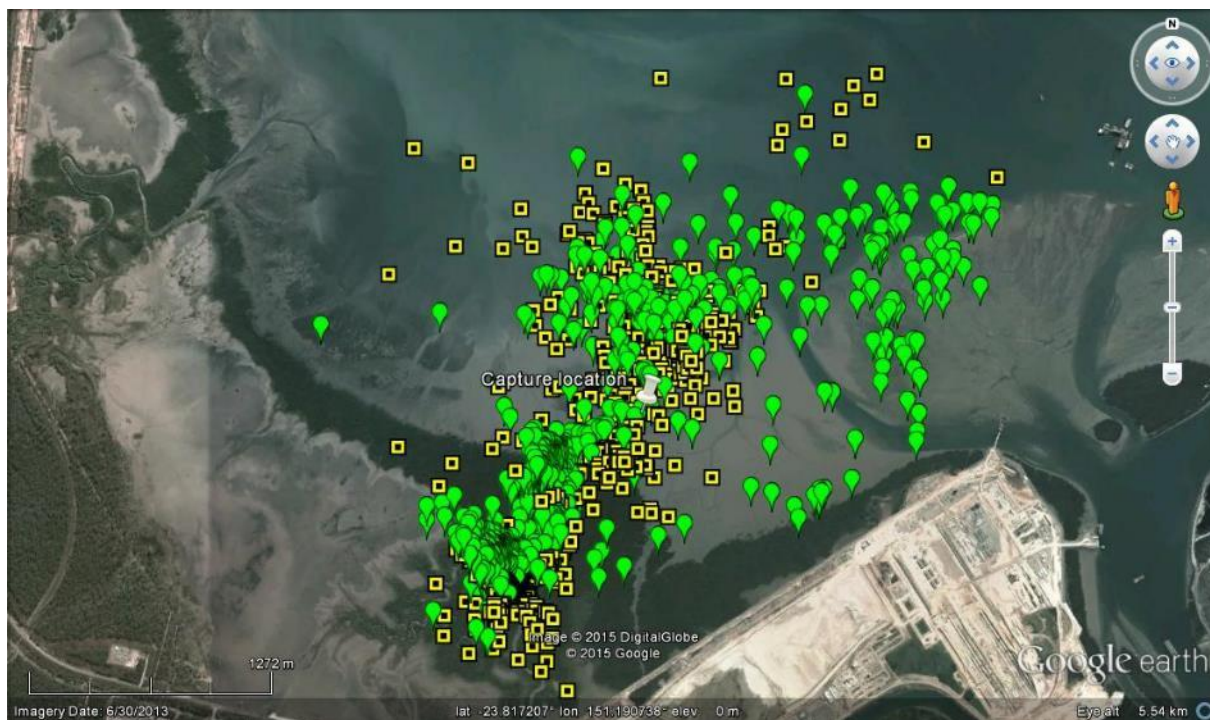
Figure 116 Fastloc detection of satellite tag 131872 (yellow squares; juvenile of 52.7 cm CCL) and 131862 (green drops; juvenile of 52.1 cm CCL) around Wiggins Island and the mangrove drain. Capture Locations of both individuals shown by white pin.
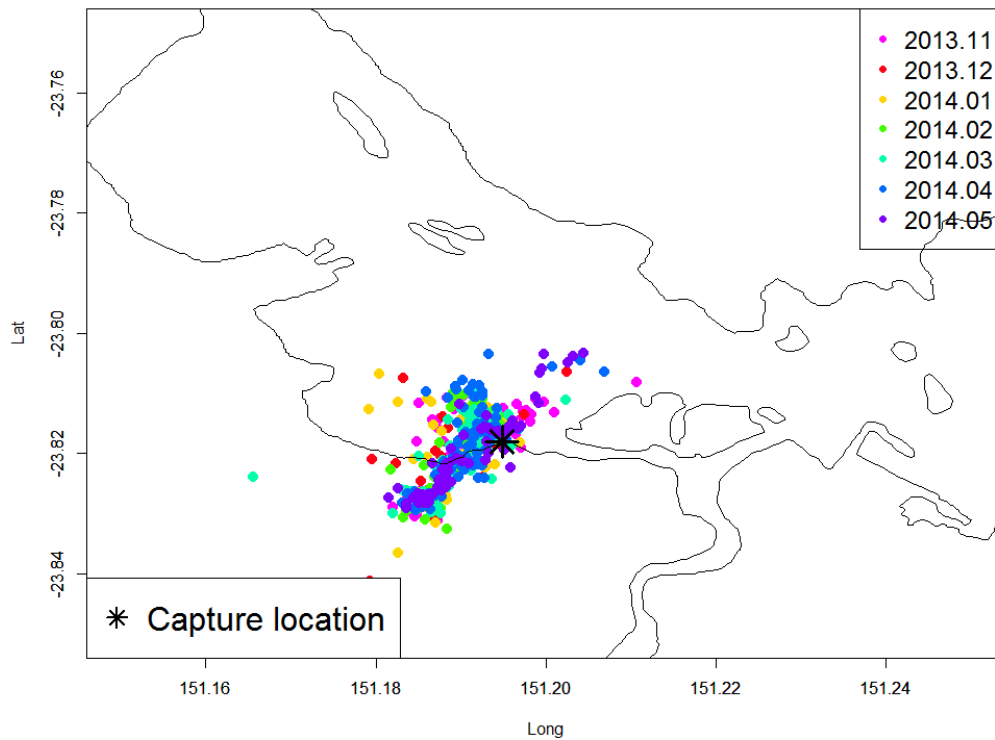
Figure 117 Map of turtle movement (satellite tag PTT = 131872). Monthly GPS (Fastloc) detections of satellite tag (PTT = 131872, Acoustic Tag ID = 29771) from November 2013 – May 2014 of a juvenile (unknown sex) of 52.7 cm CCL.
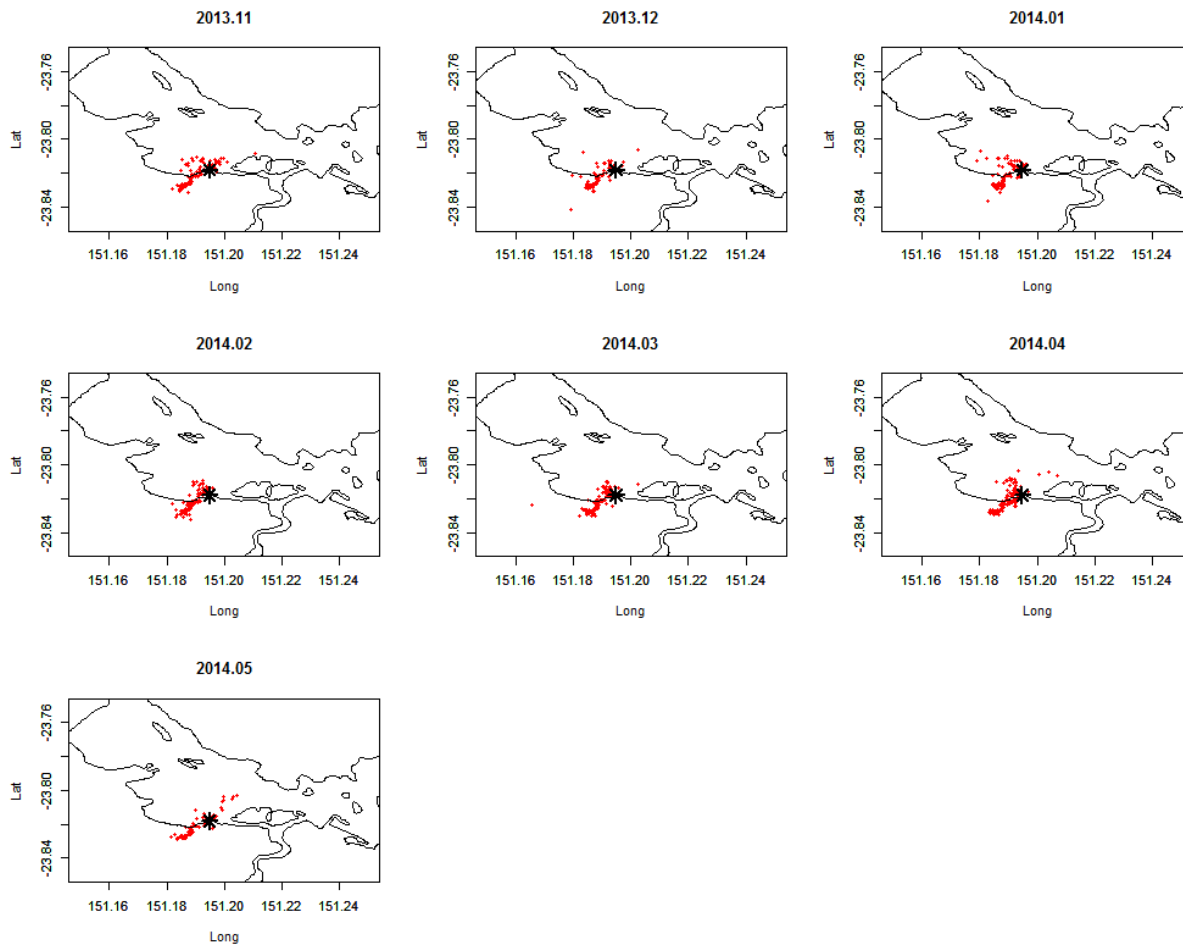
Figure 118 Monthly GPS detections of satellite tag 131872 (juvenile (unknown sex) of 52.7 cm CCL) with each panel representing a month. Capture location indicated by black asterisk.
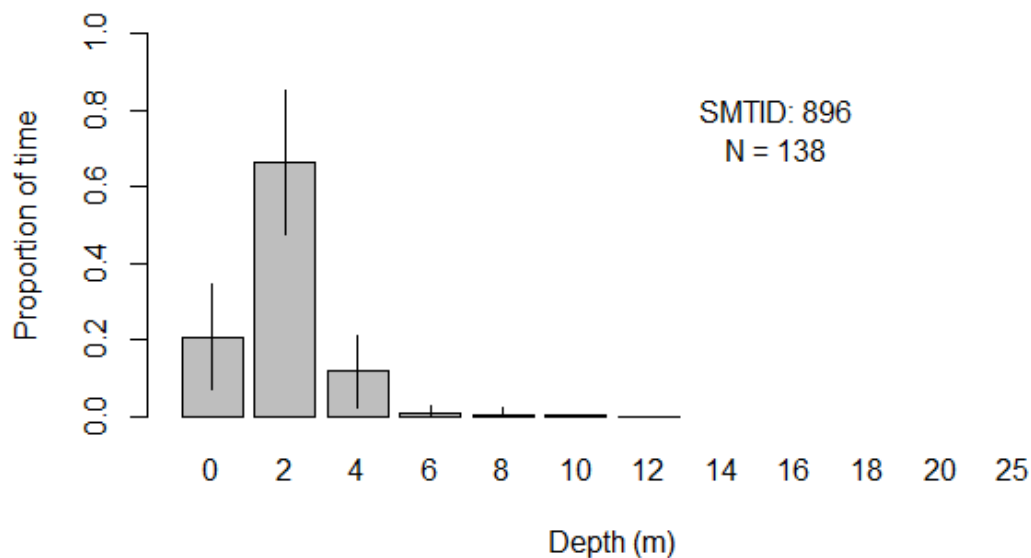
Figure 119 Proportion of time (SD) spent in depth for a juvenile turtle (tag 131872, 52.7 cm CCL).
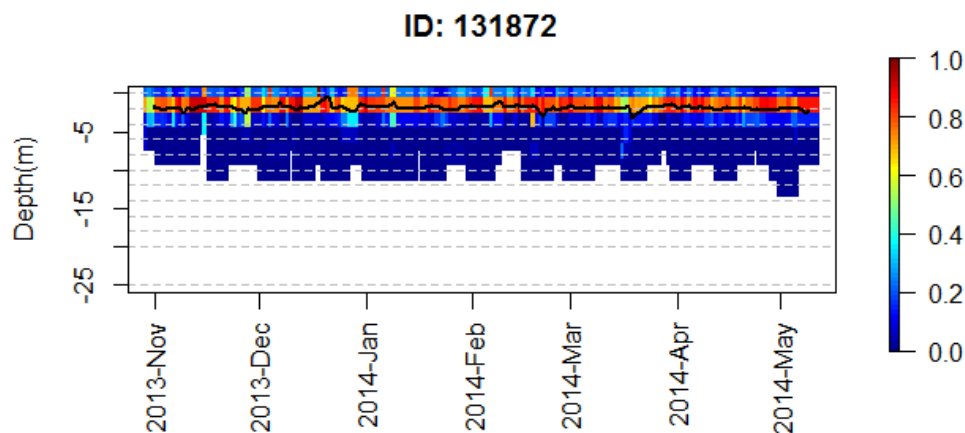
Figure 120 Plot of average time spent at depth per day (black line) for a juvenile turtle (tag 131872, 52.7 cm CCL).

3.12 Comparison of satellite and acoustic data

For animals that departed the array shortly after tagging (satellite tag ID 126273, 126274 and 131869), satellite tags provide the only long term data on the movement and habitat use with the detection span from satellite tags greater than that for acoustic tags (Table 3.8). Interestingly, of these animals that moved away from Gladstone, both animals that moved north and then south (satellite tag IDs 126273 and 131869) were detected by the array of receivers on their way past Gladstone in August 2013 and January 2014, respectively, suggesting that strategically placed acoustic receivers along the Queensland and New South Wales coastline would provide long term data on the timing and distance of foraging and nesting movements for this species.

For all animals with both tag types the average detection span from satellite tags was 7.2 (± 0.9 SE) months and for acoustic tags 9.0 (± 2.1) months, which was not significantly different (p = 0.4, t-test). For animals that remained within the array, the detection span from acoustic tags was significantly

greater (12.6 ± 1.5 months) than satellite tags (7.6 ± 1.4 months) (p <0.03, t-test). For all double tagged animals, acoustic tags provided on average 57 times more detections per month than satellite tags. The significantly higher number of detections combined with a longer detection span from acoustic tags enabled a more thorough and detailed interpretation of habitat use. Two of the turtles tagged with both satellite and acoustic tags at Wiggins Island in November 2013 had the acoustic tags secured to a PVC sleeve which reduced the number of detections (see Chapter V). For these two individuals (satellite tag ID 131862 and 131872), the number of monthly detections from satellite tags was similar to or greater than acoustic tags which was attributed to the signal attenuation caused by the PVC sleeve around the acoustic tag as these animals remained within the array and in close proximity to the receivers.

The benefit of satellite tags is that that they provide information on an animal's location when it is in an area not covered by acoustic receivers. However, as the comparisons of 50 and 95% KUD's illustrate, the home range estimates of individuals generated from satellite telemetry can underestimate home range size due to the small number of detections combined with the fact that the majority of satellite detections appear to occur in sheltered waters. This was particularly apparent in small turtles at Wiggins Island with the 50% KUD primarily confined to either the upper reaches of the mangrove drain or on the lee side of Wiggins Island.

Table 3.8 Comparison of the number of detections per month for SPLASH F10 satellite tags (Fastloc detections via ARGOS) and VEMCO acoustic tags (from acoustic receivers in Gladstone Harbour) on turtles fitted with both tag types. Dark and light shading represents satellite and acoustic tag pairs on the same individual.

	May-13	Jun-13	Jul-13	Aug-13	Sep-13	Oct-13	Nov-13	Dec-13	Jan-14	Feb-14	Mar-14	Apr-14	May-14	Jun-14	Jul-14	Aug-14	Sep14
Satellite tag:126272	111	77	44	106	219	170	67	0	0	0	0	0	0	0	0	0	0
Acoustic tag:27949	2362	3568	3650	5260	3089	2941	2221	1099	1372	2001	3392	3823	3827	3532	4576	3794	1459
Satellite tag:126273	232	0	64	241	110	160	137	169	17	2	0	0	0	0	0	0	0
Acoustic tag:27926	2224	0	0	0	0	0	0	0	0	0	0	0	0	0	0	0	0
Satellite tag:126274	145	155	124	91	92	58	0	0	0	0	0	0	0	0	0	0	0
Acoustic tag:126274	136	0	0	481	0	0	0	0	0	0	0	0	0	0	0	0	0
Satellite tag:126275	74	84	88	93	94	43	64	20	91	75	31	142	30	0	0	0	0
Acoustic tag:126275	7070	1778	3093	2500	1984	903	650	940	1887	957	768	1522	2862	1549	1299	2314	1048
Satellite tag:126276	78	53	22	65	68	10	0	0	0	0	0	0	0	0	0	0	0
Acoustic tag:27950	4921	10139	13012	15785	8334	9064	5705	4195	5105	4199	6543	4986	6306	7066	10582	8348	2847
Satellite tag:131862							275	441	191	207	0	0	0	0	0	0	0
Acoustic tag:31598							1157	664	160	45	58	139	234	80	568	352	47
Satellite tag:131868							254	202	55	130	356	353	312	64	0	0	0
Acoustic tag:26568							1045	1390	1320	1435	2138	1498	3611	3382	0	0	0
Satellite tag:131869							143	249	116	16	0	0	0	0	0	0	0
Acoustic tag:16229							9	0	7	0	0	0	0	0	0	0	0
Satellite tag:131872							251	168	186	179	222	236	129	0	0	0	0
Acoustic tag:29771							9	18	19	24	41	34	107	173	0	0	0
Satellite tag:131871*							0	0	0	0	0	0	0	0	0	0	0
Acoustic tag:27629							1300	1446	1013	627	499	903	863	691	1200	919	125

* satellite tag failed

For animals that remained within the array or receivers, the size and shape of KUD's calculated from satellite and acoustic detections were broadly similar. For animals that maintained a relatively small home range (50% KUD < 2.7km^2), in four out of five instances, the 50% KUD from acoustic telemetry was 1.5–2.9 times greater than that calculated using satellite telemetry over the same time period (Table 3.9). In these four animals, 95% KUD area from acoustic telemetry were more similar to those from satellite telemetry but were still 1.12–1.4 times greater (Table 3.9). For the animals captured at Pelican Banks, only one animal remained in the vicinity of where it was captured. The distribution of the 50% KUD area from satellite telemetry of this animal (satellite tag ID 126272) had a slight overlap with the 50% KUD from acoustic telemetry whereas the 95% KUD from both tags were similar (Figure 121). The other animal tagged at Pelican Banks moved between Pelican Banks and Wiggins Island with the 50 and 95% KUD's from satellite telemetry due primarily to the fact that the area between Wiggins Island and Pelican Banks did not have receiver coverage but also due to satellite detection upstream of the most upstream receiver within the mangrove drain (Figure 122).

For those animals tagged at Wiggins Island, the estimate of KUD area from satellite telemetry was larger than that from acoustic telemetry for only one individual (satellite tag ID 126276) due to the fact that this animal was detected both within the array of receivers but also upstream of the most upstream receiver within the mangrove drain where it could be detected by acoustic receivers (Figure 123). This resulted in the 50 and 95 % KUD area from satellite detections being 2.3 times and 1.8 times greater than those acoustic detections.

For the other three animals tagged at Wiggins Island (tag ID 131862, 131872, 126275), satellite telemetry underestimated KUD with the 50 % KUD centred around the upper reaches of the mangrove drain for animals captured in this habitat (Figure 124 and Figure 125) or on the northwest side of Wiggins Island for the individual captured at this location (Figure 126). In all three animals, there were high numbers of detections on acoustic receivers in locations where there were few satellite detections resulting in the 50% KUD from acoustic detections being centred on different areas. For animals tagged in the mangrove drain, the use of the intertidal and subtidal flats to the north of the mangrove drain was underestimated from satellite telemetry. Similarly, for the animal tagged at Wiggins Island, the 50% KUD from acoustic detection illustrated that the animal spent a considerable amount of time immediately to the south of Wiggins Island and also to the west of the northern tip of Wiggins Island (Figure 126).

Table 3.9 Comparison of 50 and 95% KUD area (km^2) calculated from satellite telemetry and acoustic telemetry (in parenthesis) for six individual green turtles tagged with both tag types that remained within the array for long periods of time. Turtles that remained within a small area are denoted by an asterisk.

Satellite tag ID	50 % KUD area (km^2)	95 % KUD area (km2)
126272*	0.62 (0.95)	3.40 (4.11)
126275*	0.19 (0.54)	2.14 (2.67)
126276*	2.64 (1.12)	10.29 (5.76)
131862*	0.46 (1.32)	4.28 (4.79)
131868	7.28 (4.50)	64.11 (25.20)
131872*	0.29 (0.56)	2.53 (3.62)
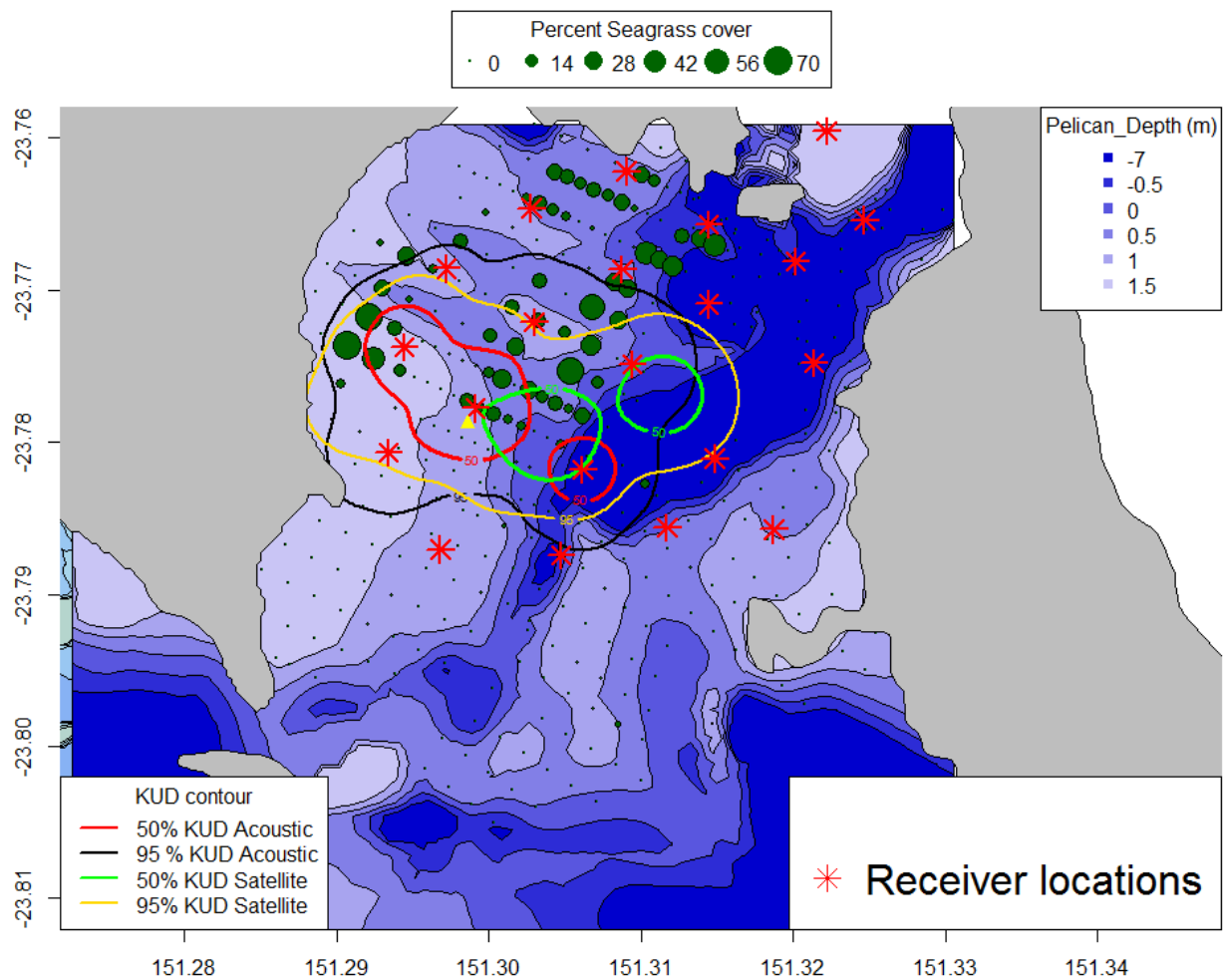
Figure 121 Plot of 50 and 95% KUD contours from satellite and acoustic tag data for turtle 126272 (mature female, 106.2 cm CCL, acoustic tag ID 27949). Capture location shown as yellow triangle.
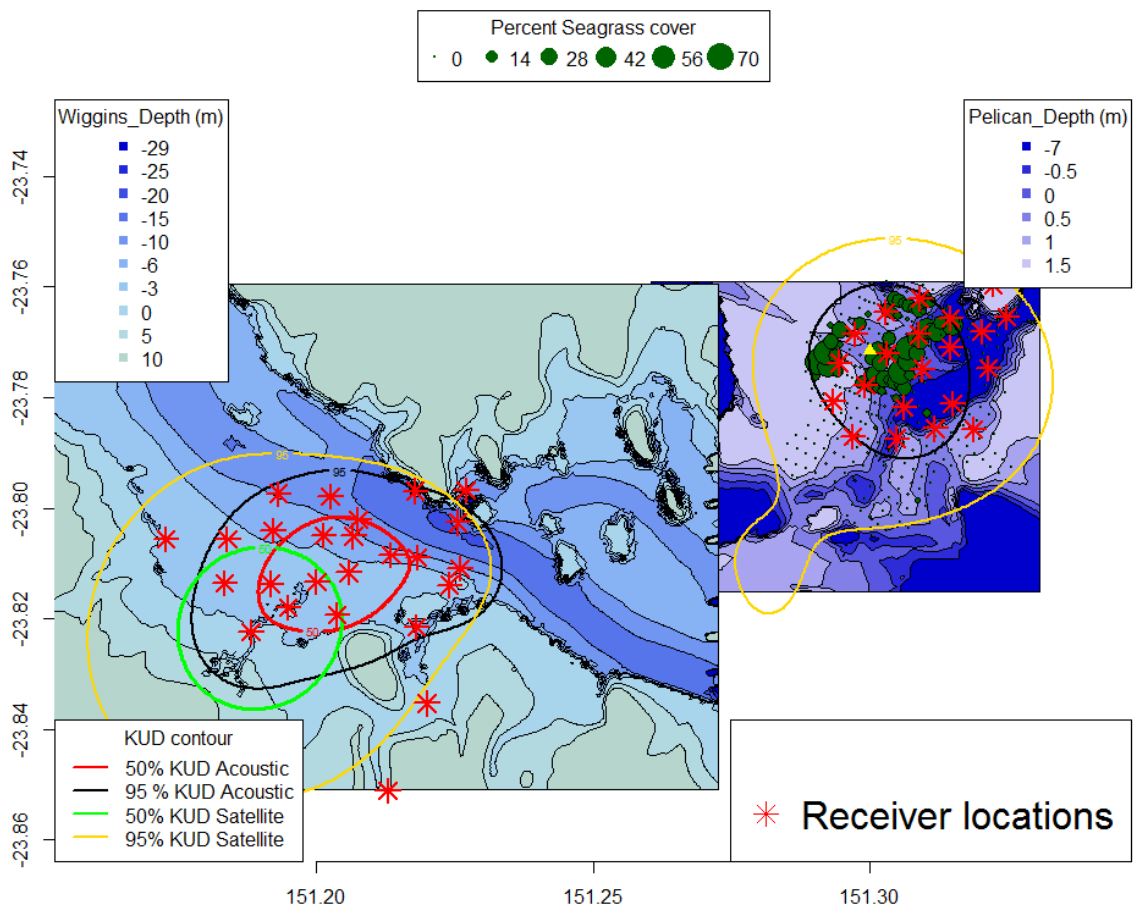
Figure 122 Plot of 50 and 95 % KUD contours from satellite and acoustic tag data for turtle 131868 (mature male, 97.7 cm CCL, acoustic tag ID 26568). Capture location shown as yellow triangle. This individual spent little time at Pelican therefore this area was not encompassed by the 50% KUD contour.
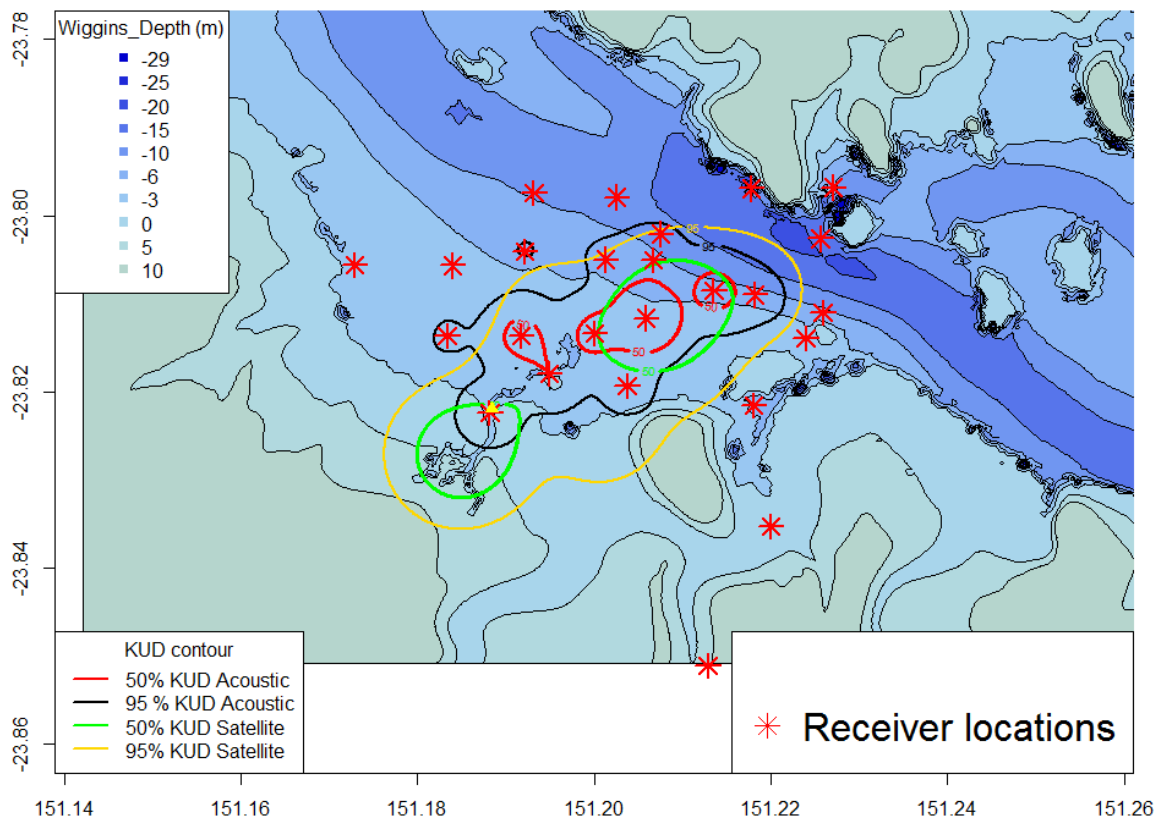
Figure 123 Plot of 50 and 95% KUD contours from satellite and acoustic tag data for turtle 126276 (juvenile male, 54.6 cm CCL, acoustic tag ID 27950). Capture location shown as yellow triangle.
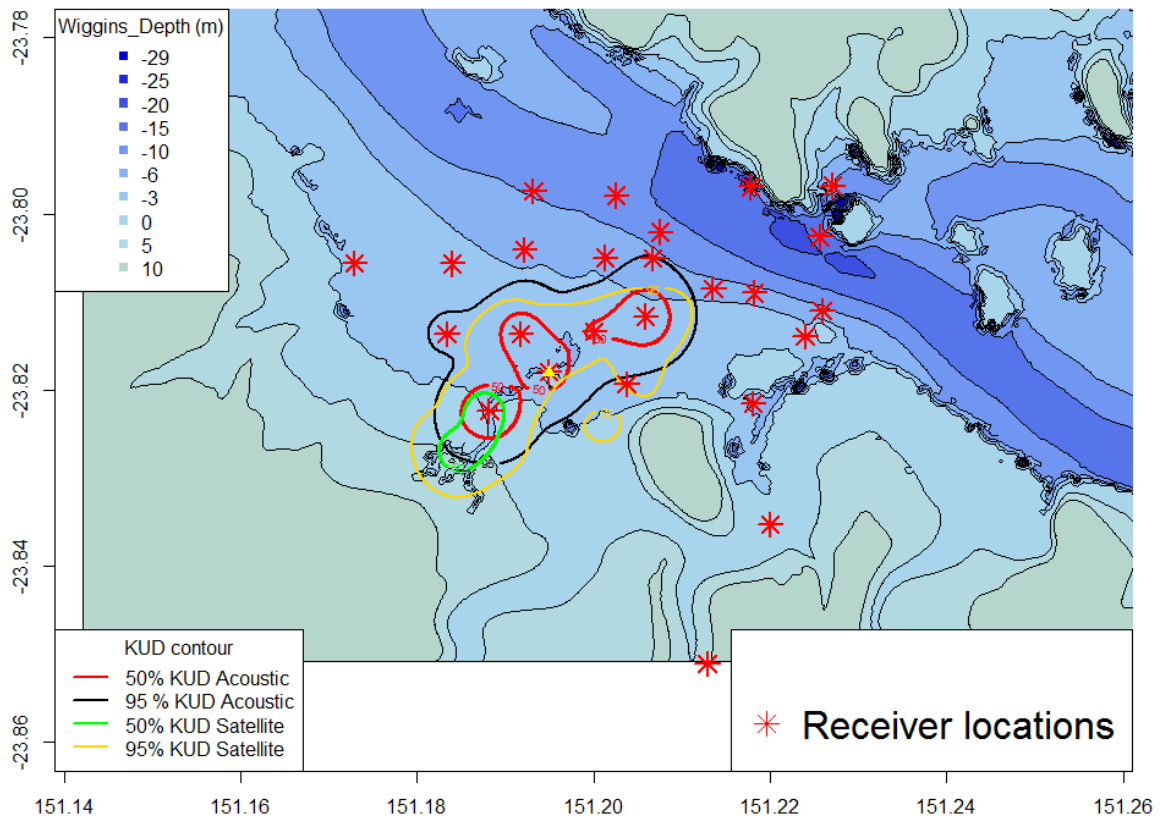
Figure 124 Plot of 50 and 95% KUD contours from satellite and acoustic tag data for turtle 131862 (juvenile (unknown sex), 52.1 cm CCL, acoustic tag ID 31598). Capture location shown as yellow triangle.
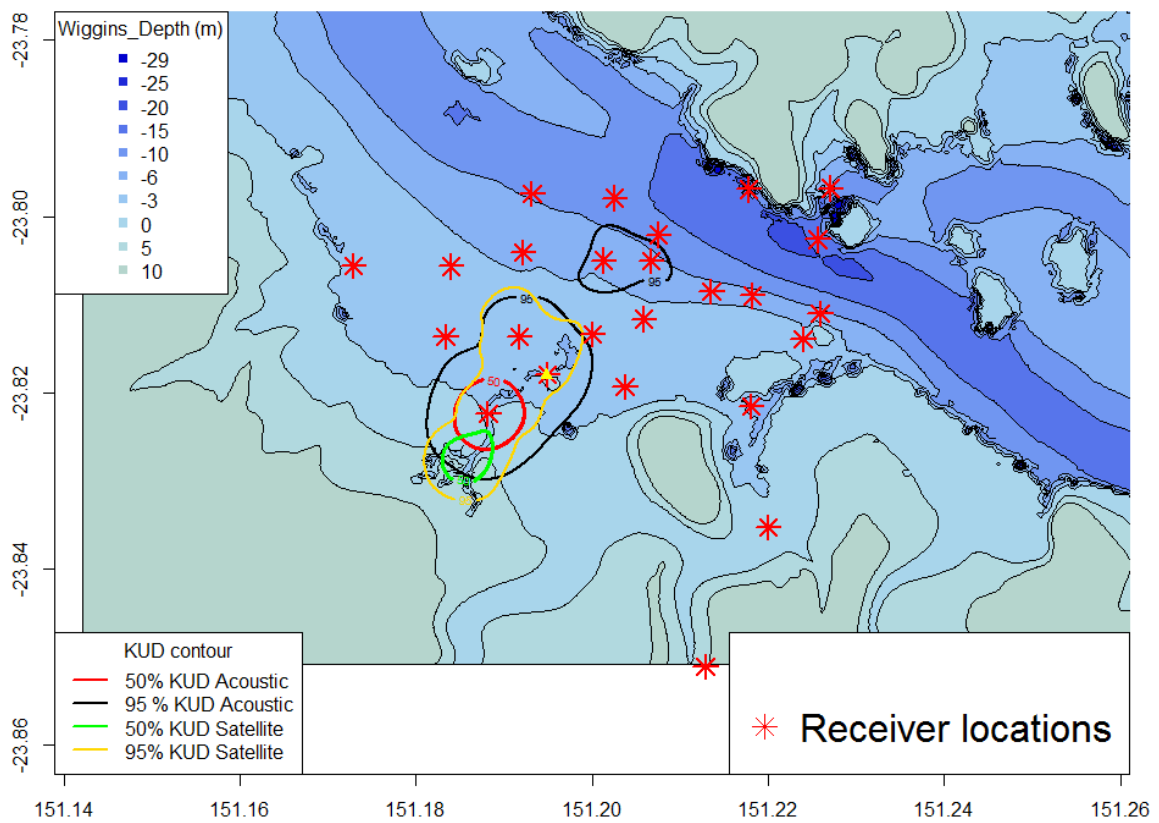
Figure 125 Plot of 50 and 95% KUD contours from satellite and acoustic tag data for turtle 131872 (juvenile (unknown sex), 52.7 cm CCL, acoustic tag ID 29771). Capture location shown as yellow triangle.
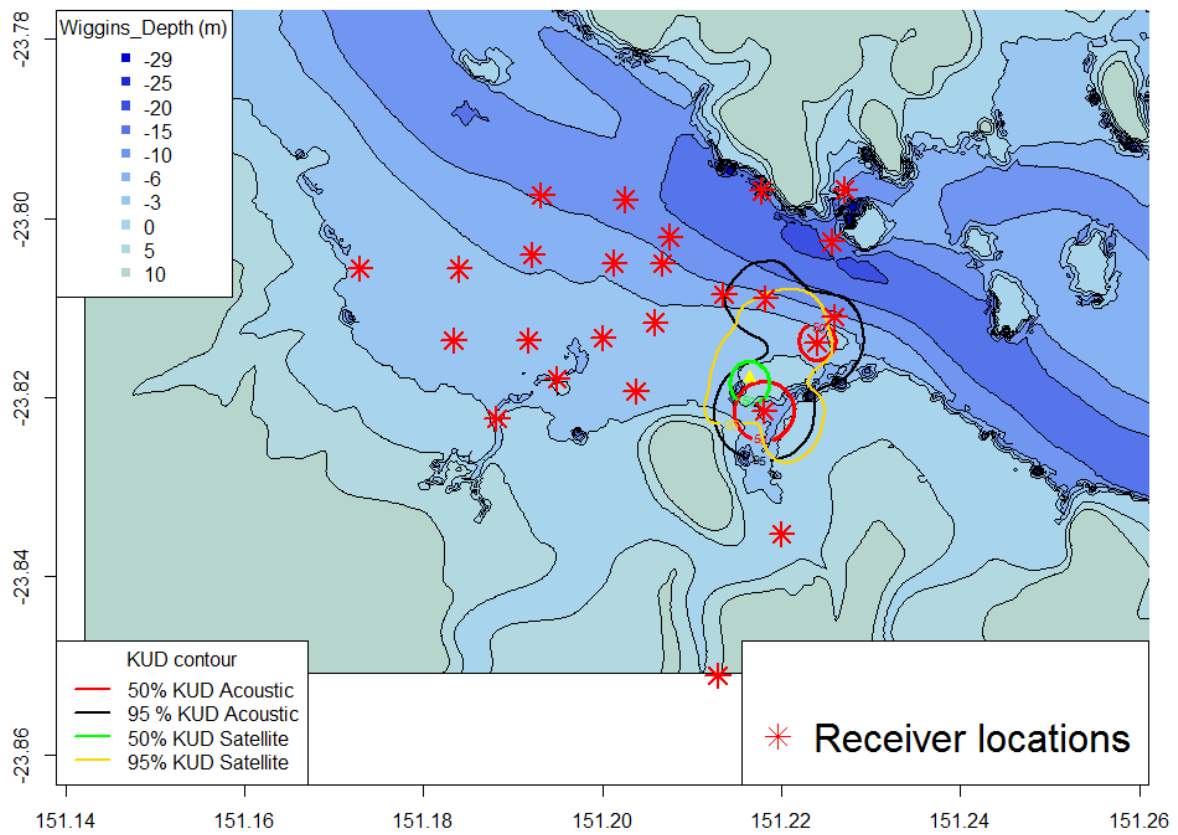
Figure 126 Plot of 50 and 95% KUD contours from satellite and acoustic tag data for turtle 126275 (juvenile male, 58.8 cm CCL, acoustic tag ID 27947). Capture location shown as yellow triangle.
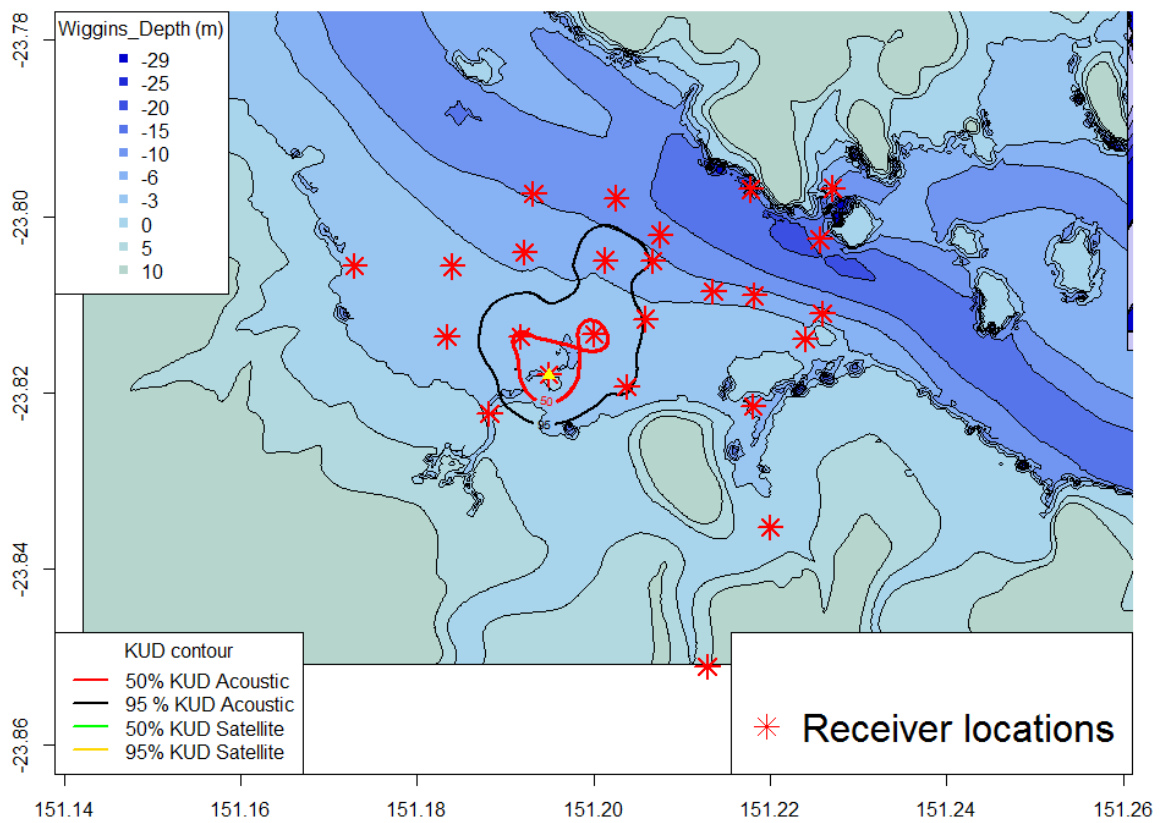
Figure 127 Plot of 50 and 95% KUD contours from satellite and acoustic tag data for turtle 131871 (juvenile (unknown sex), 60 cm CCL, acoustic tag ID 27629). Capture location shown as yellow triangle.

4 Discussion

4.1 Turtle Movement

The results of the current study have demonstrated that for juvenile and adult green turtles in Gladstone, average cumulative home range was 1.3 ± 0.2 km^2 and 6.7 ± 0.8 km^2 for 50 and 95% KUD's, respectively. These estimates of home range are within the range of other studies using a variety of methods from tag returns, visual observations, active boat based acoustic telemetry, satellite telemetry and passive acoustic telemetry to estimate home range. Mark recapture studies demonstrate long term fidelity of juvenile (Hirth et al. 1992) and adult green turtles (Limpus and Read 1985; Limpus et al. 1992) but do not provide data on the extent of habitat use and movement between recaptures. Limpus et al. (1992) also demonstrated adult females return to the same foraging area following extensive breeding migrations. Frequent resighting and acoustic telemetry of juvenile turtles demonstrated that juveniles remained within the same small area over a period of 10 weeks (Brand-Gardner et al. 1999). The majority of research has demonstrated that green turtles use a restricted areas with either 95% KUD and or Minimum Convex Polygon (MCP) estimates less than 10 km^2 and 50% KUD between 0.18–4.04 km^2 (Mendoca 1983; Brill et al. 1995; Renaud et al. 1994; Whiting and Miller 1998; Seminoff et al. 2002; Makowski et al. 2006; MacDonald et al. 2012).

Mendonca (1983) studied the home ranges of nine juvenile green turtles in Mosquito Lagoon, Florida, and found that the turtle's daily movements were confined to areas between 0.48 and 5.06 km^2 and centred around shallow estuarine flats that contained concentrated beds of seagrass (*Syringodium filiforme* and *Halodule wrightii*). Brill et al. (1995) found that the home ranges of 12 immature green turtles in Kaneohe Bay, Oahu (Hawaii, USA) were restricted to an average of 2.62 km^2 (± 0.96 km^2) and were confined to tightly spaced coral-covered patches where macroalgae growth was most abundant.

Short-term foraging ranges of ten adult green turtles in Repulse Bay, Australia, were between 0.84 and 8.50 km^2 with some animals moving up to 25 km between foraging areas (Whiting and Miller 1998). MacDonald et al. 2012 used acoustic telemetry to monitor movement of 25 juvenile and adult green turtles in San Diego Bay over a period of up to 370 days. Home range estimates (50% KUD) were between 0.49–4.04 km^2. Some of the smallest movements of juvenile green turtles have been recorded on structured habitats such as reef or jetties where food resources are limited to areas of hard substrate. Renaud et al. (1994) recorded daily movements for juvenile green turtles along a rock wall in South Padre Island, Texas, with nine home ranges between 0.22 and 3.11 km^2. Similarly Makowski et al. (2006) demonstrated a 50% KUD of between 0.18–1.17 km^2 in six juvenile green turtles along worm-rock reef in Florida.

The largest green turtle home ranges have been described by Seminoff et al. (2002) who reported home ranges of 12 green turtles in Bahia de los Angeles, Gulf of California, Mexico from 5.84 to 39.08 km^2. The large size of home ranges in these animals was attributed to the large distance between macroalgal food resources and benthic shelter. Although some of the turtles in the current study moved between Pelican Banks and Wiggins Island, these individuals generally had a small foraging area at each site and did not travel between areas on a daily basis as would be consistent with animals moving between a foraging and resting area.

The current study has demonstrated that turtles at Pelican Banks had a home ranges significantly larger than individuals at Wiggins Island. The majority of animals at Pelican Banks were adults compared to only juveniles at Wiggins Island which may suggest that adults may forage over larger distances than juveniles which is consistent with data of Whiting and Miller (1998) who demonstrated that this was the case for green turtles in Shoalwater Bay. However, MacDonald et al (2012) demonstrated that larger adults have a smaller home range than juveniles which was primarily attributed to adults having a better knowledge of habitat. Reasons for any differences between home range size of individuals from Pelican Banks and Wiggins Island are likely to be complex since, in addition to differences in the age of individuals at the two sites, food resources also differ. The diet of animals we tagged in November 2013 has been analysed using oesophageal lavage and stable isotope analysis (Prior 2014). Last bite analysis showed that animals at Pelican Banks fed primarily on seagrass (*Zostera muelleri* and *Halophila ovalis*) as opposed to red algae (*Catenella nipae, Chondria* sp., *Hypnea* sp., and *Bostrychia tenella)* at Wiggins Island (Prior, 2014). It is apparent that small scale differences in the size and shape of an individual's home range/foraging area are common and that these differences are likely to be the result of complex interactions between individual dietary preferences, spatio-temporal food availability, habitat complexity (shelter and distribution of food resources) as well as knowledge of habitat (experience) and presence of predators and threatening processes.

4.2   Tide related movements, channel use and shipping interactions

Tide related movement has been described previously with turtles observed moving into intertidal foraging areas as water depth allowed them to access these areas and then retreating to deeper water on the ebb tide (Limpus et al. 1994). At Pelican Banks, movement onto the intertidal flats at high tide was consistent across all animals tagged in this area. Both the cumulative 50% KUD figures as well as plots of habitat occupied against water depth, consistently demonstrated that animals were using intertidal areas during the high tide and retreating to the edge of the channel or the channel at low tide. This movement up onto the flats at high tide is presumably related to the availability of food resources, however the seagrass cover within low tide KUD's was not appreciably different to high tide KUD's suggesting that other types of preferred algae and/or seagrass have been more abundant in the intertidal areas only available at high tide. Analysis of the diet of green turtles at Shoalwater Bay (Limpus et al. 2005) demonstrated that as different habitats become available to the turtles through the tidal cycle, the major food types consumed may change. Analysis of the diet of green turtles at Pelican Banks showed that these animals fed primarily on *Zostera muelleri* and *Halophila ovalis*, with our data showing no appreciable difference in density of these species between the high and low tide cumulative KUD's.

At Wiggins Island, plots of habitat used against water depth demonstrated that animals were detected more often by receivers on the channel edge at low tide whereas at high tide animals were detected more often in the mangrove drain. Plots of KUD at high and low tide for animals at Wiggins Island were less informative in regards to fine scale tidal movement. This was presumably due to the reduced receiver coverage at the mangrove fringe where turtles are feeding at high tide. However, it was evident from the number of detections within the mangrove drain (GH7) and at the deep hole at the top of this drain (GH49) that animals were moving up the drain and then into the mangrove forest as the tide rose. The number of detections in the mangrove drain at low tide was 3425 and increased over the rising tide to 57,807 at high tide.

All the turtles tagged at Wiggins Island and Pelican Banks were sampled for diet by oesophageal lavage following capture (Prior, 2014). In turtles from Wiggins Island, the variety of algae species (*Catenella nipae, Chondria* sp., *Hypnea* sp*.,* and *Bostrychia tenella*) found in lavage samples support the observed tidal related movement with these species known to be associated with mangrove vegetation (Cribb 1996). Furthermore, the presence of pieces of mangrove bark and root in the diet of these turtles suggests that turtles were foraging on epiphytic algae on mangroves.

Despite the strong tidal signal in these data, there was individual variation with a few animals not showing a marked difference in home range size or distribution at high and low tide. This individual variation is presumably in response to changes in the availability of preferred food resources (seasonally and with water depth) resulting in subtle variation in the home range and tidal related movements of individuals.

Highest commercial shipping traffic occurred in the deep shipping channels to the north of Wiggins Island (see Chapter V of this report). Although there was some commercial traffic within the channel at Pelican Banks, this was limited to vessels of shallower draft. At Wiggins Island there was virtually no overlap between 50 and 95% KUD's of turtles (both satellite and acoustic telemetry) with high commercial shipping traffic (Chapter V). Similarly, depth data from satellite tags on turtles at Wiggins Island showed that animals were very rarely at depth greater than 10 m indicating that they did not use the shipping channel for feeding or resting. Similar results have been demonstrated for green turtles feeding on man-made structures (Renaud et al. 1994) and seagrass beds (MacDonald et al. 2012) with both these studies showing very little overlap with channels adjacent to either feeding grounds. Around Wiggins Island, there was no seagrass on the intertidal and subtidal flats or any other obvious source of food such as epiphytic algae outside of the mangrove forest, suggesting that absence of food may have caused animals to remain close to available food sources.

At Pelican Banks, there was a greater degree of overlap with the channel and channel edge which was most likely due to the presence of seagrass across a depth gradient. Despite the home range of animals at Pelican Banks encompassing the channel, very few animals crossed over to the eastern side of the channel nearer to Facing Island, which may partially be explained by the reduced density of seagrass in this area of Pelican Banks (Chapter II).

The use of intertidal areas by both turtles and small recreational craft during high tides holds reasonably high potential for interaction. The speed of recreational boats has been shown to put dugongs, turtles and other marine species at higher risk of collision or disturbance (Grant and Lewis 2010; Hazel et al. 2007; Hodgson and Marsh 2007; Maitland et al. 2006) and we frequently observed recreational vessels travelling in excess of 15 knots over the intertidal flats at Pelican Banks and to a lesser extent at Wiggins Island.

While diurnal changes in habitat use have not been examined in this report, this will form part of future work. Turtles at Pelican Banks showed a peak in the number of detections between 0400 and 1300 (Chapter V) which coincides roughly with the high tide (0.2-0.45 d since low tide). At Wiggins Island, the number of detections had two peaks, one at 0400-0800 between 0.1-0.3 days since the last low water, with another peak over the period 0000-1500 centred on 0.5 days since the previous low (this is the period approaching the next low water – on average). These data suggest turtles at Pelican Banks may have a stronger diurnal pattern than turtles at Wiggins Island or that turtles are more likely to be detected during daylight hours at Pelican Banks suggesting a diurnal shift in habitat use.

Hazel et al. (2009) demonstrated that green turtles utilised different areas by day and by night, and depth at night was greater than during the day. These short term data were consistent with intermittent observations (visual — Bjorndal 1980; and acoustic — Mendonca 1983; Renaud et al. 1994; Taquet et al. 2006) and from short-term records of diving behaviour (Seminoff et al. 2001; Makowski et al. 2006; Hazel et al. 2009) and support the theory that green turtles prefer to travel and forage by day and then rest much of the night. While we don't present day and night habitat use in the current report, the data collected from acoustic telemetry will enable us to do this and it will be conducted in the future to determine the extent of habitat differences at day and night.

4.3 Comparison between areas and climatic variability

For animals tagged in May 2013, juveniles of both sexes at Wiggins Island were more than twice as likely to remain in the same foraging area for more than six months as either juveniles or adults at Pelican Banks. The small and uneven sample size prevented a statistical comparison between those animals tagged in May and November by sex and age class. However, the higher proportion of animals leaving the foraging area at Pelican Banks up to six months after tagging in May 2013 may be due to the decline in food resources following record floods caused by ex-tropical cyclone Oswald which resulted in significant seagrass loss throughout Gladstone Harbour and surrounding areas (McCormack et al. 2013). Prior (2014) showed that animals at Pelican Banks were feeding primarily on seagrass, so this decline in food resources may have caused animals to move to areas that were not as impacted by the flooding. The lack of movement away from Wiggins Island may be related to the fact that animals in this area were feeding primarily on red algae as opposed to seagrass (Prior, 2014).

Data from satellite tags show that for at least three of the adult females that left the array following tagging in May 2013, these animals moved more than 100 km away from Gladstone Harbour and established new foraging areas either until the tag stopped transmitting or in the case of two animals for period of 1-2 months before moving south and establishing another restricted home range. Such long range movements away from a foraging area by animals that are not partaking in courtship or breeding activities are uncommon (Balazs 1980; Limpus et al. 1994; C Limpus pers. comm. March 2015). While it is common for animals to move tens of kilometres between foraging areas (Whiting and Miller 1998) and even between reefs (Gredzens et al 2014), the scale of movement demonstrated by three of the satellite tagged turtles at Pelican Banks is unprecedented for green turtles on the east coast of Queensland. Recapture data from Queensland turtle tagging program (tens of thousands of individuals) as well satellite tracks from more than 60 green turtles tagged along the Queensland coast, have only demonstrated one similar case of large scale movement where a resident adult female turtle, tagged in Moreton Bay, moved to Mon Repos (~320 km by water) and then between Mon Repos and Platypus Bay (~70 km by water) (C Limpus pers. comm.). Gredzens et al (2014) reported the movement of a "transient" adult female turtle in Torres Strait, however, this individual moved at a much smaller linear scale (approximately 40 km between reefs) than the turtles in the current study.

The movement of immature and subadult turtles between distant foraging areas is consistent with the "developmental migration" hypothesis (Carr 1980) that turtles utilise a series of foraging areas throughout their life. However, shifts in foraging area among immature and sub-adult turtles along the Queensland coast are also very uncommon with only four such movements reported in the literature from tens of thousands of animals tagged along the Queensland coast (Limpus et al. 1994, Limpus et al. 2005).

4.4   Long term monitoring of turtle habitat use in Gladstone Harbour.

The size and shape of home range estimates were very similar for turtles tagged with both satellite and acoustic tags that remained in the array and were detected by both telemetry methods. Estimates of home range from satellite and acoustic telemetry were also within the range of Australian studies (Whiting and Miller 1998; Gredzens et al. 2014). For animals that departed the foraging areas during the life span of the satellite tag (60% at Pelican Banks and none at Wiggins Island), the data from satellite tags provided the only information on habitat use and the scale of movement following departure. However for the remaining animals, data from acoustic tags provided significantly more daily detections as well as a much longer detection span. The longest time a satellite tag provided data for was 13 months whereas acoustic tags provided data for more than 17 months (the entire monitoring period).

The ability to obtain hundreds of detections per day enabled determination of high and low tide KUDs over long periods of time. On average, less than 10 satellite detections were recorded per day reducing the ability for fine scale analyses of habitat use over short and long time periods. Overall, the difference in home range estimates from satellite and acoustic tags were similar (at least for animals that remained within the arrays of receivers) with the main benefit of acoustic tags being their reduced cost and longer retention times. Being able to apply more tags, for a longer time period and on a greater proportion of the population, is the main advantage of acoustic tags as it enables long term data not only on movement but also population level residency. The benefits of these attributes can be illustrated with reference to the anomalously high rate of long distance movement observed in animals tagged at Gladstone in 2013, after major flooding. Unbiased estimates of movement parameters could have been obtained from animals tagged before the flooding and followed through subsequent years, allowing a clearer interpretation of cause and effect.

The detection span and proportion of animals remaining within the array provide data on the proportion of animals moving away from foraging areas. This information has also identified differences in the home range persistence in juveniles feeding on algae in the western part of Port Curtis and adults feeding on seagrass around Pelican Banks. Animals at Wiggins Island were 2–4 times more likely to remain within the Wiggins Island array than animals at Pelican Banks with the data also demonstrating that females were 2–4 times more likely to remain in an area than males. These subtle differences have important implications for the conservation of green turtles and can help identify which areas are more or less influenced by changes in food resources either due to natural or anthropogenic causes.

Of those foraging areas where data are available for the southern GBR stock, Moreton Bay has the highest female breeding rate (Limpus et al. 2013) and also the highest growth rates (Chaloupka et al. 2004), while western Shoalwater Bay which has the lowest female breeding rate also was recorded with the lowest growth rates. These data are indicative of a significant role of habitat condition, possibly forage abundance or quality in growth rate and annual breeding rate. Data on the size and stability of home range from foraging areas would help determine whether animals forage over greater distances or undertake more frequent shifts in home range. Similarly, long term acoustic telemetry (10 year tag life) will shed light on the bimodal size frequency distribution observed in some populations (e.g. Limpus et al. 2005; Hamabata et al. 2014), a pattern which suggests that large juveniles (50-70 cm CCL) occupy a different habitat to small juveniles and adults. Indeed it has been suggested that that the green turtle foraging aggregations along the coasts of the western Japanese main islands are not maintained by long-term residents, but by periodic and continually dynamic populations resulting from ontogenetic habitat shifts (Hamabata et al. 2014).

The trade-off between cost and benefit of satellite and acoustic telemetry for dugongs has been determined by Zeh et al (2014). Given that acoustic tags are less than a tenth of the cost of satellite tags and acoustic receivers are a fifth of the cost of satellite tags, satellite telemetry costs are largely related to equipment or capital-type expenses while acoustic telemetry costs are dominated by the installation and maintenance of the array. In instances where arrays have already been installed and research is active and ongoing (such as Gladstone Harbour) research that aims to determine long term movement and habitat use would therefore benefit more from tagging many animals with acoustic tags as opposed to a few animals with satellite tags. Similar conclusions were reached by Zeh et al (2014) who stated that acoustic transmitters should become the preferred methods of tracking dugong habitat use in the vicinity of ports because they enable more animals to be tracked for longer and with fewer animal welfare problems than those caused by GPS transmitters. The longevity of acoustic tag attachment on green turtles (and all other species) would be significantly enhanced with internal attachment either within the peritoneal cavity as in done in fish and sharks or alternatively, under the skin.

4.5 Summary

Juvenile (n = 21), sub-adult (n = 7) and adult (n = 21) green turtles were tagged with acoustic tags within two arrays of acoustic receivers in Gladstone Harbour. At Pelican Banks, 33 animals (5 juveniles, 7 sub-adults and 21 adults) were tagged while at Wiggins Island 16 juveniles were tagged. Between May 2013 and September 2014, over 1.4 million detections of tagged turtles were recorded by 44 acoustic receivers within Gladstone Harbour.

Individual turtles were detected up to 240 000 times with the median number of detections greater than 17 000. Turtles tagged in May and November 2013 were monitored until September 2014 when receivers were last downloaded. Maximum potential detection span for animals tagged in May and November 2013 was 502 and 313 days, respectively. The average detection span for all turtles was 273 (± 19) days with turtles at Wiggins Island having a greater detection span (337 ± 34 days) than turtles at Pelican Bank (242 ± 31 days). The average number of days turtles were detected was 218 (± 20) with turtles at Wiggins Island being detected on more days (295 ± 34 days) than turtles at Pelican Bank (181 ± 25 days).

Home range estimates (50 and 95% KUD (Kernel utilisation distribution)) were calculated for those individuals that were detected for more than 30 days on two or more receivers (n = 42). Green turtles at Gladstone had small home ranges which persisted for months. The average 50 and 95% KUD of animals at Pelican Banks was 1.4 ± 0.2 km2 and 6.7 ± 0.9 km2, respectively which was significantly greater than animals at Wiggins Island (0.7 ± 0.1 km2 and 3.8 ± 0.4 km2, t-test, p <0.01), however, like many animals for which long term data are now becoming available, a large proportion move away from previously established home range and set up a home range tens to hundreds of kilometres away. In Gladstone, after 1 year of monitoring nearly 20% of turtles at Wiggins Island and 53% of turtles at Pelican Banks had moved outside the array of receivers within Gladstone Harbour.

Satellite tagging showed that animals at Pelican Banks moved up to 150 km north and 230 km south of where they were tagged. None of the satellite tagged animals at Wiggins Island moved away from where they were tagged and the proportion that moved outside of the array was much less, suggesting that juveniles are more likely to establish smaller home ranges for longer periods. However, food sources presumably play a role in home range size and site fidelity with animals at

Wiggins Island feeding predominantly on epiphytic red algae growing on intertidal mangroves. Animals at Pelican Banks were feeding predominantly on seagrass with the home range of most animals overlapping areas of highest seagrass density.

At both Wiggins Island and Pelican Banks there was a high degree of overlap of habitat used by individuals with a strong signal of tide related movements. Animals at both areas moved into shallow water with high seagrass cover at high tide and retreated to subtidal flats and the edges of the channel at low tide. At Wiggins Island, the majority of animals moved up into the mangroves at high tide, frequently utilising a mangrove drain.

For animals at Wiggins Island where commercial shipping traffic was greatest, there was very little overlap between home range and areas of highest shipping traffic. At Wiggins Island, less than 1% of all acoustic tag detections occurred on the northern side of the shipping channel between Wiggins Island and Curtis Island. Furthermore, there were also no detections of satellite tagged turtles in the channel or on the northern side of it. Shipping traffic was primarily confined to the shipping channel and water depths greater than 10 m, whereas turtles were very rarely detected on receivers in the channel and depth data from four animals with satellite tags showed that turtles spent the majority of time less than 3 m below the surface with very occasional dives to 7 m.

At Pelican Banks where commercial shipping traffic was low, there was a greater degree of overlap between home range and channel habitat, however the majority of turtles spent very little time in the channel and this was primarily restricted to low tide. Given that most commercial vessels using the Pelican Banks channel travel at less than 10 knots, the risk of boat strike is lower than that from recreational vessels which frequently travel through this area at high speed.

At both Wiggins Island and Pelican Banks, recreational and commercial fishers regularly travel across the intertidal and subtidal flats, however there are no estimates of overall vessel density to enable us to evaluate the risk of boat strike. Despite the fact that so few of the turtles at Wiggins Island were recorded in the channel or across it, we only monitored the movement of a small proportion of the turtle population in Gladstone due to difficulties in capturing animals along the western shore of Curtis Island. Data on the movement patterns and habitat use of animals from the area directly impacted by heavy traffic are therefore required.

Home range estimates from satellite and acoustic tags were very similar for animals that remained within the receiver array, with acoustic tags providing significantly more fine scale data on habitat use than satellite tags. It was clear from both data sets that satellite detections underestimated home range due to fewer detections. However, for some animals that moved far up the mangrove drain at Wiggins Island, where there was no receiver, receiver data failed to show the full extent of movement. In the majority of instances, home range estimates from acoustic data provide better resolution of spatial distribution within the home range. Furthermore, data from acoustic tags enabled tidal patterns in movement to be evaluated due to several hundred detections from individuals each day, as opposed to satellite tags where only 1-15 detections per day were obtained.

Chapter V Spatial modelling of green turtle habitat use with reference to shipping frequency

Toby Patterson, Natalie Kelly, Richard Pillans, Scott Cooper, Russ Babcock

1 Introduction

Boat strike has been listed as one of the major sources of human induced mortality on marine turtles ("Key Threatening Process Nomination Form - Fatal injury to marine mammals, reptiles, and other large marine species through boat strike on the Australian coast - nomination-boat-strike-2012.pdf" n.d., Preen 2000) and other marine mega fauna (Maitland et al. 2006, Williams and O'Hara 2010, Conn and Silber 2013, Redfern et al. 2013). Several studies have attempted to use models to predict the distribution of marine animals for the purpose of assessing risks posed by boat strike (Maitland et al. 2006, Bauduin et al. 2013, Conn and Silber 2013). In many cases, telemetry data is the only available information on the distribution of animals in a region. Despite common problems of relatively low sample sizes, non-uniform distribution of tagging and capture effort and often short term data, several studies have employed telemetry data to produce resource selection functions from which distributions can be inferred (e.g. Godley et al. 2002, Olivier and Wotherspoon 2005, Raymond et al. 2014). Determining optimal methods for constructing resource selection functions ("habitat use") is a subject of ongoing research and debate in ecology (Boyce 2006, Meyer and Thuiller 2006).

Our goal in this study is to analyse the acoustic telemetry data collected in two receiver arrays in Port Curtis in order to build predictive habitat preference models for turtles in Port Curtis. A subset of animals was also tagged with satellite tags. We characterise the habitat of turtles using several environmental covariates and construct statistical models which predict the relative preference of turtles for these habitats. We then examine how these are distributed throughout various regions within Port Curtis. If the model predictions are reliable, this exercise may be useful in determining likely areas of relatively high turtle usage. This relies on being able to predict turtle habitat outside of those areas which were not directly sampled (either with the satellite telemetry data or the acoustic receiver networks).

We also consider available data on movements of commercial vessels within the harbour. Determining regions of relatively high risk to turtles provides useful background information for implementing various management measures such as 'go-slow' zones, which are commonly considered in order to reduce the risk of ship-strike mortality on turtles. Our underlying assumption is that areas with high numbers of boats, travelling at higher speeds should be more risky for any turtles that use these areas (Hazel et al. 2007). We therefore want to characterise regions which are associated with two factors: (1) high usage (i.e. areas containing a large number of vessel positions), and (2) high speeds. Finally, we consider the habitat predictions along with the analysis of shipping data and examine whether the analysis presented here is likely to be informative regarding vessel strike risk.

The overarching assumption in this study is that the number of detections at a receiver is related to the turtles' preference for the set of habitat conditions associated with that receiver. While the reception characteristics of the receivers vary, this assumption is probably reasonable, given sufficient data. The acoustic receivers recorded a large number of individual detections (Chapter IV). Dealing with this large number of individual detections becomes unwieldy in a statistical model, especially if we consider time-varying predictors of turtle habitat. Undoubtedly, complex spatio-temporal processes and interactions between the dynamics of turtle populations, environment and exogenous variables will influence the spatial dynamics and apparent habitat preference of individual

turtles (Chapter IV). However, considerable simplification is required for tractable spatial prediction of habitats from the data collected in this study. Below we detail how raw-detection data was summarized for modelling and the extraction of spatial covariates to be used as predictors.

Moreover, for logistical reasons the coverage of receivers was not evenly spread, either spatially or with respect to habitat. Thus, the habitat conditions observed by the array do not stratify or even bound the range of conditions which might be expected in the harbour. In this sense we have a problem of extrapolating beyond the range of the data, and the observations are such that we have only N=47 (the number of receivers) independent observations of habitat. Some variables which are likely to be important drivers of green turtle habitat usage, such as seagrass distribution were known relatively patchily or from only certain areas (Chapter II; Davies et al. 2012). However, a key goal of this exercise is to attempt to predict distribution of turtles throughout the harbour. Chiefly this is in order to make an initial assessment of the overlap of likely turtle habitat and available data on shipping intensity. Therefore, we restricted the models to physical proxies of habitat (bathymetry, slope, site, etc.) which were available in all locations. Further studies should endeavour to include factors of more direct biological relevance. Partly as a response to this uncertainty and lack of uniform data coverage and in an attempt to examine potential variability due to the differences in habitat between the Wiggins Island and Pelican Banks arrays, we also investigated separate models for the Pelican Banks and Wiggins Island areas. As the models were fitted to spatial variables which are measured throughout the harbour, spatial prediction of favourable habitat throughout is technically possible, but with caveats.

In the following we first describe the predictor variables used for model building. We then describe how the acoustic detection data were treated for input into statistical models. Next, the models themselves are described. This focuses on models for predicting distribution within arrays, which examine individual variability between turtles, and constrained models which are used to make extrapolations of habitat over wider regions. We describe the available Australian Marine Safety Agency (AMSA) vessel tracking data for the region and examine trends in shipping intensity and distributions of vessel speed. Finally, we comment on how the current modelling might be expanded, both with further data collection and improved models.

2 Methods

2.1 Covariate extraction

We extracted the following variables as descriptors of habitat for each receiver location, and examined pairwise scatter plots and correlation coefficients to assess co-linearity between covariates. Covariates were estimated based on data extracted from the Gladstone seagrass growth model (Chapter III), and from data provided by MSQ.

2.1.1 DISTANCE TO HIGH WATER MARK.

The distance (km) from the receiver location to the high water mark was calculated by taking the minimum straight line distance from each grid point in the harbour to the nearest coastline point (Figure 128).
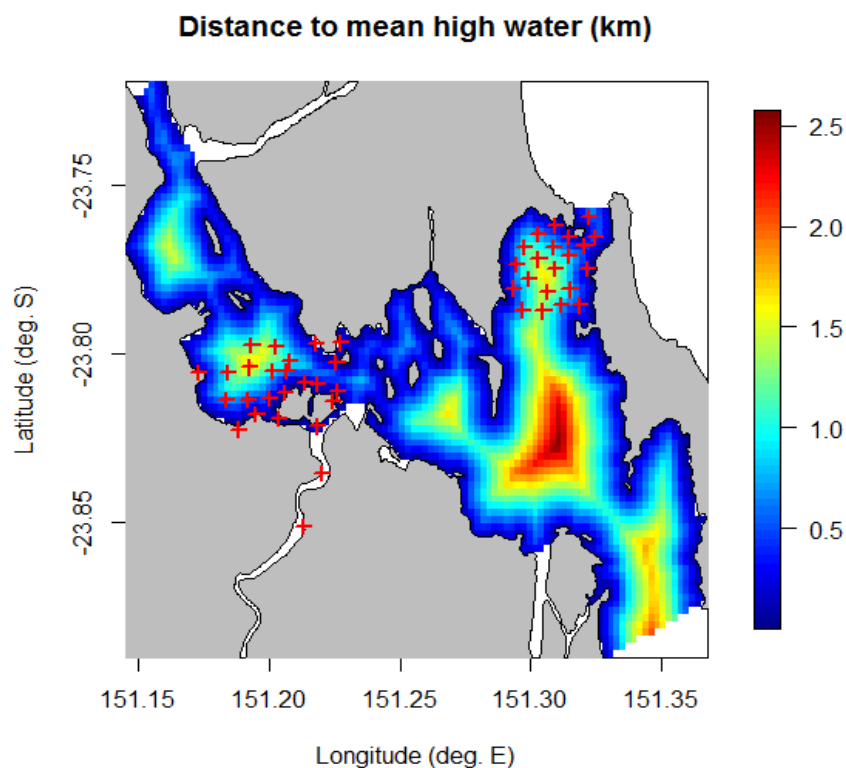
Figure 128 Distance to high water. Positions of receivers are given in the red crosses.

2.1.2 THE DEPTH AT LOW-WATER OF THE RECEIVER (M)

Receiver depth at low tide was obtained by rasterizing collections of point soundings collected by Marine Safety Queensland (https://www.operations.amsa.gov.au/Spatial/) to obtain a continuous estimate of bathymetry for the Port (Figure 129). Depth may be a useful descriptor of habitat as it (a) determines whether an area is accessible to turtles (i.e. if an area remains inundated at lower water, it is accessible at all times) and (b) may also usefully correlate with particular habitat types and forage availability.
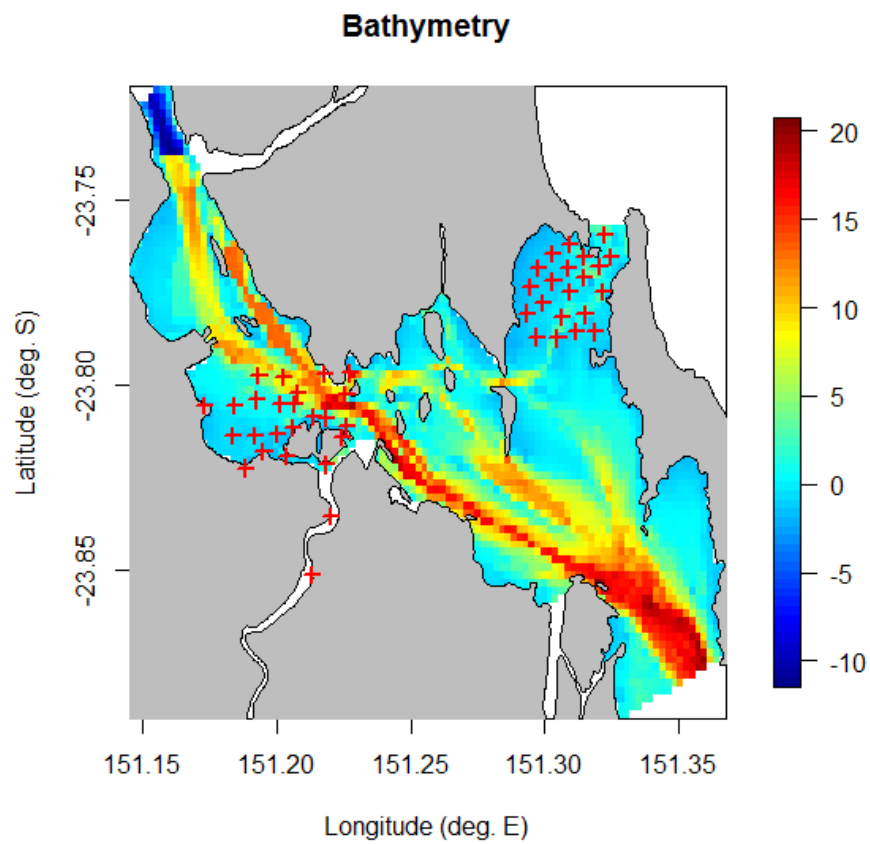
Figure 129 Bathymetry data for Port Curtis used in habitat models
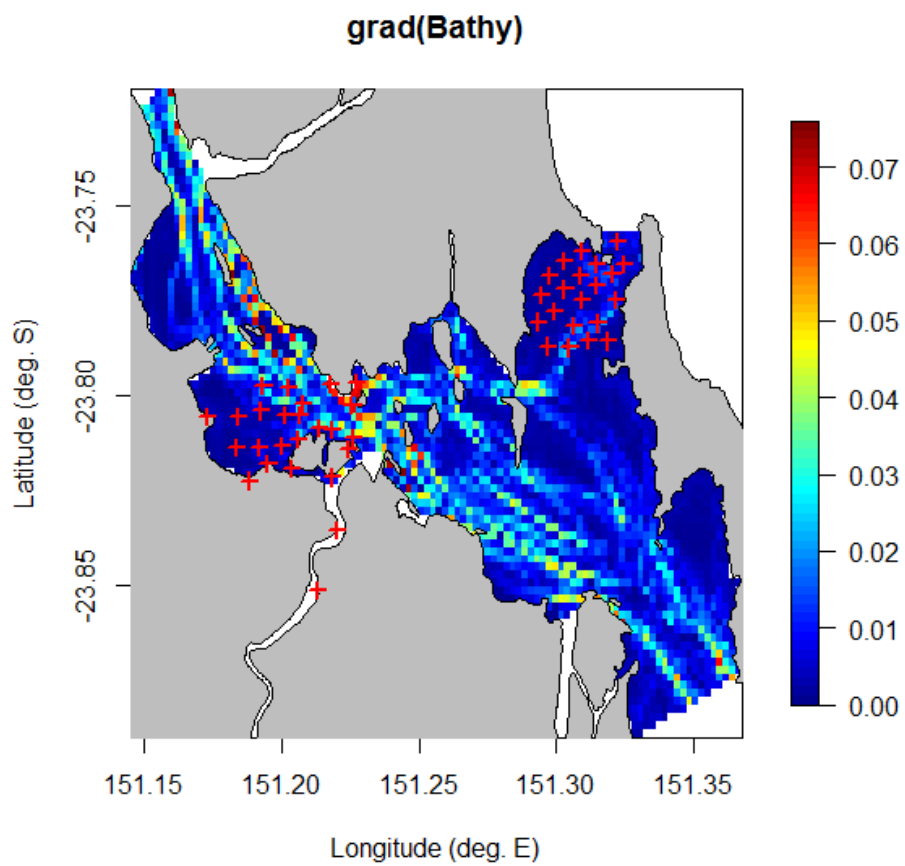
Figure 130 Gradient (radians) of the bathymetry plotted in Figure 129.

2.1.3 GRADIENT OF THE BATHYMETRY.

The gradient of the bathymetry was calculated from the surface shown in two dimensional numerical differencing (Figure 130). The variable was included to consider whether turtles prefer a flatter or more graded substrate within a given depth range.

2.1.4 TIME SINCE LOW WATER.

Times of high and low water were obtained from the tide predictions for Gladstone Harbour (Bureau of Meteorology). These data indicated that the time difference between successive high and low water marks in Port Curtis was on average 0.52 d; min=0.47, max=0.576. We made the simplifying assumption that tidal signals could be represented as the fraction of the day elapsed after the most recent low water period. While this assumption does not account for shifts in the tidal cycle, we expect that the covariate as calculated nevertheless adequately captures the effect of tide on turtle habitat preference.

2.2 Summarizing detections and response data for preference models

2.2.1 PING RATE CORRECTION

Because the ping rates of the acoustic tags varied between individuals, the data needed to be scaled so that all turtle detection data were alike. The scaling was relative to the most frequent ping rates. The Vemco tags employ a randomization scheme in order to reduce the likelihood of collisions between multiple tags in the same vicinity. Under this scheme, the tags have a minimum time interval (τ_{min} s) between pings and randomly emit an acoustic signal between $0 - \tau_{max}$ seconds. If we denote the time of the ping as t_{ping} (i.e. $\tau_{min} \leq \tau_{ping} \leq \tau_{max}$) and assume that $t_{ping} \sim$ Unif(τ_{min}, τ_{max}) then the expected value ping rate is $\mathbb{E}(t_{ping_i}) = \frac{\tau_i + \tau_{min}}{2}$. We assumed that this expected value could be used to scale the observed number of detections at each station. This was necessary as a key assumption of the habitat preference model is that the turtle's preference for a given set of covariates is proportional to the number of detections recorded by a receiver. If N_{ijt} is the number of detections of the i-*th* turtle at the j-*th* receiver over time interval t, then in the modelling described below we calculate an adjusted number of detections:

$$N_{ijt}^* = N_{ijt} + \left(N_{ijt} \times \frac{\mathbb{E}(\tau_{min})}{\mathbb{E}(\tau_{ping_i})} \right)$$

2.2.2 COMPILATION AND SUMMARIZING MODEL DATA

The tag data comprised 773,128 individual detections. In the model detailed below there is a need to compute for all individuals whether they were detected or not at any of the possible receivers, for all possible time periods under consideration. Data summaries to be used as input into spatial habitat

models were compiled as follows. All calculations were carried out in relational databases, hence the use of terms such as 'table' to refer to data sets.

1 – First an 'empty set' was created as a table with all possible combinations of receiver, tag and date and time in 1 hour interval. Given the number of 1 hour time intervals over the range of the tagging experiment, and the number of tags and receivers this created a table of 28 million rows.

2 - A second table was created whereby the detections were grouped into 1 hour bins by tag and receiver, and a detection count was calculated.

3 - These two tables were joined using an outer join so that all the records were kept from our 'empty set' with zero detections, and the detection count with the matches from the second table was updated.

4 - A further update was required to find the time since the last low tide for each one hour time period. So, the time elapsed since the previous low tide was calculated for the midpoint of each period of a given day of the year.

5 As a necessary simplification step which avoided the need to model millions of individual records, the absolute time intervals were discarded and the number of detections for each hour in the day calculated, as a truncated value of time-since-low-tide. These were truncated into intervals of [0-0.09], [0.1-0.19]…. [0.9-1]. This created a data set of around 3×10^4 rows which was used as the final input to the models. Since the other covariates (listed above) are not time varying, these could be extracted for each row in this final detection + time-since-low-tide table.

2.3 Habitat preference modelling

For the purposes of extrapolating across the broader Gladstone Harbour region, an 'explanatory' approach was used to model acoustic detections/habitat preference (Mac Nally 2000, Shmueli 2010) . In this approach to statistical modelling, care is taken to select covariates that are likely to meaningfully influence the underlying process of interest. In such instances, it is also best to ensure that the shapes of modelled relationships are biologically or ecologically reasonable (for example, distributions of species are not likely to be multimodal with relation to a given environmental covariate). This is to be contrasted with the situation when a model is developed for prediction, and all available (reasonable) covariates are considered for their predictive power and the model is largely unconstrained to fit the data as closely as possible.

Models of turtle habitat preference were implemented using Generalized Additive Models (GAMs) and Generalized Additive Mixed-Models (GAMMs, see Wood 2006). These are linear-in-the-predictor models which employ non-parametric smooth functions to model non-linear relationships between observations and covariates. In this study our response variables are the number of observations in a 1 hour time bin over a 24 hour cycle.

All models considered here take the general form

$$\log \mathbb{E}(N_{ljt}^*) \sim f_1(x_1, x_2, ..) + f_2(x_3, ..) + \cdots + \epsilon$$

where $f_1(.), f_2(.), \ldots$ are smoothing functions of predictor variables $x_1, x_2, \ldots$ and ϵ is a residual error term. Commonly count data like this are modelled using a Poisson distribution (Wood 2006). But in this case our response variable $N^*_{j,t}$ containing many zeros and the $\mathbb{E}(N^*_{j,t}) \neq \mathbb{V}(N^*_{j,t})$, as is assumed by a Poisson error distribution. Accordingly, we assumed that errors could be modelled with a Tweedie distribution which generalized across the spectrum between Poisson distributions and Gamma distribution and has been used successfully in a variety of settings (e.g. Candy 2004, Woehler et al. 2014).

The predictor variables listed above are abbreviated as follows:

- `land.dis` - distance of a point to the nearest mean-high-water point
- `bat` - depth of the water (m)
- `slop` - gradient of bathymetric data (radians)
- `timel` - time-since-low-water (fraction of a 24 hour period).

Modelling proceeded by first considering a model which sought to capture the broader habitat preference over the entire harbour - i.e. in regions well outside sites of data collection. To do this we used semi-constrained additive models (SCAMs) (SCAMs, Pya and Wood 2014). These are a recent addition to the suite of additive models that allow constraints on the shape of smooth terms in a model to be employed. The constraints take the form of enforcing that smooths are convex or monotonically increasing or decreasing. The reason why constraints are useful in this context is that from previous analysis, expert opinion and other data sources (e.g. satellite tracking positions) indicate particular relationships with habitat variables. Additionally, we expect that unconstrained models are likely to overfit to some degree. In other words they are likely to be overly complex in order to model the variability within the data in the array. For the task of making extrapolatory predictions in areas outside the regions where data are collected, a simpler model is likely to behave better.

For the harbour wide model to be used for extrapolation into unobserved regions, we aggregated the counts of detections by summing over receivers. The response variable was therefore $N^*_{j,t} = \sum_i N^*_{ijt}$ In the notation used to specify GAMS in the R library `mgcv` (Wood 2006) the constrained model used for harbour wide prediction was

$$\log \mathbb{E}(N^*_{j,t}) \sim f_1(\texttt{timelo}, k = 5) + f_2(\texttt{land.dist}) + f_3(\texttt{bath})$$

with the errors specified as $\texttt{Tweedie}(p = 1.8)$. In this case we considered several constraints:

- that `timelo` was a smooth function, but with a small number of knots k (set to k=5)
- that habitat preference is related to `bath` in a convex relationship (a single maxima, or peak, is allowed in $f_1(.)$)
- that habitat preference is related to `bath` in a convex relationship (a single maxima, or peak, is allowed in $f_2(.)$).

In general terms, the point of the constrained models is that for the purpose of extrapolating with which to capture the broad scale features of the data without being driven by signals specific to any given location or the behaviour of particular individual turtles.

2.3.1 INVESTIGATING SITE DIFFERENCES AND INDIVIDUAL LEVEL VARIABILITY.

In order to examine the potentially different turtle habitat usage at Pelican Banks and Wiggins Island, we considered two further Generalized additive Mixed Models (GAMMs). In these we used bivariate tensor-spline smooths between `TIMELO` and `land.dist` in order to include any potential interaction between these two variables, and a single smooth term for `bath`,

$$\log \mathbb{E}(N^*_{ijt}) \sim f_1(\text{TIMELO,land.dist}) + f_2(\text{bath}) + b_i$$

where the turtle-wise random effect $b_i \sim N(0, \sigma_b^2)$ and with the residual error distribution specified as $\text{Tweedie}(p = 2)$ (with generalises to a Gamma distribution). Here f_1 and f_2 were non-parametric tensor-splines smooths. In these models a large number of knots ($k = 20$) was used so as to allow a high degree of flexibility in fitting the observations. Of interest in these models are the individual turtle-level random effects, b_i, whose size gives some notion of the degree of variability between turtles.

2.4 Vessel movement data

The Australian Marine Safety Authority (AMSA) collects vessel presence and movement data from a variety of sources, including terrestrial and satellite shipborne Automatic Identification System (AIS) systems. This vessel traffic data is stored in a database called the Craft Tracking System (https://www.operations.amsa.gov.au/Spatial/). A summarized version of this data is available to download from the AMSA data portal (https://www.operations.amsa.gov.au/Spatial/).

The vessel traffic data is collected by AMSA at a 5-60 second frequency, but the data available from the data portal has been down-sampled to the closest hour (or slightly more), i.e., the raw data are not averaged over that hour, but just include whichever data points are closest, and/or greater than, than one hour apart. Future work should explore the possibility of gaining access to the entire relevant AMSA dataset (which is a number of terabytes), however this was not feasible at this time.

The vessel traffic data are downloaded as unprojected point shapefiles. Each location of a vessel is tagged with a time stamp (in UTC), and an indication of vessel speed and dimensions (and other associated data). For the publicly accessible data, all vessel identification has been removed, but an anonymous unique identifier has been supplied for each vessel. We found numerous instances in both vessel dimension and speed data, particularly which were likely to be erroneous as vessels were listed as travelling at implausibly fast speeds. These have not been further analysed here, but were removed from the core shipping dataset. Again, in future, it would be worthwhile to check for errors in vessel dimension to allow for a vessel size-based analysis of ship-strike risk; it is assumed that errors in vessel speed could be dealt with by looking at the higher frequency data.

Australia-wide vessel traffic data was obtained from the AMSA website for the period September 2012 to August 2014 (data comes in monthly bundles); this data was clipped to the local Port Curtis region. After this, basic quality control was carried out on the vessel tracking data. This entailed removal of data where vessel length was zero or greater than 300 m, where vessel speed was greater than 40 knots, and where speed was greater than 16 knots for vessels greater than 40 m in length.

We examined the distribution of vessel sizes and the number of positions in the data as a function of vessel size. The aim of characterizing these distributions was to examine whether particular vessel sizes are represented relatively highly in the AUSREP data. This is necessary to determine which sector of the vessel traffic the data describes. It's important to note that AIS have been mandated by the International Maritime Organization (IMO) on large vessels. This includes vessels of 300 gross tonnage and upwards engaged on international voyages, cargo ships of 500 gross tonnage and upwards not engaged on international voyages, as well as passenger ships (more than 12 passengers), irrespective of size. For vessels smaller than these capacities, AIS is voluntary.

To produce a 'vessel density' map we defined the hourly, or near-hourly, records of vessel presence to characterize a 'vessel hour'. That is, we assume that the location at which any vessel was logged is representative of the location of a vessel over an hour period. Summed up over space and time, this would give an indication of the total number of vessel hours in a particular region, which could be viewed as a proxy for vessel density. To avoid the natural oversampling that would occur for stationary vessels, all location data for vessels travelling at a speed of 0.1 knots or less were removed. Obviously, vessels can move a long distance in an hour. But our assumption here is that the one hour data, when aggregated over space and time, is sufficient for characterizing density on average.

3 Results

3.1 Exploratory analysis of detection patterns

The mean number of detections per individual was 62.3495 (SD = 160). The number of detections per hour was higher at the Wiggins Island site (mean = 76 compared to Pelican Banks (mean = 52.87)). The variability in detections was slightly higher at Pelicans Banks (SD = 160) versus Wiggins Island (SD = 150).

It is important to recall that these are not detection rates for a particular hour, but rather the number of detections at a given combination of `timelo` and hour of the day summed over all days in the data set. Box and whisker plots (Figure 131 and Figure 132) show considerable variation in detection rates between tagged turtles and in some case within individual data sets.
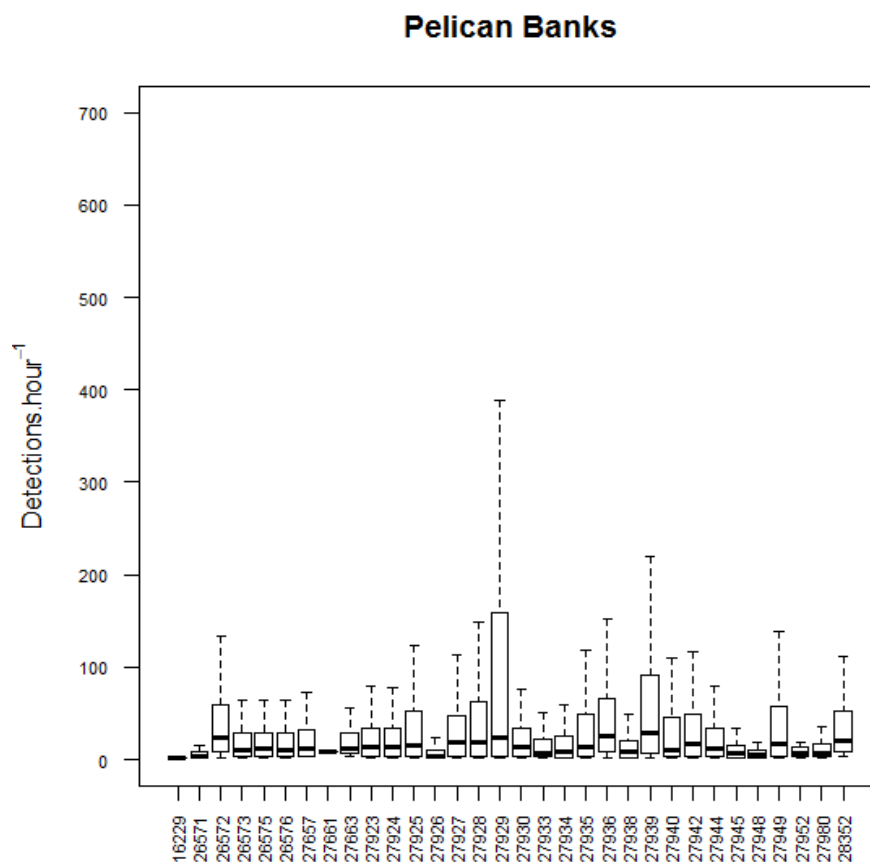
Pelican Banks

Figure 131 Detections per hour for each acoustically tagged turtle at Pelican Banks.

By plotting the number of detections (over all individuals) associated with a combination of hour of the day and time since low water, we generated a surface to look for patterns in detection rates through the tidal cycle and over the day (Figure 133). At Pelican Banks, there was a strong peak in detections in the morning and early afternoon (0400-1300). This ranged over approximately 0.2-0.45 days since the last low tide. The pattern at Wiggins Island (Gladstone Harbour) showed two peaks in detection; one was focused at 0400-0800 between 0.1-0.3 days since the last low water, with another peak over the period 0000-1500 centred on 0.5 days since the previous low (this is the period approaching the next low water - on average).
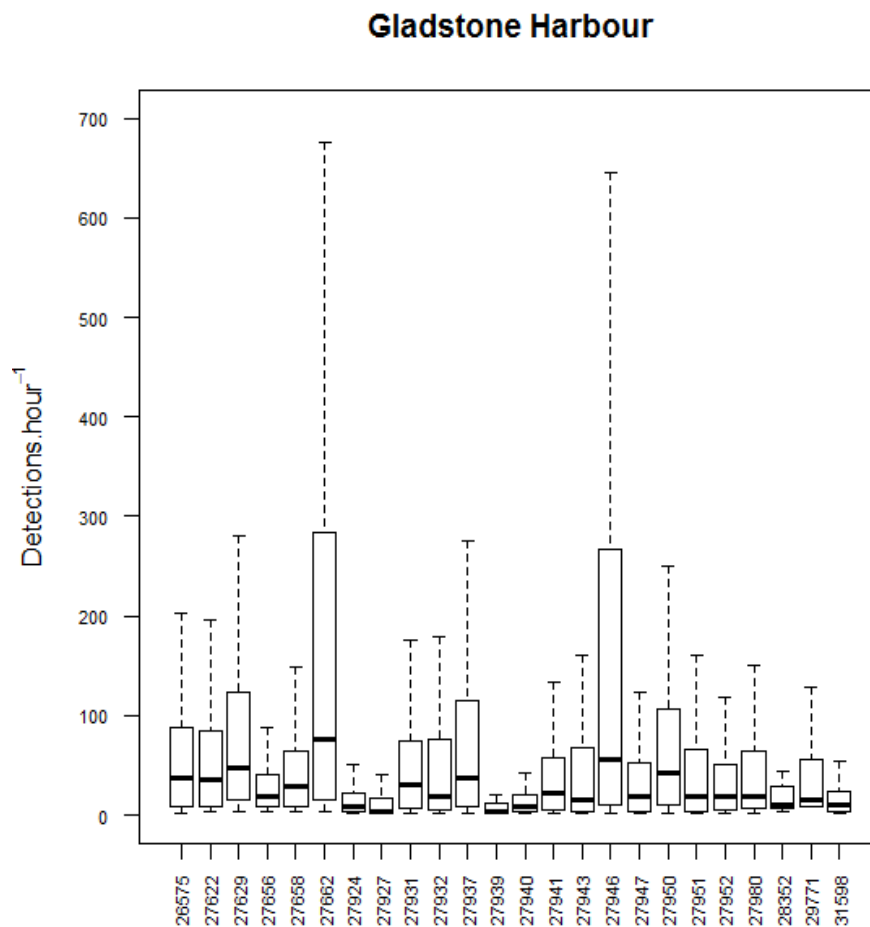
Figure 132 Detections per hour for each acoustically tagged turtle detected at the Wiggins Island Array.
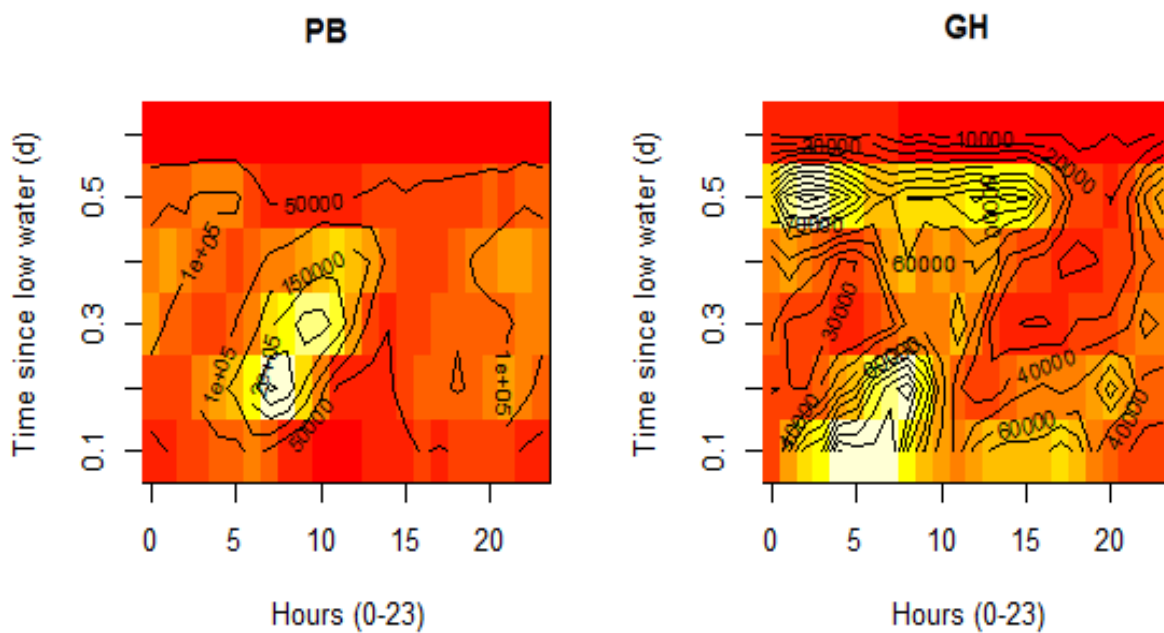
Figure 133 Number of detections as a function of time since low water and hour of the day for (left) Pelican Banks (PB) and (right) Wiggins Island (WI)..

3.1.1 CORRELATIONS BETWEEN PREDICTOR VARIABLES.

The degree of co-linearity between the predictor variables was generally low. One exception was between `bath` and `slope` which had a relatively large negative correlation (approximately - 0.6). However, examination of the scatter plot between these two variables shows that this correlation was largely driven by one data point and was also subject to several large outliers. Accordingly, we found that there was minimal concern that the selected covariates would present significant problems stemming from co-linearity.
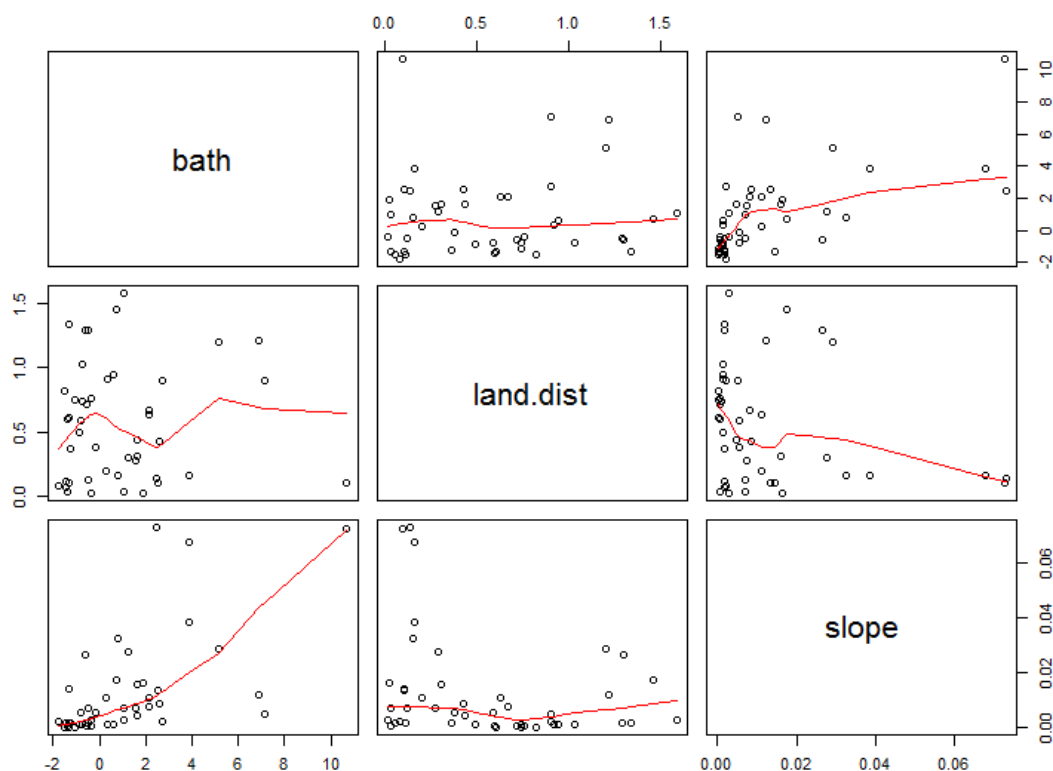
Figure 134 Pairwise scatter plot of covariates for examination of problematic co-linearity. From these plots it can be seen there are no major indications of co-linearity.

3.2 Habitat model results

3.2.1 RELATIONSHIPS WITH COVARIATES OF SELECTED EXTRAPOLATION MODEL

The constrained extrapolation model (i.e., that produced using data summarised over both Pelican Banks and Wiggins Island) predicted that higher rates of detection would occur between 0-5 hours after a low tide (Figure 135 - left). A dip in detections was predicted 7.2 hours after the low (roughly in line with the next high tide) followed by another increase on the subsequent low (roughly at 12 hours from the previous low). Additionally, the number of detections tailed off considerably at 0.6 days (14.4 hours since previous low). Despite the model only being constrained to have convex relationships between detection rates and distance-from-land and bathymetry, for both these variables the model suggested diminishing presence of turtles with increasing values of each covariate (Figure 135). The rate of decrease in detections with distance-from-land was only slight, but was considerably steeper with deepening water.
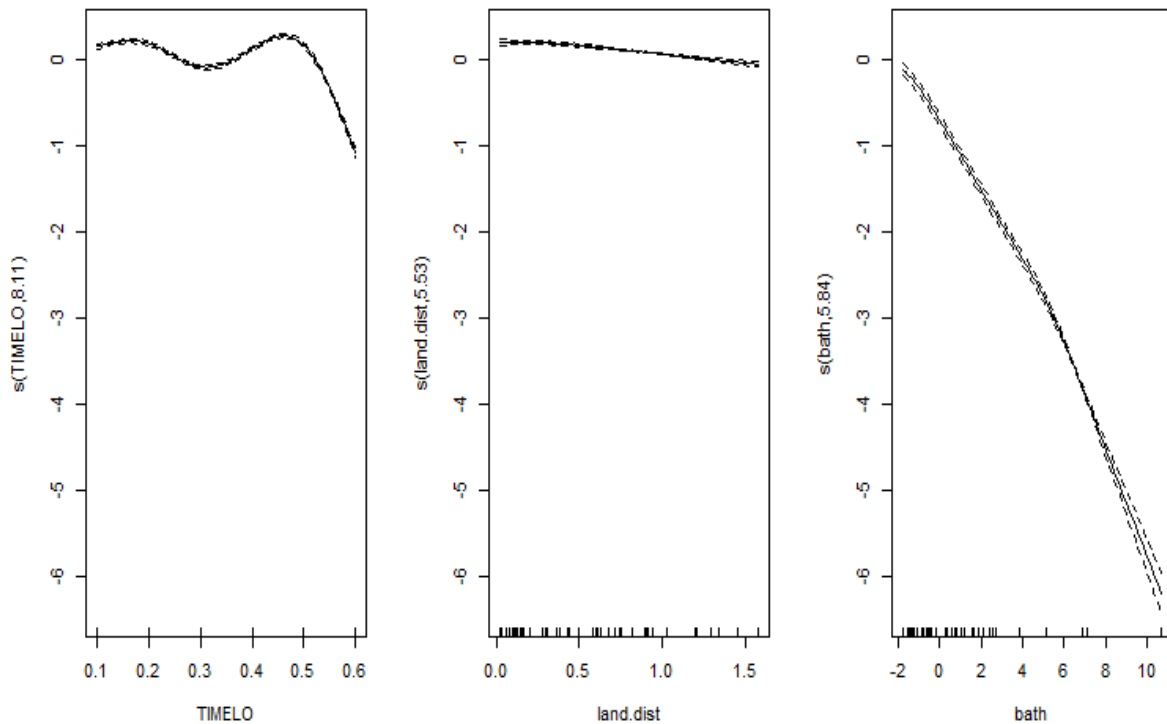
Figure 135 Partial effects plots of the semi-constrained model with respect to (left) time-since low water (centre) distance-from-land and (right) bathymetry.

3.2.2 MODEL DIAGNOSTICS

The diagnostics of the constrained extrapolation model were generally acceptable given the constraints on the model, the highly variable data, and large number of zero detections (Figure 136). However, the diagnostics were far from ideal; the distribution of residuals was approximately Gaussian but with several outliers. The plot of fitted versus response values showed unexplained patterning in the residuals. This indicates that the model fit is not as good as would be hoped - again not a surprising a result given the nature of the data. By this, we mean that given the highly (left) skewed nature of the numbers of detections (within each individual turtle x receiver x various environmental covariate cells), that even a Gamma distribution could not fully account for this variation. The residuals, however, indicate that for the most part, the Gamma distribution assumption did handle the skewness; this is, of course, open to further improvement in the future. Additionally, the model explained only a low proportion of the variation in the observations (deviance explained = 21%). Some of this may be due to the constraints on the functional shape of the smooth terms.
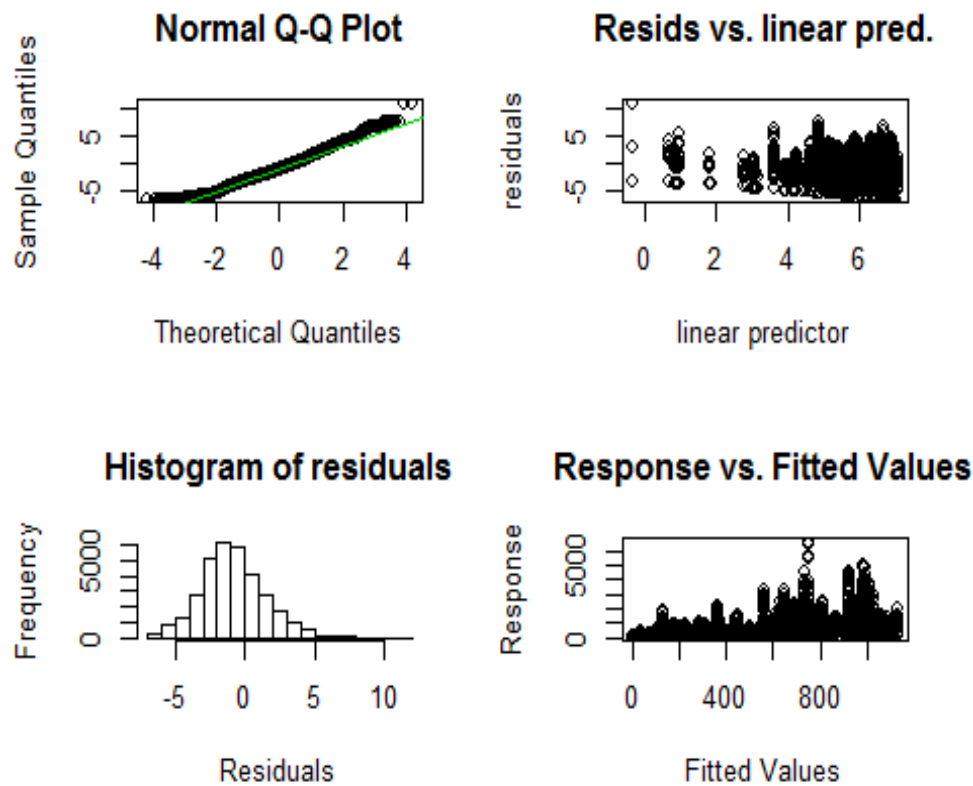
Figure 136 Diagnostic plots for the fitted SCAM model used to extrapolate throughout the Port Curtis region.

3.2.3 SITE-SPECIFIC MODELS: FITTED RELATIONSHIPS WITH COVARIATES

The GAMMs fitted to data by site indicated differing responses between the Wiggins Island (GH) and Pelican Banks (PB) arrays. For the WI array, a high number of hits was predicted for regions close to the high-water mark, declining to near zero at roughly 1 km from land (Figure 137). A relationship with `timelo` similar to the constrained 'extrapolatory' model mentioned above, was indicated. The number of hits decreased markedly after values >0.5 d since the previous low.

The bivariate smooth terms in the GAMMs, which included `slope` and `bath`, showed a complex relationship with bathymetry/water depth, but simpler responses with gradient (Figure 138). Generally, the effect of the `slope` variable was minimal. The smooth on Timelo showed a peak between 2-6 m at WI while at PB there were several peaks. Note that the water depth was considerably shallower for the PB data. It is difficult to interpret these plots in biological or ecological terms, and it is likely that they reflect the depths at which receivers happened to be placed more than any underlying behaviour by the turtles.

GH

PB
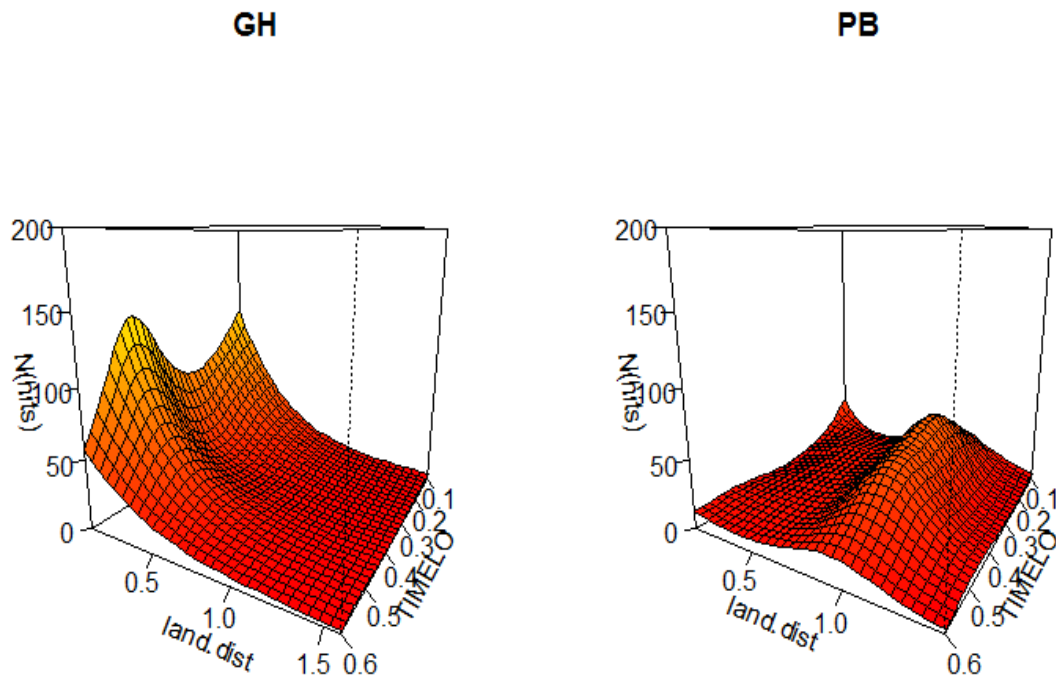
Figure 137 Fitted relationships between distance-to-land (land.dist), time since previous low water ("Timelo") and number of detections (N[hits]) from the GAMM models for (left) Wiggins Island (GH) and (right) Pelican Banks (PB) data.

GH

PB
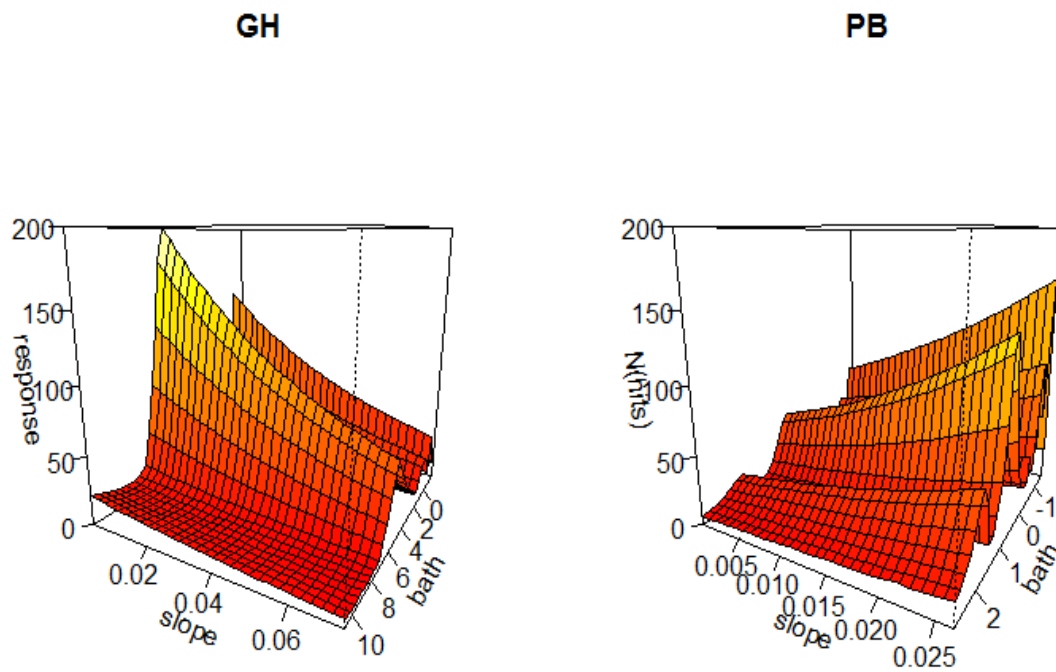
Figure 138 Fitted relationships between gradient (slope), depth ("bath") and number of detections (N[hits]) from the GAMM models for (left) Wiggins Island (GH) and (right) Pelican Banks (PB) data.

3.2.4 RANDOM EFFECTS

The random effects on individual turtles indicated, in general, that the variability between turtles, as characterized by the random intercept terms, was relatively small compared to main effects. Put into non-statistical terms, this indicates that the inclusion of random intercept terms did not drastically change the model predictions of the expected number of detections with respect to covariates. At the upper end of the fitted random effects, we'd expect only +/- 2 acoustic pings (our index of habitat preference) from an individual whose intercept was out in the tails of the distribution.
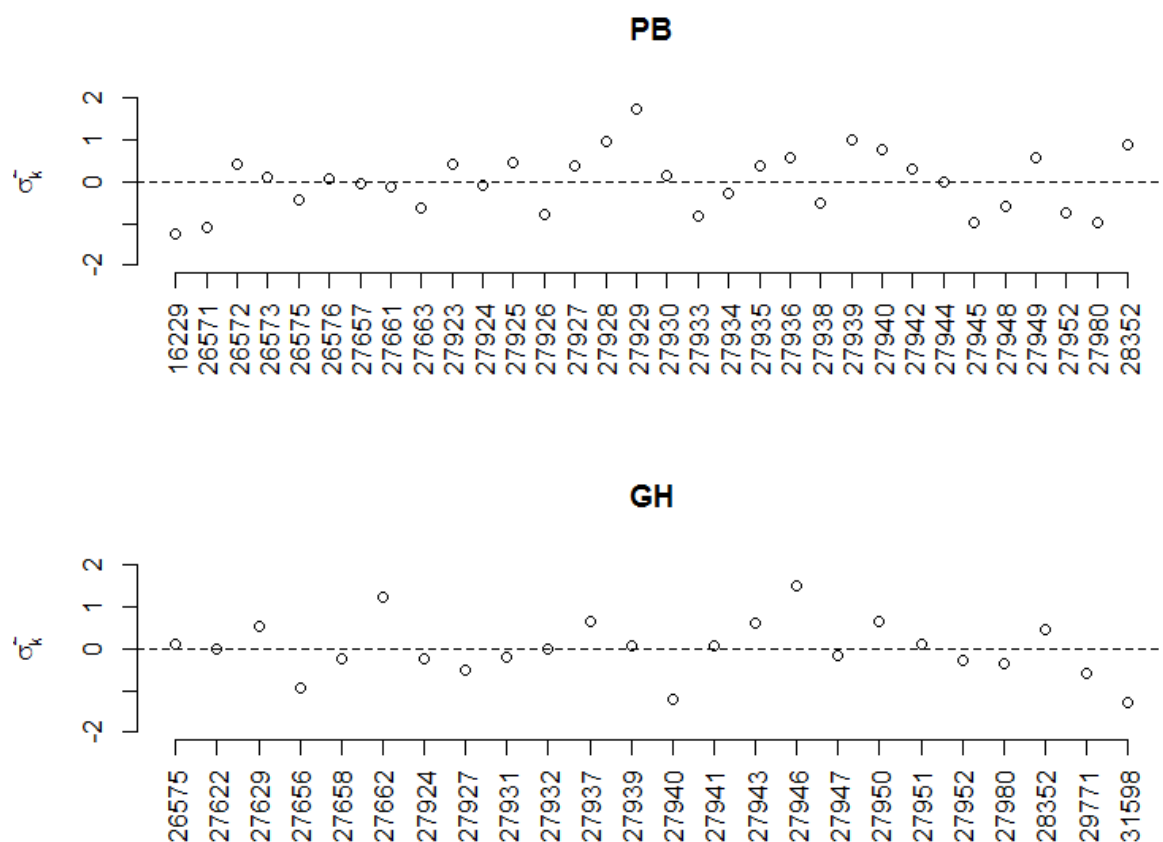
Figure 139 GAMM Estimates of random intercept terms for each individual turtle for (top) Pelican Banks (PB) data and (bottom) Wiggins Island (WI) data.

3.2.5 SPATIAL PREDICTION

By applying the three models to covariate data within an array region, and across the harbour (i.e. in places where no receivers were located), we compiled spatial predictions of likely turtle habitat. GAMM predictions from Pelican Banks indicated that turtles preferred areas away from the Eastern shore of Pelican Banks, with less preferred habitat in the middle of the bay being surrounded by areas of more preferred habitat (Figure 140).
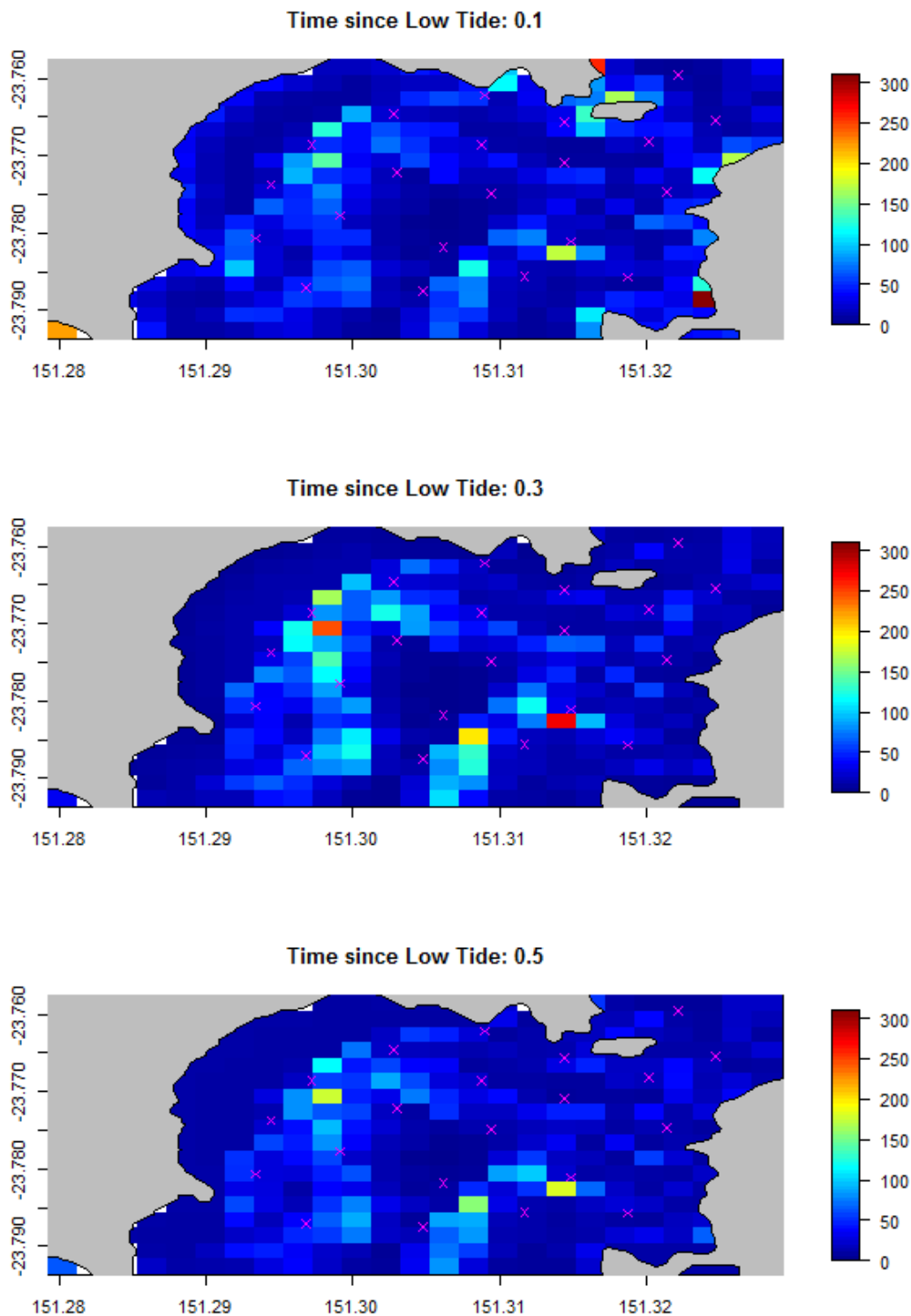
Figure 140 GAMM spatial predictions of expected number of hits / preferences at Pelican Banks with respect to time-since-previous low water.

Around high tide (0.3 d since previous low water), the models predicted some increased preference in localized hotspots at the same locations. At approximately the next low (0.5 d since previous low water) the predicted number of hits had dropped appreciably.

Predictions for the GAMM fitted to Wiggins Island (Figure 141) were that shallower water was preferred on the low tide (0.1 and 0.3 d since previous low water). Preference for inshore areas decreased on the higher tide (0.3 d since previous low). At Wiggins, tidal movement variations across the tagged population were less clear than those at Pelican Banks due mainly to individual variation

and the data being biased by a few individuals with large numbers of detections. Overall number of detections 1 hour from low tide was ~154,000 vs 77,000 at 1 h from high tide. This is likely to be due to increased chance of detecting tagged animals around low tide given that there was one receiver close to the mangroves. When detections at the two receivers in the Mangrove drain there was a steady increase in the number of detections as the tide rises indicating animals were moving into the mangroves where they could not be detected (Chapter IV).
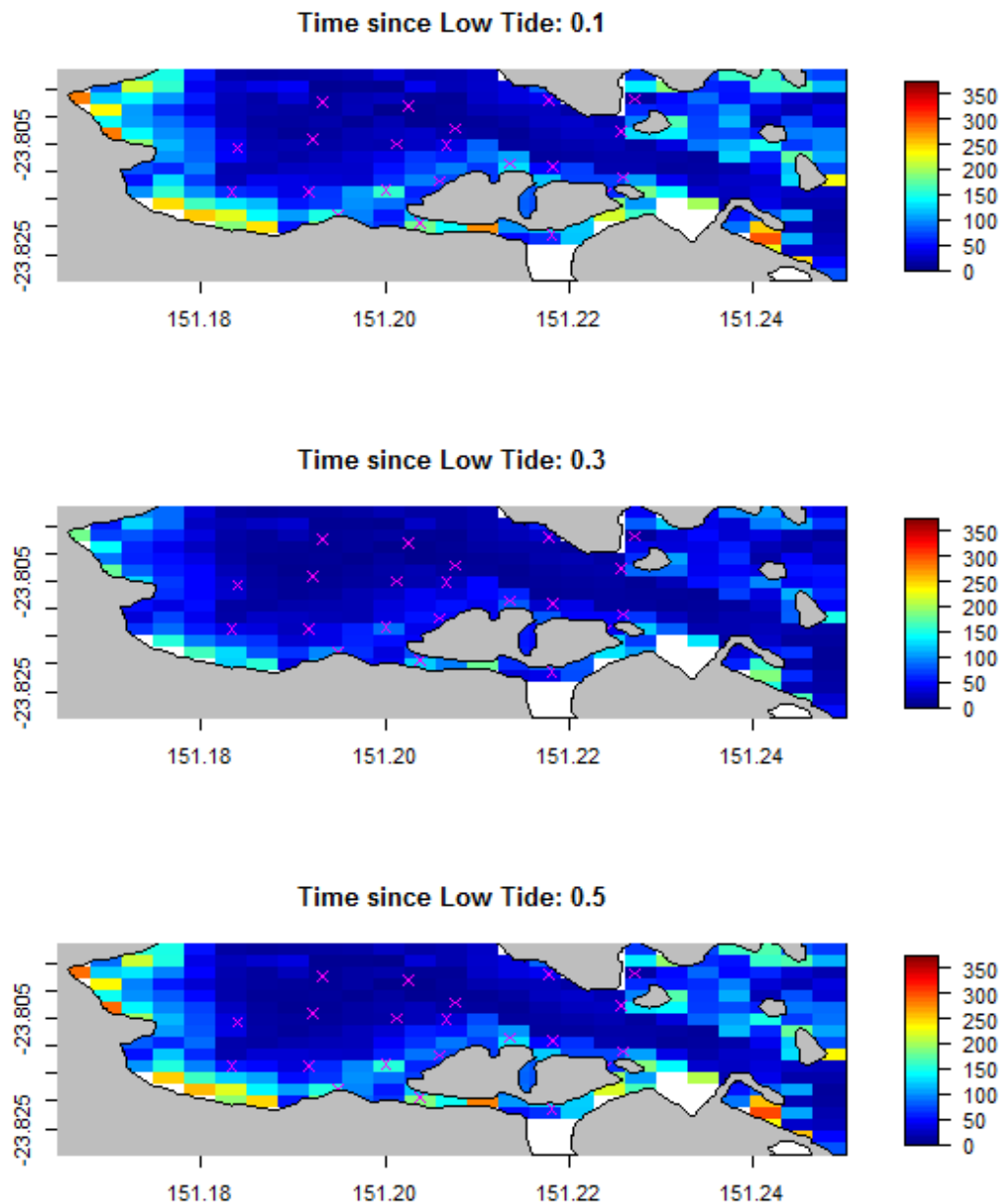
Figure 141 GAMM spatial predictions of expected number of hits / preferences at Wiggins Island with respect to time-since-previous low water.

3.2.6   EXTRAPOLATION/PREDICTION OF MODELS TO THE ENTIRE HARBOUR

The constrained extrapolation model (the SCAM model), predicted that shallow water habitats throughout the Gladstone region would be favoured by turtles (Figure 142). Similar to the GAMM fitted to Wiggins Island, the predictions with respect to the progression of tides was implausible as

the model predicted that the highest preference for inshore would occur on or soon after low water. While the model indicated that it fit the data reasonably well (from the diagnostic plots above in Figure 136), this prediction is clearly unlikely. Given the satellite data and the results presented in Chapter IV the turtles do appear to spend the majority of time in shallow coastal water. So there is an indication from the individual level analysis of acoustic data and the independent satellite data, that the overall spatial predictions of the model are tenable, but that it is not capturing the dynamics of turtles with respect to the progression of the tidal cycle. The general summary of the model prediction is therefore that areas of deep water, relatively far from the high water mark, are generally not preferred. Despite the inclusion of only moderate constraints on the model, the relationship with bathymetry was one of the stronger relationships to come out of these models.
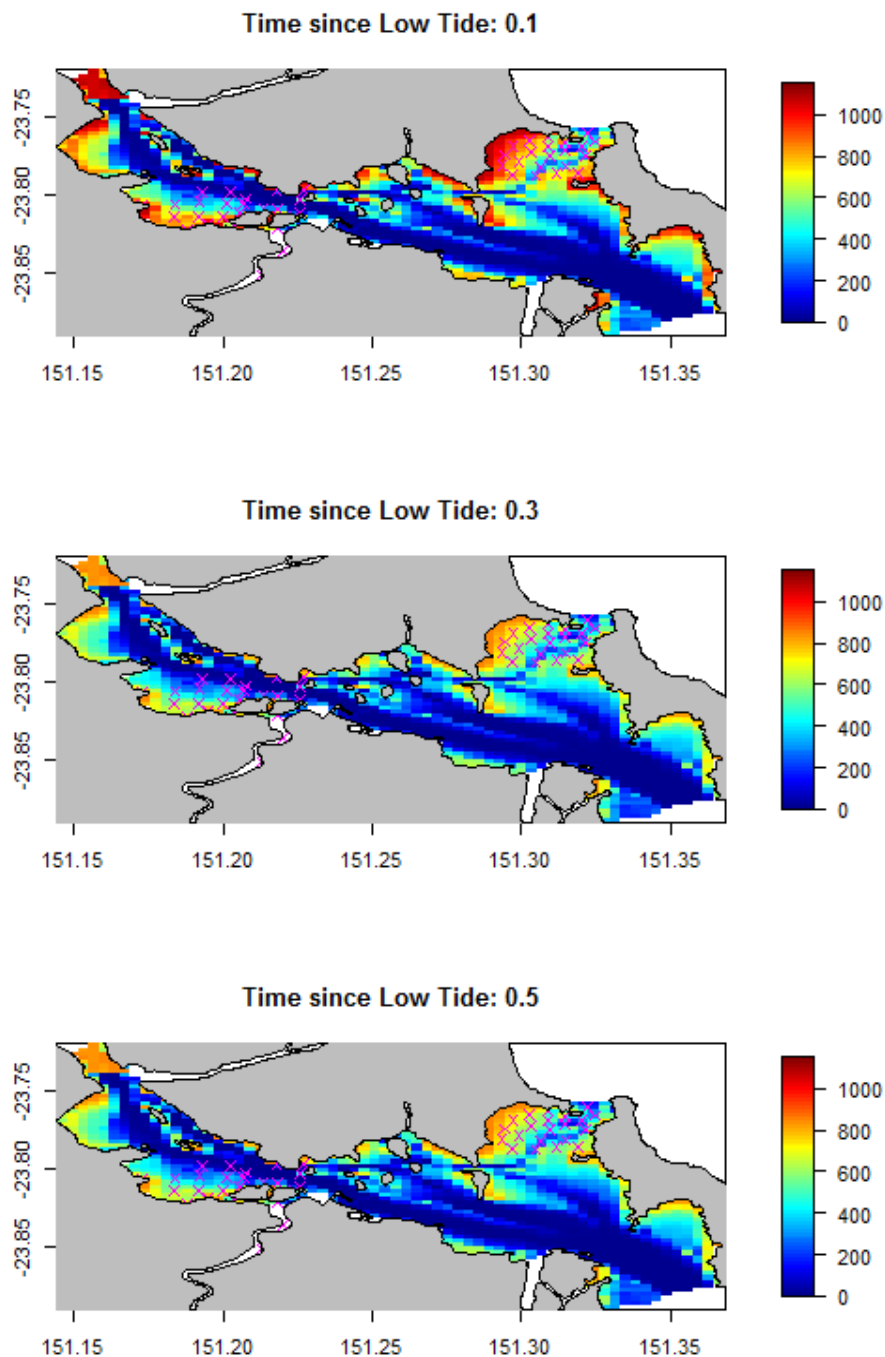
Figure 142 Spatial predictions from the SCAM model used to extrapolate to a larger region of the harbour.

3.3   Shipping analysis results

3.3.1   TRENDS IN SHIPPING TRAFFIC

The vessel data indicates that shipping intensity decreased markedly in Port Curtis between 2012 and 2014 (Figure 143). The maximum number of vessel positions (i.e. vessel-hours) was in October 2012 with 19,165 positions. The largest drop (of 58%) occurred between January and February of 2013. From this point on, the intensity of shipping traffic continued to decline but at a slower rate. The data for the last 3 months (June - August 2014), had an average number of 4,710.67 vessels.
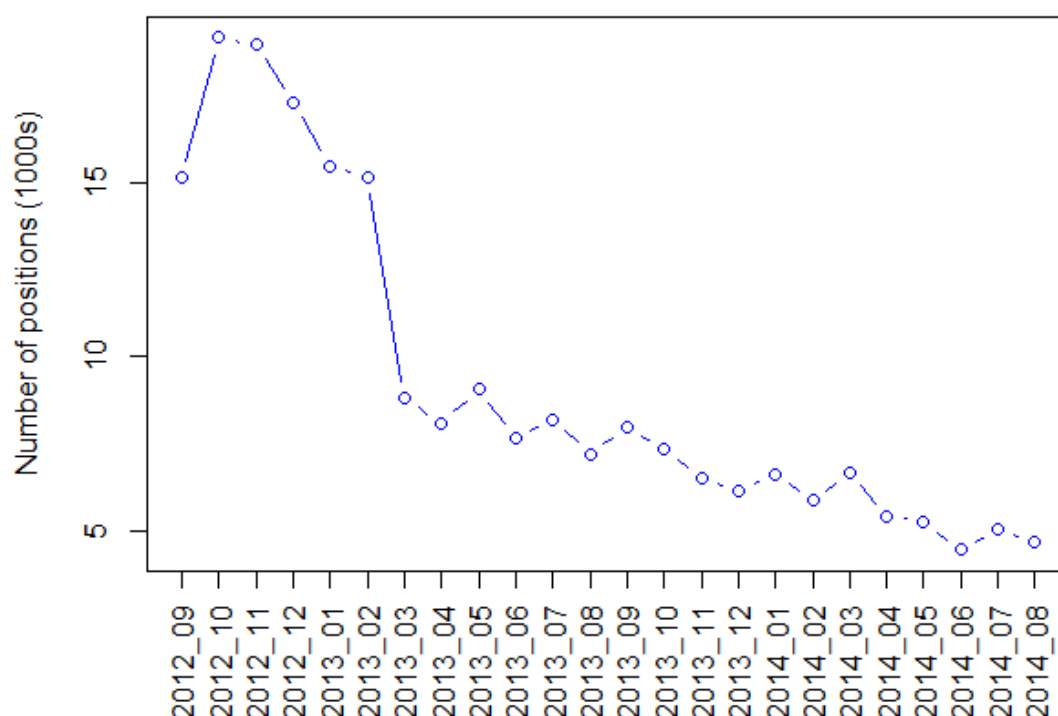
Figure 143 Trends in total vessel traffic in the local Port Curtis area, as represented by the AMSA AUSREP data for September 2012 - August 2014.

3.3.2   VESSEL SPEED AND SIZE DISTRIBUTION:

When restricted to the Port Curtis region, the AMSA shipping data held information from 1941 unique vessels. For these vessels there were 596,009 position fixes after the quality control measures had been applied. It was apparent that even though the majority of vessels in the AUSREP data were large, the majority of vessels which constituted the location data within the harbour were smaller craft; 61.76% of locations came from vessels which were less than 50 m length.

The majority of the vessel speeds in the shipping data were also relatively slow; speeds under 5 knots made up 63.41% of the positions or vessel-hours.
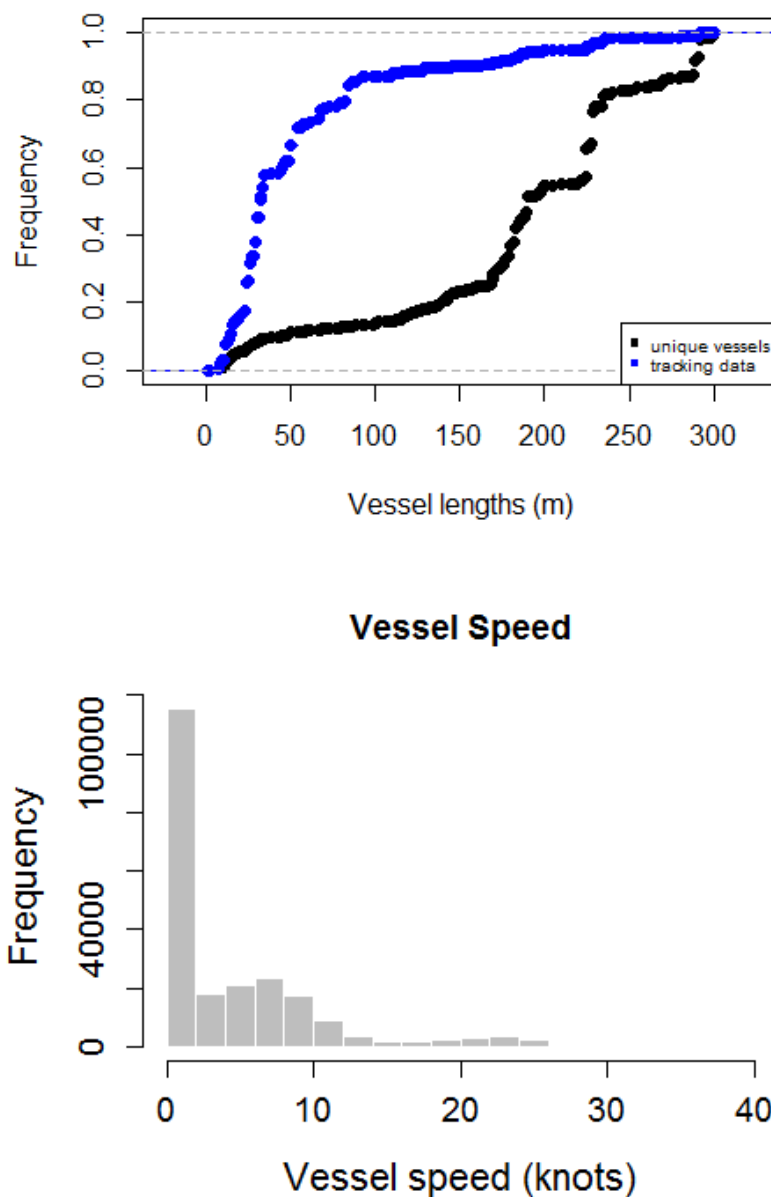
Vessel Speed

Figure 144 Vessel size and speed distributions in Gladstone Harbour. (Top) Empirical cumulative distribution functions for unique vessel lengths (black) and the representation of vessels by size in the AUSREP data (blue). (Bottom) Frequency distribution of vessel speeds.

The average speed of vessels was 4.4 ± 5.76 SD knots, indicating a large degree of variability in vessel speeds, overall. But given the highly skewed nature of the distribution of speeds, the median (median = 1.6 knots) is probably not a good measure of the general distribution of vessel speeds as it may represent vessels swinging at anchor yet moving at speeds greater than the 0.1 knot cut-off point.

3.3.3   DISTRIBUTION OF SHIPPING INTENSITY

From maps of the distribution of vessels at various speeds it was apparent that the majority of the data from AMSA pertains to large vessels using the major shipping channels through the centre of the harbour (Figure 145). The entrance into the Calliope River around Wiggins Island, and the channel to open water between Facing Island and Curtis Island were also used, but to a lesser degree. The most dense areas of shipping traffic were along the major shipping channel running   from

the central port areas to the south-western tip of Curtis Island (site of several LNG developments) with a high concentration of positions indicating speeds >20 knots.
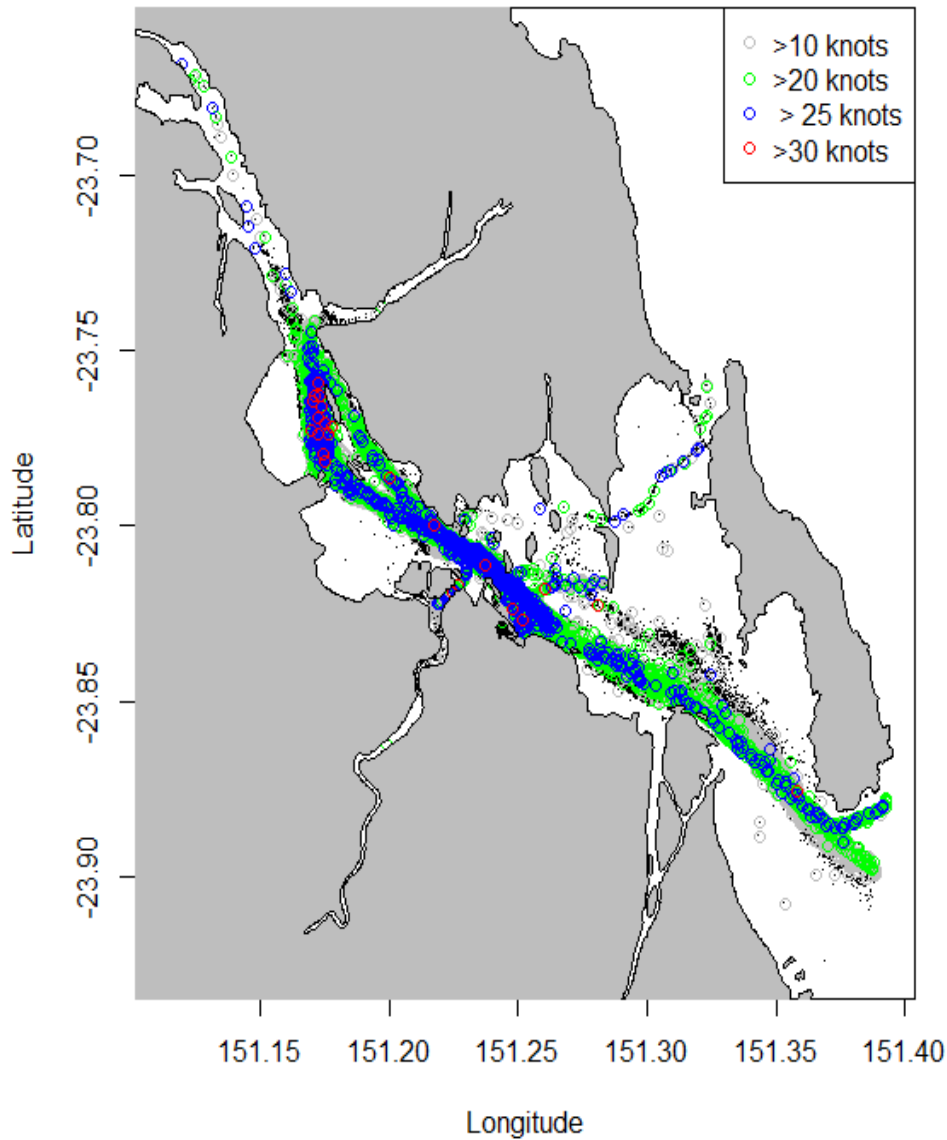
Figure 145 AUSREP shipping positions for Port Curtis labelled by speed thresholds.

By averaging spatially across all years of data we see that, generally, mean speeds are less than 15 knots. Particular outlier speeds do increase the average, but this is likely to be rare. Additionally, plotting the standard deviation of speeds shows that there is a high degree of variability in the areas which tend to contain the largest density of fast vessel traffic.

mean vessel speed (knots)

$$\sqrt{Var(speed)}$$
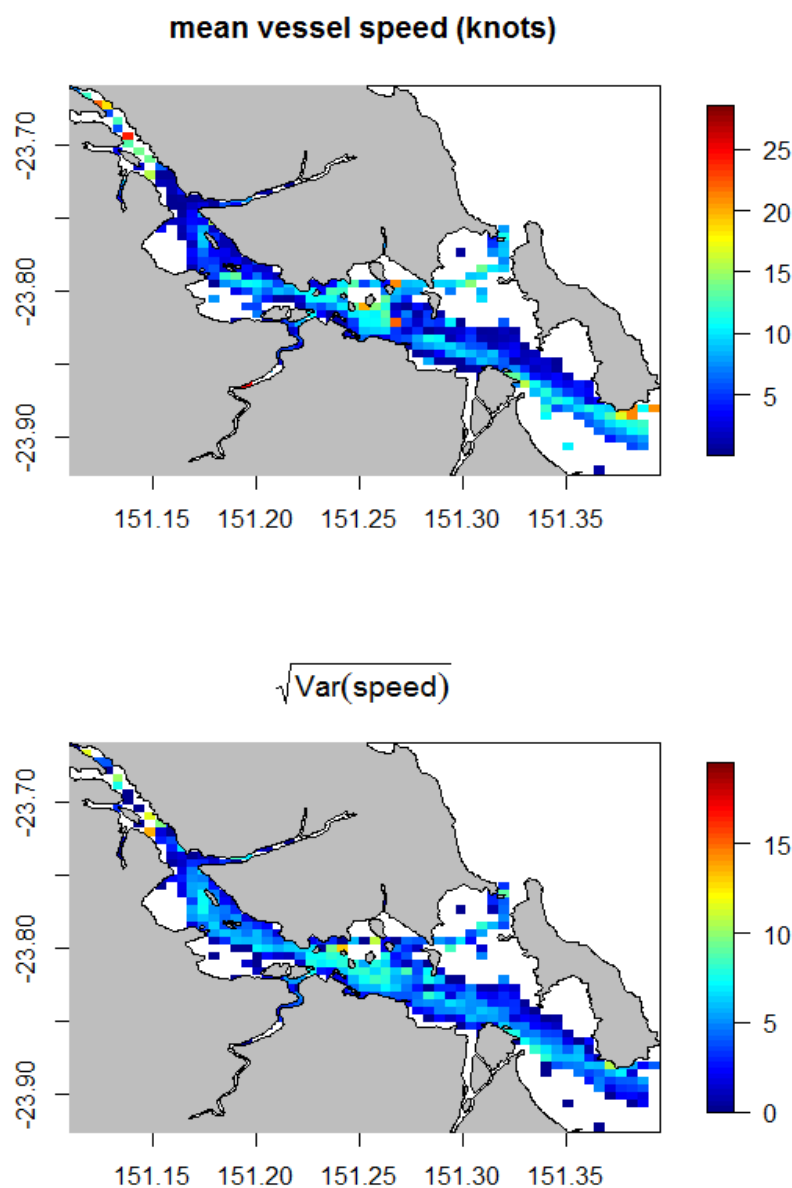
Figure 146 Mean (top) and standard deviation (bottom) of vessel speeds throughout the harbour.

3.3.4 OVERLAP OF HABITAT MODELS AND ZONES OF HIGH SPEED/DENSITY.

Plots of the relationships between predicted number of detections in each of the cells containing vessel traffic showed very little correlation between predicted number of detections, habitat preference and either average vessel speed or the intensity of shipping usage (Figure 147). Note that these predictions of habitat models plotted are on a log scale to visually accentuate the contrast in the predictions. The estimated smooth relationships between shipping speed and intensity indicated were influenced by a few points of high speed/intensity which coincided with predictions of high preference. Considering just the relationship between preference and intensity, without these few points there would likely be a reasonably clear negative relationship – i.e. turtles are predicted to prefer areas which as associated with less shipping traffic, at least for shipping of the types covered by the AUSREP data. Outlier points with high vessel speed and occurrence as well as high turtle habitat preference may be areas with unusually high risk for turtles. At least one such area appears to be the banks to the northeast of the Auckland channel which are shallow enough to represent potential habitat while being close to the main shipping channel. This area has never been recorded as supporting a seagrass bed (Bryant et al. 20140 and is in fact unlikely to constitute significant turtle habitat.
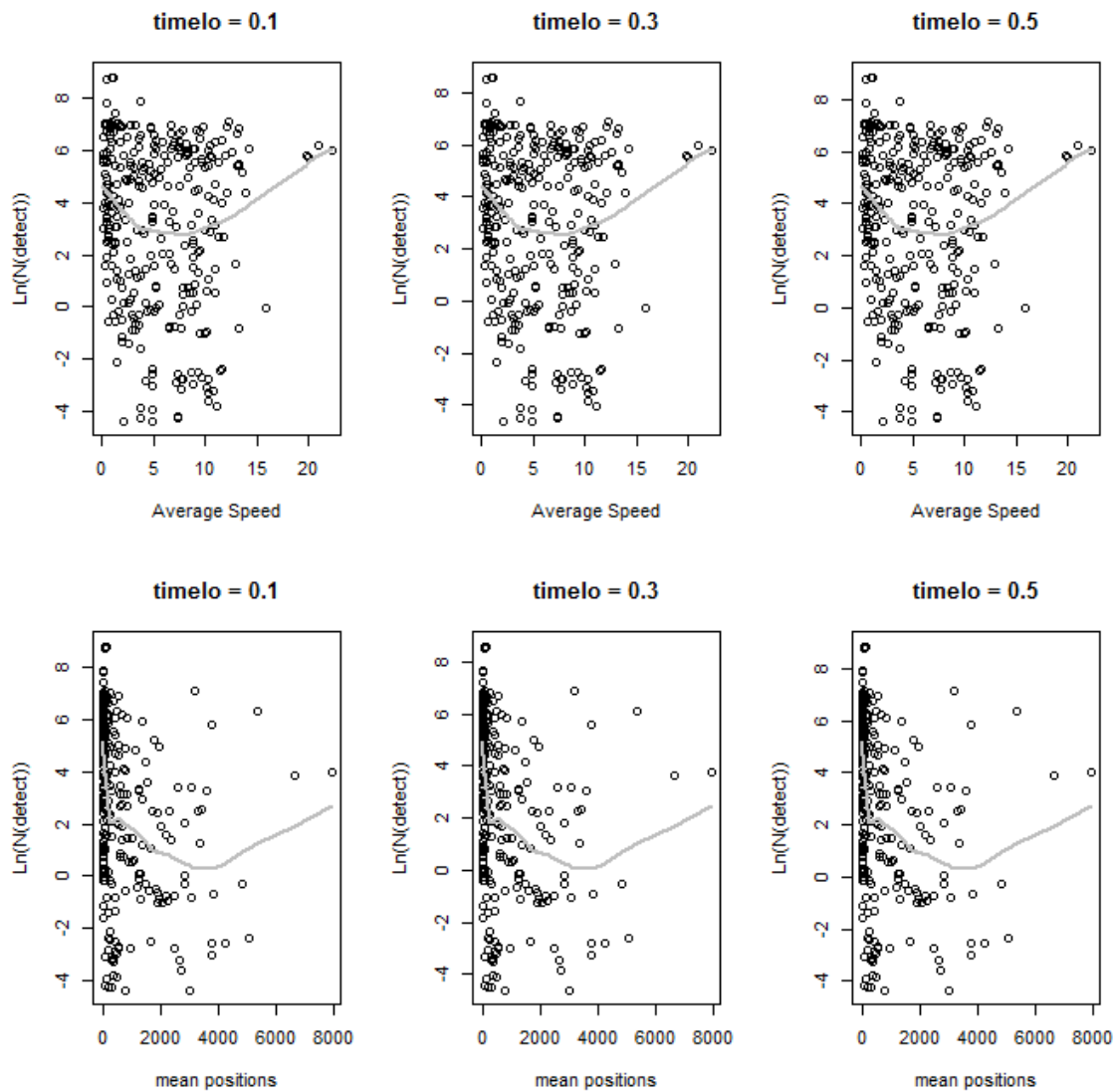
Figure 147 Log predictions from the preference models as a function of average speed (top row) and shipping intensity (average number of positions – bottom row). The lines are non-parametric Loess smoothers, which were used to detect any likely correlations. Each column is for the values of time-since-low water used throughout.

The same information can be view spatially by overlaying the habitat predictions and summaries of vessel traffic (Figure 148). Again, the degree of spatial overlap between the shipping data and the habitat models was generally small as areas predicted to be preferred by turtles were around the shore, while areas of high shipping intensity were in the deeper shipping channels. The narrows area to the north of Wiggins Island was an area of demonstrably high shipping intensity which is in close proximity to areas of high preference – although there was little direct overlap with the model. Given the high degree of uncertainty in the habitat preference model, and some of their limitations, it would be prudent to consider areas such as this in more depth in any future studies.
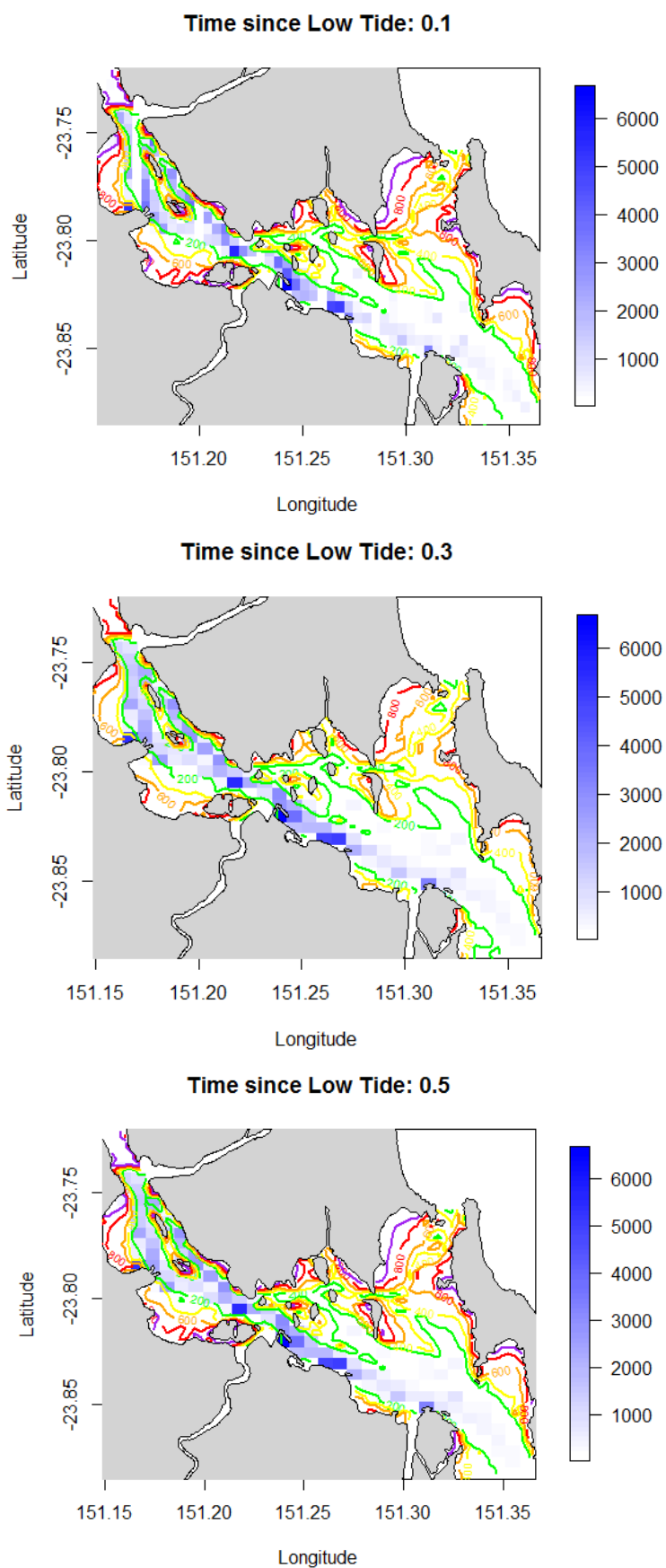
Figure 148 Maps of habitat preference (coloured contours give the expected number of detections – green lowest, purple highest). The blue shading gives average number of vessel positions per month.

4 Discussion

4.1 Adequacy of habitat models

The Generalized Additive Models of various forms presented in this report uniformly predicted higher preference for shallow water habitats, though in some respects they were qualifications based on the ability to track turtles in all parts of the harbour. If the question is whether turtles are in deeper channels in the middle of the harbour versus shallower water close inshore, then the predictions appear plausible and consistent with the satellite tracking data and the previously presented analysis of acoustic data in Part IV. This is important for consideration of ship strike risk as it would suggest that the risk of ship strike is likely to be lower in deeper waters further from the high water mark. Since these are the areas to where shipping is largely restricted, the potential for interactions with turtles is likely to be reduced.

The role of other factors was less clear. Slope of bathymetry did not appear to increase the predictive power of the models and was generally indicated to be a minor factor. This is not altogether surprising. The main reason for including slope as a predictor variable was to include a variable which would allow regions at the same depth to be differentially preferred. Additionally, areas such as steeper banks could have been avoided or preferred by turtles and at Barrow Island newly created (dredged) channels were shown to be used by resting turtles, increasing their risk of ship-strike (C Limpus pers. comm. 2014). On both these counts there seems to be little indication to support these hypotheses.

The models did predict clear signals with respect to tide, but they were at odds with previous data on movements over the tidal cycle. This probably reflects some structural inadequacies of the GAMMS, as well as potential artefacts and limitations in the acoustic data with regard to habitat prediction. Turtles have been observed to move into shallow areas at high tide and retreat to deeper areas as the tide falls (Limpus et al. 1994). There is strong evidence from previous results (Chapter IV) that turtles at Wiggins Island move towards the mangrove edge at high tide via mangrove drains, however these tidal movements were less obvious than those at Pelican Banks due to the sparse receiver coverage along the mangrove edge where turtles were foraging at high tide. It was only once data from individual receivers within the mangrove drain were investigated that this pattern of movement was obvious so it is not completely surprising that the model fitted to the Wiggins Island array data did not reproduce this result. The Pelican Banks GAMM, however, did predict deeper habitats to be favoured on a low tide.

The reason why the extrapolatory SCAM model and Wiggins Island GAMM did not reproduce plausible results through the tidal cycle could be twofold. First, the data used to fit the models does not capture the full spectrum of possible depth/tide combinations - at least over the space required for prediction. Few receivers were placed very close inshore at Wiggins Island. This means that if turtles were moving inshore on an incoming tide, the receivers in deeper water could gather fewer detections at high tide whereas around low tide, when turtles were forced off the flats and mangrove forest by lack of water, the number of detections could increase. Indeed, this was the case at Wiggins Island where the total number of detections 1 hour from low tide was ~154,000 vs 77,000 at 1 h from high tide due to the fact that there were 11 receivers regularly detecting animals in habitat accessible at low tide only but only 2 receivers in areas only accessible at mid to high tide. However,

the number of detections on these two receivers steadily increased as the tide rose, indicating animals were moving into the mangroves where the chances of detecting them were lower. This would produce the effect seen in the GAMMs from Wiggins Island data. It is noteworthy that the Wiggins Island array was situated in a more diverse range of depths, relative to Pelican Banks, and relatively few hits were collected on deep water stations. This would further enhance the effect of apparently predicting greater preference for inshore areas on a low tide.

Additional acoustic receivers placed in areas which dry at low tide may be necessary to determine when turtles move in and out of shallow waters with respect to tide. On the face of it, this may appear to entail significant effort to deploy instruments which will often collect no data. However, from a habitat prediction perspective, true absences are as useful as presence data. In the case of acoustic data, absences can arise not just from the animals actually being distant from a receiver, but also from poor detection rates. The analysis in this report of detection data suggests that turtles are probably being detected at distances <300 m. Given the layout of the arrays (with average spacing around 800 m), it is unlikely that long distance detections are biasing the results. However, depth and currents due to tide could be influential in determining detection rates in shallow habitats in particular. Any future studies need to bear these aspects in mind and explicitly factor in detection probability when designing arrays for monitoring habitat usage.

4.2   Predicted overlap between turtle habitat and shipping

Notwithstanding the issues with the habitat preference models employed here, the prediction that turtles mostly prefer tidal flats and areas inshore is plausible. This has clear implication for characterizing shipping risk. Larger shipping traffic (i.e. the type observed in the AMSA data used here) is restricted to the shipping channels which were predicted to be used to a minimal extent by turtles.

From the outset it is clear that a full risk analysis is not possible given current data. This would require an estimate of spatial density of turtles which is currently not available and would require dedicated surveys (e.g. see Williams and O'Hara 2010, Redfern et al. 2013). Therefore both the exercises of predicting habitat distribution and preference, and that of looking for more risk-prone areas of the harbour, can be better quantified by including spatial density estimates. Nonetheless, the broad approach outlined here should be useful as further data accumulates on the movements of turtles.

Tracking of turtles (Chapter IV) has demonstrated the importance algae as food source and determinant of habitat use for green turtles in Gladstone Harbour, in addition to seagrass and mangroves. Accurate maps of seagrass and mangrove distribution are available for Gladstone Harbour, and similar information is required for reefs and macroalgal habitat if these are to be incorporated into assessments of risk to turtles.

The analysis here strongly indicates that collection of the spatial distribution of small vessel traffic (recreational and commercial traffic without AIS) is needed if overall risk to turtles is to be accurately assessed. Similar conclusions have been reached in a recent assessment of risk to megafauna in Port Curtis (Richardson et al. 2014). If the predictions of the habitat models are supported in general (i.e. that shallow waters are key habitat) then it is possible that larger vessels may represent a smaller direct risk to turtles. This conclusion is somewhat different than the overall finding of Richardson et al. (2014) in part due to their assessment that large vessels pose greater risks due to their size, but possibly also in part because of the larger scale of their data on the likely distribution and habitat use

of turtles. It is important to note, however, that the results here cannot be interpreted as supporting the idea that large vessels are not a cause of ship strikes. However, these analyses do support the need to consider other types of vessel traffic beyond that represented in AMSA's AUSREP dataset.

Because small craft such as recreational vessels or small boats operated by commercial fishers are not routinely tracked, collecting this data would be challenging but very important given that the speed of recreational boats has been shown to put dugongs, turtles and other marine species at higher risk of collision or disturbance (Grant and Lewis 2010, Hazel et al. 2007, Hodgson and Marsh 2007 Maitland et al. 2006). Other platforms for data collection such as cameras or surveys would need to be considered to gather such information.

4.3 Summary

Modelling of turtle habitat use has addressed key goals of GISERA by providing a means of translating insights from turtle tracking into a harbour-wide picture of potential interactions with shipping traffic. While the potential for vessel interactions clearly exists, it appears to be lower than expected due to relatively high site fidelity of turtles in the harbour, their small core habitat use areas, and their preference for feeding in shallow areas. Their use of deeper areas such as channels is higher during low tide, when potential for interaction with commercial shipping may be higher, though potentially still low since most appeared to stay close to channel edges, and crossed channels infrequently. Potentially management of the risk of ship strike could incorporate this information by focusing shipping movements on periods of high tide. Such practices may already be in place in some parts of the harbour or for larger vessels. Other possibilities include public education campaigns, as suggested by Richardson et al. (2014) which would not face the legal complexities encountered when proposing "go-slow" zones.

A key information gap that requires further study is to quantify the spatial pattern and intensity of small boat (recreational) vessel traffic which is less restricted to deep channel areas, particularly at high tide when small craft are more likely cross shallow intertidal habitat. This is also the same time when green turtles are most likely to be found in shallow water. Such risks could be reduced, as they are elsewhere, by a combination of awareness and education programs and go slow zones in critical areas.

Tagging studies and habitat models while a key component of quantification of turtle risk, do not provide all the information required to evaluate risks across the harbour. To truly characterize the probability of ship strike, fine scale spatial density estimates of turtles throughout the harbour are required. These would be useful in also generating an associated abundance estimate for turtles in Port Curtis. The latter would also go part way to determining the population consequences of a given rate of turtle mortality on the local population and would provide a key indicator for future monitoring. Without this it is impossible to determine in any absolute terms, what the ship strike risk associated with any area or which sector of the vessels in Port Curtis pose the greatest risk.

Overall summary & recommendations

Summary

During both field campaigns, water column sampling showed the dominant component of the total absorption was the detrital or non-algal component, being greater than 70% of total absorption in the central region of the harbour. This component was greater than 77% inorganic material at all sites. CDOM was also a significant contributor to the total absorption coefficient and, because of the high particulate and CDOM loadings, light penetration in the water column was low resulting in low phytoplankton biomass. Diatoms were the dominant algal group at all sites within the harbour. Interestingly, although the September 2013 results showed lower particulate and CDOM loadings than the November 2012 results, the phytoplankton biomass, as indicated by chl-a is lower in 2013. This is likely due to the time of year; the September 2013 samples were probably collected prior to the spring bloom while the November 2012 samples were collected during a late spring bloom.

The observations of water quality parameters provided here constitute a key step for GISERA in developing a verifiable biogeochemical model of Gladstone Harbour. They can be used for validation purposes in their own right, but more importantly they form the link between modelling, point observations made in the field, and synoptic broad scale observations of water quality parameters provided by remote sensing platforms. Water quality in turn is a key factor influencing seagrass growth, therefore these observations are integral to the broader goals of GISERA in developing a reliable seagrass growth model for Gladstone Harbour.

Seagrass distribution throughout the harbour was patchy, particularly in more turbid parts of the inner harbour. The use of AUVs shows promise as a means of surveying seagrass but was not viable in areas of high turbidity and/or high current flow such as prevail in much of Gladstone Harbour. It was effective in other areas such as Pelican Banks, Seal Rocks and, during suitable conditions, in parts of outer Rodds Bay. Maximum depth of seagrass beds within the harbour ranged from -3.39 m to 1.42 m above datum. This depth range, when measured across the range of sites, corresponded to light levels of around 13% (±2.99 SE) of available surface PAR at Mean Low Water Neap Tide. Depth distribution (maximum depth range) of seagrass beds combined with water quality measurements provided a harbour wide means of assessing model skill in predicting seagrass depth distribution.

The seagrass growth model, which includes a newly developed set of equations, simulated observed seagrass distributions with a reasonably high degree of accuracy both in terms of depth range and spatial coverage. Other innovations in this model include the ability to use predicted ocean colour outputs to provide a broad scale means of not only visualise variations in water quality but to quantitatively validate or calibrate the model using remotely sensed data. The model includes sediment re-suspension and inputs of freshwater and sediments from river discharges (and potentially other sources as well). In combination with the new characteristics of the model this mean that it has the potential to be used to predict the impact of events such as flooding on the growth of seagrasses weeks or months in advance. Such capabilities may prove useful in terms of managing aspects of harbour use, in order to reduce risk to important natural assets such as turtles which are dependent on seagrasses.

Detailed mapping of seagrass biomass at Pelican Banks combined with observations of the fine scale movements of green turtles show that turtle habitat use (presumably feeding) is closely linked to seagrass distribution on the banks. In areas with lower seagrass biomass, other food sources such as mangroves and macroalgae are more important and are also related to turtle habitat use. Turtle

habitat use also showed significant variation in relation to water depth and tides, with turtles tending to stay in shallow waters at high tide, mainly retreating to channel edges or other deeper areas at low tide when seagrass beds or other feeding areas were exposed. In general turtles, particularly juveniles, showed a high level of site fidelity, not travelling far from the areas where they were captured, though for unknown reasons a higher than expected number of tagged animals did move significant distances, including outside the array and outside the Gladstone region. The experience of operating a large acoustic array in Gladstone harbour demonstrated the viability of acoustic tagging of turtles for providing data on habitat use and other behaviour of resident turtles. Acoustic tagging provided similar data to the more commonly used satellite tagging methods, but in larger volumes, over longer periods and at lower cost. However, until a more effective network of receivers is deployed along the Queensland coast, satellite tags remain the best option for informing us of larger scale turtle movements.

Risk assessment models for the Gladstone Harbour turtle population suggest that the risk to turtles from commercial shipping is likely to be relatively low. Characteristics of turtle movements such as the preference for shallow nearshore areas and infrequent movements outside the core habitat area, mean that they spend relatively little time in high risk areas such as channels used by commercial shipping. However other risks such as from recreational vessels and coastal fishing operations remain unquantified.

The work of the GISERA marine program has provided the basis for further development of tools such as seagrass growth and water quality modelling, as well as for seagrass risk modelling. To some extent this potential is already being capitalised on by programs such as the Gladstone Healthy Harbours Program which is further developing the biogeochemical water quality and seagrass growth model for the purposes of both hindcasting and forecasting conditions in the harbour. Opportunities for further development of risk assessments have not yet been taken up, but given adequate resources these can quickly be activated should the need arise. The following recommendations are suggested as key means of further capitalising on the experience and outcomes from GISERA Marine.

Recommendations

1. Optics sampling conducted in GISERA Marine focused on sampling spatial variability. Additional optical measurements quantifying temporal variability at fixed points, for example throughout a tidal cycle or encompassing wind events or floods, would be particularly useful in terms of understanding the dynamics of biophysical processes in the harbour and in assessing and better calibrating the biogeochemical and seagrass growth model.

2. Broad-scale, remotely-sensed observations of benthic primary producers such as seagrass have the potential to be incorporated into the seagrass growth model but, in order for this to be possible, spectrally-resolved measurements of simultaneous up-welling and down-welling irradiance, characteristic of these primary producers and their habitats, are required.

3. Grazing by turtles and dugongs as well as herbivorous fish and small marine invertebrates has the potential to significantly affect the distribution of seagrass, its absolute biomass and the ratios of above:below ground biomass. Rates of grazing require much better quantification in order for interactions between grazers and seagrass to be incorporated into predictions of seagrass biomass and rates of recovery.

4. The habitat modelling presented in this report has highlighted the need for broader and/or more targeted coverage of acoustic receivers throughout the harbour in order to reduce

uncertainty in habitat prediction. Further monitoring should consider using arrays with expanded coverage that cover harbour areas of high operation concern as well as spanning the range of habitats that used by turtles in the harbour. This could be investigated by stratifying the placement of arrays with respect to depth, habitat type and other variables. The modelling detailed in the current report could be used as an initial tool in formal statistical design of an expanded monitoring array.

5. Tracking of turtles has demonstrated the importance algae as food source and determinant of habitat use for green turtles in Gladstone Harbour, in addition to seagrass and mangroves. Accurate maps of seagrass and mangrove distribution are available for Gladstone Harbour, and similar information is required for reefs and macroalgal habitat if these are to be incorporated into assessments of risk to turtles.

6. Better characterisation of the risk of ship strike requires estimates of the average spatial density of turtles and its associated uncertainty. Additionally, gathering data on the spatial distribution of small craft usage is likely to be a key component in understanding all sources of mortality. As discussed in the Chapter V, both visual surveys of turtle density and data on small boat traffic are required if risks to turtles are to be fully quantified. Surveys of turtles would have the added benefit of providing a harbour-wide estimate of abundance. Such estimates would allow monitoring of trends in the local turtle population. Initial design work indicates that such surveys are feasible.

Appendix A Site information for optics field work

Apx Table A.1 Site code information for November 2012 field trip.

Site code	Date (local)	Time (local)	Latitude (^{O}S)	Longitude (^{O}E)	Bottom depth (m)
PBN	20 Nov 2012	10:40	23.7688	151.2988	NA
PBS	20 Nov 2012	12:50	23.7903	151.2983	1.9
SFT1	22 Nov 2012	08:22	23.8979	151.3715	5
SFT2	22 Nov 2012	09:19	23.8920	151.3677	16.6
SFT3	22 Nov 2012	10:02	23.9008	151.3637	4.5
SFT4	22 Nov 2012	10:31	23.9008	151.3605	6.4
SFT5	22 Nov 2012	11:01	23.9183	151.3554	1.9
MF1	22 Nov 2012	11:35	23.8642	151.3495	19.0
MF2	22 Nov 2012	12:08	23.8450	151.3259	12.1
SFt1B	22 Nov 2012	12:47	23.8812	151.3714	4.5
SFt2B	22 Nov 2012	13:25	23.8920	151.3677	17.6
SFt3B	22 Nov 2012	14:02	23.9007	151.3635	5.4
SFt4B	22 Nov 2012	14:26	23.9087	151.3603	7.5
DCT1	23 Nov 2012	09:16	23.7304	151.1527	1.4
DCT2	23 Nov 2012	09:45	23.7297	151.1555	10.5
DCT3	23 Nov 2012	10:26	23.7287	151.1581	10.0
DCT4	23 Nov 2012	10:50	23.7274	151.1608	1.8
BST1	23 Nov 2012	12:08	23.6756	151.1296	5.0
RCT1	23 Nov 2012	12:41	23.7033	151.1425	7.5
FLT1	23 Nov 2012	13:20	23.7442	151.1602	4.4
PNT1	23 Nov 2012	13:49	23.7950	151.1876	5.3
PMT1	23 Nov 2012	14:25	23.8041	151.2275	9.1
SCD1	24 Nov 2012	08:30	23.7507	151.3175	7.9
PBMT1	24 Nov 2012	09:17	23.7858	151.3058	2.2
PBMT2	24 Nov 2012	09:35	23.7832	151.3047	3.1
PBMT3	24 Nov 2012	10:00	23.7849	151.3057	4.8
QN1	24 Nov 2012	10:30	23.7990	151.2852	13.2
COMT1	24 Nov 2012	11:40	23.7944	151.2628	3.7
COMT2	24 Nov 2012	12:00	23.7942	151.2619	10.2
COMT3	24 Nov 2012	12:36	23.7938	151.2614	7.8
WIT1	24 Nov 2012	14:51	23.7983	151.2421	8.1
QI2	25 Nov 2012	08:07	23.8109	151.2937	2.6
QI3	25 Nov 2012	08:50	23.8069	151.3027	5.9
EN1	25 Nov 2012	10:00	23.7766	151.2618	5.4

Apx Table A.2 Site code information for September 2013 field trip.

Site code	Date (local)	Time (local)	Latitude (°S)	Longitude (°E)	Bottom depth (m)
PBN	13 Sept 2013	11:50	23.7688	151.2988	0.9
SCD1	13 Sept 2013	13:00	23.7507	151.3175	8.1
PBS	13 Sept 2013	13:50	23.7903	151.2983	1.9
QI1	13 Sept 2013	14:25	23.7995	151.2850	5.4
QI2	13 Sept 2013	15:10	23.8109	151.2937	NA
QI3	13 Sept 2013	15:40	23.8069	151.3027	NA
RB5	14 Sept 2013	09:00	24.0388	151.6050	NA
RB6	14 Sept 2013	09:35	24.0342	151.5736	NA
RB4	14 Sept 2013	10:25	24.0200	151.6229	NA
RB3	14 Sept 2013	10:52	24.0307	151.6264	2.9
RB1A	14 Sept 2013	11:20	24.0602	151.6463	0.9
RB2A	14 Sept 2013	11:50	240695	151.6464	3.7
SFT1	15 Sept 2013	09:47	23.8979	151.3715	3.8
SFT2	15 Sept 2013	09:15	23.8920	151.3677	16.9
SFT3	15 Sept 2013	08:30	23.9008	151.3637	4.5
SFT4	15 Sept 2013	08:03	23.9008	151.3605	6.5
SFT5	15 Sept 2013	07:30	23.9183	151.3554	1.7
MF1	15 Sept 2013	10:25	23.8642	151.3495	18.6
MF2	15 Sept 2013	11:05	23.8450	151.3259	12.1
OF1	16 Sept 2013	08:35	23.8244	151.4056	11.9
OF2	16 Sept 2013	09:30	23.8573	151.4278	12.9
PBMT1	16 Sept 2013	11:00	23.7858	151.3058	3.1
PBMT2	16 Sept 2013	11:35	23.7832	151.3047	2.8
PBMT3	16 Sept 2013	12:00	23.7849	151.3057	2.9
EN1	16 Sept 2013	12:35	23.7766	151.2618	3.5
COMT1	17 Sept 2013	06:55	23.7944	151.2628	3.9
COMT2	17 Sept 2013	07:20	23.7942	151.2619	12.5
COMT3	17 Sept 2013	07:45	23.7938	151.2614	9.1
PMT1	17 Sept 2013	08:18	23.8041	151.2275	12.8
WIT1	17 Sept 2013	09:05	23.7983	151.2421	10.5
PNT1	17 Sept 2013	10:00	23.7950	151.1876	6.1
WI	18 Sept 2013	06:58	23.8125	151.2052	2.0
BST1	18 Sept 2013	08:20	23.6756	151.1296	7.8
RCT1	18 Sept 2013	09:15	23.7033	151.1425	9.7
DCT1	18 Sept 2013	09:43	23.7304	151.1527	3.2
DCT2	18 Sept 2013	10:00	23.7297	151.1555	12.1
DCT3	18 Sept 2013	10:30	23.7287	151.1581	11.5
DCT4	18 Sept 2013	11:00	23.7274	151.1608	2.8
FLT1	18 Sept 2013	11:25	23.7442	151.1602	5.3

Site code	Date (local)	Time (local)	Latitude ($^{\circ}$S)	Longitude ($^{\circ}$E)	Bottom depth (m)
CP1	19 Sept 2013	07:10	23.8270	151.2489	10.5
CP2	19 Sept 2013	07:45	23.8378	151.2757	11.9
CP3	19 Sept 2013	08:30	23.8256	151.2911	14.6
PBS2	19 Sept 2013	09:10	23.7901	151.2985	2.6
PBN2	19 Sept 2013	09:25	23.7670	151.2991	2.6
CP4	19 Sept 2013	09:45	23.8170	151.2606	5.0

Appendix B Bio-optical properties terminology

Symbol/ Abbreviation	Description	Units
chl-a	chlorophyll-a	mg m^{-3}
CDOM	coloured dissolved organic matter	
TSM	total suspended matter	g m^{-3}
a	total absorption coefficient	m^{-1}
a$_{CDOM}$	absorption coefficient for CDOM	m^{-1}
a$_{ph}$	absorption coefficient for phytoplankton	m^{-1}
b	total scattering coefficient	m^{-1}
c	beam attenuation coefficient	m^{-1}
u	ratio of backscattering to backscattering + absorption	-
γ	backscattering coefficient	m^{-1}
r$_{rs}$	below water remote sensing reflectance	sr^{-1}
R$_{rs}$	above water remote sensing reflectance	sr^{-1}
λ	wavelength	nm

Appendix C Biogeochemical and seagrass modelling

This section derives from first principles Eq. 3, the relationship between the nitrogen-specific leaf area, Ω, the aboveground biomass of the seagrass, B (SG_A in the main text), and the fraction of the bottom, as viewed from above, covered by seagrass, or the effective projected area of seagrass, A_{eff}.

First assume that the change in the effective projected area with the addition of biomass is proportional to the available area:

$$\frac{dA_{eff}}{dB} = k(1 - A_{eff}) \tag{A.1}$$

where k is a constant. Rearranging, and integrating both sides:

$$\int \frac{dA_{eff}}{1 - A_{eff}} = \int k\,dB \tag{A.2}$$

Solving the integration terms gives:

$$-\ln⬚(1 - A_{eff})⬚ = kB + C \tag{A.3}$$

where C is the integration constant. Taking the exponential of both sides, and rearranging, gives:

$$A_{eff} = 1 - exp(-kB - C) \tag{A.4}$$

At zero biomass, there is zero effective surface area, thus 0 = 1-exp(-0-C). Rearranging, exp(-C) = 1, thus C = 0. So Eq. A.4 becomes:

$$A_{eff} = 1 - exp(-kB) \tag{A.5}$$

To show that the constant k is the nitrogen-specific leaf area, Ω, differentiate Eq. A.5 with respect to biomass:

$$\frac{dA_{eff}}{dB} = k\,exp(-kB) \tag{A.6}$$

At zero biomass, when the surface is completely uncovered, placing a leaf of biomass B on the surface covers an area of ΩB. Thus at zero biomass,

$$⬚\frac{dA_{eff}}{dB}⬚ = \Omega = kexp(-k0) = k \tag{A.7}$$

So $k = \Omega$, and we reach, as required A_{eff} = 1-exp(-Ω B).

Thus this simple form provides a link between the physical characteristic of a leaf, Ω, the seagrass biomass, B, and the fraction of bottom covered A_{eff}. It is relatively straightforward to show that A_{eff} ~ Ω B when B is small, and $A_{eff} \rightarrow 1$ when B is large.

This form is also used in the shallow water biogeochemical model for determining coral cover Gustafsson et al. (2013), macroalgae cover (CEM, 2014) and bottom reflectance of the optical model. In the simple representation here, it is assumed that the placement of each leaf is independent of all others. That is, the change of the effective leaf area is dependent on the fraction of available space remaining (Eq. A.1). A more sophisticated representation might consider that additional seagrass

shoots are more likely to be located close to existing shoots. This appears to be a small effect, and of course, it is likely that plant anatomy might have evolved, as far as possible, to avoid such an effect.

A preliminary assessment of Eq. 3 is given in Figure B.1, showing observations of the fraction of the bottom covered against seagrass biomass from Gladstone Harbour. Uncertainty exists in the estimates of both biomass and effective area at low biomass. At low biomass, $A_{eff} \sim \Omega_B$, so any model error at low biomass is due is errors in estimating Ω, rather than the form of Eq. 3. At higher biomasses, Eq. 3 appears to well represents the effect of reduced bottom coverage due to shoots overlying each other.

In a study of canopy density and photosynthesis in *Amphilibolis griffithii* (Hedley et al. 2014) used observations to fit the percentage of light transmitted through a seagrass canopy to the leaf area index, LAI: percentage = exp(-0.29 LAI). In our model, the transmitted fraction is exp(-sin $\beta_{blade} A_L \Omega_B$ B). Given that Ω_B B = LAI, their form is identical to ours, with our model having a geometrically-determined coefficient of A_L sin β_{blade} = 0.35 for *Zostera*, compared to their empirically-determined coefficient for *Amphilibolis* of 0.29. Thus both the form of Eq. 3, and our physical means of determining the coefficient, work well.
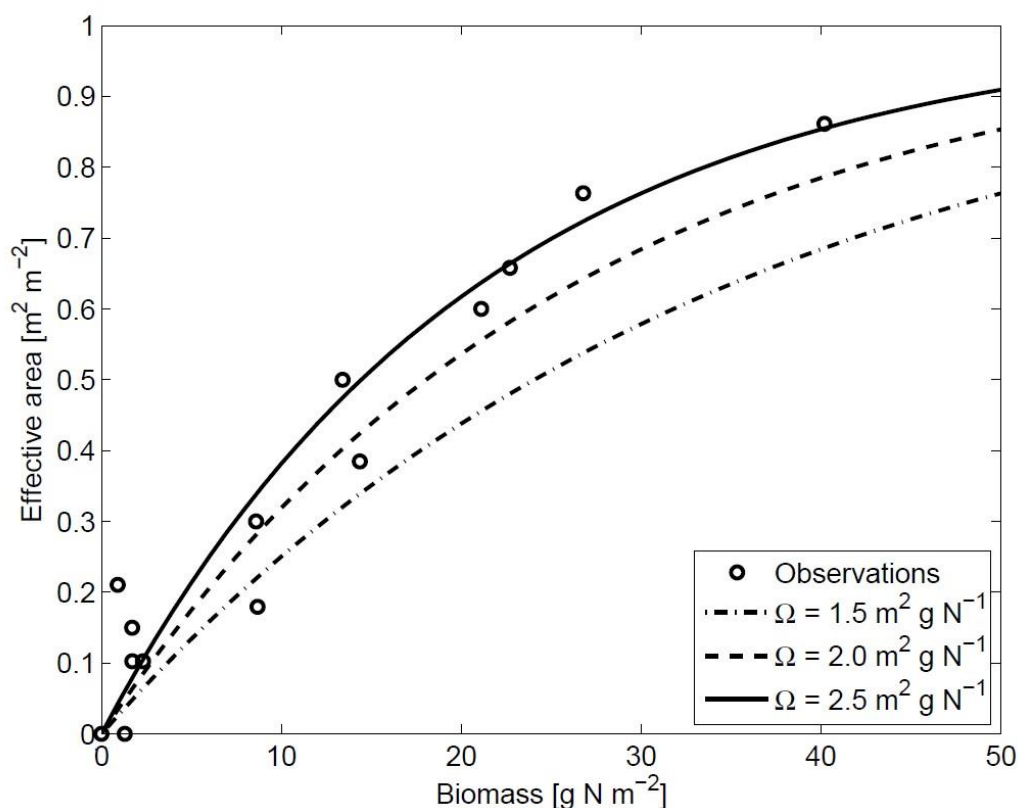
Apx Figure C.1 Observations (o) and model estimates (lines) of the relationship between the effective projected area fraction, A_{eff}, and seagrass biomass, B (Eq. 3). The conversion between dry weight and leaf nitrogen is 0.0192 g N g dw[-1] (Duarte, 1990). Observations are derived from data in Chapter II, Figure 38.

Is acoustic tracking appropriate for air-breathing marine animals? Dugongs as a case study

Daniel R. Zeh[a,b], Michelle R. Heupel[a,b,c], Colin J. Limpus[d], Mark Hamann[b], Mariana M. P. B. Fuentes[b], Russel C. Babcock[e], Richard D. Pillans[e], Kathy A. Townsend[f], Helene Marsh[a,b]

[a]*AIMS@JCU, Australian Institute of Marine Science, College of Marine and Environmental Sciences, James Cook University, Townsville, QLD 4811, Australia*
[b]*College of Marine and Environmental Sciences, James Cook University, Townsville, Australia*
[c]*Australian Institute of marine Science & Centre for Sustainable Tropical Fisheries and Aquaculture, James Cook University, Townsville, Australia*
[d]*Aquatic Threatened Species Unit, Department of Environment and Heritage Protection, 41 Boggo Road, Dutton Park, Australia*
[e]*Commonwealth Scientific and Industrial Research Organization, Marine and Atmospheric Research, Cleveland, Queensland 4163, Australia*
[f]*School of Biological Sciences, Moreton Bay Research Station, University of Queensland, Dunwich, Queensland 4183, Australia*

Abstract

Marine animals face increased pressure through expanded shipping and recreational activities. Effective conservation and management of large species like marine mammals or sea turtles depends on knowledge of movement and habitat use. Previously studies have used data collected from either satellite or acoustic telemetry but rarely both. In this study, data from satellite and acoustic technologies were used to: Determine the efficacy of satellite and acoustic telemetry to define dugong movement patterns; compare the benefits and limitations of each approach; examine the costs of each approach in relation to the amount and type of data provided; and relate telemetry data to the boundaries of a Go Slow area designed to protect dugongs and turtles from vessel strike within an urbanised coastal embayment (Moreton Bay, Queensland, Australia). Twenty-one dugongs were captured in seagrass habitats on the Eastern Banks of Moreton Bay in July - September 2012 and July 2013 and fitted with GPS and acoustic transmitters. Both satellite and acoustic telemetry produced reliable presence and movement data for individual dugongs. When the dugongs were within the range of the acoustic array, there was relatively good correspondence between the overall space use measures derived from GPS and acoustic transmitters, demonstrating that acoustic tracking is a potentially valuable and cost-effective tool for monitoring local dugong habitat use in environments equipped with acoustic receiver arrays. Acoustic technology may be particularly useful for species that establish home ranges with stable residency especially near large urban or port environs. However, the relative merits of the two technologies depend on the research question in the context of the species of interest, the location of the study and whether the study site has an established acoustic array.

Keywords: *Dugong dugon*, marine wildlife, acoustic, satellite, telemetry, GPS

1. Introduction

The growth of coastal ports and urban areas has increased pressure on marine animals through expanded shipping and recreational activities. For example, the speed of recreational boats has been shown to put dugongs, turtles and other marine species at higher risk of collision or disturbance (Maitland et al., 2006; Hazel et al., 2007; Hodgson and Marsh, 2007; Grant and Lewis, 2010). Data showing the presence and movement patterns of animals in relation to factors such as critical habitat and human use of coastal waters fill a key knowledge gap for managing coastal developments and provide important insights for the effective conservation of exploited or endangered species (Cooke, 2008; Bograd et al., 2010). For managers responsible for protecting these species, defining movement and behavioural variables is challenging due to the dynamic nature of these coastal environments and the difficulty in determining what an individual is doing (e.g., feeding, moving) at a given time. Researchers have used various forms of telemetry to understand these aspects of marine animal behaviour. Telemetry data have been employed to elucidate a wide array of biological factors including: migration, home range, habitat use, mortality, site fidelity, diel and seasonal patterns and habitat preference (see reviews by Hart and Hyrenbach, 2009; Hazen et al., 2012 and Heupel and Webber, 2012). Telemetry analyses have also been used to address management and conservation challenges (Bograd et al., 2010).

The two main approaches are satellite and acoustic telemetry (e.g., Marsh and Rathbun, 1990; Sheppard et al.,

*Corresponding author
Email address:* daniel.zeh@my.jcu.edu.au (Daniel R. Zeh)

2006; Cooke, 2008; Heupel and Webber, 2012). For example, data from acoustic telemetry have been used to calculate the mortality rates of juvenile sharks to improve stock assessment models for fisheries management (Heupel and Simpfendorfer, 2002; Knip et al., 2012a; Pillans et al., 2014) to evaluate the efficacy of marine protected areas (Heupel and Simpfendorfer, 2005; Knip et al., 2012b) and have provided data on the locations and dive movements of humpback (Baumgartner et al., 2008) and right whales (Winn et al., 1995). Similarly, data from satellite tagging have been used to analyse home range and habitat use for management and conservation (James et al., 2005; Shillinger et al., 2008; Slone et al., 2013; Jaine et al., 2014) and for understanding animal movements including migrations in relation to coastal development (Sheppard et al., 2006; Costa et al., 2012; Pendoley et al., 2014).

Passive acoustic telemetry arrays offer considerable benefit for studying behaviours of marine species because the associated small transmitters are light, less expensive and have longer battery life than satellite transmitters. Indeed, acoustic receiver arrays have been used to track over 80 species of marine animals to study migration, home range and habitat use (Heupel et al., 2006; Heupel and Webber, 2012). This approach has been facilitated to some extent by the installation of passive acoustic arrays through national networks such as the Integrated Ocean Observing System (IOOS, United States, Malone, 2004; Raynor, 2010; Luczkovich et al., 2012), the Australian Animal Tagging and Monitoring System (Heupel and Simpfendorfer, 2014) of the Integrated Marine Observing System (IMOS, Australia), and the Pacific Ocean Shelf Tracking Array (POST, Canada, Welch et al., 2009). Large arrays are being considered on all United States and Canadian coasts with plans to be integrated through the Ocean Shelf Tracking and Physics Array (Grothues, 2009). Large arrays that are installed and maintained collectively rather than by individual researchers offer considerable benefits to marine wildlife tracking because many species can be tracked using the same acoustic array (due to the pseudo-random repeat rate of each individual transmitter, designed to avoid signal collision) offering solutions to understanding the behaviour of animals in and around ports and industrial development. The main limitation of acoustic arrays is that movements and activity are not recorded while the animals are outside the array.

However, when continuous spatial and temporal information is required across long distances, most marine mammal and reptile studies have used satellite telemetry (Cooke, 2008; Block et al., 2011; Costa et al., 2012). A major limitation of satellite tracking is that tags are externally attached to the animal (e.g., by attachment to the dorsal fin, Pennisi, 2005; Gales et al., 2012) or attached via a tether with a weak link (Marsh and Rathbun, 1990; Deutsch et al., 1998; Reid et al., 2001) which makes them susceptible to bio-fouling and early loss. In addition, deployment times are limited by battery life; thus, animals are typically tracked only for relatively short periods (often

weeks to months; Hart and Hyrenbach, 2009) depending on the size of the battery pack and programming of transmission rates. Also some satellite tags are large, restricting tracking to adult animals. However, recent advances in miniaturising the tags allow tracking of small immature turtles (Mansfield et al., 2014). Understanding the relative costs and performance metrics of both acoustic and satellite technologies is important because both approaches offer the potential to obtain important insights into behaviour of animals, especially around coastal developments. Despite the broad application of both acoustic and satellite technologies to track animal movements, few studies have fitted animals with both technologies to test and compare the efficacy of each.

While application of both technologies is not appropriate for many small species, larger marine animals provide an opportunity to examine the benefits and limitations of each approach. The dugong, *Dugong dugon*, which is listed as Vulnerable to extinction by the IUCN (Marsh, 2008) and is one of the Great Barrier Reef region's World Heritage Values (GBRMPA, 1981), provides an excellent research opportunity. Individuals are large enough to carry both satellite and acoustic transmitters and they are not likely to be disturbed by the acoustic transmitter frequency of 69 kHz since it is probable their hearing range is similar to the 400 Hz to 46 kHz range of manatees, *Trichechus spp.* (Marsh et al., 2011 and D. Ketten, *pers. comm.*).

Human activities that affect populations of dugongs and other threatened marine wildlife must be managed more intensively in high human-use areas to reduce the potential for reproductive isolation of populations that remain in the dwindling number of coastal wild places. Although many dugong habitats in eastern Queensland have been protected from incidental fishing by spatial closures (Dobbs et al., 2008; Fernandes et al., 2010), several critical habitats are adjacent to current major or proposed port developments. Managers face significant challenges in protecting dugongs from anthropogenic impacts in these areas. High density human activities occurring within and adjacent to dugong habitat at several of Queenslands major ports such as Brisbane, Gladstone and Townsville greatly increase the risk of exposure to a host of threats that may not exist in less developed areas (Chilvers et al., 2005).

We collected data from acoustic and satellite technologies to describe the presence and movement patterns of dugongs in an urbanised area (Moreton Bay, Queensland) adjacent to the Port of Brisbane, Australias third busiest port. The study focused on an area of shallow seagrass and an associated Go Slow Zone to define use of this region by dugongs and the efficacy of the current management arrangements to protect dugongs from boat strikes. Go Slow Zones are reduced speed zones designed to reduce the likelihood of risk of vessel collision (Laist and Shaw, 2006; Calleson and Frohlich, 2007; Marsh et al., 2011). Study site selection was based on persistent dugong pres-

ence in this area as representative of conditions in coastal port environs to provide proof of concept for using acoustic telemetry on dugongs.

Data analyses from satellite and acoustic technologies were used to: 1) determine the efficacy of satellite and acoustic telemetry to define dugong movement patterns; 2) compare the benefits and limitations of each approach; 3) examine costs of each approach in relation to the amount and type of data provided and 4) relate telemetry data to the boundaries of a Go Slow area designed to protect dugongs and turtles from recreational vessel strike in an area of considerable recreational and commercial boat traffic. We also evaluate the relative merits of the two technologies for other species of air-breathing marine animals.

2. Materials and Methods

The movements of dugongs were examined in Moreton Bay, Queensland adjacent to Brisbane, the third largest city in Australia with a population over 2 million in 2011 and the nations third largest cargo port (AustralianGovernment, 2013). The study site, an important dugong habitat area (Lanyon, 2003; Chilvers et al., 2005), includes both shallow and deep water regions in the Eastern Banks-South Passage area adjacent to Moreton and North Stradbroke Islands (Figure 1). The multiple-use Moreton Bay Marine Park encompasses the entire bay and adjacent waters and includes a range of no-take, limited activity and Go Slow zones. Water depths within the study site ranged from 2 to 20m with variable benthic habitat types including sand and seagrass (Roelfsema et al., 2009). The study site was defined by two areas: the acoustic telemetry array and the Moreton Bay Region (Figure 1).

Field Methods. For deployment of the acoustic array, an area dominated by seagrass in eastern Moreton Bay was selected because it consistently supports large numbers of dugongs (Lanyon, 2003). An array of 28 acoustic receivers (VR2W, Vemco, NS, Canada) was installed over 170 km^2 of this high density dugong habitat (Figure 1). Acoustic receivers were deployed on paving slabs with metal poles, auger anchors or float and anchor systems depending on depth and current. The array was deployed in March 2012, removed in December 2012 and redeployed at the same locations in May 2013.

Dugongs were captured in seagrass habitats on the Eastern Banks in July - September 2012 and July 2013 using the rodeo method developed by Marsh and Rathbun (1990) and refined by Lanyon et al. (2002). For each dugong, total body length was measured (cm) in a straight line from snout to fluke notch, sex was noted and a titanium ID tag, satellite transmitter and an acoustic transmitter were attached as standard protocol (Limpus, 1992). An ARGOS GPS transmitter (Gen 4 Marine Unit, Telonics, USA) was attached to 21 dugongs using a 3m tether and padded tailstock harness developed by Marsh and Rathbun (1990) and modified following Holley et al. (2006) in

2012. In 2013, the harness design was altered again based on the design used for tracking manatees (J. Powell, *pers. comm.*). Both harness designs used here incorporated a weak link designed to break under stress to enable harness release if the tether snagged and corrodible links designed to release the tailstock harness and tether after several months.

An ARGOS GPS transmitter (Gen 4 Marine Unit, Telonics, USA) was attached to each dugong using a 3 m tether and padded tailstock harness developed by Marsh and Rathbun (1990) and modified following Holley et al. (2006) in 2012. In 2013, the harness design was altered based on the design used for tracking manatees (J. Powell, *pers. comm.*). Both harness designs incorporated a weak link designed to break under stress to enable harness release if the tether snagged, and a corrodible link to release the harness and tether after several months.

The ARGOS GPS transmitters were programmed to emit a GPS position every hour. Location data for each animal were collected daily through the ARGOS website via the unique satellite tag ID. GPS data were available after converting ARGOS DS (all satellite messages) data using the Telonics Data Converter software (Telonics Inc. USA, 2007). These data were used for all analyses after filtering as outlined below. Location data were defined from the time the dugongs were released until a transmitter stopped transmitting or detached. Immediate post-capture locations were not removed from the dataset as studies of the behaviour of dugongs fitted with time-depth recorders (TDR) in 2012 indicated no behavioural changes after capture and handling (Hagihara et al., 2011). The tag detachment date was determined by the characteristics of the animals track. While attached, the track pattern was visibly irregular and after detachment the track reflected drift with the current. The clear difference between the pre- and post- detachment tracks enabled accurate estimation of the overall time of GPS transmitter deployment and aided tag recovery. All tracking data were truncated at the estimated detachment date, to ensure activity spaces excluded drift data.

Each tailstock harness was fitted with an acoustic transmitter (V16TP, Vemco, NS, Canada) to facilitate acoustic tracking. Acoustic transmitters had an estimated battery life of 824 days and emitted a unique code ID, depth (m) and temperature (°C) with data transmitted at 69 kHz at a pseudo-random interval every 45 - 90 seconds. The pseudo-random repeat rate was used to avoid signal collision with other deployed transmitters. Acoustic receivers detected the presence of acoustic transmitters that passed within 500 m based on data collected from moored sentinel tags in the study site (M. Heupel unpublished data). Data were downloaded in November 2012, August 2013, December 2013 and April 2014.

Data Filtering. Data from GPS and acoustic transmitters were standardised by binning into three hour periods to allow direct comparisons of the data from the two tech-
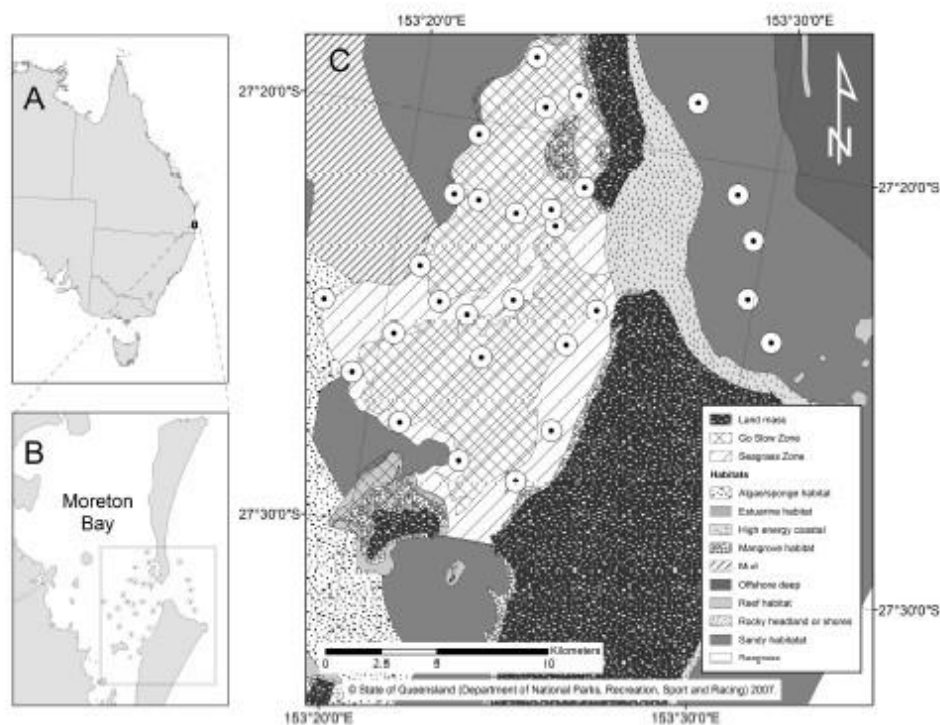
Figure 1: The study site located on A) the mid-eastern Australian coast. Research was conducted within B) the Moreton Bay Region and C) the acoustic array. The acoustic array encompassed a variety of habitats as indicated in the figure legend. The acoustic receiver locations were mostly deployed in areas mostly dominated by seagrass as indicated by the symbols.

nologies and to minimize autocorrelation. GPS data binning and filtering were accomplished using a custom R script based in part on previous speed-filters (McConnell et al., 1992; Flamm et al., 2001; Austin et al., 2003; Freitas et al., 2008). GPS data filters included filtering to: 1) eliminate duplicate times or duplicate consecutive locations, 2) retain only Successful and Resolved QFD data (i.e., the most accurate and most reliable data) and, 3) remove spurious consecutive data points that resulted in calculated speeds greater than 20 km/hour for maximum burst swimming speed (Marsh et al., 1981) or calculated speeds greater than 10 km/hour for maximum cruising speed (Marsh et al., 1981). Outlier data occurring on land were also deleted.

Acoustic monitoring does not provide GPS location data for individuals since the data consist of receiver based detections. To compare between methods, acoustic data were processed to provide positional locations for individuals using a centre-of-activity approach (Simpfendorfer et al., 2002) that produced mean locations from detections in each three hour time bin. Animal positions were calculated based on a weighted mean of the number of detections at each receiver in the array within each time period.

Duration of Tracking. All GPS data from the Moreton Bay Region (Figure 1B) were used to analyse the duration of satellite tag deployment; the duration of acoustic tag deployment was estimated from the data recorded by the array. A subset of 21 consecutive days of tracking for 13 individuals (see Supplementary Material Appendix A for dates) was used for detailed comparative analysis for indices derived from GPS and acoustic data within both the Moreton Bay Region and the acoustic array (Table 1). The range of 21 consecutive days was the maximum number of days that data were simultaneously available from both technologies for the greatest number of dugongs. Further, using the same time range for all individuals enabled the calculation of composite estimates of activity space of all individuals within the array. GPS data only were used to calculate Array Presence, Seagrass Presence and Go Slow Zone Presence because those analyses are a percentage of the movement in the Moreton Bay region (not only within

Table 1: Analyses applied to the 21 day subset of GPS and acoustic data from 13 dugongs within the Moreton Bay region (MBR) (i.e., including areas beyond the acoustic array Ref.1-5) and comparison of acoustic and GPS data within the array (Ref. 6-8) where MCP = minimum convex polygon, KUD = kernel utilisation distribution.

Ref	Term	Description	Use
1	Array Presence	Percentage of GPS postions inside the acoustic array relative to the MBR	Calculate proportion of locations within the acoustic array
2	Seagrass Presence	Percentage of GPS positions inside seagrass beds relative to the MBR	Calculate proportion of locations within the seagrass
3	Go Slow Zone Presence	Percentage of GPS postions inside the Go Slow Zone relative to the MBR	Calculate proportion of locations within the Go Slow Zone
4	Array Use	GPS MCP within the acoustic array relative to GPS MCP of movement the entire MBR	Measure the overlap in area between MBR
5	Spatial Overlap: MCP	Measure of overlap between acoustic and GPS MCP areas within array	Determine how similar MCP area estimates were between methods
6	Spatial Overlap: 50%	Measure of overlap between acoustic KUD and GPS 50% KUD areas within array	Determine how similar 50% KUD estimates were between methods
7	Spatial Overlap: 95%	Measure of overlap between acoustic KUD and GPS 95% KUD areas within array	Determine how similar 95% KUD estimates were between methods

the acoustic array itself).

Comparison of Acoustic and GPS Data Outputs. Eight dugongs were omitted from the analyses because their GPS transmitters detached after a few days or because they remained within the array for only a few days (See Supplementary Material Appendix A). Minimum convex polygons (MCP) were calculated to define the extent of movement of individuals. Space use was further refined by calculating 50% and 95% kernal utilisation distributions (KUD). The 50% KUD represents the core use area of an individual while the 95% KUD represents the extent of movement, similar in scale to MCP estimates. Acoustic telemetry data were restricted to the confines of the acoustic array but the GPS data extended to the Moreton Bay Region. Composite activity space estimates were produced by combining the 13 individual data files into a single file each for GPS and acoustic tracking datasets respectively.

MCPs were calculated using the using the Convex Hull tool in ArcGIS 10.1 (ESRI, 2013). KUDs were calculated using the kde and isopleth tools in the Geospatial Modelling Environment (Beyer, 2012). KUDs are sensitive to sample size and smoothing parameter (Millspaugh et al., 2006; Pillans et al., 2014). After exploratory data analysis, likelihood cross-validation (CVh) was chosen as the most biologically relevant smoothing parameter to compare the acoustic and GPS KUDs given the small sample sizes present (Seaman and Powell, 1996; Horne and Garton, 2006); e.g., sample sizes for 21-day acoustic activity centres size were less than 44. This approach is consistent with Gredzens et al.'s 2014 work on dugong home ranges. Land masses were excluded from all KUDs and MCPs using the XTools Pro 9.2 extension for ArcGIS (DataEast, 2013).

Size and overlap of activity spaces (21 day data for 13 dugongs). Activity space estimates were used to define the amount of space used and identify whether different metrics (MCP, KUD) produced overlapping spatial outputs. Intersections of activity space estimates were calculated between (GPS and acoustic) MCPs, 50% KUDs and 95% KUDs for individuals using the Intersection tool in ArcGIS. Areas of intersection were calculated and the ratio of intersected area to GPS area calculated as a percentage for each individual. The percentage of intersection provided an indication of the level of agreement between activity space estimates.

Day-Night Comparisons. Data from the composite 21 day GPS and acoustic tracking data were divided into day (0600 to 1800 hrs) and night (1800 to 0600 hrs) time periods. Activity space estimates were used to define the amount of space used during day and night periods. Intersections of activity space estimates were calculated between (GPS and acoustic) MCPs, 50% KUDs and 95% KUDs for the composite data set using the Intersection tool in ArcGIS. Areas of intersection were calculated and the ratio of intersected area to GPS area calculated as a percentage for the composite data set. The percentage of intersection provided an indication of whether different areas were used during the day or night.

Stability of Activity Space. Patterns of residency and habitat usage within Moreton Bay, the acoustic array, the seagrass area, and Go Slow Zone (Figure 1C) for each dugong were estimated using indices of time, distance and area (Table 1). To determine whether the full extent of activity space had been identified based on GPS and acoustic telemetry, activity space stability was calculated using

Table 2: Activity spaces of the 13 dugongs within the array over the 21 day periods using both GPS and acoustic data.

Tag ID	GPS	Acoustic	Spatial Overlap (%)	GPS	Acoustic	Spatial Overlap (%)	GPS	Acoustic	Spatial Overlap (%)
QA30696	93.4	12.1	12.3	6.8	5.4	24.4	46.5	34.4	50.3
QA30723	94.5	54.5	52.7	10.2	15.7	2.1	68.3	92.4	72.4
QA30677	39.1	61.2	69.3	5.6	26.6	100.0	24.5	169.5	100.0
QA30541	45.0	15.4	33.6	3.3	3.5	42.8	22.1	24.2	60.3
QA30710	104.4	181.1	99.7	10.2	48.3	100.0	81.5	247.1	95.3
QA30676	31.5	14.7	46.6	5.8	1.1	7.3	22.5	7.1	20.9
QA30712	101.0	42.5	41.8	5.9	0.5	0.9	39.1	4.5	8.3
QA30694	41.4	52.8	88.4	2.9	1.3	3.4	16.7	9.2	15.8
QA30709	34.2	21.9	44.9	3.7	10.2	88.9	19.3	56.8	88.6
QA18399	122.1	84.9	68.9	7.4	4.9	19.3	61.9	38.6	33.3
K88240	67.5	50.0	72.2	3.1	7.6	44.4	33.2	47.3	59.8
T71561	113.9	104.8	85.1	85.0	17.0	55.6	55.5	95.5	74.5
QA33315	93.3	37.2	38.6	2.5	8.2	0.0	46.5	54.2	45.0
Composite	167.1	196.0	92.2	6.2	1.2	4.5	64.0	16.3	11.4
Mean	75.5	56.4	58.0	5.8	11.6	376	41.4	67.8	55.7
SD	33.2	46.5	25.0	2.7	13.3	38.1	20.8	70.5	30.2

cumulative area analysis. Cumulative analysis consisted of weekly MCP areas summed across weeks (e.g. week 1+week 2, week 1+week 2+week 3) to determine whether activity space plateaued over time.

Cost Comparisons. To determine the cost effectiveness of acoustic versus satellite telemetry, the cost of tracking dugongs fitted with GPS and acoustic transmitters was compared for nine scenarios. Scenarios included the two tracking methods (GPS and acoustic) times three levels of logistical difficulty: 1) easy catching and accessible location (e.g. Moreton Bay), 2) difficult catching and accessible location (e.g. Townsville), and 3) difficult catching and remote location (e.g. Boigu, Torres Strait). In addition, scenarios with and without an established acoustic array were considered. Costs were based on dugong catching trips conducted by James Cook University in 2012 and 2013 (e.g., Gredzens et al., 2014). Logistical assumptions are presented as Supplementary Material Appendix B. Total cost estimates were based on the cost of different parameters, including equipment, travel, salary, and operating costs. Only direct costs were considered.

3. Results

The tailstock harness that contained the acoustic tag tended to remain on the dugong longer than the tether to which the GPS transmitter was attached. Thus the mean tracking period for acoustic transmitters was 107 days (SD = 95 days, median = 60 days), significantly greater than the mean tracking period of 39 days for GPS (SD = 26 days, median = 35 days, Welch Two Sample t-test, p <0.01). Four dugongs were still being acoustically tracked at the last download in early April 2014, 256-266 days after

deployment. The longest GPS track period was 108 days which reflected the battery life of the GPS transmitter.

Table 3: Comparison of the presence of 13 dugongs and composite data in the acoustic array, seagrass and Go Slow Zone over the 21 day periods in which each animal was tracked.

Tag ID	GPS Points in MCP	Array Presence (%)	Seagrass Presence (%)	Go Slow Zone Presence (%)
QA30696	157	87.9	77.1	79.0
QA30723	170	88.8	68.8	69.4
QA30677	171	94.7	89.5	91.8
QA30541	65	92.3	83.1	84.6
QA30710	141	83.0	85.8	79.4
QA30676	172	98.3	95.3	97.7
QA30712	162	77.8	73.5	73.5
QA30694	160	84.4	60.6	17.5
QA30709	169	91.7	89.9	89.3
QA18399	121	76.0	63.6	60.3
K88240	162	93.8	84.6	87.7
T71561	141	88.7	80.1	76.6
QA33315	173	97.1	42.2	63.6
Composite	1964	89.1	76.3	74.6

Habitat use was calculated from GPS data and compared for 13 dugongs. Array Presence values, Seagrass Presence values and Go Slow Zone Presence values all showed high presence of dugongs in these areas (Table 3). Despite this, only five individuals had Go Slow Zone Presence values greater than 80% and one animal spent less than 18% of its time within the Go Slow Zone. Habitat use from composite data also indicated that most of the dugongs time was spent within these three Go Slow areas. Array Presence for 13 dugongs over the 21 day period had

a mean value of 78% (median = 90%; SD = 23%; range = 32-96%) providing further evidence that the activity spaces of tagged dugongs were mostly within the acoustic array.

Size and Overlap of Activity Spaces (21 day data for 13 dugongs). The estimates of MCPs, 50% KUDs and 95% KUDs varied between dugongs for the two technologies (Table 2), which is to be expected as the data generated by the two techniques are not directly comparable. The results were very close for some dugongs, but varied for others (Figure ??), suggesting individual dugong movements played a role in resulting activity space estimates. However, these metrics also reflect the acoustic array geometry, the number of acoustic receivers recording individual animal signals and the analytical methods used. The intersection of (GPS and acoustic) MCPs as a percentage of the GPS MCP ranged from 12% to almost 100% (Table 2). The corresponding figures for 50% KUDs ranged from 0-100%, and 8-100% for 95% KUDs. The composite GPS and acoustic MCPs overlapped by 92%, composite 50% KUDS by 4.5%, and composite 95% KUDs by 11%. These data indicate that a reliable picture of the activity space use of dugongs in the confines of an acoustic array can be obtained by acoustic tracking several animals.

Day-Night Comparisons (21 day data for 13 dugongs). The resulting MCP, 50% KUD and 95% KUD estimates calculated for day and night periods were nearly identical indicating that for the 13 animal composite data there was little difference in behaviour between day and night periods. The intersections of the acoustic and GPS day and night MCPs were 87% (day) and 84% (night) as percentages of the corresponding GPS MCPs, indicating a high level of agreement. The overlap of KUD areas was much smaller with only 4.2% (day) and 20.3% (night) overlap of the 50% KUDs and 33.8% (day), 25.0% (night) overlap of the 95% KUDs. Although these 50% and 95% KUD ratios were small, the mapped KUDs (Figure ??C) show that the locations of the respective GPS and acoustic 50% and 95% KUDs were spatially close. Thus comparisons using both technologies indicated little difference between day and night use of the array area by the tagged dugongs.

Stability of Activity Space. Analysis of cumulative MCP home ranges indicated space use of dugongs in the Moreton Bay Region continued to increase over five weeks for the 13 dugongs for which the requisite acoustic tracking data were available. However, MCP estimates stabilised after two weeks for the nine dugongs tracked using GPS technology. These data suggest that during this short term study, GPS tracking captured the extent of movement more quickly than acoustic tracking although there was a high degree of overlap and agreement in activity space size using both methods (Figure 2). However, it is not possible to separate confounding influences of technology and the analytical methods used and so these conclusions are tentative.
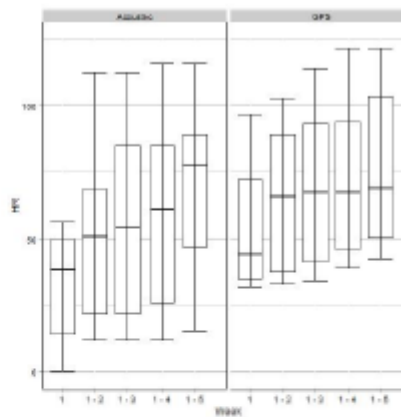
Figure 2: Cumulative space use of dugongs based on MCP analysis. The horizontal bar shows the median value of days tracked, boxes indicate 75th and 25th percentiles and whiskers show the maximum and minimum values of y (activity space area).

Cost Comparisons. Regardless of the method used, tracking is least costly in easily accessible areas where dugongs are easy to catch, such as in Moreton Bay. In areas where acoustic arrays are established, acoustic tracking is more economical than GPS tracking regardless of the scenario (Figure 3). However, if an array is not in place, it is likely to be more cost-effective to use GPS tracking unless tracking longevity is a priority or an array can also be used for other species to spread costs across projects or among collaborators. Difficulty of capture also increased costs because catching dugongs in areas of high turbidity will take a greater amount of time and necessitates the use of spotter aircraft compared with catching in clear water where dugongs are more easily spotted. A high proportion of the costs associated with GPS tracking are from equipment costs (>35%), whereas most (>50%) of the expenses with acoustic tracking are associated with operating costs. The proportion of operational costs increases by approximately 20% when acoustic arrays need to be deployed (see Supplementary Material Appendix C).

4. Discussion

Data indicated that both satellite and acoustic telemetry produced reliable presence and movement data for individual dugongs. When the dugongs were within the range of the acoustic array, there was relatively good correspondence between the overall space use measures derived from GPS and acoustic transmitters, demonstrating that acoustic tracking is a potentially valuable and cost-effective tool for monitoring local dugong habitat use in environments equipped with acoustic receiver arrays.

The duration of acoustic tracking was greater than that of satellite tracking although the range of tracking days
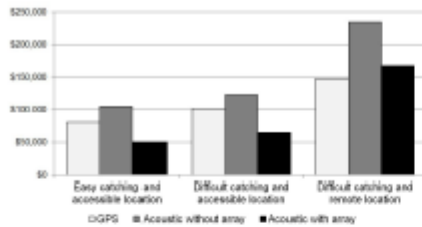
Figure 3: Costs for each tracking method for each scenario; Scenario 1- easy catching and accessible location (e.g., Moreton Bay, where the water is clear); Scenario 2 - difficult catching and accessible location (e.g., Townsville, where the water has high levels of suspended sediment); and Scenario 3 - difficult catching and remote location (e.g., Boigu, Torres Strait, where the water can be clear but mangroves and corals make for difficult access).

was highly variable for both technologies largely due to the attachment mechanism (see Supplementary Material Appendix A). The median number of days tracked for dugongs fitted with GPS tags was 35 days compared to 60 days for acoustic transmitters. The factors contributing to these differences in longevity between technologies include: 1) operational difficulties with the tether attachment in 2013, which caused several GPS units to detach in a few days; 2) the tether arrangement which is designed to break if the tether becomes entangled; 3) the duty cycle of the GPS transmitters which limited the battery life (108 days); 4) the corrodible link in the tailstock belt which in 2012 detached after a maximum of 69 days (before the array was disbanded) but lasted for up to 108 days in the redesigned tag arrangement in 2013 enabling the acoustic tracking to continue for more than 266 days and 5) acoustically tracked animals leaving the array area.

The requirement to maintain the GPS tag at the surface via a tether mechanism produces a significant limitation to tag life because of the need to incorporate a weak link in the attachment mechanism for animal welfare reasons (Deutsch et al., 1998; Reid et al., 2001). In contrast, acoustic tags are much smaller, producing less drag and enabling a more durable attachment (in this case a tailstock belt) with the capacity to provide data for longer periods. If the acoustic tags had been surgically implanted in the dugongs, the differences in the longevity of the two techniques should have been much greater. The acoustic tags have longevity of 894 days; the battery life of the GPS tags would have lasted no more than a year even with a duty-cycle designed to maximise battery-life.

Both technologies provided important insights into habitat use within the array even though overlaps of space use estimates of satellite and acoustic telemetry data within the confines of the acoustic array were variable. Comparison of core use areas (50% KUD) indicated low overlap in location estimates for approximately half of individuals. However, for two individuals, core area overlap was 100% indicating the two methods captured the location

of these individuals equally well. Comparison of extent of movement (MCP and 95% KUD) showed greater than 50% overlap for over half of the individuals providing results similar to those for core areas. In most cases MCPs based on acoustic estimates were smaller than those for satellite tags, presumably a result of the spacing and distance between receivers in the array which was, of course, not a factor for satellite locations. In contrast KUD estimates based on acoustic detection were larger than for GPS data. Again, this was likely due to the geometry of the array in this case because of the relatively sparse nature of the array (non-overlapping detection radii) and consequent reduction in positional accuracy. The relative differences between methods were smaller for the 95% KUD than for the 50% KUD, probably for the same reason. The differences in the relative size of MCP and KUD estimates for the two methods highlight the unavoidable tension between acoustic array size and accuracy.

Cumulative home range analyses indicated that home ranges did not increase by large amounts over the tracking period which also suggests residence within defined spaces for the dugongs that did not leave the area during the tracking period. Spatial residency in various locations was high for many individuals, a result consistent with (Sheppard et al., 2006). Although most of these data only span periods of several weeks, they suggest high use of specific areas over the short to medium term, a result confirmed by our 21-day analyses. Most data collected during the 21 day periods (>75% of satellite locations) were within the acoustic array. Similarly, 70% of individuals spent over 85% of their time within the array when considering the entire GPS tracking period with limited movement into deeper regions outside the barrier islands. This pattern indicates high fidelity to this region and highlights the importance of the seagrass meadows around the Moreton Banks for dugongs as has been established by other studies (e.g., Lanyon, 2003) and is part of the rationale for the Go Slow Zone on the Eastern Banks.

Our studies indicated that in the area of the array, there was very little evidence of diurnal differences in dugongs activity space. Most information suggests that sirenians do not have well defined periods of circadian activity (see Marsh et al., 2011, for review). This lack of marked diel activity patterns is consistent with the absence of a pineal organ in the brain of sirenians, which can act as a regulator of daily rhythms in temperate zone mammals (Ralph et al., 1985).

The boundaries of the Go Slow Zone overlap much of the mapped seagrass areas. All tracked individuals spent large amounts of time over seagrass areas so it was not surprising that the spatial residence of most individuals examined in the 21 day analyses overlapped extensively with Go Slow Zones (¿60% of space used was in Go Slow Zones). However, location data indicated that individuals regularly moved in and out of the Go Slow Zone. This result suggests that the spatial extent of the Go Slow Zone is providing some protection for dugongs from boat
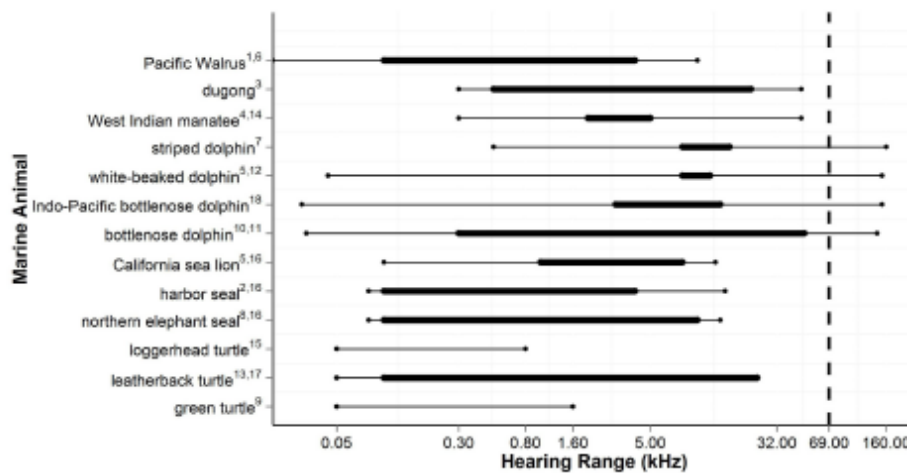
Figure 4: Comparison of marine animals' hearing ranges with the frequency of the acoustic transmitter, 69 kHz. (shown by a dashed line). Thin lines represent animal hearing ranges and thick lines represent vocalisation ranges. ([1]Stirling et al., 1987, *Odobenus rosmarus rosmarus*, [2]Hanggi and Schusterman, 1994, *Phoca vitulina*, [3]Anderson and Barclay, 1995, [4]Gerstein et al., 1999, *Trichechus manatus*, [5]Wartzok and Ketten, 1999, *Zalophus californianus*, [6]Kastelein et al., 2002, *Odobenus rosmarus divergens*, [7]Kastelein et al., 2003, *Stenella coeruleoalba*, [8]Southall et al., 2003, *Mirounga angustirostris*, [9]Bartol and Ketten, 2013, *Chelonia mydas*, [10]Popov et al., 2007, *Tursiops truncatus*, [11]Sayigh et al., 2007, *Tursiops truncatus*, [12]Nachtigall et al., 2008, *Lagenorhynchus albirostris*, [13]Dow Piniak et al., 2012, *Dermochelys coriacea*, [14]Gaspard III et al., 2012, *Trichechus manatus latirostris*, [15]Martin et al., 2012, *Caretta caretta*, [16]Reichmuth et al., 2013, *Zalophus californianus*, [17]Ferrara et al., 2014, *Dermochelys coriacea*, [18]Gridley et al., 2014, *Tursiops aduncus*)

strikes but that it is unlikely to be 100% effective. There was a high degree of individual variability in the number of recorded locations within the Go Slow Zone indicating that some dugongs will receive more protection than others from that regulatory initiative. Thus, our data indicate that the current Go Slow Zone does not provide full protection for all dugongs within this region but will mitigate some of the potential interactions with boaters.

Cost is a big factor in decision making for both scientists and funding agencies. Which methodology is more appropriate should be considered in light of the scientific question asked as well as resource availability. Cost-benefit analysis indicated that each method (GPS vs acoustic) can be justifiably costed depending on questions and resources. Satellite telemetry costs are largely related to equipment or capital type expenses while acoustic telemetry costs are dominated by the installation and maintenance of the network resulting in higher personnel costs. Array costs would of course have been much higher if we had installed a denser array with overlap between the ranges of individual receivers.

A large, national network of acoustic receivers (the Australian Animal Tagging and Monitoring System facility of the Integrated Marine Observing System) provides a platform for the detection of acoustically tagged animals at a broad scale (Heupel and Simpfendorfer, 2014). This network includes receivers in an array of habitats around

Australia although there is no guarantee equipment will be located in areas useful to specific study species. Satellite tracking of dugongs had one distinct advantage over acoustic tracking; it could record locations for individuals beyond the boundaries of the acoustic array. This is an important consideration for dugongs as animals are known to make large and meso-scale movements (Sheppard et al., 2006). For example, our GPS tracking data showed all animals moved beyond the boundaries of the acoustic array and two animals moved over 250 km to Hervey Bay.

This raises the question about which is easier or cheaper to cost and support: Equipment or people. The answers to this question will vary based on location, agency and funding body. Disregarding costs that are common across approaches at the same location (e.g., animal capture costs), it is more cost-effective to use acoustic telemetry if an array already exists within the focal area and if the research questions are directly related to a local study site. If broader-scale movement questions are being asked, a larger acoustic network would be required and satellite telemetry would be a more cost effective option. Costs of both approaches also differ depending on the study site. Working in remote locations is better suited to satellite telemetry than acoustic telemetry, a direct result of the differences in costs within approaches.

The suitability of using acoustic and satellite tracking technologies with dugongs was dependent upon animal
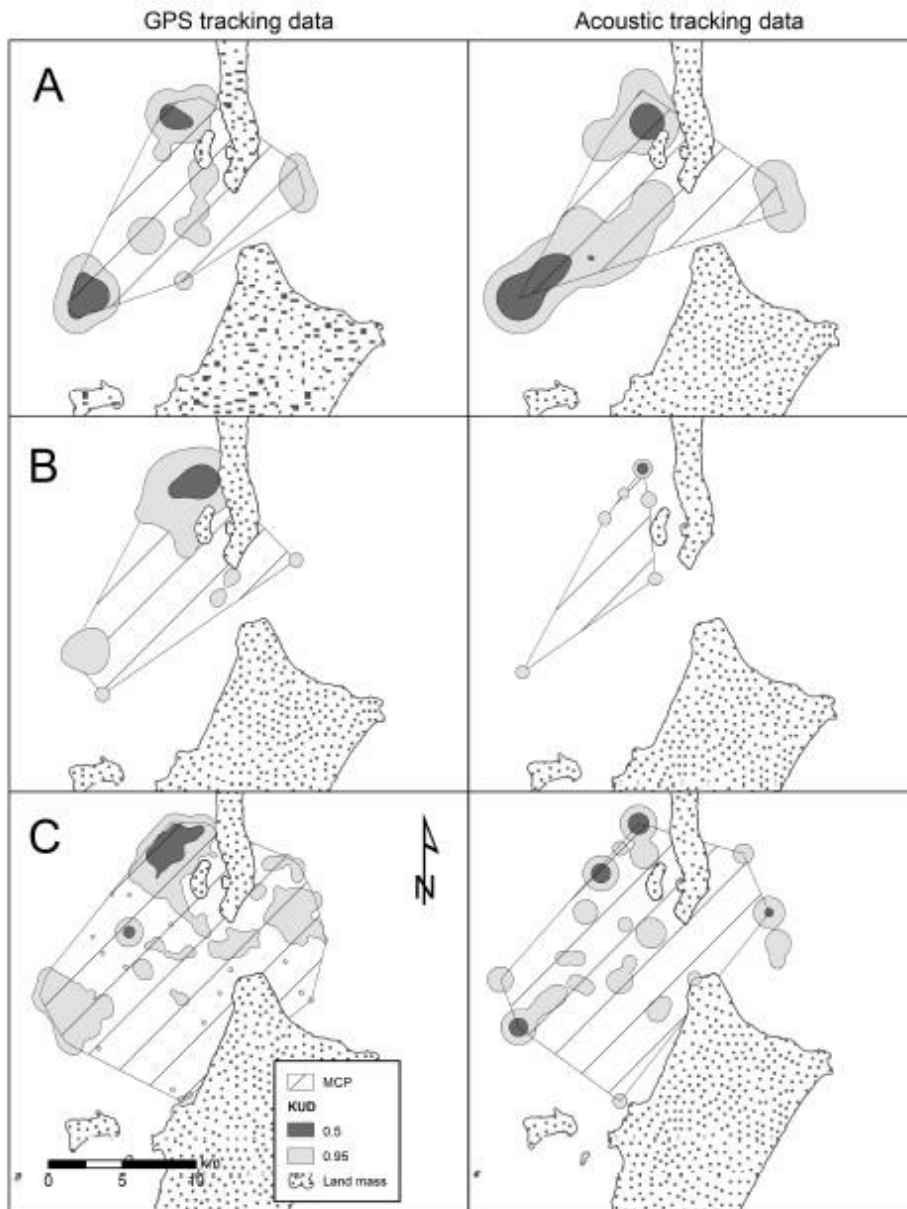
Figure 5: Maps illustrating the variation in MCP, 50% KUD and 95% KUD estimates for the 21-day data using GPS (left hand column) and acoustic (right hand column) technologies. A) An individual with good agreement between the methods where MCP, 50% KUD and 95% KUD estimates were very similar for GPS and acoustic tracking data. B) An individual with low agreement between methods where 50% KUD estimates had similar locations but MCP and 95% KUD estimates were different in area although locations were consistent. C) Comparison of daytime composite data from the 13 animals.

size and hearing range of the species. When considering acoustic tracking for other coastal marine mammals, the use of acoustic transmitters makes size less critical smaller species could be tracked. Hearing range of the species is important: 69 kHz is within the hearing range of many marine mammals, especially dolphins (Wartzok and Ketten 1999; Ketten 2000; D. Ketten *pers. comm.*) and could interfere with their intra-species communications or searching for prey. Hearing ranges of most pinnipeds and sea turtles have maxima well less than 69 kHz, the frequency of the acoustic transmitter and thus might be considered suitable candidates for acoustic tracking (Wartzok and Ketten 1999; Ketten 2000; D. Ketten *pers. comm.*, 2014). Tubelli et al. (2012) predicted that the hearing range of the minke whale is below 10 kHz making it another possible candidate. Dolphins, however, appear to have hearing ranges clearly including the 69 kHz transmitter frequency. Therefore acoustic tracking using currently available technologies is unlikely to be suitable for all marine mammal species.

5. Conclusion

Both GPS and acoustic technologies provided reliable location data for individuals for comparable periods of time although failure of the attachment device used in this study led to early loss of satellite transmitters in many cases. The two technologies each have benefits and limitations in the data they provide. Cost-benefit analysis indicated that each method (GPS vs acoustic) can be appropriate depending on questions and resources. The cost-effectiveness of using acoustic rather than GPS technology for tracking dugongs clearly depends on the research question and the location. When the dugongs are within the range of an acoustic array, this research has shown overall good correspondence between the MCPs and KUDs of the GPS and acoustic transmitters.

Ultimately, the cost effectiveness of the method applied must be driven by the species and the research question. Researchers should then consider what resources are on hand. Is an existing array present or can a collaborative array be established? Is the study site remote? Is staff time limited? Does the animal exhibit stable residency? Careful consideration of available resources in conjunction with the question being addressed should lead to a clear conclusion about which of these two technologies is most cost effective in gaining a research outcome.

We conclude that acoustic tracking is a potentially valuable and cost-effective tool for monitoring dugong habitat use in environments equipped with acoustic receiver arrays. As dugongs are not wilderness animals (Marsh et al., 2011) and ports in developed countries are increasingly fitted with acoustic arrays, we conclude that acoustic transmitters should become the preferred methods of tracking dugongs habitat use in the vicinity of ports because they enable more animals to be tracked for longer and with fewer animal welfare problems than GPS transmitters. We expect similar methods will work as well for some other marine species but advise that each species hearing and sound production ranges will need to be considered.

References

Anderson, P. K., Barclay, R. M. R., 1995. Acoustic signals of solitary dugongs: Physical characteristics and behavioral correlates. Journal of Mammalogy 76 (4), 1226–1237.

Austin, D., McMillan, J. I., Bowen, W. D., 2003. A three-stage algorithm for filtering erroneous argos satellite locations. Marine Mammal Science 19 (2), 371–383.

AustralianGovernment, 2013. State of australian cities 2013: Brisbane. Report, Department of Infrastructure and Transport.

Bartol, S., Ketten, D. R., 2013. Sea turtle and pelagic fish sensory biology: Developing techniques to reduce sea turtle bycatch in longline fisheries. technical memorandum nmfs-pifsc-7. Report, National Ocean and Atmospheric Administration (NOAA), U.S. Dept. of Commerce.

Baumgartner, M., Freitag, L., Partan, J., Ball, K., Prada, K., April 2008. Tracking large marine predators in three dimensions: The real-time acoustic tracking system. Oceanic Engineering, IEEE Journal of 33 (2), 146–157.

Beyer, H. L., 2012. Geospatial modelling environment (Version 0.7.2.1). (software).

Block, B. A., Jonsen, I. D., Jorgensen, S. J., Winship, A. J., Shaffer, S. A., Bograd, S. J., Hazen, E. L., Foley, D. G., Breed, G. A., Harrison, A. L., Ganong, J. E., Swithenbank, A., Castleton, M., Dewar, H., Mate, B. R., Shillinger, G. L., Schaefer, K. M., Benson, S. R., Weise, M. J., Henry, R. W., Costa, D. P., 2011. Tracking apex marine predator movements in a dynamic ocean. Nature 475 (7354), 86–90, 10.1038/nature10082.

Bograd, S. J., Block, B. A., Costa, D. P., Godley, B. J., 2010. Biologging technologies: New tools for conservation. introduction. Endangered Species Research 10, 1–7.

Burgess, E. A., Lanyon, J. M., Brown, J. L., Blyde, D., Keeley, T., 2012. Diagnosing pregnancy in free-ranging dugongs using fecal progesterone metabolite concentrations and body morphometrics: A population application. General and Comparative Endocrinology 177 (1), 82–92.

Calleson, C. S., Frohlich, R. K., 2007. Slower boat speeds reduce risks to manatees. Endangered Species Research 3, 295–304.

Chilvers, B. L., Lawler, I. R., Macknight, F., Marsh, H., Noad, M., Paterson, R., 2005. Moreton bay, queensland, australia: an example of the co-existence of significant marine mammal populations and large-scale coastal development. Biological Conservation 122 (4), 559–571.

Cooke, S. J., 2008. Biotelemetry and biologging in endangered species research and animal conservation: Relevance to regional, national and iucn red list threat assessments. Endangered Species Research 4, 165–185.

Costa, D. P., Breed, G. A., Robinson, P. W., 2012. New insights into pelagic migrations: Implications for ecology and conservation. Annual Review of Ecology, Evolution, and Systematics 43 (1), 73–96.

DataEast, 2013. X Tools Pro (version 9.2), ArcView Extension. (software).

Deutsch, C. J., Bonde, R. K., Reid, J. P., 1998. Radio-tracking manatees from land and space: Tag design, implementation, and lessons learned from long-term study. Marine Technology Society. Marine Technology Society Journal 32 (1), 18–29.

Dobbs, K., Fernandes, L., Slegers, S., Jago, B., Thompson, L., Hall, J., Day, J., Cameron, D., Tanzer, J., Macdonald, F., Marsh, H., Coles, R., 2008. Incorporating dugong habitats into the marine protected area design for the Great Barrier Reef Marine Park, Queensland, Australia. Ocean & Coastal Management 51 (4), 368–375.

Dow Piniak, W. E., Eckert, S. A., Harms, C. A., Stringer, E. M., 2012. Underwater hearing sensitivity of the leatherback sea turtle (Dermochelys coriacea): Assessing the potential effect of anthropogenic noise. Report, U.S. Department of the Interior, Bureau of Ocean Energy Management, Headquarters, Herndon, VA. OCS Study BOEM 2012-01156.

ESRI, 2013. ArcGIS (Version 10.1). (software).

Fernandes, L., Dobbs, K., Day, J., Slegers, S., 2010. Identifying biologically and physically special or unique sites for inclusion in the protected area design for the great barrier reef marine park. Ocean & Coastal Management 53 (2), 80–88.

Ferrara, C. R., Vogt, R. C., Harfush, M. R., Sousa-Lima, R. S., Albavera, E., Tavera, A., 2014. First evidence of leatherback turtle (Dermochelys coriacea) embryos and hatchlings emitting sounds. Chelonian Conservation and Biology 13 (1), 110–114.

Flamm, R. O., Ward, L. I., Weigle, B. L., 2001. Applying a variable-shape spatial filter to map relative abundance of manatees (Trichechus manatus latirostris). Landscape Ecology 16 (3), 279–288.

Freitas, C., Lydersen, C., Fedak, M. A., Kovacs, K. M., 2008. A simple new algorithm to filter marine mammal Argos locations. Marine Mammal Science 24 (2), 315–325.

Gales, R., Alderman, R., Thalmann, S., Carlyon, K., 2012. Satellite tracking of long-finned pilot whales (Globicephala melas) following stranding and release in tasmania, australia. Wildlife Research 39 (6), 520–531.

Gaspard III, J. C., Bauer, G. B., Reep, R. L., Dziuk, K., Cardwell, A., Read, L., Mann, D. A., 2012. Audiogram and auditory critical ratios of two florida manatees (Trichechus manatus latirostris). The Journal of Experimental Biology 215, 1442–1447.

GBRMPA, 1981. Nomination of the great barrier reef by the commonwealth of australia for inclusion in the world heritage list. Report, UNESCO 37pp.

Gerstein, E. R., Gerstein, L., Forsythe, S. E., Blue, J. E., 1999. The underwater audiogram of the west indian manatee (Trichechus manatus). The Journal of the Acoustical Society of America 105 (6), 3575–3583.

Grant, P. B. C., Lewis, T. R., 2010. High speed boat traffic: A risk to crocodilian populations. Herpetological Conservation and Biology 5 (3), 456–460.

Gredzens, C., Marsh, H., Fuentes, M. M. P. B., Limpus, C., Shimada, T., Hamann, M., 2014. Satellite tracking of sympatric marine megafauna can inform the biological basis for species co-management. PLoS ONE 9 (6), 1–12.

Gridley, T., Cockcroft, V. G., Hawkins, E. R., Blewitt, M. L., Morisaka, T., Janik, V. M., 2014. Signature whistles in free-ranging populations of indo-pacific bottlenose dolphins, Tursiops aduncus. Marine Mammal Science 30 (2), 512–527.

Grothues, T. M., 2009. A review of acoustic telemetry technology and a perspective on its diversification relative to coastal tracking arrays. In: Nielsen, J. L., Arrizabalaga, H., Fragoso, N., Hobday, A., Lutcavage, M., Sibert, J. (Eds.), Tagging and tracking of marine animals with electronic devices. Vol. 9 of Reviews: Methods and technologies in fish biology and fisheries: Making fisheries management work:. Springer, pp. 77–90.

Hagihara, R., Jones, R. E., Sheppard, J. K., Hodgson, A. J., Marsh, H., 2011. Minimizing errors in the analysis of dive recordings from shallow-diving animals. Journal of Experimental Marine Biology and Ecology 399 (2), 173–181.

Hanggi, E. B., Schusterman, R. J., 1994. Underwater acoustic displays and individual variation in male harbour seals, Phoca vitulina. Animal Behaviour 48 (6), 1275–1283.

Hart, K. M., Hyrenbach, K. D., 2009. Satellite telemetry of marine megavertebrates: the coming of age of an experimental science. Endangered Species Research 10, 9–20.

Hazel, J., Lawler, I. R., Marsh, H., Robson, S., 2007. Vessel speed increases collision risk for the green turtle Chelonia mydas. Endangered Species Research 3, 105–113.

Hazen, E. L., Maxwell, S. M., Bailey, H., Bograd, S. J., Hamann, M., Gaspar, P., Godley, B. J., Shillinger, G. L., 2012. Ontogeny in marine tagging and tracking science: Technologies and data gaps. Marine Ecology Progress Series 457, 221–240.

Heupel, M. R., Semmens, J. M., Hobday, A. J., 2006. Automated acoustic tracking of aquatic animals: scales, design and deployment of listening station arrays. Marine and Freshwater Research 57 (1), 1–13.

Heupel, M. R., Simpfendorfer, C. A., 2002. Estimation of mortality of juvenile blacktip sharks, Carcharhinus limbatus, within a nursery area using telemetry data. Canadian Journal of Fisheries and Aquatic Sciences 59 (4), 624–632.

Heupel, M. R., Simpfendorfer, C. A., 2005. Using acoustic monitoring to evaluate MPAs for shark nursery areas: The importance of long-term data. Marine Technology Society Journal 39 (1), 10–18.

Heupel, M. R., Simpfendorfer, C. A., 2014. Importance of environmental and biological drivers in the presence and space use of a reef-associated shark. Marine Ecology Progress Series 496, 47–57.

Heupel, M. R., Webber, D. M., 2012. Trends in acoustic tracking: Where are the fish going and how will we follow them?

Hodgson, A. J., Marsh, H., 2007. Response of dugongs to boat traffic: The risk of disturbance and displacement. Journal of Experimental Marine Biology and Ecology 340 (1), 50–61.

Holley, D., Lawler, I., Gales, N., 2006. Summer survey of dugong distribution and abundance in Shark Bay reveals additional key habitat area. Wildlife Research 33 (3), 243–250.

Horne, J. S., Garton, E. O., 2006. Likelihood cross-validation versus least squares cross-validation for choosing the smoothing parameter in kernel home range analysis. The Journal of Wildlife Management 70 (3), 641–648.

Jaine, F. R. A., Rohner, C. A., Weeks, S. J., Couturier, L. I. E., Bennett, M. B., Townsend, K. A., Richardson, A. J., 2014. Movements and habitat use of reef manta rays off eastern australia: Offshore excursions, deep diving and eddy affinity revealed by satellite telemetry. Marine Ecology Progress Series 510, 73–86.

James, M. C., Andrea Ottensmeyer, C., Myers, R. A., 2005. Identification of high-use habitat and threats to leatherback sea turtles in northern waters: New directions for conservation. Ecology Letters 8 (2), 195–201.

Kastelein, R. A., Hagedoorn, M., Au, W. W. L., de Haan, D., 2003. Audiogram of a pacific dolphin (*Stenella coeruleoalba*). The Journal of the Acoustical Society of America 113 (2), 1130–1137.

Kastelein, R. A., Mosterd, P., van Santen, B., Hagedoorn, M., de Haan, D., 2002. Underwater audiogram of a pacific walrus (*Odobenus rosmarus divergens*) measured with narrow-band frequency-modulated signals. The Journal of the Acoustical Society of America 112 (5), 2173–2182.

Ketten, D. R., 2000. Cetacean ears. In: Au, W. W. L., Popper, A. N., Fay, R. R. (Eds.), Hearing by Whales and Dolphins. SHAR Series for Auditory Research. Springer-Verlag, New York, Ch. Cetacean Ears, pp. 43–108.

Knip, D. M., Heupel, M. R., Simpfendorfer, C. A., 2012a. Evaluating marine protected areas for the conservation of tropical coastal sharks. Biological Conservation 148 (1), 200–209.

Knip, D. M., Heupel, M. R., Simpfendorfer, C. A., 2012b. Mortality rates for two shark species occupying a shared coastal environment. Fisheries Research 125126 (0), 184–189.

Laist, D. W., Shaw, C., 2006. Preliminary evidence that boat speed restrictions reduce deaths of florida manatees. Marine Mammal Science 22 (2), 472–479.

Lanyon, J. M., 2003. Distribution and abundance of dugongs in Moreton Bay, Queensland, Australia. Wildlife Research 30 (4), 397–409.

Lanyon, J. M., Sneath, H. L., Kirkwood, J. M., Slade, R. W., 2002. Establishing a mark-recapture program for dugongs in Moreton Bay, southeast Queensland. Australian Mammalogy 24 (1), 51–56.

Limpus, C. J., 1992. Estimation of tag loss in marine turtle research. Wildlife Research 19 (4), 457–469.

Luczkovich, J. J., Sprague, Mark W.and Krahforst, C. S., Corbett, D. R., Walsh, J. P., 2012. Passive acoustics monitoring as part of integrated ocean observing systems. The Journal of the Acoustical Society of America 132 (3), 1915–1915.

Maitland, R. N., Lawler, I. R., Sheppard, J. K., 2006. Assessing the risk of boat strike on dugongs (*Dugong dugon*) at Burrum Heads, Queensland, Australia. Pacific Conservation Biology 12, 321–326.

Malone, T. C., 2004. The coastal component of the u.s. integrated ocean observing system. Environmental Monitoring and Assessment 81 (1-3), 51–62.

Mansfield, K. L., Wyneken, J., Porter, W. P., Luo, J., 2014. First satellite tracks of neonate sea turtles redefine the lost years oceanic niche. Proceedings of the Royal Society B: Biological Sciences 281 (1781).

Marsh, H., 2008. *Dugong dugon*, In: IUCN 2012. IUCN Red List of Threatened Species. (version 2012.1).

Marsh, H., Gardner, B. R., Heinsohn, G. E., 1981. Present-day hunting and distribution of dugongs in the Wellesley Islands (Queensland): Implications for conservation. Biological Conservation 19 (4), 255–267.

Marsh, H., O'Shea, T. J., Reynolds III, J. E., 2011. Ecology and Conservation of the Sirenia: Dugongs and Manatees. Conservation Biology 18. Cambridge University Press, New York.

Marsh, H., Rathbun, G. B., 1990. Development and application of conventional and satellite radio tracking techniqes for studying dugong movements and habitat use. Australian Wildlife Research 17, 83–100.

Martin, K. J., Alessi, S. C., Gaspard, J. C., Tucker, A. D., Bauer, G. B., Mann, D. A., 2012. Underwater hearing in the loggerhead turtle (*Caretta caretta*): a comparison of behavioral and auditory evoked potential audiograms. The Journal of Experimental Biology 215 (17), 3001–3009.

McConnell, B. J., Chambers, C., Fedak, M. A., 1992. Foraging ecology of southern elephant seals in relation to the bathymetry and productivity of the southern ocean. Antarctic Science 4 (04), 393–398.

Millspaugh, J. J., Nielson, R. M., McDonald, L., Marzluff, J. M., Gitzen, R. A., Rittenhouse, C. D., Hubbard, M. W., Sheriff, S. L., 2006. Analysis of resource selection using utilization distributions. The Journal of Wildlife Management 70 (2), 384–395.

Nachtigall, P. E., Mooney, T. A., Taylor, K. A., Miller, L. A., Ras-

mussen, M. H., Akamatsu, T., Teilmann, J., Linnenschmidt, M., Vikingsson, G. A., 2008. Shipboard measurements of the hearing of the white-beaked dolphin *Lagenorhynchus albirostris*. Journal of Experimental Biology 211 (4), 642–647.

Pendoley, K. L., Schofield, G., Whittock, P. A., Ierodiaconou, D., Hays, G. C., 2014. Protected species use of a coastal marine migratory corridor connecting marine protected areas. Marine Biology 161 (5), 1455–1466.

Pennisi, E., 2005. Satellite tracking catches sharks on the move. Science 310 (5745), 32–33.

Pillans, R. D., Bearham, D., Boomer, A., Downie, R., Patterson, T. A., Thomson, D. P., Babcock, R. C., 09 2014. Multi year observations reveal variability in residence of a tropical demersal fish, *Lethrinus nebulosus*: Implications for spatial management. PLoS ONE 9 (9).

Popov, V. V., Supin, Alexander Ya.and Pletenko, M. G., Tarakanov, M. B., Klishin, V. O., Bulgakova, T. N., Rosanova, E. I., 2007. Audiogram variability in normal bottlenose dolphins (*Tursiops truncatus*). Aquatic Mammals 33 (1), 24–33.

Ralph, C. L., Young, S., Gettinger, R., O'Shea, T. J., 1985. Does the manatee have a pineal body? Acta Zoologica 166, 55–60.

Raynor, R., 2010. The us integrated ocean observing system in a global context. Marine Technology Society Journal 44 (6), 26–31.

Reichmuth, C., Holt, M. M., Mulsow, J., Sills, J. M., Southall, B. L., 2013. Comparative assessment of amphibious hearing in pinnipeds. Journal of Comparative Physiology A 199 (6), 491–507.

Reid, J. P., Butler, S. M., Easton, D. E., Deutsch, C. J., 23-25 April 2001 2001. Fifteen years of success in tracking manatees with the argos system: An overview of programs and techniques.

Roelfsema, C. M., Phinn, S. R., Udy, N., Maxwell, P., 2009. An integrated field and remote sensing approach for mapping seagrass cover, moreton bay, australia. Journal of Spatial Science 54 (1), 45–62.

Sayigh, L. S., Esch, H. C., Wells, R. S., Janik, V. M., 2007. Facts about signature whistles of bottlenose dolphins, *Tursiops truncatus*. Animal Behaviour 74 (6), 1631–1642.

Seaman, D. E., Powell, R. A., 1996. An evaluation of the accuracy of kernel density estimators for home range analysis. Ecology 77 (7), 2075–2085.

Sheppard, J. K., Preen, A. R., Marsh, H., Lawler, I. R., Whiting, S. D., Jones, R. E., 2006. Movement heterogeneity of dugongs, *Dugong dugon* (Müller), over large spatial scales. Journal of Experimental Marine Biology and Ecology 334 (1), 64–83.

Shillinger, G. L., Palacios, D. M., Bailey, H., Bograd, S. J., Swithenbank, A. M., Gaspar, P., Wallace, B. P., Spotila, J. R., Paladino, F. V., Piedra, R., Eckert, S. A., Block, B. A., 2008. Persistent leatherback turtle migrations present opportunities for conservation. PLoS Biology 6 (7), e171.

Simpfendorfer, C. A., Heupel, M. R., Hueter, R. E., 2002. Estimation of short-term centers of activity from an array of omnidirectional hydrophones and its use in studying animal movements. Canadian Journal of Fisheries and Aquatic Sciences 59 (1), 23–32.

Slone, D. H., Reid, J. P., Kenworthy, W. J., 2013. Mapping spatial resources with gps animal telemetry: Foraging manatees locate seagrass beds in the Ten Thousand Islands, Florida, usa. Marine Ecology Progress Series 476, 285–299.

Southall, B. L., Schusterman, R. J., Kastak, D., 2003. Acoustic communication ranges for nothern elephant seals (*Mirounga angustirostris*). Aquatic Mammals 29 (2), 202–213.

Stirling, I., Calvert, W., Spencer, C., 1987. Evidence of stereotyped underwater vocalizations of male atlantic walruses (*Odobenus rosmarus rosmarus*). Canadian Journal of Zoology 65, 2311–2321.

Telonics Inc. USA, 2007. Telonics Data Converter (Version 2.13). (software).

Tubelli, A., Zosuls, A., Ketten, D., Mountain, D. C., 2012. Prediction of a mysticete audiogram via finite element analysis of the middle ear. In: Popper, A., Hawkins, A. (Eds.), The Effects of Noise on Aquatic Life. Vol. 730 of Advances in Experimental Medicine and Biology. Springer New York, pp. 57–59.

Wartzok, D., Ketten, D. R., 1999. Marine mammal sensory systems.

In: Reynolds, J., Rommel, S. (Eds.), Biology of Marine Mammals. Smithsonian Institution Press, pp. 117–175.

Welch, D. W., Melnychuk, M. C., Rechisky, E. R., Porter, A. D., Jacobs, M. C., Ladouceur, A., McKinley, R. S., Jackson, G. D., 2009. Freshwater and marine migration and survival of endangered cultus lake sockeye salmon (*Oncorhynchus nerka*) smolts using post, a large-scale acoustic telemetry array. Canadian Journal of Fisheries and Aquatic Sciences 66 (5), 736–750.

Winn, H. E., Goodyear, J. D., Kenney, R. D., Petricig, R. O., 1995. Dive patterns of tagged right whales in the Great South Channel. Continental Shelf Research 15 (45), 593 – 611.

6. Supplementary Material A

Table 4: Tagging details for dugongs fitted with GPS and acoustic transmitters in 2012 and 2013. The number of days indicate total monitoring period (i.e., date from first detection to last). During 2012 the acoustic array was removed for six months from December 2012. In 2013, presence at the date of latest download is indicated by +.

Tag ID	Maturity stage[1]	Sex	Size (cm)	Date tagged	Days tracked GPS	Days tracked Acoustic	Total data points GPS	Total data points Acoustic	Max distance GPS (km)	21 day analysis period
QA30696	Adult	F	312	4/9/2012	32	55	242	40	27.2	4/9-24/9
QA30723	Adult	M	288	4/9/2012	57	56	690	74	31.9	24/7-14/8
QA30677	Juvenile	F	216	4/9/2012	38	32	420	44	2.3	4/9-25/9
QA30541	Juvenile	M	200	4/9/2012	62	73	701	123	1.3	7/9-28/9
QA30710	Adult	M	298	24/8/2012	41	21	254	39	15.4	24/8-14/9
QA30676	Juvenile	F	239	4/9/2012	34	33	268	46	6.4	4/9-25/9
QA30712	Subadult	M	248	24/8/2012	23	27	210	41	7.3	24/8-13/9
QA2685	Subadult	M	245	24/8/2012	8	48	368	32	3.0	-
QA30694	Juvenile	F	209	4/9/2012	55	54	459	107	21.9	4/9-26/9
QA30709	Subadult	F	257	24/8/2012	61	60	599	71	31.9	24/8-14/9
QA18400	Adult	F	290	12/7/2013	35	263	176	18	280.0	-
QA18391[3]	Adult	M	286	12/7/2013	3[2]	262	14	153	0.0	-
QA33322[3]	Subadult	F	253	8/7/2013	6[2]	265	30	203	18.0	-
No tag	Subadult	M	250	8/7/2013	108[2]	1	388	4	320.0	-
QA33400[3]	Subadult	F	250	8/7/2013	4[2]	266	72	232	19.7	-
QA18399	Juvenile	M	239	12/7/2013	32	140	850	277	29.4	12/7-1/8
QA33313	Subadult	M	247	8/7/2013	16	40	102	41	6.1	-
K88240	Adult	M	297	8/7/2013	34	74	452	75	16.9	11/7-1/8
T71561	Adult	M	279	8/7/2013	80	121	554	131	3.1	8/7-29/7
QA33315	Adult	M	285	11/7/2013	38	105	301	31	1.4	11/7-1/8
QA33314[3]	Adult	M	292	11/7/2013	4[2]	256	22	497	10.1	-
				mean	38.5	107.2	342.0	108.5	40.7	
				SD	26.0	94.6	241.8	115.7	87.1	
				median	35	60	301	71	15.4	

[1] based on Lanyon (2003) and Burgess et al. (2012).
[2] excluded from Moreton Bay Region analyses due to limited GPS tracking records.
[3] In 2014, transmitter still active at the date of latest acoustic download.

7. Supplementary Material B

Assumptions considered for tracking and each scenario

1. Tagging assumptions

   - 10 dugongs tracked.
   - GPS tracked animals assumed to transmit data for 3 months; acoustic-one year.
   - Acoustic arrays have 30 receivers.
   - Acoustic downloads every three months taking 5 days on water and requiring certified divers.
   - Costs do not account for new GPS or acoustic battery changes (annual expense).
   - Costs assume that GPS VHF receiving equipment and programs are available.
   - Field gear not costed (safety, wetsuits, hats, etc.).
   - The capital cost of the array is included as an equipment cost only for the sites without an existing array.

2. Scenario 1 (Moreton Bay trips)

   - Assume personnel are local / no accommodation or travel cost.
   - Assume local personnel used for acoustic data download and array establishment.
   - Catching 9 people (2 skippers + 4 catchers + 1 veterinarian + 1 data recorder + 1 extra).
   - 5 people (4 divers + 1 skipper) to set up array and download data.
   - 2 vessels for catching; one vessel to set up array and download data (assume JCU vessels).
   - 5 days catching; 5 days establish array; 5 days download data
   - No plane charter.
   - Array set up based on costs in Moreton Bay in May 2013 (prices and material may vary).

3. Scenario 2 (Townsville trips)

   - Assume local personnel / no accommodation or travel cost
   - Catching 9 people (2 skippers + 4 catchers + 1 veterinarian + 1 data recorder + 1 extra)
   - 5 people (4 divers + 1 skipper) to set up array and download data.
   - 2 vessels for catching; one vessel to set up array and to download data (assume JCU vessels).
   - 10 days catching; 5 days set array; 5 days download data.
   - Plane charter is necessary to spot dugongs.
   - Array set up based on costs in Moreton Bay in May 2013 (prices and material may vary).

4. Scenario 3 (Torres Strait trips)

   - Assume personnel are from Townsville.
   - Catching 9 people (4 catchers + 2 skippers + 1 veterinarian + 2 rangers/locals).
   - 5 people (4 divers + 1 skipper) to set up array and download data.
   - 3 vessels (1 JCU + 2 local boats)
   - No in kind support from Torres Strait Regional Authority.
   - 20 days catching; 5 days set array; 5 days download data.
   - Assume out of the 20 days, in the water catching for only 10 days.
   - No plane charter necessary
   - Array set up based on costs in Moreton Bay in May 2013 + 10% of costs to account for more expensive material in Torres Strait (prices and material may vary).
   - Assumes gear sent to Torres Strait with JCU boat to reduce freight costs.

8. Supplementary Material C
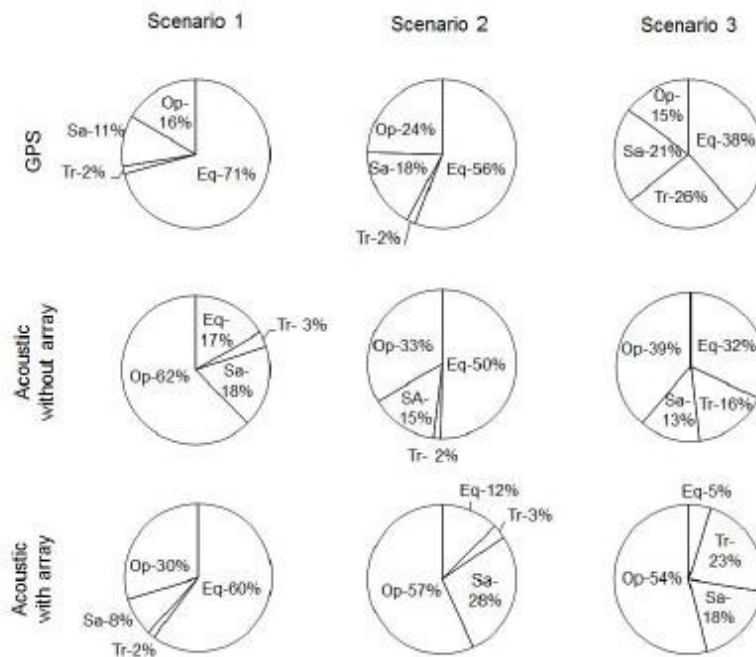
Figure 6: Breakdown of costs associated with each tracking method for each scenario: Scenario 1- easy catching and accessible location (e.g., Moreton Bay); Scenario 2 - difficult catching and accessible location (e.g., Townsville); and Scenario 3 - difficult catching and remote location (e.g., Boigu, Torres Strait). Percentages relate to overall cost: Eq: Equipment cost, Tr: Travel cost (catching only), Salary cost (catching only), Op: Operations cost. The capital cost of the array is included as an equipment cost only for sites without an existing array.

Appendix E Location of acoustic receivers

Apx Table E.1 Location of acoustic receivers deployed in the GISERA CSIRO Gladstone Harbour receiver array. (All receiver location and download information can be accessed at the IMOS AATAMS website https://aatams.emii.org.au/aatams/installation/list). Receivers remain deployed at the time of writing.

Name	Receiver Serial #	Lat	Long	Deployment Date	Depth
CALPSANC	103617	-23.8511	151.2129	19/03/2013 7:47	3.2
CAL2ANC	103611	-23.8353	151.22	19/03/2013 8:26	2.8
CAL1ANC	121457	-23.8215	151.2181	19/03/2013 8:58	2.9
GH1ANC	121459	-23.811	151.2259	19/03/2013 9:30	3.9
GH2ANC	103605	-23.8139	151.224	19/03/2013 10:10	2.5
GH3ANC	121461	-23.805	151.2067	19/03/2013 10:54	4
GH4ANC	103609	-23.8116	151.2059	19/03/2013 11:39	2
GH6ANC	103608	-23.8133	151.2001	19/03/2013 12:11	2.5
GH5ANC	121474	-23.805	151.2013	19/03/2013 12:54	
GH8ANC	121470	-23.8041	151.1922	19/03/2013 13:37	3.1
GH9ANC	121464	-23.8137	151.1917	19/03/2013 14:04	1.5
GH7ANC	103628	-23.8179	151.1949	19/03/2013 14:40	2.8
GH11ANC	121462	-23.8136	151.1834	19/03/2013 15:11	1.7
GH10ANC	109857	-23.8057	151.184	19/03/2013 15:36	2.5
GHC17ANC	109860	-23.7974	151.1932	19/03/2013 16:04	8.5
GHC16ANC	121475	-23.7979	151.2025	19/03/2013 16:27	9
GH01ANC	121477	-23.8193	151.2037	19/03/2013 16:56	2.5
GHC14ANC	109859	-23.8021	151.2076	20/03/2013 7:37	9
GHC18ANC	103606	-23.7969	151.2178	20/03/2013 8:01	8
GHC13ANC	121460	-23.8026	151.2256	20/03/2013 8:31	5.5
GHC19ANC	121468	-23.7968	151.227	20/03/2013 9:14	8
PB2ANC	109861	-23.7874	151.3048	20/03/2013 11:02	3.2
PB1ANC	103625	-23.7871	151.2968	20/03/2013 11:40	1.4
PB5ANC	109866	-23.7807	151.2934	20/03/2013 12:23	0.7
PB6ANC	121463	-23.7778	151.2991	20/03/2013 13:22	1.5
PB9ANC	103607	-23.7737	151.2944	20/03/2013 13:57	1
PB10ANC	103610	-23.7721	151.303	20/03/2013 14:27	1.3
PB13ANC	121458	-23.7686	151.2972	20/03/2013 14:54	1.1
PB17ANC	121469	-23.7646	151.3028	20/03/2013 15:16	1.2
PB18ANC	103614	-23.7622	151.309	20/03/2013 15:32	1.3
PB21ANC	121453	-23.7596	151.3222	21/03/2013 7:41	5.5

Name	Receiver Serial #	Lat	Long	Deployment Date	Depth
PB20ANC	103618	-23.7654	151.3247	21/03/2013 8:14	5
PB16ANC	121454	-23.7681	151.3202	21/03/2013 8:43	5.3
PB19ANC	121473	-23.7657	151.3144	21/03/2013 9:11	3
PB14ANC	103603	-23.7686	151.3088	21/03/2013 9:36	1.4
PB11ANC	121472	-23.7749	151.3094	21/03/2013 10:01	1.4
PB15ANC	121476	-23.7709	151.3144	21/03/2013 10:35	3.6
PB4ANC	103619	-23.7748	151.3214	21/03/2013 11:05	3.6
PB8ANC	121456	-23.7811	151.3148	21/03/2013 11:33	4
PB12ANC	121466	-23.7857	151.3187	21/03/2013 12:00	1.4
PB3ANC	121455	-23.7856	151.3117	21/03/2013 12:41	1.8

References

Abal, E.G. and Dennison, W.C. 1996 Seagrass Depth Range and Water Quality in Southern Moreton Bay, Queensland, Australian Marine and Freshwater Research 47:763-71.

Addison, D.S., Gore, J.A., Ryder, J. and Worley, K. 2002. Tracking postnesting movements of loggerhead turtles (*Carettacaretta*) with sonic and radio telemetry on the southwest coast of Florida, USA. Marine Biology 141:201–205.

Aragones, L. and Marsh, H. 2000. Impact of dugong grazing and turtle cropping on tropical seagrass communities. Pacific Conservation Biology 5:277-288.

Arthur, K., Boyle, M.C. and Limpus, C.J. 2008. Ontogenetic changes in diet and habitat use in green sea turtle (*Chelonia mydas*) life history. Marine Ecology Progress Series 362:303-311.

Arthur, K., McMahon, K.M., Limpus, C.L., and Dennison, W.C. 2009. Feeding ecology of green turtles (*Chelonia mydas*) from Shoalwater Bay, Australia. Marine turtle newsletter, 6.

Atkinson, M.J. 1992. Productivity of Eniwetak atoll reef predicted from mass-transfer relationships. Cont. Shelf Res. 12:799–807.

Australia Pacific LNG Project Appendix I - Marine Mammal and Turtles Management Plan LNG Facility.

Baird, M.E. and Middleton, J.H. 2004. On relating physical limits to the carbon: nitrogen ratio of unicellular algae and benthic plants. J. Mar. Sys. 49:169– 175.

Baird, M.E. and Suthers, I.M. 2007. A size-resolved pelagic ecosystem model. Ecol. Model. 203:185–203.

Baird, M.E., Walker, S.J., Wallace, B.B., Webster, I.T. and Parslow, J.S. 2003. The use of mechanistic descriptions of algal growth and zooplankton grazing in an estuarine eutrophication model. Est., Coastal and Shelf Sci. 56:685–695.

Balazs, G.H. 1980. Synopsis of biological data on the green turtle in the Hawaiian Islands. National Oceanic and Atmospheric Administration Technical Memorandum No. 7. National Marine Fisheries Service Southwest Fisheries Centre. pp. 1-141.

Balazs, G.H. 1994. Homeward bound: satellite tracking of Hawaiian green turtles from nesting beaches to foraging pastures. Proceedings of the Thirtheen annual Symposium on Sea Turtle Biology and Conservation. U.S. Dep. Commer., NOAA Tech. Memo. NMFS, pp. 135-138.

Bass, A.L. and Witzell, W.N. 2000. Demographic composition of immature green turtles (*Chelonia mydas*) from the east central Florida coast: evidence from mtDNA makers Herpetologica, 56: 357–367.

Bauduin, S., Martin, J, Edwards, H.H., Gimenez, O., Koslovsky, S.M. and Fagan, D.E. 2013. An index of risk of co-occurrence between marine mammals and watercraft: example of the Florida manatee. Biological Conservation 159:127–136.

Bjorndal, K.A. 1980. Nutrition and grazing behavior of the green turtle *Chelonia mydas*. Marine Biology 56:147-154.

Bjorndal, K.A. 1997. Foraging ecology and nutrition of sea turtles. In: Lutz, P.L. and Musick, J.A. (eds) The biology of sea turtles. CRC Press, Boca Raton, FL, p 199–231.

Blondeau-Patissier, D., Brando, V.E., Oubelkheir, K., Dekker, A.G., Clementson, L.A. and Daniel, P. 2009. Bio-optical variability of the absorption and scattering properties of the Queensland inshore and reef waters, Australian Journal of Geophysical Ressearch (Oceans) 114: C05003.

Bolten, A.B. 2003. Variation in sea turtle life history patterns: Neritic vs. oceanic developmental stages. In: Lutz, P.L., Musick, J.A. and Wyneken, J. (eds) The Biology of Sea Turtles. Vol II. CRC Press: Boca Raton, FL, p 243–257.

BOM 2012. http://www.bom.gov.au/climate/enso/history/ln-2010-12/rainfall-flooding.shtml.

Bowen, B.W., Meylan, A.B., Ross, P.J., Limpus, C.J., Balazs, G.H. and Avise, J.C. 1992. Global population structure and natural history of the green turtle (*Chelonia mydas*) in terms of matriarchal phylogeny. Evolution 46:865–881.

Boyce, M.S. 2006. Scale for resource selection functions. Diversity and Distributions 12:269–276.

Brand, S.J., Lanyon, J.M. and Limpus, C.J. 1999. Digesta composition and retention times in wild immature green turtles, *Chelonia mydas*: a preliminary investigation. Marine and Freshwater Research 50:145-147.

Brando, V. E., Dekker, A. G., Park, Y. J., & Schroeder, T. 2012. Adaptive semianalytical inversion of ocean color radiometry in optically complex waters. Applied Optics, *51*(15): 2808-2833.

Brand-Gardner, S.J., Limpus, C.J. and Lanyon, J.M. 1999. Diet selection by immature green turtles, *Chelonia mydas*, in subtropical Moreton Bay, south-east Queensland. Australian Journal of Zoology 47:181-191.

Brill, R.W., Balazs, G.H., Holland, K.N., Chang, R.K.C., Sullivan, S. and George, J.C., 1995. Daily movements, habitat use and submergence intervals of normal and tumor-bearing juvenile green turtles (*Chelonia mydas* L) within a foraging area in the Hawaiian islands. J. Exp. Mar. Biol. Ecol. 185:203–218.

Bryant, C.V., Davies, J.D., Jarvis, J.C., Tol, S. and Rasheed, M.A. 2014. Seagrasses in Port Curtis and Rodds Bay 2013: Annual Long Term Monitoring, Biannual Western Basin Surveys & Updated Baseline Survey, Centre for Tropical Water & Aquatic Ecosystem Research (TropWATER) Publication 14/23, James Cook University, Cairns, 71 pp.

Bryant, C.V. and Rasheed, M.A. 2013. Gladstone permanent transect seagrass monitoring monthly report December 2013. Update Report, Centre for Tropical Water and Aquatic Ecosystem Research Publication 13/50 James Cook University, Cairns, 9 pp.

Bustard, R. 1972. Sea Turtles: Their Natural History and Conservation. Collins, London.

Byrne, R. Fish, J., Doyle, T.K. and Houghton, J.D.R. 2009. Tracking leatherback turtles (*Dermochelys coriacea*) during consecutive inter-nesting intervals: Further support for direct transmitter attachment. Journal of Experimental Marine Biology and Ecology 377:68–75.

Calenge, C. 2006. The package "adehabitat" for the R software: A tool for the analysis of space and habitat use by animals. Ecological Modelling 197:516–519.

Cambridge, M.L. and Lambers, H. 1998. Specific leaf area and functional leaf anatomy in Western Australian seagrasses. In: Lambers, H., Poorter, H. and Vuren, M.M.I.V. (eds.),

Inherent variations in plant growth: physiological mechanisms and ecological consequences. Backhuys, Leiden, pp. 88–99.

Campbell, S.J., McKenzie, L.J., Kerville, S.P and Bite, J.S. 2007. Patterns in tropical seagrass photosynthesis in relation to light, depth and habitat. Estuarine, Coastal and Shelf Science 73:551-562.

Candy, S.G. 2004. Modelling catch and effort data using generalised linear models, the Tweedie distribution, random vessel effects and random stratum-by-year effects. CCAMLR Science 11:59–80.

Carr, A. 1980. Some problems in sea turtle ecology. American Zoologist 20:489-498.

Carr, J.A., D'Odorico, P., McGlathery, K.J. and Wiberg, P.L. 2012. Stability and resilience of seagrass meadows to seasonal and interannual dynamics and environmental stress. J. Geophys. Res. 117:G01007.

Chartrand, K., Ralph, P.J., Petrou, K.K. and Rasheed, M. A. 2012. Development of a Light-Based Seagrass Management Approach for the Gladstone Western Basin Dredging Program. Tech. rep., DAFF Publication. Fisheries Queensland, Cairns 126 pp.

Chartrand, K, Rasheed, M.A. and Unsworth, R.K.F. 2009. Long term seagrass monitoring in Port Curtis and Rodds Bay, November 2008. Tech. rep., DEEDI Publication PR09-4407 (QPIF, Cairns), 34 pp.

Chaloupka, M., Limpus, C. and Miller, J. 2004. Green turtle somatic growth dynamics in a spatially disjunct Great Barrier Reef metapopulation. Coral Reefs 23:325–335.

Clementson, L.A. 2013. The CSIRO method. In: Hooker, S.B., L. Clementson, C.S. Thomas, L. Schlüter, M. Allerup, J. Ras, H. Claustre, C. Normandeau, J. Cullen, M. Kienast, W. Kozlowski, M. Vernet, S. Chakraborty, S. Lohrenz, M. Tuel, D. Redalje, P. Cartaxana, C.R. Mendes, V. Brotas, S.G. Prabhu Matondkar, S.G. Parab, A. Neeley and E. Skarstad Egeland, 2013. The Fifth SeaWiFS HPLC Analysis Round-Robin Experiment (SeaHARRE-5). NASA Technical Memorandum 2012-217503, NASA Goddard Space Flight Center, Greenbelt, Maryland.

Coles, R.G., Rasheed, M.A., McKenzie, L.J., Grech, A., York, P.H., Sheaves, M. McKenna, S. and Bryant, C. 2014. The Great Barrier Reef World Heritage Area seagrasses: Managing this iconic Australian ecosystem resource for the future. Estuarine, Coastal and Shelf Science 153:A1-A12.

Collier, C.J., Waycott, M. and McKenzie, L.J. 2012. Light thresholds derived from seagrass loss in the coastal zone of the northern Great Barrier Reef, Australia. Ecological Indicators 23:211–219.

Conn, P. B. and Silber, G.K. 2013. Vessel speed restrictions reduce risk of collision-related mortality for North Atlantic right whales. Ecosphere 4:43.

Costanza, R., de Groot, R., Sutton, P., van der Ploeg, S., Anderson, S.J., Kubiszewsk, I., Farber, S. and Turner, R.K. 2014. Changes in the global value of ecosystem services. Glob. Environ. Change 26:152-158.

Cribb, A.B. 1996. Seaweeds of Queensland: a naturalist's guide. The Queensland Naturalist's Club, Brisbane, QLD.

CSIRO Coastal Environmental Modelling Team 2014. CSIRO Environmental Modelling Suite: Scientific description of the optical, carbon chemistry and biogeochemical models parameterised for the Great Barrier Reef. CSIRO, Hobart, Australia.

Davies, J.N., McCormack, C.V. and Rasheed, M.A. 2012. Gladstone Permanent Transect Seagrass Monitoring – November 2012 Update Report, DAFF Publication, Fisheries Queensland, Cairns, 17 pp.

Davies, J.D., McCormack, C.V. and Rasheed, M.A. 2013. Port Curtis and Rodds Bay seagrass monitoring program, Biannual Western Basin & Annual Long Term Monitoring November 2012. Tech. rep., Centre for Tropical Water & Aquatic Ecosystem Research (TropWATER) Publication, James Cook University, Cairns, 54 pp.

Dethmers, K.E.M., Broderick, D., Moritz, C., Fitzsimmons, N.N., Limpus, C.J., Lavery, S., Whiting, S., Guinea, M., Prince, R.I.T. and Kennett, R. 2006. The genetic structure of Australasian green turtles (*Chelonia mydas*): exploring the geographical scale of genetic exchange. Molecular Ecology 15:3931–3946.

Dethmers, K.E.M., Jensen, M.P., FitzSimmons, N.N., Broderick, D., Limpus, C.J. and Moritz, C. 2010. Migration of green turtles (*Chelonia mydas*) from Australasian feeding grounds inferred from genetic analyses. Mar. Freshw. Res. 61:1376-1387. http://dx.doi.org/10.1071/MF10084.

Doody, S.J., Roe, J. Mayes, P. and Ishiyama, L. 2009. Telemetry tagging methods for some freshwater reptiles. Marine and Freshwater Research 60: 293–298.

Duarte, C.M. 1990. Seagrass nitrogen content. Mar. Ecol. Prog. Ser. 67:201–207.

Duarte, C.M. 1991. Seagrass depth limits. Aquatic Botany 40:363-377.

Duarte, C.M. 2002. The future of seagrass meadows. Environmental Conservation 29:192-206.

Duarte, C.M. and Chiscano, C.L. 1999. Seagrass biomass and production: a reassessment. Aquatic Botany 65:159–174.

Dwyer, R.G., Campbell, H.A., Irwin, T.R. and Franklin, C.F. 2014. Does the telemetry technology matter? Comparing estimates of aquatic animal space-use generated from GPS-based and passive acoustic tracking. Marine and Freshwater Research http://dx.doi.org/10.1071/MF14042.

Elkalay, K., Frangoulis, C., Skliris, N., Goffart, A., Gobert, S., Lepoint, G. and Hecq, J.-H., 2003. A model of the seasonal dynamics of biomass and production of the seagrass Posidonia oceanica in the Bay of Calvi (Northwestern Mediterranean). Ecol. Mod. 167:1–18.

Erftemeijer, P.L.A. and Lewis, R.R. 2006. Environmental impacts of dredging on seagrasses: A review. Marine Pollution Bulletin 52:1553-1572.

Flint, M., Eden, P.A., Limpus, C.J., Owen, H., Gaus, C. and Mills, P.C. 2014. Clinical and pathological findings in green turtles (*Chelonia mydas*) from Gladstone, Queensland: Investigations of a stranding epidemic. EcoHealth DOI: 10.1007/s10393-014-0972-5.

Frouin, R. and Murakami, H. 2007. Estimating photosynthetically available radiation at the ocean surface from ADEOS-II Global Imager data. Journal of Oceanography 63:493-503.

Gaus, C., Grant, S., Jin, N.L., Goot, K., Chen, L., Villa, A.C., Neugebauer, F., Qi, L. and Limpus, C. 2012. Investigation of contaminant levels in green turtles from Gladstone. National Research Centre for Environmental Toxicology (Entox). 160 pp.

Gitzen, R.A., Millspaugh, J.J. and Kernohan, B.J. 2006. Bandwidth selection for Fixed-Kernel Analysis of animal utilization distributions. Journal of Wildlife Management 70:1334–1344.

Godley, B. J., Richardson, S., Broderick, A.C., Coyne, M.S., Glen, F. and Hays, G.C. 2002. Long-term satellite telemetry of the movements and habitat utilisation by green turtles in the Mediterranean. Ecography 25:352–362.

Gordon, H. R., Brown, O. B., Evans, R. H., Brown, J. W., Smith, R. C., Baker, K. S., & Clark, D. K. 1988. A semianalytic radiance model of ocean color. Journal of Geophysical Research: Atmospheres (1984–2012), 93(D9): 10909-10924.Gras, A.F., Koch, M.S. and Madden, C.J., 2003. Phosphorus uptake kinetics of a dominant tropical seagrass Thalassia testudinum . Aquatic Botany 76:299–315.

Grech, A., Coles, R.G. and Marsh, H. 2011. A broad-scale assessment of the risk to coastal seagrasses from cumulative threats. Mar. Policy 35:560-567.

Grech, A., Chartrand-Miller, K., Erftemeijer, P., Fonseca, M., McKenzie, L., Rasheed, R., Taylor, H. and Coles, R.G. 2012. A comparison of threats, vulnerabilities and management opportunities in global seagrass bioregions. Environ. Res. Lett. 7:024006.

Gredzens, C., Marsh, H., Fuentes, M.M.P.B., Limpus, C.J., Shimada, T. and Hamman, M. 2014. Satellite tracking of sympatric marine megafauna can inform the biological basis for species co-management. PLoS ONE 9(6): e98944. doi:10.1371/journal.pone.0098944.

Gumley, L., Descloitres, J. and Shmaltz, J. 2010. Creating reprojected true color modis images: A tutorial, tech. rep 1.0.2, 17 pp. Tech. rep., Univ. of Wisc.-Madison, Madison.

Gustafsson, M.S.M., Baird, M.E. and Ralph, P.J. 2013. The interchangeability of autotrophic and heterotrophic nitrogen sources in scleractinian coral symbiotic relationships: a numerical study. Ecol. Model. 250:183–194.

Hamabata, T., Kamezaki, N. and Hikida, T. 2014. Genetic structure of green turtle (*Chelonia mydas*) peripheral populations nesting in the northwestern Pacific rookeries: evidence for northern refugia and postglacial colonization. Mar. Biol. 161:495–507.

Han, B.-P. 2002. A mechanistic model of algal photoinhibition induced by photodamage to photosystem-II. J. Theor. Bio. 214:519–527.

Hansen, J.W., Udy, J.W., Perry, C.J., Dennison, W.C. and Lomstein, B. A. 2000. Effect of the seagrass Zostera muelleri on sediment microbial processes. Mar. Ecol. Prog. Ser. 199:83–96.

Hastings, A., Byers, J. E., Crooks, J.A., Cuddington, K., Jones, C.G., Lambrinos, J.G., Talley, T.S. and Wilson, W.G. 2007. Ecosystem engineering in space and time. Ecological Letters 10:153–164.

Hazel, J. 2009. Evaluation of fast-acquisition GPS in stationary tests and fine-scale tracking of green turtles. Journal of Experimental Marine Biology and Ecology 374:58–68.

Hazel, J., Lawler, I.R. and Hamann, M. 2009. Diving at the shallow end: Green turtle behaviour in near-shore foraging habitat. Journal of Experimental Marine Biology and Ecology 371:84-92.

Hazel, J., Lawler, I.R., Marsh, H. and Robson, S. 2007. Vessel speed increases collision risk for the green turtle *Chelonia mydas*. Endangered Species Research 3:105-113.

Hedley, J.D., McMahon, K. and Fearns, P. 2014. Seagrass canopy photosynthetic response is a function of canopy density and light environment: A model for *Amphibolis griffithii* . PLOS One 9:e111454.

Herzfeld, M., 2006. An alternative coordinate system for solving finite difference ocean models. Ocean Modelling 14:174–196.

Herzfeld, M., Condie, S., Andrewartha, J.R. and Gorton, B. 2015. Project ISP007: Development of Connectivity Indicators for the Gladstone Healthy Harbour Report Card Draft Final Technical Report. Tech. rep., CSIRO.

Herzfeld, M., Parslow, J.S., Andrewartha, J.R., Sakov, P.V. and Webster, I.T. 2004. Hydrodynamic modelling of the Port Curtis region, Project CM2.11. Indooroopilly. Qld.: Cooperative Research Centre for Coastal Zone, Estuary and Waterway Management. Tech. rep., Cooperative Research Centre for Coastal Zone, Estuary and Waterway Management, 51 pp.

Hirth, H.F., Huber, M., Frohm, T. and Mala, T. 1992. A natural assemblage of immature green (*Chelonia mydas*) and hawksbill (*Eretmochelys imbricata*) turtles on the fringing reef of Wuvulu Island, Papua New Guinea. Micronesica 25:145-153.

IUCN 2014. The IUCN Red List of Threatened Species. Version 2014.3. <www.iucnredlist.org>. Downloaded on 08 April 2015.

Jeffrey, S.W. and Vesk, M. 1997. Introduction to marine phytoplankton and their pigment signatures. In: Jeffrey, S.W., Mantoura, R.F.C. and Wright, S.W. (eds.) Phytoplankton Pigments in Oceanography: guidelines to modern methods. UNESCO Publishing, pp. 37-84.

Jeffrey, S.W. and Wright, S.W. 2006. Photosynthetic pigments in marine microalgae: insights from cultures and the sea. In: Subba Rao, D.V. (ed.) Algal Cultures, Analogues of Blooms and Applications, Science Publishers, pp. 33-90.

Kaldy, J.E., Brown, C.A. and Andersen, C.P. 2013. In situ 13C tracer experiments elucidate carbon translocation rates and allocation patterns in eelgrass *Zostera marina*. Mar. Ecol. Prog. Ser. 487:27–39.

Kehoe, M., O'Brien, K., Grinham, A. and Burford, M. 2015. Primary production of lake phytoplankton, dominated by the cyanobacterium *Cylindrospermopsis raciborskii*, in response to irradiance and temperature. Inland Waters 5:93–100.

Kemp, W.M., Murray, L., Borum, J. and Sand-Jensen, K. 1987. Diel growth in eelgrass *Zostera marina*. Mar. Ecol. Prog. Ser. 41:79–86.

Kernohan, B.J., Gitzen, R.A. and Millspaugh, J.J. 2001. Analysis of animal space use and movements. In: Millspaugh, J.J. and Marzluff, J.M. (eds) Radio Tracking and Animal Populations. Academic Press, San Diego, California. pp. 126-166.

Key Threatening Process Nomination Form - Fatal injury to marine mammals, reptiles, and other large marine species through boat strike on the Australian coast - nomination-boat-strike-2012.pdf. (n.d.).

Kohler, K.E. and Gill, S.M. 2006. Coral point count with excel extensions (CPCe): A Visual Basic program for the determination of coral and substrate coverage using random point count methodology. Computers & Geosciences 32:1259–1269.

Lahanas, P.N., Bjorndal, K.A., Bolten, A.B., Encalada, S.E., Miyamoto, M.M., Valverde, R.A. and Bowen, B.W. 1998. Genetic composition of a green turtle (*Chelonia mydas*) feeding ground population: evidence for multiple origins. Mar. Biol. 130:345–352. http://dx.doi.org/10.1007/s002270050254.

Lal, A., Arthur, R., Marbà, N., Lill, A.W.T. and Alcoverro, T. 2010. Implications of conserving an ecosystem modifier: Increasing green turtle (*Chelonia mydas*) densities substantially alters seagrass meadows. Biological Conservation 143:2730–2738.

Lee, K.-S. and Dunton, K.H. 1999. Inorganic nitrogen acquisition in the seagrass *Thalassia testudinum*: Development of a whole-plant nitrogen budget. Limnol. Oceanogr. 44:1204–1215.

Lee, Z., Carder, K. L., & Arnone, R. A. 2002. Deriving inherent optical properties from water color: a multiband quasi-analytical algorithm for optically deep waters. Applied Optics, 41(27): 5755-5772.

Limpus, C.J. 1993. The green turtle, *Chelonia mydas*, in Queensland: breeding males. Wildlife Research 20:513–523.

Limpus, C.J. 2008. A biological review of Australian marine turtle species: green turtle, *Chelonia mydas* (Linnaeus). The State of Queensland. Environmental Protection Agency 2008, ISBN:978-0-9803613-2-2. 95 pp.

Limpus, C.J., Couper, P.J. and Read, M.A. 1994. The green turtle, *Chelonia mydas*, in Queensland: population structure in a warm temperate feeding area. Memoirs of the Queensland Museum 35:139–154.

Limpus, C.J. and Limpus, D.J. 2000. Mangroves in the diet of *Chelonia mydas* in Queensland, Australia. Marine turtle newsletter 13-15.

Limpus, C.J. and Limpus, D.J. 2003. Biology of the loggerhead turtle in western South Pacific Ocean foraging areas. In: Bolten, A.B. and Witherington, B.E. (eds.) Loggerhead Sea Turtles. Smithsonian Institution, Washington, D.C., p 93–113.

Limpus, C.J., Limpus, D.J., Arthur, K.E. and Parmenter, C.J. 2005. Monitoring green turtle population dynamics in Shoalwater Bay 2000-2004. Queensland Environmental Protection Agency and the Great Barrier Reef Marine Park Authority. Research Publication No. 83.

Limpus, C.J., Limpus, D.J., Savige, M. and Shearer, D. 2012. Health assessment of green turtles in south and central Queensland following extreme weather impacts on coastal habitat during 2011. Department of Environment and Resource Management, Brisbane. 13 pp.

Limpus, C.J., Miller, J.D., Paramenter, C.J., Reimer, D., McLachlan, N. and Webb R. 1992. Migration of green (*Chelonia mydas*) and loggerhead (*Caretta caretta*) turtles to and from eastern Australian rookeries. Wildlife Research 19:347–357.

Limpus, C.J., Parmenter, C.J. and Chaloupka, M. 2013. Monitoring of Coastal Sea Turtles: Gap Analysis 2. Green turtles, *Chelonia mydas*, in the Port Curtis and Port Alma Region. Report produced for the Ecosystem Research and Monitoring Program Advisory Panel as part of Gladstone Ports Corporation's Ecosystem Research and Monitoring Program.

Limpus, C.J. and Reed, P.C. 1985. The green turtle, *Chelonia mydas*, in Queensland: population structure in a coral reef feeding ground. In: Grigg, G., Shine, R., and Ehmann, H. (eds.) Biology of Australian Frogs and Reptiles. Surrey Beatty and Sons, Sydney, p 47-52.

Longstaff, B.J. 2003. Investigations into the light requirements of seagrasses in northeast Australia. Ph.D. thesis, University of Queensland.

Luke, K., Horrocks, J.A., LeRoux, R.A. and Dutton, P.H. 2004. Origins of green turtle (*Chelonia mydas*) feeding aggregations around Barbados, West Indies. Mar. Biol. 144:799–805. http://dx.doi.org/10.1007/s00227-003-1241-2

Lutcavage, M.E., Plotkin, P.T., Witherington, B. and Lutz, P.L. 1997. Human impacts on sea turtle survival. In: Lutz, P. and Musick, J. (eds.) The Biology of Sea Turtles. CRC Press, Boca Raton, FL, pp. 387-410.

MacDonald, B.D., Lewison, R.L., Madrak, S.V., Seminoff, J.A. and Eguchi, T. 2012. Home ranges of East Pacific green turtles *Chelonia mydas* in a highly urbanized temperate foraging ground. Marine Ecology Progress Series 461:211-221.

MacNally, R. 2000. Regression and model-building in conservation biology, biogeography and ecology: the distinction between–and reconciliation of–"predictive" and "explanatory" models. Biodiversity & Conservation 9:655–671.

Macreadie, P.I., Baird, M.E., Trevathan-Tackett, S.M., Larkum, A.W.D. and Ralph, P.J. 2014. Quantifying and modelling the carbon sequestration capacity of seagrass meadows - a critical assessment. Mar. Pollut. Bull. 83:430-439.

Maitland, R. N., Lawler, I.R. and Sheppard, J.K. 2006. Assessing the risk of boat strike on Dugongs *Dugong dugon* at Burrum Heads, Queensland, Australia. Pacific Conservation Biology 12:321.

Makowski, C.A., Seminoff, J.A., Salmon, M.A. and English, G. 2006. Home range and habitat use of juvenile Atlantic green turtles (*Chelonia mydas* L.) on shallow reef habitats in Palm Beach, Florida, USA. Marine Biology 148(5):1167-1179.

Margvelashvili, N. 2009. Stretched Eulerian coordinate model of coastal sediment transport. Computer Geosciences 35:1167–1176.

Margvelashvili, N., Andrewartha, J., Herzfeld, M., Robson, B. and Brandob, V. 2013. Satellite data assimilation and estimation of a 3D coastal sediment transport model using error-subspace emulators. Env. Model. Soft. 40:191–201.

Maxwell, P.S., Pitt, K.A., Burfeind, D.D., Olds, A.D., Babcock, R.C. and Connolly, R.M. 2014. Phenotypic plasticity promotes persistence following severe events: physiological and morphological responses of seagrass to flooding. Journal of Ecology 102:54–64.

McCormack, C., Rasheed, M.A., Davies, J., Carter, A., Sankey, T. and Tol, S. 2013. Long term seagrass monitoring in the Port Curtis Western Basin. In: TropWATER (ed.) Quarterly Seagrass Assessments & Permanent Transect Monitoring Progress Report November 2009 to Nov 2012. James Cook University, Cairns, 88pp.

McKenzie, L.J., Lee Long, W.J., Coles, R.G. and Roder, C.A. 2000. Seagrass-watch: community based monitoring of seagrass resources. Biol. Mar. Mediterr. 7:393-396.

McKenzie, L.J., Yoshida, R.L., Grech, A. and Coles, R. 2014. Composite of Coastal Seagrass Meadows in Queensland. Australia-November 1984 to June 2010. http://dx.doi.org/10.1594/PANGAEA.826368.

McKenzie, L.J., Finkbeiner, M.A. and Kirkman, H. 2001. Methods for mapping seagrass distribution. In: Short, F.T. and Coles, R.G. (eds.), Global Seagrass Research Methods. Elsevier Science, Amsterdam, pp. 101-121.

Meager, J.J. and Limpus, C.J. 2012. Marine wildlife stranding and mortality database annual report 2011. III. Marine Turtles. Conservation technical and data report 2012(3):1-46.

Mendonca, M.T. 1983. Movements and feeding ecology of immature green turtle (*Chelonia mydas*) in a Florida lagoon. Copeia 4:1013–1023.

Meyer, C.B. and Thuiller, W. 2006. Accuracy of resource selection functions across spatial scales. Diversity and Distributions 12:288–297.

Miller, R.L. and McKee, B. A. 2004. Using MODIS terra 250 m imagery to map concentrations of suspended matter in coastal waters. Remote Sens. Environ. 93:259-266.

Mitchell, B.G. 1990. Algorithms for determining the absorption coefficient for aquatic particulates using the quantitative filter technique. Ocean Optics X. 1302:137-148.

Mongin, M. and Baird, M. E. 2014. The interacting effects of photosynthesis, calcification and water circulation on carbon chemistry variability on a coral reef flat: a modelling study. Ecol. Mod. 284:19–34.

Moriarty, D.J.W., Inverson, R.L. and Pollard, P.C. 1986. Exudation of organic carbon by the seagrass *Halodule wrightii* Aschers. and its effect on bacterial growth in the sediment. J. Exp. Mar. Biol. Ecol. 96:115–126.

Newell, R.I. and Koch, E.W. 2004. Modeling seagrass density and distribution in response to changes in turbidity stemming from bivalve filtration and seagrass sediment stabilization. Estuaries 27:793–806.

Pope, R.M. and Fry, E.S. 1997. Absorption spectrum (380-700 nm) of pure water: II. Integrating cavity measurements. Applied Optics 36:8710-8723.

O'Brien, K.R., Burford, M.A. and Brookes, J.D. 2009. Effects of light history on primary productivity in a phytoplankton community dominated by the toxic cyanobacterium *Cylindrospermopsis raciborskii*. Freshwater Bio. 54:272–282.

Olivier, F. and Wotherspoon, S.J. 2005. GIS-based application of resource selection functions to the prediction of snow petrel distribution and abundance in East Antarctica: comparing models at multiple scales. Ecological Modelling 189:105–129.

Orth, R.J., Carruthers, T.J.B., Dennison, W.C., Duarte, C.M., Fourqurean, J.W., Heck, K.L., Randall Hughes, A., Kendrick, G.A., Kenworthy, J.W., Olyarnik, S., Short, F.T., Waycott, M. and Williams, S.L. 2006. A global crisis for seagrass ecosystems. Bioscience 56:987-996.

Pedersen, T.M., Gallegos, C.L. and Nielsen, S.L. 2012. Influence of near-bottom re-suspended sediment on benthic light availability. Estuarine, Coastal and Shelf Science 106:93-101.

Penhale, P.A. and Thayer, G.W. 1980. Uptake and transfer of carbon and phosphorus by eelgrass (*Zostera marina* L.) and its epiphytes. J. Exp. Mar. Biol. Ecol. 42:113–123.

Petrou, K., Jimenez-Denness, I., Chartrand, K., McCormack, C., Rasheed, M. and Ralph, P.J. 2013. Seasonal heterogeneity in the photophysiological response to air exposure in two tropical intertidal seagrass species. Mar. Ecol. Prog. Ser. 482:93–106.

Petus, C., Devlin, M. and da Silva, E.T., submitted. Use of MODIS satellite imagery to monitor turbidity variations in anthropogenically-modified coastal environments: A case study in the Great Barrier Reef World Heritage Area (Port of Gladstone, Australia). J. of Env. Manag.

Pillans, R.D., Bearham, D., Boomer, A., Downie, R., Patterson, T.A., Thomson, D.P. and Babcock, R.C. 2014. Multi year observations reveal variability in residence of a tropical demersal fish, *Lethrinus nebulosus*: implications for spatial management. PLoS One 9(9): e105507. doi:10.1371/journal.pone.0105507.

Preen, A. 2000. Dugongs, boats, dolphins and turtles in the Townsville-Cardwell region and recommendations for a boat traffic management plan for the Hinchinbrook Dugong Protection Area. Great Barrier Reef Marine Park Authority.

Prior B.R. 2014. Diet of green turtles (*Chelonia mydas*) from different habitats within Port Curtis (Gladstone Harbour), Queenland. University of Queenlsand Honours Thesis. 45 pp.

Pya, N. and Wood, S.N. 2014. Shape constrained additive models. Statistics and Computing: 1–17.

Ralph, P.J., Durako, M., Enriquez, S., Collier, C. and Doblin, M. 2007. Impact of light limitation on seagrasses. J. Exp. Mar. Biol. Ecol. 350:176–193.

Rasheed, M.A., Davies, J.D. and McCormack, C.V. 2013. Port Curtis and Rodds Bay seagrass monitoring program, November 2012. Tech. rep., JCU Publication, Centre for Tropical Water & Aquatic Ecosystem Research, Cairns.

Rasheed, M.A., Dew, K.R., McKenzie, L.J., Coles, R.G., Kerville, S.P. and Campbell, S.J. 2008a. Productivity, carbon assimilation and intra-annual change in tropical reef platform seagrass communities of the Torres Strait, north-eastern Australia. Cont. Shelf Res. 28:2292-2304.

Rasheed, M.A., McKenna, S.A., Carter, A.B. and Coles, R.G., 2014. Contrasting recovery of shallow and deep water seagrass communities following climate associated losses in tropical north Queensland, Australia. Mar. Poll. Bull. 83:491–499.

Rasheed, M.A., McKenna, S.A., Taylor, H.A. and Sankey, T.L. 2008b. Long term seagrass monitoring in Port Curtis and Rodds Bay, Gladstone October 2007. Tech. rep., DPI&F Publication PR07-3271 (Cairns), 32 pp.

Rasheed, M.A., McKenna, S.A. and Thomas, R. 2005. Long-term seagrass monitoring in Port Curtis and Rodds Bay, Gladstone - October/November 2004. Tech. rep., DPI&F Information Series QI05032 (Cairns), 27 pp.

Rasheed, M.A., Taylor, H.A. and Thomas, R. 2006. Long-term seagrass monitoring in Port Curtis and Rodds Bay, Gladstone - October 2005. Tech. rep., DPI&F Information Series QI06030 (Cairns), 30 pp.

Rasheed, M.A. and Unsworth, R.K.F. 2011. Long-term climate-associated dynamics of a tropical seagrass meadow: implications for the future. Mar. Ecol. Prog. Ser. 422:93-103.

Raymond, B., Lea, M.-A., Patterson, T., Andrews-Goff, V., Sharples, R., Charrassin, J.-B., Cottin, M., Emmerson, L., Gales, N. and Gales. R. 2014. Important marine habitat off east Antarctica revealed by two decades of multi-species predator tracking. Ecography 38:121–129.

Read, M.A. and Limpus, C.J. 2002. The green turtle, *Chelonia mydas*, in Queensland: Feeding ecology of immature turtles in Moreton Bay, southeastern Queensland. Memoirs of the Queensland Museum 48:207-214.

Redfern, J.V., McKenna, M.F., Moore, T.J., Calambokidis, J., Deangelis, M.L., Becker, E.A, Barlow, J., Forney, K.A., Fiedler, P.C. and Chivers, S.J. 2013. Assessing the risk of ships striking large whales in marine spatial planning. Conservation Biology 27:292–302.

Renaud, M.L., Carpenter, J.A. and Williams, J.A. 1994. Activities of juvenile green turtles, *Chelonia mydas*, at a jettied pass in South Texas. Fisheries Bulletin 93:586–593.

Rheuban, J.E., Berg, P. and McGlathery, K.J. 2014. Multiple timescale processes drive ecosystem metabolism in eelgrass (*Zostera marina*) meadows. Mar. Ecol. Prog. Ser. 507:1–3.

Richardson, D., Toki, B., Moran, D., Wulf, P. 2014. Assessment and Review of Marine Traffic, Marine Fauna Incidents and the Necessity of Go Slow Zones. Report to Gladstone Ports Corporation by BMT WBM Pty Ltd. Brisbane Australia. 81 pp.

Roberts, D.G. 1993. Root-hair structure and development in the seagrass *Halophila ovalis* (R. Br.) Hook. f. Aust. J. Mar. Freshw. Res. 44:85–100.

Schiller, A., Herzfeld, M., Brinkman, R. and Stuart, G. 2014: Monitoring, predicting, and managing one of the seven natural wonders of the World. Bull. Amer. Meteor. Soc. 95:23–30.

Schroeder, T., Devlin, M. J., Brando, V. E., Dekker, A. G., Brodie, J. E., Clementson, L. A., & McKinna, L. 2012. Inter-annual variability of wet season freshwater plume extent into the Great Barrier Reef lagoon based on satellite coastal ocean colour observations. Marine Pollution Bulletin, *65*(4): 210-223.

Seminoff, J.A., Resendiz, A. and Nichols, W.J. 2002. Home range of green turtles *Chelonia mydas* at a coastal foraging area in the Gulf of California, Mexico. Marine Ecology Progress Series 242:253–265.

Seminoff, J.A., Resendiz, A., Smith, T.W. and Yarnell, L. 2001. Diving patterns of green turtles (*Chelonia mydas agassizii*) in the Gulf of California. In: Coyne, M.S. and Clark, R.D. (eds.), Proceedings of the Twenty-First Annual Symposium on Sea Turtle Biology and Conservation. NOAA, Philadelphia.

Shmueli, G. 2010. To explain or to predict? Statistical Science 25:289–310.

Silverman, B.W. 1986. Density estimation for statistics and data analysis. New York: Chapman and Hall. 176 pp.

Spring, C.S. and Pike, D. 1998. Tag recovery supports satellite tracking of a green turtle. Marine Turtle Newsletter 82:8.

Sullivan, J.M., Twardowski, M.S. Zaneveld, J.R.V, Moore, C.M., Barnard, A.H., Donaghay, P.L. and Rhoades B. 2006. Hyperspectral temperature and salt dependencies of absorption by water and heavy water in the 400–750 nm spectral range, Appl. Opt., 45(21):5294–5309.

Stoeckl, N., Hicks, C.C., Mills, M., Fabricius, K., Esparon, M., Kroon, F., Kaur, K. and Costanza, R. 2011. The economic value of ecosystem services in the Great Barrier Reef: our state of knowledge. In: Costanza, R., Limburg, K. and Kubiszewski, I. (eds.) Ecological Economics Reviews. Annals of the New York Academy of Sciences 1219:113–133.

Taquet, C., Tacquet, M., Dempster, T., Soria, M., Ciccione, S., Roos, D. and Dagorn, L., 2006. Foraging of the green sea turtle *Chelonia mydas* on seagrass beds at Mayotte Island (Indian Ocean), determined by acoustic transmitters. Mar. Ecol. Prog. Ser. 306:295–302.

Taylor, H., Rasheed, M.A., Dew, K. and Sankey, T.L., 2007. Long term seagrass monitoring in Port Curtis and Rodds Bay, Gladstone November 2006. Tech. rep., DPI&F Publication PR07-2774 (Cairns), 30 pp.

Thomas, R., Unsworth, R.K.F. and Rasheed, M.A. 2010. Seagrasses of Port Curtis and Rodds Bay and long term seagrass monitoring, November 2009. DEEDI, Cairns.

Troeng, S., Evans, D.R., Harrison, E. and Lagueux, C.J. 2005. Migration of green turtles Chelonia mydas from Tortuguero, Costa Rica. Marine Biology 148:435-447.

van Dam, R.P. and Diez, C.E. 1996. Diving behavior of immature hawksbills (*Eretmochelys imbricata*) in a Caribbean cliff wall habitat. Marine Biology 127:170–178.

van der Heide, T., van Nes, E., Geerling, G., Smolders, A., Bouma, T. and van Katwijk, M. 2007. Positive feedbacks in seagrass ecosystems: Implications for success in conservation and restoration. Ecosystems 10:1311–1322.

Vermaat, J.E., Agawin, N.S.R., Duarte, C.M., Fortes, M.D., Marba, N. and Uri, J.S. 1995. Meadow maintenance, growth and productivity of a mixed Philippine seagrass bed. Mar. Ecolo. Prog. Ser. 124:215–225.

Webster, I.T. and Harris, G. P. 2004. Anthropogenic impacts on the ecosystems of coastal lagoons: modelling fundamental biogeochemical processes and management implications. Mar. Fresh. Res. 55:67–78.

Wetzel, R.G. and Penhale, P.A. 1979. Transport of carbon and excretion of dissolved organic carbon by leaves and roots/rhizomes in seagrasses and their epiphytes. Aquat. Bot. 6:149–158.

Wild-Allen, K., Herzfeld, M., Thompson, P.A., Rosebrock, U., Parslow, J. and Volkman, J.K. 2010. Applied coastal biogeochemical modelling to quantify the environmental impact of fish farm nutrients and inform managers. J. Mar. Sys. 81:134–147.

Williams, R. and O'Hara, P. 2010. Modelling ship strike risk to fin, humpback and killer whales in British Columbia, Canada. Journal of Cetacean Research and Management 11:1–8.

Woehler, E., Patterson, T.A., Bravington, M.V., Hobday, A.J. and Chambers, L.E. 2014. Climate and competition in abundance trends in native and invasive Tasmanian gulls. Mar. Ecol. Prog. Ser 511:249–263.

Wand, M.P. and Jones, M.C. 1995. Kernel smoothing. In: Monographs on Statistics and Applied Probability. Chapman and Hall, London, UK, p. 7.

White, G.C. and Garrott, R.A. 1990. Analysis of wildlife radio-tracking data. Academic, New York.

Whiting, S.D. and Miller, J.D. 1998. Short term foraging ranges of adult green turtles (*Chelonia mydas*). Journal of Herpetology 32:330–337.

Wood, S. 2006. Generalized additive models: an introduction with R. CRC press.

Worton, B.J. 1989. Kernel methods for estimating the utilization distribution in home-range studies. Ecology 70:164–168.

York, P. and Smith, T. 2013. Research, monitoring and management of seagrass ecosystems adjacent to port developments in central Queensland: literature review and gap analysis. Tech. rep., Deakin University, Waurn Ponds, Victoria.

Zaneveld, R.V., Kitchen, J.C. and Moore, C. 1994. The scattering error correction of reflecting-tube absorption meters, Ocean Opt. XII, 2258: 44–55.

Zeh, D.R., Heupel, M.R., Limpus, C.J., Hamann, M., Fuentes, M.M.P.B., Babcock, R.C., Pillans, R.D., Townsend, K.A. and Marsh, H. 2014. Is acoustic tracking appropriate for air-breathing marine animals? Dugongs as a case study. Journal of Experimental Marine Biology and Ecology 464:1–10.

Zimmerman, R.C., 2003. A biooptical model of irradiance distribution and photosynthesis in seagrass canopies. Limnol. Oceanogr. 48:568–585.

Zimmerman, R.C. and Alberte, R.S. 1996. Effect of light/dark transition on carbon translocation in eelgrass *Zostera marina* seedlings. Mar. Ecol. Prog. Ser. 136:305–309.

Zimmerman, R.C., Reguzzoni, J.L. and Alberte, R.S. 1995. Eelgrass (*Zostera marina* L.) transplants in San Francisco Bay: Role of light availability on metabolism, growth and survival. Aquatic Bot. 51:67–86.